Jarkko Paavola

Signature Ensembles and Receiver Structures for Oversaturated Synchronous DS-CDMA Systems

Turku Centre *for* Computer Science

TUCS Dissertations

No 91, October 2007

Signature Ensembles and Receiver Structures for Oversaturated Synchronous DS-CDMA Systems

Jarkko Paavola

To be presented, with the permission of the Faculty of Mathematics and Natural Sciences of the University of Turku, for public criticism in Auditorium Lambda in ICT building on December 14 2007, at 12 noon.

University of Turku
Department of Information Technology
Communication Systems

2007

Supervisors

Adjunct professor Valery Ipatov
Department of Information Technology
University of Turku
FIN-20014 University of Turku
Finland

Professor Jouni Isoaho
Department of Information Technology
University of Turku
FIN-20014 University of Turku
Finland

Reviewers

Professor Evgueni A. Krouk
Department of Safety in Information Systems
St. Petersburg State University of Aerospace Instrumentation
67, Bolshaya Morskaya, St Petersburg, 190000
Russia

Professor Tapani Ristaniemi
School of Information Technology
University of Jyväskylä
P.O.Box 35 (Agora), FIN-40014 University of Jyväskylä
Finland

Opponent

Associate professor Alexander Sergienko
Department of Theoretical Fundamentals of Radio Engineering
St. Petersburg Electrotechnical University
5, Professor Popov Street, St. Petersburg, 197376
Russia

ISBN 978-952-12-1959-7
ISSN 1239-1883
Painosalama Oy

Abstract

This thesis considers aspects in signature ensemble design for oversaturated synchronous DS-CDMA systems. CDMA is a multiple access method, where different users are distinguished with a unique code signal, or signature, assigned to each user because with DS-CDMA all users transmit simultaneously in the common frequency band. The set of all signatures is called signature ensemble. Synchronized signatures permit orthogonality between them but the number users is limited by the code signal space dimension, which is determined by available bandwidth and required data rate. If more users are to be served beyond the signal space dimension, the system becomes oversaturated making multiple access interference unavoidable. In such a situation a trade-off must be decided between the increase in the number of users, reduced performance due to inflicted interference and the complexity of a receiver, since the performance of a conventional matched filter receiver is poor in an oversaturated situation.

Two criteria of optimality are of essence when signature ensembles are assessed. Channel capacity is a measure of how well available resources are utilized. On the other hand, a crucial factor is the error probability in the receiver. Oversaturated CDMA can reach the theoretical limit of channel capacity, but only with Gaussian distributed signals. With a binary data transmission, which is also considered in this thesis, the optimization of signature ensemble for the maximization of channel capacity should be performed the same way with low signal-to-noise ratios as with Gaussian distributed signals. For high signal-to-noise ratios the Euclidean distance between transmitted signals should be maximized. This optimization direction also results in optimal error performance.

In this thesis oversaturated signature ensembles are designed for a group orthogonal system meaning that users are divided to non-interfering groups, which are then oversaturated with additional users. Group orthogonality permits using very simple receiver structure. The signature ensemble design criterion is to maximize the minimum Euclidean distance between all possible superpositions of user signatures modulated by antipodal information bits. That is, the minimum bit error probability is targeted. When one transmitter controls all transmissions, such as a base station in a cellular environment, data bits can be collaboratively encoded to improve the performance of group orthogonal oversaturated system. This way the minimum Euclidean distance can even surpass the minimum Euclidean distance of orthogonal signaling. It is concluded in this thesis that oversaturated systems can serve more users than the conventional orthogonal scheme with tolerable performance loss and with a very simple receiver. Analytical results are confirmed with simulations.

Acknowledgments

As my thesis project is nearing completion I want to express my gratitude to individuals who have had an important role in it during the last six years.

First of all, I would like to thank professor Valery Ipatov for continuous and patient guidance during my PhD studies. Without him this thesis would not have ever become reality. The supervision I've received has made this process a rewarding learning experience. Uncompromising demands for high scientific quality have ensured that I was focused on producing the best possible thesis. I would also like to thank professor Jouni Isoaho for giving me the opportunity to work towards a PhD thesis first in the Department of Physics and nowadays in the Department of Information Technology.

Professor Evgueni Krouk and professor Tapani Ristaniemi have reviewed this thesis. I thank them for their time and effort. Their kind and encouraging words are greatly appreciated.

This thesis have been funded by University of Turku and Turku Centre for Computer Science (TUCS). I would also thank Nokia foundation, HPY research foundation, Ulla Tuomisen säätiö and Turun suomalainen yliopistoseura ry for financial support.

Several people have helped with my thesis work. I would like to thank Alexey Dudkov for proof-reading the thesis and for many helpful suggestions; Sami Nuuttila for support with LaTeX typesetting, MATLAB® software, and with all my other computer related problems in general; Mika Oksanen for correcting language errors from the manuscript. I also thank PhD students and colleagues in our department for good company and an inspiring working environment. Especially, I want to mention Mikko Jalonen and all whose work is related to Dtv group's project activities. It has given me a great pleasure to see what can be achieved with the combination of determination and talent.

I am grateful to my mother Marja Hautamäki and step-father Matti Hautamäki for loving support. My thoughts also go to my late father Jorma Paavola. I wish I could have shared these moments with him. My mother-in-law Riitta Tala-Saramäki has shown sincere interest towards my progress with the thesis throughout the years.

Finally, two the most important persons in my life – I thank my wife Liisa for her companionship for better or for worse during the last twelve years, which has also brought us our daughter Elsa – my little angel.

Turku, October 24, 2007

Jarkko Paavola

Contents

List Of Acronyms

1G	First Generation of mobile phones
2G	Second Generation of mobile phones
3G	Third Generation of mobile phones
3GPP	Third Generation Partnership Project
4G	Fourth Generation of mobile phones
AWGN	Additive White Gaussian Noise
BER	Bit Error Rate
BLVP	Balanced Lattice Volume Packing
BPSK	Binary Phase Shift Keying
CCGO-CDMA	Collaboratively Coded Group Orthogonal CDMA
CCMA	Collaborative Coding Multiple Access
DSSS	Direct Sequence Spread Spectrum
CDMA	Code Division Multiple Access
fcc	face-centered cubic
FDM	Frequency Division Multiplexing
FDMA	Frequency Division Multiple Access
FHSS	Frequency Hopping Spread Spectrum
FIR	Finite Impulse Response
GO-CDMA	Group orthogonal CDMA
GSM	Global System for Mobile Communication
HSDPA	High Speed Downlink Packet Access
IIR	Infinite Impulse Response
ISDN	Integrated Services Digital Network
kbps	kilobits per second
LVP	Lattice Volume Packing
MAI	Multiple Access Interference
Mbps	Megabits per second
Mcps	Megachips per second
MIMO	Multiple Input Multiple Output
MMSE	Minimum Mean Square Error
MUD	Multiuser Detector
OVSF	Orthogonal Variable Spreading Factor
PC	Personal Computer

pdf	probability density function
PN	Pseudo Noise
POTS	Plain Old Telephone Service
PSK	Phase Shift Keying
QAM	Quadrature Amplitude Modulation
QoS	Quality of Service
S-CDMA	Synchronous Code Division Multiple Access
SINR	Signal-to-Interference-and-Noise Ratio
SIR	Signal-to-Interference Ratio
SLVP	Symmetric Lattice Volume Packing
SSP	Sphere Surface Packing
SNR	Signal-to-Noise Ratio
TDM	Time Division Multiplexing
TDMA	Time Division Multiple Access
TSC	Total Squared Correlation
UMTS	Universal Mobile Telecommunication System
WBE	Welch Bound Equality
WLAN	Wireless Local Area Network
WMAN	Wireless Metropolitan Area Network
ZFE	Zero Forcing Equalizer
ZSSP	Sphere Surface Packing including Zero vector

List of Symbols

$A, \mathbf{A}$	Amplitude, Diagonal amplitude matrix
$a, \mathbf{a}$	Chip, chip vector
$b, \mathbf{b}$	Data symbol, data symbol vector
$\mathbf{c}$	Filter tap vector
C	Channel capacity
d	Euclidean distance
d_H	Hamming distance
δ_{kl}	Kroenecker delta
Δ	Gilbert distance
Δ_c	The duration of chip
d_k	Decision statistics for user k
$\mathbf{g}$	Channel impulse response vector
γ	Energy loss
$\mathbf{H}_n$	Hadamard matrix of size n
$\mathbf{h}$	Orthonormal signature
$H(X)$	Entropy
$H(Y\|X)$	Conditional entropy
$\mathbf{I}_n$	Identity matrix of size n
$I(X;Y)$	Mutual Information
E	Energy
$E[\cdot]$	Expectation
$\boldsymbol{\varepsilon}$	Error vector
e_{ov}	Oversaturation efficiency
f	Frequency
G_p	Gray code penalty
G_{pk}	Peak gray code penalty
K	The number of users
L	Subspace dimension
l_g	The length of channel impulse response vector
λ	Eigenvalue
M	M-ary modulation
n	The number of equalizer taps
$n(t), \mathbf{n}$	Noise

n_I	Interleaver length
N	The dimension of signal space
N_0	Noise spectral density
M	The number of distinct signals
Ω	The number of supplementary signatures
$\mathbf{p}$	Constellation point vector
$\mathbf{P}$	Constellation point matrix
P	Power
P_e	Average probability of error
$P(X)$	Probability density function
Ψ	Remainder after division of N by four
$Q(x)$	Q-function
q^2	Signal-to-noise ratio
q_I^2	Signal-to-interference ratio
ρ	Correlation coefficient
$\mathbf{R}$	Correlation coefficient matrix
R	Data rate
$\Re$	Real part of complex number
s	The number of supplementary users in one subspace
$s(t), \mathbf{s}$	Signature, signature vector
$\dot{s}(t)$	Complex envelope of signal
$\dot{s}_o(t)$	Chip pulse shape
$\mathbf{S}$	Signature matrix
σ^2	Variance of noise
t	Time
T	Duration of signal
$T(h, \alpha)$	Owen's T-function
w	The weight of vector
W	The bandwidth of signal
$x(t), \mathbf{x}$	Transmitted group signal, group signal vector
$y(t), \mathbf{y}$	Observation, observation vector
$z, \mathbf{z}$	Matched filter output, matched filter output vector
Z_I	Zero-padding length
Z_j	Decision region of user j

Chapter 1

Introduction

During the recent decade personal wireless communication has become enormously popular. For example, in Finland the number of mobile phone subscribers have passed the number of using plain old telephone service (POTS) in the beginning of the current decade [1] and the penetration of mobile subscribers exceeded 90% of the population in 2004 [1]. The first generation (1G) of mobile phones was based on analog technology, and was capable of only transmitting speech. After the introduction of the second generation (2G) of mobile phones, such as Global System for Mobile communication (GSM), the wireless communication industry has experienced huge growth. In addition to speech transmission the 2G systems also had capability for simple data services which attracted users. World-wide, the number of GSM subscribers surpassed 500 million in 2001 [2]. The rapid progress of the Internet, which coincides with the time frame of expanding popularity of cellular communications, has revolutionized communication between people and created a market for wireless data services with wired-like capacity. People are accustomed to accessing multimedia services from the Internet with speeds of several tens of megabits per second (Mbps).

In the aftermath of the success of the 2G mobile phone systems, the wireless communication community envisioned *wireless access available anywhere, anytime* as a guideline for the designing third generation (3G) mobile phone standards [2,3]. The standardization within the third generation partnership project (3GPP) [2, 4] is a significant step towards a wireless system, which would give the same services users receive with a personal computer (PC) connected to the wired network regardless of user location. However, as the first commercial 3G networks opened in 2005, ten years after the deployment of GSM, it was evident that many steps are still required before this goal is achieved. The first 3G networks achieve data rates that are only in the region of the Integrated Services Digital Network (ISDN) [5], which is well below one Mbps (even 384 kilobits per second (kbps) is rare).

Also, the deployment of 3G systems has experienced difficulties due to high licensing costs in some countries and unrealistically high expectations of consumers [5]. The third generation is not nearly as revolutionary from the consumer point-of-view as the second generation was, since the development between standard generations is an evolutionary process. Although the 3G systems do not offer unparalleled services, they offer flexibility and configurability, which the 2G systems lacked. Thus, on the road towards the future high data rate cellular standards, the third generation will serve as a basis for evolution and development.

The evolution of 3G systems has been continuous, and several enhanced releases of the standard have been published since the original version was released. It has been reported [6] that High Speed Downlink Packet Access (HSDPA) -capable 3G networks are able to deliver data rates of approximately 10 Mbps, or even 20 Mbps if multiple input - multiple output (MIMO) technique is utilized [7].

It is easy to predict that the fourth generation (4G) of mobile phones will evolve from 3G systems [6]. Mobile phone standards will probably also experience convergence with other wireless communication networks such as wireless local/metropolitan area networks (WLAN/WMAN), broadcasting systems, and wireless personal area networks [5,6,8]. Each network type will be utilized in user terminals to provide required quality of service (QoS) to the users while network resources are exploited efficiently [9, 10].

The most critical resource which limits achieving high data rates in wireless communication, is *bandwidth*, or frequency resource. Bandwidth is a very scarce resource, and therefore it is strictly regulated by authorities. Thus, the greatest challenge of future wireless systems is the efficient utilization of existing frequency resources [11]. Especially challenging are multiuser systems, which experience fading and are power limited.

The fundamentals on digital communication systems and factors affecting transmission fidelity and bandwidth requirements can be found, for example, from [12–16]. Within fixed modulation mode and code rate the higher data rate needs a wider bandwidth. In digital communications information symbols are transmitted with signals modulated by data symbols. A communication system containing M distinct signals is able to deliver $\log_2 M$ bits with one signal. Each signal has finite duration T. The definition for bandwidth is ambiguous [15]. The definition adopted here is following: the bandwidth required by the signal, W, is $W \approx 1/T$, which corresponds to a frequency band from zero to the first null in spectrum for rectangular signals having sinc[1]-shaped spectrum [16]. To be precise, the bandwidth of a finite duration signal is infinite, but the single-sided main lobe of its frequency response is adequate to characterize the baseband signal in the frequency

[1] $\mathrm{sinc}\ (x) = \sin\ (\pi x)/\pi x$

domain. The data rate, R, available through the channel is $R = \log_2 M/T$. The data rate entering the modulator (gross rate) can, in practical systems, be higher than the original data rate (source rate). It is meant to compensate the added redundancy used for error encoding on source data to protect it from channel disturbances.

In practice, it is not enough that a single high data rate stream can be transmitted through the air from the transmitter to the receiver. Wireless communication systems must be able to serve tens or even hundreds of users simultaneously with multimedia applications requiring very high data rates. The method allowing several users to communicate simultaneously is called *multiple access*. Different strategies to implement multiple access are presented next, along with essential information of the cellular environment where mobile receivers typically operate.

1.1 Multiple access techniques and the cellular communication environment

In a cellular system, the coverage area is divided into parts called cells. Each cell has a base station, which is connected with all user terminals inside the cell. In cellular telecommunication systems, the transmission from base station to user terminal (downlink, forward link) and the transmission from terminal to base station (uplink, reverse link) must be separated. Traditionally downlink and uplink transmissions use different frequencies or they occur consecutively. These two options are referred to as frequency division multiplexing (FDM) and time division multiplexing (TDM). The method allowing several users to communicate simultaneously inside a cell is called a multiple access technique. The capacity of multiple access techniques refers to the maximum number of users ($K_{\max}$) served inside one cell [17]. In this thesis, the term capacity refers specifically to multiple access capacity $K_{\max}$. The information theoretic maximal data rate through the channel established by Claude Shannon [18] is referred to as *channel capacity* to make a distinction with the latter. Classical multiple access methods are orthogonal, thus they do not inflict multiple access interference (MAI) to systems. To provide orthogonality signals can be non-overlapping in the time domain or in the frequency domain, but the non-overlapping condition is only sufficient, not necessary. In code-division systems signals overlap in both domains, being orthogonal due to proper code structure. The capacity of orthogonal multiple access methods is $K_{\max} = WT$ [19,20]. Adding users to systems beyond this limit inflicts MAI. The number of allowed extra users depends on the tolerable amount of interference.

The analog first generation systems used frequency division multiple access (FDMA), where different users communicate on different frequencies.

The FDMA is not very convenient from the implementation point-of-view, since K parallel passband filters are required in the receiver and orthogonality is difficult to preserve in practice [19]. In the cellular communication environment the cells must be clustered to ensure that the same frequencies are not used in adjacent cells, which would cause inter-cell interference.

Most of the 2G systems used a combination of time division multiple access (TDMA) with FDMA. In TDMA, the time axis is divided into slots allocated to different users. Pure TDMA allows all users to have the whole bandwidth at their disposal. The practically achievable capacity of pure TDMA is limited by peak power[2] requirements, since small duration of time slots entails big power emission, which is impractical in battery powered mobile devices. Also, in cellular environment the frequency re-use restricts the maximum emitted power. In GSM the number of time slots is eight. Thus, in order to function in real systems, TDMA must be combined with FDMA [19].

The 3G systems and one 2G system have adopted code division multiple access (CDMA) as their multiple access technique. In CDMA users communicate simultaneously in the same frequency band. Different users are separated in the receiver with the help of an individual code signal called *signature*. The set of all signatures is called a *signature ensemble*. In the time of deployment of the 2G systems, CDMA seemed to be too complex from the implementation point-of-view. Thus, only one 2G standard, called IS-95 or cdmaOne [19,21,22], uses CDMA. The rapid development in digital technology has enabled large scale implementations of CDMA in consumer electronics nowadays.

Three discussed multiple access methods are illustrated in Fig. 1.1. Orthogonal multiple access can also provided by spatial space division [13] or by polarization of carrier waves [15].

CDMA capacity is not equal in the downlink and in the uplink, since orthogonal, and therefore MAI free transmission in the uplink, is not possible unless some complex procedures are used in the mobile transmitter controlling transmission epoch to provide synchronous arrival of all signals from mobile transceivers at the base station receiver. An example of a such a procedure is implemented in 3G TDM (Time Division Multiplexing) [5, 23, 24]. There, uplink transmissions are arranged by a control procedure, which delays the transmissions of mobile terminals according to their distance from the base station.

The capacity of CDMA has traditionally been limited by uplink capacity [16,21] due to asynchronous signaling, which inflicts MAI to the system. However, modern wireless data communication sets more stringent require-

[2]High peak power, which is the maximal amount of power emitted by transmitter, should not be dramatically higher than the average power which is emitted energy per time unit.

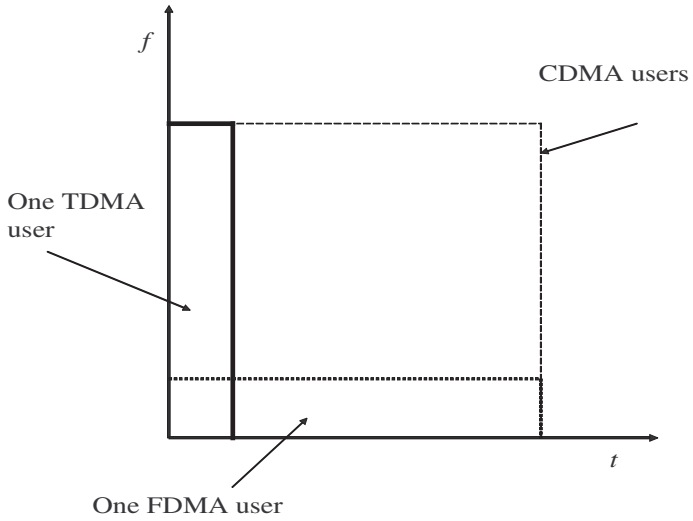

Figure 1.1: Illustration of different multiple access techniques

ments for the downlink due to the asymmetric nature of data. Much more data is downloaded to the user terminal than is sent to the network [6]. Video telephony might have different aspects, however [6, 9].

1.2 Objectives of thesis

The aim of this thesis is to analyze and propose bandwidth efficient methods for multiple access in the downlink of CDMA systems. Current state-of-the-art wireless communication systems use solutions such as multicarrier modulation [25] and MIMO [26] to achieve very high data rates. CDMA will certainly also be an integral part of future wireless communication standards, such as 4G mobile phones, but it will probably be combined with other aforementioned techniques [6]. Due to the importance of CDMA downlink, this thesis concentrates on methods of increasing user-capacity by examining signature ensembles and receiver structures that accomplish that goal. In the CDMA downlink, it is possible to use synchronous signaling. This special multiple access technique is called *synchronous CDMA* (S-CDMA). The method of increasing the capacity of S-CDMA in this thesis is called *oversaturation*, or overloading. The aim is to find adequate trade-offs between oversaturation efficiency (capacity growth), performance loss due to inflicted MAI and additional receiver complexity due to efforts to mitigate extra MAI.

It should be noted that regardless of current trends of limiting the S-CDMA to downlink only, it is also possible to utilize it in the uplink. As the cell size is shrinking in so called hot-spot areas, where extremely high data rates are required, pico cells are utilized. They have coverage areas in the scale of meters or few tens of meters. There, the synchronism can be maintained within a fraction of chip interval also in the uplink due to very small distance between transmitter and receiver. Other such quasi-synchronous systems are also proposed for satellite [27] systems, which use a special spreading code to transmit timing information, and microcellular [28] environments, where receiver processing transforms an asynchronous channel to the synchronous equivalent. The S-CDMA system developed by Cylink relied on network synchronization for both downlink and uplink [29]. Special orthogonal signals can be constructed to such a quasi-synchronous channel to combat possible small synchronization errors [30, 31].

Increasing the capacity of S-CDMA with the design of signature ensembles and corresponding receiver structures is the topic of this thesis. In CDMA system design the signature or receiver optimization cannot be performed independently [32–35]. The selection of employed receiver structures depend on restrictions on complexity and requirements on the performance, which are highly dependent on the signature ensemble selection. For the oversaturated situation, there are no signature ensembles which could provide multiple access interference free transmission. Therefore, when capacity increase is desired with existing time-frequency resources, the trade-off between complexity of receiver and performance defines the selection of receiver type and signature ensemble. A complex receiving algorithm introduces large delays to transmission and dissipates a lot of power [11]. On the other hand, high signal energy can also be problematic in cellular networks [19]. The analysis of oversaturated S-CDMA starts with a brief review of previous achievements reported in the literature.

1.3 Previous work on oversaturated CDMA

Next, a brief review of previous work on oversaturated CDMA techniques is presented. A more detailed study of discussed receivers is given in chapter 4. Oversaturated signature ensembles are discussed in chapters 5, 6 and 7. The work by Ross and Taylor has been the basis for many other authors. In [36, 37] they propose a signature ensemble which is optimal in the minimum Euclidean distance [32]. That is, the asymptotic bit error probability is minimized if an optimal receiver is employed. The scheme is investigated in detail in chapter 5 along with an extension of the scheme to arbitrary numbers of users and a method to produce a binary signature ensemble that follows the minimum distance requirement. The utilization of Ross

and Taylor signature ensembles requires the optimal receiver algorithm [38] to be used while the obtained oversaturation efficiency is modest. This has led to active research for ways to reduce exponential complexity by exploiting cross-correlation properties of signatures, or to utilize sub-optimal algorithms at the receiver. Signature ensembles providing high oversaturation efficiency have been discovered also.

In [33] Learned et.al. proposed a polynomial complexity optimal receiver algorithm for a signature cross-correlation matrix that has tree-structure which is obtained, for example, with the Ross and Taylor signature ensemble. Another proposed option for signatures in [33] is to utilize wavelet basis to create real valued signatures. More information about oversaturation using wavelets can be found in [34, 39, 40]. Polynomial complexity of multiuser receivers is also possible if all values in a signature ensemble cross-correlation matrix are identical [35, 41] or negative [42].

Shi and Schlegel [43] propose a trellis decoder [12] based receiver for signature ensembles having a band-diagonal cross-correlation matrix, which can be obtained by interpolating and linearly combining Walsh-Hadamard codes. The complexity of the trellis decoder is linear in the number of users and exponential in the number of trellis states.

Suboptimal multiuser receivers aim to cause minimal decrease in the performance of the receiver while providing simple implementation. Suboptimal receivers can be divided into linear [44, 45] and non-linear [46–49] categories, where the latter is also referred to as decision-driven multiuser receiver. Developments in the field of multiuser detection have been studied profoundly in [50], which also contains extensive reference list on the subject. Out of the linear receivers a decorrelating detector [44] cannot be used in the oversaturated case due to impossibility of decorrelation of linearly dependent signals, but a minimum mean square error (MMSE) receiver [45] suits well to this purpose. The theory of decorrelating receiver and the MMSE receiver are generalized to group pseudo-correlator and group MMSE detector algorithms in [51]. Both of them specialize in receiving a group of linearly dependent users while the interfering subspace is linearly independent from the desired subspace.

When using linear receivers the signature ensemble that reaches the minimum MAI power level is obtained by minimizing the total squared correlation (TSC) among all users. Such a signature set is called a Welch bound equality (WBE) ensemble. Rupf and Massey found [52] that a WBE ensemble maximizes the channel capacity for equal energy users, and the issue has been under extensive study since. The result was later extended to case of different amplitudes in [53] and the term generalized WBE signatures was adopted to differentiate them from the equal energy case. The connection of WBE signatures to user capacity is analyzed in [54, 55]. WBE ensembles will be analyzed in more detail in section 5.2.

In [56] a group orthogonal system was proposed, where signatures are divided to non-interfering groups making an optimal multiuser receiver feasible in each group due to the small number of users inside the group. MAI occurs only between users inside a group. No specific signature ensembles providing group orthogonality were given in [56]. Group orthogonal signal design to maximize minimum Euclidean distance inside the group is analyzed in detail in chapters 6 and 7. Group orthogonality based on spatial division of signatures is investigated in [57]. In [58] the trade-off between inter-group and intra-group interference is analyzed for the system where each group utilizes the same signatures but different chip waveforms.

Vanhaverbeke et. al. [59–61] have investigated oversaturation based on different kind of combinations of two different initial sets to produce oversaturation. Both initial sets can be orthogonal or the other set can be pseudo-random. The receiver is based on successive interference cancellation. Several variations and improvements of the original idea are investigated in [62–66]. The approach can be considered opposite in group orthogonal strategy, where MAI occurs inside the group instead of between groups. Proposed methods are collected and thoroughly analyzed in PhD thesis by Vanhaverbeke published in 2005 [20].

In addition to multiple access capacity of oversaturated communications, information theoretic channel capacity has received a lot of attention during the recent decade. It is proved in [52] that Shannon capacity can be obtained in oversaturated S-CDMA transmission with a WBE signature ensemble. The channel capacity of oversaturated S-CDMA is further discussed in chapter 3.

Some of the contributions of this thesis have been published in [67–72]. Here, results published in aforementioned references are significantly extended and presented more accurately in systematic manner.

1.4 Overview of thesis

Thesis is organized as follows: First, the fundamentals of spread spectrum and S-CDMA are investigated in chapter 2, and a method to increase S-CDMA capacity called oversaturation is presented. Chapter 3 serves as a motivation for the topic selection and for the work performed for this thesis. Two criteria of optimality of communication systems are discussed there. The conclusion is that it is possible for oversaturated S-CDMA to obtain Shannon's channel capacity and also to have optimal asymptotic error performance in terms of minimum Euclidean distance. Next, a problem with receiving CDMA transmission is illustrated and several receiver algorithms for oversaturated situations are presented. It is seen that the performance of conventional receiver is not adequate, and the optimal receiver is difficult

to implement in practice due to its high complexity. Therefore, a number of suboptimal algorithms are investigated from which the group orthogonal receiver is treated in the most detail. After describing CDMA receivers the focus shifts to designing oversaturated signature ensembles. Optimal signature ensemble is presented in chapter 5 along with ensembles, which obtain higher efficiency but exhibit energy loss when compared to the optimal ensemble. The main contribution of this thesis is the signature ensemble design provided for group orthogonal receiver, which is presented in chapter 6 for unique signature per user strategy, and in chapter 7 for collaboratively encoded data bits of users. Collaborative encoding entails that each user does not posses a unique signature. For both schemes, the performance is analyzed theoretically in an additive white Gaussian noise (AWGN) channel. In chapter 8, theoretical performance analysis of chapters 6 and 7 is verified with simulations. Also, the performance in multipath channel is analyzed, which is a more realistic channel model for mobile terminals in cellular communications. Finally, the concluding remarks are given.

Chapter 2

The fundamental concepts of synchronous CDMA systems

2.1 Spread spectrum concept

The emphasis of this thesis is on CDMA technology, which is completely based on the spread spectrum concept. Therefore, some very well known aspects of spread spectrum are discussed briefly to establish notations used throughout this thesis and to provide necessary information to thoroughly understand oversaturation of S-CDMA. The literature is crowded with excellent material on spread spectrum methods. An interested reader can find detailed material from for example references [17,21,22,32,73]. Spread spectrum has been utilized in military communications for several decades. Historical milestones of spread spectrum systems and its military applications are presented in [17]. The commercial communication benefits from exactly the same properties as military systems. Books devoted to commercial implementations of CDMA in general are [19,21]. After the selection of CDMA as an air interface technique for 3G mobile systems several books describing UMTS (Universal Mobile Telecommunication System) and cdma2000 systems have emerged [3, 5, 23, 24, 74–76].

Spread spectrum system is defined in many sources [15, 16, 21, 22] as a system, which employs much wider bandwidth than required by the data rate to be transmitted. This definition, however, is ambiguous. For example, in the GSM cellular standard users reserve the bandwidth of approximately 200 kHz to transmit data at rate between 9.6-13 kbps, but GSM does not involve any spread spectrum methods in the transmission of user data[1]. Here, we use older and more universal definition which can be found for example in [32]. There a *spread spectrum signal* is defined as a signal, whose time-

[1]To enhance frequency re-use between adjacent cells slow frequency-hopping spread spectrum method is employed between base stations [22].

frequency product that is the product of signal duration, T, and its required bandwidth, W, is much greater than one:

$$WT >> 1. \tag{2.1}$$

For plain signals that are not employing spread spectrum methods, the relation in question is

$$WT \approx 1. \tag{2.2}$$

System employing spread spectrum signals is referred to as *spread spectrum system*.

In principle, spread spectrum systems have numerous merits when compared to systems utilizing plain signals. These merits include good performance in a multipath environment, resistance to narrow-band interference, privacy, possibility for exact time and location measurement, and good electromagnetic compatibility. The most important merit regarding this thesis is the possibility of employing CDMA as multiple access method, which will be inspected in detail in the next section. In addition, in a cellular environment CDMA makes universal frequency re-use possible, which increases the capacity and enables the use of soft handover, which enhances the performance [21].

The basic principles of spread spectrum are illustrated in Fig. 2.1. Originally narrow-band signal in Fig. 2.1(a) is spread at the transmitter without adding extra energy, thus making the transmitted signal spectrum wide and power spectrum density low as shown in Fig. 2.1(b). At the receiver an opposite operation, called despreading illustrated in 2.1(c), is performed to return to the original spectrum. Some of the merits of spread spectrum are easily explained with Fig. 2.1. Low probability of interception and good electromagnetic compatibility are due to the fact that power spectrum density of a spread spectrum signal can be close or even below the noise level. Resistance to narrow-band jamming is achieved due to the fact that after the despreading in the receiver the jammer spectrum is spread to wider spectrum having low power level.

Good time resolution is due to the time compression effect in the time domain. It enables measuring time accurately, and also separating signals arriving at receiver with different delays from a multipath channel. This is illustrated in Fig. 2.2, where the matched filter output is presented for two copies of the original signal. It is seen that even though the delayed copy of the transmitted signal is overlapping in time with the original signal, they are easily separated after the matched filter processing. Privacy is protected against non-authorized receivers when only intended receiver is aware of the code signal used in transmission.

In practice, the spreading of the signal is accomplished by modulating information bits with a spread spectrum signal. At the receiver a reverse

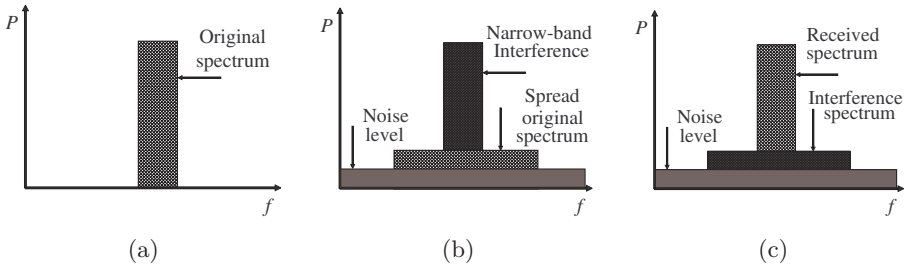

Figure 2.1: The basic principle of spread spectrum.

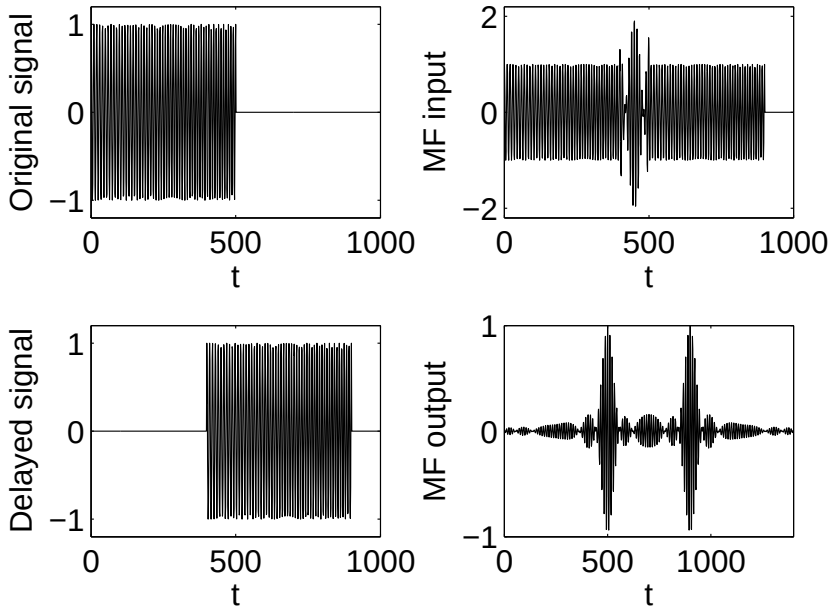

Figure 2.2: The time compression effect of spread spectrum signals.

operation called despreading is performed to restore the original transmitted signal. Despreading is in fact exactly the same operation as spreading, where the received signal is modulated with synchronized replica of the original spread spectrum signal. Here, we discuss only discrete spread spectrum signals. Continuous spread spectrum signals are not that typical in contemporary commercial communication systems but remain in wide use for example in radar and sonar systems [77, 78].

2.2 Discrete spread spectrum signals

In the baseband, a discrete spread spectrum signal is a chip, or code, sequence. The term chip is introduced to separate elementary pulses from information bearing symbols. Formally, the complex envelope of the spreading signal, $\dot{s}(t)$, can be given as

$$\dot{s}(t) = \sum_{i=-\infty}^{\infty} a_i \dot{s}_0(t - i\Delta_c)\exp(j2\pi f_i t), \tag{2.3}$$

where a_i, f_i are complex amplitude and frequency of chip number i, and $\dot{s}_0(t)$ is the pulse waveform with the duration Δ_c. The real signal, $s(t)$, is obtained from the complex envelope as $s(t) = \Re\{\dot{s}(t)\exp(j2\pi f_c t)\}$, where f_c is the frequency of the carrier wave.

The spread spectrum systems can be divided into two main categories, which are direct sequence spread spectrum (DSSS) and frequency hopping spread spectrum (FHSS). It is also possible to use time hopping or the three alternatives can be utilized simultaneously in a hybrid mode [17]. The entire available bandwidth is utilized in DSSS systems continuously by the all spread signals. In FHSS transmission the bandwidth reserved by the signal hops according to the spreading signal inside the boundaries of the whole bandwidth allocated for the system. The hopping is realized with the modulation of f_i in (2.3). The FHSS can be further divided into fast and slow hopping, but since the emphasis of the thesis is on DSSS, the interested reader is directed to [17] for more information on frequency hopping. In DSSS, only the complex amplitude of spread spectrum signal is modulated. Thus, $f_i = 0$ and the (2.3) reduces to

$$\dot{s}(t) = \sum_{i=-\infty}^{\infty} a_i \dot{s}_0(t - i\Delta_c). \tag{2.4}$$

In this thesis only phase shift keying (PSK) modulation of chips is considered, which means that $|a_i| = 1$. The spreading and despreading operations of binary PSK (BPSK) modulated DSSS are illustrated in Fig. 2.3, where the transmission of four bits of single user $\mathbf{b} = \{1, -1, 1 - 1\}$ (Fig. 2.3(a)) is spread with chip sequence $\mathbf{a} = \{1, 1, 1, 1, -1, -1, 1, -1\}$ using rectangular pulse shape (Fig. 2.3(c)). The result of spreading is illustrated in (Fig. 2.3(e)). The spread baseband signal is BPSK modulated and sent through the channel (here the noisy waveforms are not illustrated for sake of clarity). At the receiver, the observed signal (Fig. 2.3(b)) is despread with the synchronized copy of original spreading code (Fig. 2.3(d)) and demodulated to obtain transmitted bits (Fig. 2.3(f)).

The quality of transmission in spread spectrum systems is determined by

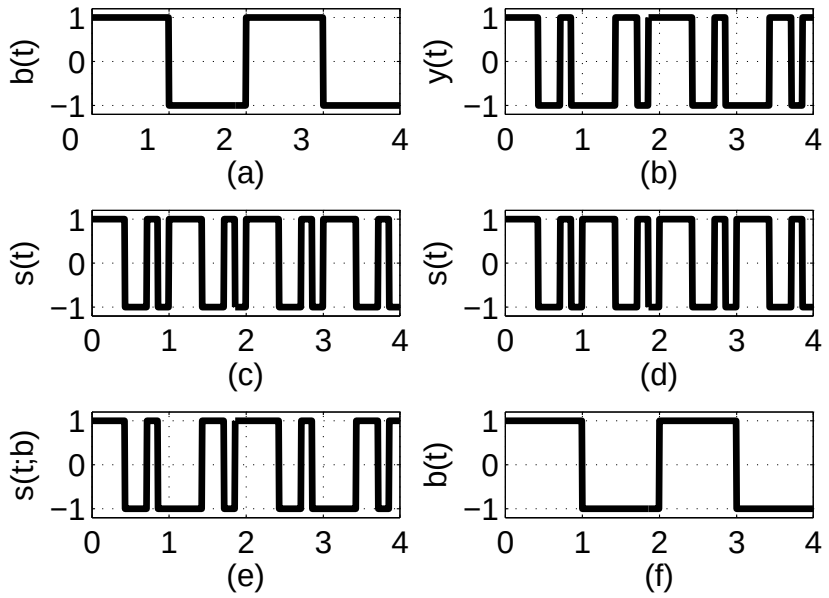

Figure 2.3: The principle of DSSS.

the correlation properties of signals[2]. The performance of a CDMA system is dependent on the cross-correlation property. Other applications of spread spectrum require good autocorrelation properties.

2.3 Code division multiple access

CDMA is a multiple access method, where each user k is assigned unique discrete spread spectrum signal, $s_k(t)$, which enables distinguishing users from each other even though all transmissions occur simultaneously in the same frequency band. This signal is referred to as signature in this thesis. The set of all users' signatures is referred as signature ensemble. Correlation properties of signature ensemble are critically dependent on the available signal space dimension, or the length of signature per one data symbol, N, which is also called spreading factor or processing gain. The spreading factor is determined by signal bandwidth, W, and data symbol duration, T [17]

$$N = WT. \tag{2.5}$$

[2]which is furthermore fully determined by the correlation properties of code sequences for fixed pulse shape of $\dot{s}(t)$.

In the case of binary data transmission, the bit rate, R_b, is the inverse of symbol duration, and

$$N = \frac{W}{R_b}, \tag{2.6}$$

where N now directly indicates how many times the bandwidth is greater than the actual data rate. There are exactly N orthogonal signatures having the length of N chips. The number of users served, $K_{\max}$, in CDMA equals the number of orthogonal signatures available. For the case of M-PSK data modulation

$$K_{\max} = \begin{cases} N, & \text{for } M\text{-PSK, } M > 2 \\ 2N, & \text{for BPSK} \end{cases}. \tag{2.7}$$

2.3.1 Synchronous CDMA

In the time domain the CDMA can be characterized as synchronous or asynchronous CDMA. The CDMA system is synchronized if there are no mutual delays between signatures of different users at the receiver input. If all signatures are synchronized the orthogonal signature ensemble is optimal due to zero cross-correlations, which completely eliminates MAI. Synchronism between signatures can be maintained on the downlink of cellular system, since the base station is controlling all transmissions. However, the uplink transmission is usually asynchronous and the orthogonal multiple access cannot be guaranteed. As a result, MAI appears and its intensity is determined by cross-correlations of signatures under their arbitrary time-shifts. Because of this, the definition of CDMA uplink capacity is not as straightforward as for synchronous case. The capacity is considered to be interference limited, meaning that the maximum number of users depends on the tolerable amount of MAI.

In the downlink, the signal transmitted by base station is a *group signal*, which is the superposition of all data modulated user signatures. Let us limit the consideration to one data symbol interval and denote the data symbol of k-th user as b_k. The data symbol modulates the signature of user k, denoted as $s_k(t)$ and consisting of chips $a_{k,i}$ (having pulse shape defined by $s_0(t)$ and duration Δ_c) , of the user k, which results in modulated signal $s_k(t; b_k)$. For binary data symbols the modulated DSSS CDMA signature is given as

$$s_k(t; b_k) = b_k s_k(t) = b_k \sum_{i=0}^{N-1} a_{k,i} s_0(t - i\Delta_c). \tag{2.8}$$

The transmitted group signal, $x(t; \mathbf{b})$ is obtained by summation of modulated user signatures, which are also multiplied by amplitudes A_k to provide

desired signal energy:

$$x(t;\mathbf{b}) = \sum_{k=1}^{K} A_k s_k(t;b_k), \tag{2.9}$$

where $\mathbf{b} = (b_1, b_2, \ldots, b_K)$ is the vector containing data symbols for all users. The signal received by terminal can be expressed as

$$y(t) = x(t;\mathbf{b}) + n(t) = \sum_{k=1}^{K} A_k s_k(t;b_k) + n(t) \tag{2.10}$$

where $n(t)$ is an AWGN component, having two-sided spectral density $N_0/2$. The immaterial common delay is omitted from the equation.

Receiver strategies to retrieve user data from the received group signal is the topic of chapter 4. For further analyses it is convenient to replace (2.10) by its discrete time vector equivalent:

$$\mathbf{y} = \mathbf{x} + \mathbf{n} = \mathbf{S}^T\mathbf{A}\mathbf{b} + \mathbf{n}, \tag{2.11}$$

where $\mathbf{y}$ is the noisy group signal column vector of length N, $\mathbf{x}$ is the transmitted group signal column vector of length N, $\mathbf{S} = [\mathbf{s}_1, \mathbf{s}_2, \ldots, \mathbf{s}_K]$ is the signature ensemble matrix of size $K \times N$ with rows as signatures $\mathbf{s}_k = (a_{k,0}$, $a_{k,1}$, $\ldots$, $a_{k,N-1})$, $\mathbf{A}$ is the $K \times K$ diagonal matrix with diagonal elements A_k, $\mathbf{b}$ is the column data bit vector of length K and $\mathbf{n}$ is the column noise vector of length N.

2.3.2 Orthogonal signature ensembles

As discussed earlier, orthogonal signature ensembles remove the MAI completely. Mathematically, orthogonality condition means that normalized correlation coefficient between user signatures i and j, ρ_{ij}, is

$$\rho_{ij} = \frac{1}{E}\int_0^T s_i(t)s_j^*(t)\,dt = \begin{cases} 1, & i = j \\ 0, & i \neq j \end{cases}, \tag{2.12}$$

where T is the duration of signature coinciding with data symbol duration, and $E = \int |s(t)|^2$ is the the energy of signatures. For DSSS signals correlation coefficient may be expressed in terms of code sequences as

$$\rho_{ij} = \frac{1}{E}\sum_{m=0}^{N-1} a_{i,m}a_{j,m}^* \begin{cases} 1, & i = j \\ 0, & i \neq j \end{cases}, \tag{2.13}$$

where E is code sequence energy $E = \sum_{i=0}^{N} |a_{k,i}|^2$. The correlation coefficients for all combinations of i and j form a cross-correlation matrix,

$\mathbf{R}$ ($\mathbf{R}_{ij} = \rho_{ij}$), and in the orthogonal signature ensemble $\mathbf{R} = \mathbf{I}$, where $\mathbf{I}$ is identity matrix. The binary orthogonal ensemble can be obtained with Hadamard matrix if rows of the matrix are employed as chip complex amplitudes of signatures [19, 32]. Hadamard matrix is a square matrix, whose components take only values ± 1, and whose all rows (and, as a consequence, columns) are orthogonal to each other. The necessary condition for Hadamard matrices to exist is that $N = 2$ or $N = 4i$, i integer. However the suffiency of that condition has not been proved. A very popular method to obtain Hadamard matrices of size 2^i is to build them recursively

$$\mathbf{H}_{2M} = \begin{pmatrix} \mathbf{H}_M & \mathbf{H}_M \\ \mathbf{H}_M & -\mathbf{H}_M \end{pmatrix} \tag{2.14}$$

starting with the matrix

$$\mathbf{H}_2 = \begin{pmatrix} + & + \\ + & - \end{pmatrix}, \tag{2.15}$$

which is obviously a Hadamard matrix. Denotation $\pm$ refers to signs of antipodal bits. Hadamard matrices for other lengths can be obtained from binary signature having optimal periodic autocorrelation function values $R(m) = -1$, $m \neq 0$. The orthogonal ensemble can be formed by creating matrix, where rows are all cyclic shifts of the binary sequence that have the minimax autocorrelation function. To have a matrix of Hadamard type, one row and one column of ones are appended to the matrix [79–81]. Suitable binary sequences for creating Hadamard matrices in this manner (m-sequences, Legendre sequences, etc.) are described in [32, 82].

2.3.3 Orthogonal signature ensembles in real applications

Orthogonal signatures are utilized, for example, in IS-95, nowadays known as cdmaOne, and in 3G standards UMTS and cdma2000.

The separation of users in the downlink of cdmaOne is achieved by orthogonal 64-length Walsh sequences [21]. In fact only 61 of them are utilized for user separation. The remaining three signatures are used for pilot, paging and synchronization channels. In the uplink, orthogonal codes are not used as signatures but to improve transmission fidelity instead [21]. Blocks of six bits are encoded with the rows of size 64 Hadamard matrix. Thus, each row represents one combination of a length six bit pattern. The 3G standard cdma2000 has evolved from cdmaOne. The system has also inherited the basic principles utilization of orthogonal codes [83].

In European 3G standard UMTS orthogonal signatures are called *channelization* codes. They are used for user separation in the downlink. They are also employed both in downlink and uplink in order to separate dedicated channels of the same user when multicode transmission takes place [5].

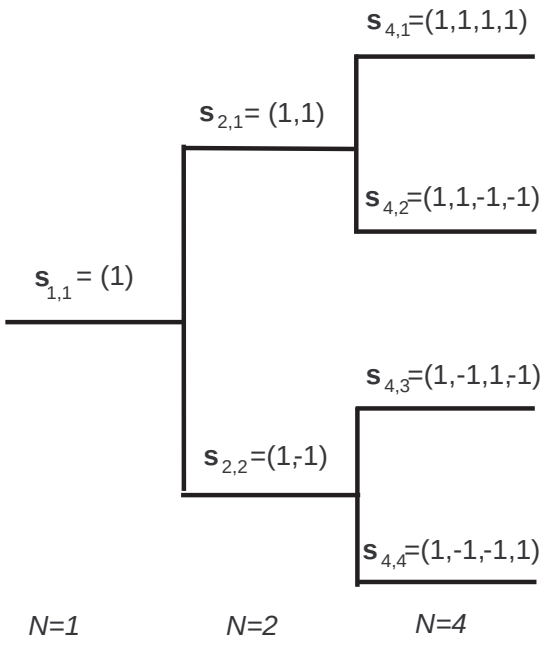

Figure 2.4: Code tree for OVSF codes

In UMTS physical channels antipodal symbols are spread using orthogonal codes. Before transmission the chip stream is scrambled with a long pseudo noise (PN) code that has good autocorrelation properties. In the uplink the scrambling codes are user-specific and they distinguish different users while in the downlink the scrambling code is cell-specific.

Orthogonal spreading codes in the UMTS standard are called orthogonal variable spreading factor codes (OVSF), which are generated with a code tree illustrated in Fig. 2.4. In practice, the OVSF codes are exactly the same as Walsh-Hadamard signatures presented in section 2.3.2. Variable spreading ensures the possibility to support variable bit rates for different physical channels of one user. The idea is to keep chip rate constant by adjusting spreading factor according to data bit rate. The higher the date rate the lower the spreading factor. Typical chip rate in the UMTS standard is 3.84 Megachips per second (Mcps). Processing gain is usually between 4 and 512 in the downlink for dedicated channels and 256 for common channels. In the uplink spreading factors are between 4 and 256 for data channels and 256 for control channels. Possible bit rates in physical channels are then from 7.5 kbps to 950 kbps corresponding to spreading factors of 512 and 4.

Each level of the code tree has N codes that have spreading factor N. Codes in each level are created from the codes of the previous level with multiplication. The code in the previous level is called mother code. Two double-length codes are created from the mother code by chaining two copies of the mother code or mother code and the same code multiplied with -1. Codes created this way maintain orthogonality if they are on the same level in the tree, or the shorter code is not found in the longer code. This means that two codes from a different level are orthogonal if the shorter code is not the mother code of the longer code. This limitation reduces the number of available codes according to bit rate requirements.

The capacity restriction imposed by OVSF codes are alleviated by different methods in the uplink and the downlink. In the uplink processing physical channels are divided into two sets, which are scrambled with two different scrambling codes. This makes it possible to use the same channelization codes to spread the two sets, which means that the capacity is doubled, i.e. the amount of physical channels is two times larger than it would be without division to two sets. In the downlink, even and odd bits of the same physical channel are processed in quadrature, which means that the bit rate of signal to be spread is halved. This implies that the spreading factor can be doubled while a constant chip rate is maintained.

2.4 Oversaturated synchronous CDMA

Orthogonal signaling is problematic in the high data rate transmission. The bandwidth for a system to operate on is defined by the authorities regulating the spectrum. Thus, it cannot be exceeded. From (2.6) and (2.7) it is seen that adding more orthogonal signatures (increasing the length) reduces available data rate, and vice versa when W is fixed. This property is totally contradictory to goals of wireless cellular system design. Thus, the problem of increasing the number of signatures without increasing bandwidth is topical. Obviously, $K > N$ signatures are not orthogonal any more. Here, the trivial doubling of K (see eq. (2.7)) is not considered as oversaturation. Thus, the goal in the thesis is to analyze methods for K to exceed N while losing as little as possible in performance versus the orthogonal signatures, and to cause minimal additional complexity to the receiver structure. The receivers for oversaturated CDMA are discussed in chapter 4.

Oversaturation efficiency, e_{ov}, is a measure of extra capacity, and it is defined as $e_{ov} = K/N = (N + \Omega)/N$, where Ω is the number of extra, or supplementary, users served beyond N. The capacity increase can be used to increase K for a given N, or to decrease N if there is no need to add more users to the system, which implies that higher data rates can be used.

2.5 Chapter summary

The fundamental issues of spread spectrum were briefly analyzed to provide necessary background knowledge on oversaturated S-CDMA. The following chapters will focus on receiver algorithms and signature ensembles for oversaturated S-CDMA, but first two criteria to label certain signature ensembles optimal are discussed in the next chapter.

Chapter 3

Criteria of optimality for oversaturated signature ensembles

In this chapter, two different criteria to label certain signature ensembles optimal are discussed. Channel capacity is a measure of efficiency for the utilization of existing energy and frequency resources. On the other hand the minimum Euclidean distance of the signature ensemble determines the performance of the receiver. The analysis starts by reproducing some crucial results on channel capacity of oversaturated S-CDMA from literature. It is seen that potential channel capacity is obtainable in an oversaturated S-CDMA transmission. After the analysis of channel capacity, the minimum distance criterion is discussed to minimize asymptotic error probability in the receiver.

3.1 Information theoretic channel capacity of synchronous CDMA

As stated before, the efficient utilization of resources is a strict demand for the contemporary wireless communication systems. In 1948, Claude Shannon [18] established the theoretical foundations of information theory. One of the most well known results is the upper bound on what error free data rates can be obtained with certain bandwidths and signal powers in an AWGN channel. The whole extent of Shannon's results and their further developments during the 50 years after initial publication are thoroughly surveyed in [84]. Next, the channel capacity of S-CDMA in an AWGN channel is analyzed based on Shannon's formulations to motivate the selection of oversaturated S-CDMA for the topic of this thesis. The results presented in

this section were published in [52] and later complemented in [53] to include results for users with unequal amplitudes. The channel capacity consideration here is valid for sum and symmetric capacity of equal energy users. Sum capacity is the total capacity of all users without any restrictions on the capacity distribution between users while symmetric capacity means that all users have an equal share of the overall capacity at their disposal.

The channel capacity, C, is obtained by maximizing the mutual information $I(X;Y)$ between the channel input and output ensembles [12,13,18,84]

$$C = \max_{P(\mathbf{x})} I(X;Y), \tag{3.1}$$

where $P(\mathbf{x})$ is the probability distribution on the ensemble X of all possible input vectors $\mathbf{x}$ and Y is the ensemble of all possible output vectors. Further, mutual information can be given by

$$I(X;Y) = H(Y) - H(Y|X), \tag{3.2}$$

where $H(Y)$ is the unconditional entropy of output ensemble, while $H(Y|X)$ is conditional entropy for fixed input vector $\mathbf{x}$. When the transmitted data bit vector is fixed the only uncertainty in the observation is caused by noise. Therefore, assuming that the channel is Gaussian, the conditional output entropy is the entropy of an N-dimensional Gaussian vector with a cross-correlation matrix $\mathbf{R}_n$ having probability density function (pdf)

$$P(\mathbf{y}|\mathbf{x}) = \frac{1}{\sqrt{(2\pi)^N \det \mathbf{R}_n}} \exp\left(-\frac{1}{2}\left(\mathbf{y}-\mathbf{x}\right)^T \mathbf{R}_n^{-1}\left(\mathbf{y}-\mathbf{x}\right)\right), \tag{3.3}$$

which, for memoryless channel, results in [13,18]

$$H\left(Y|X\right) = \frac{1}{2}\log\left((2\pi e\,\sigma^2)^N\right) \tag{3.4}$$

for $\mathbf{R}_n = \sigma^2\mathbf{I}_N$ when noise samples are uncorrelated. The denotation $\mathbf{I}_N$ is used for identity matrix of size N. The result of (3.4) means that to maximize (3.2) it is enough to maximize $H(Y)$, since $P(\mathbf{x})$ is not present in (3.4). The observation vector was defined in (2.11), which is rewritten here for convenience:

$$\mathbf{y} = \mathbf{S}^T\mathbf{A}\mathbf{b} + \mathbf{n}. \tag{3.5}$$

Given amplitude and fixed signature ensemble matrix (signatures in rows), the cross-correlation matrix of $\mathbf{y}$ is fixed

$$\begin{aligned}\mathbf{R}_y &= \overline{(\mathbf{y}-\overline{\mathbf{y}})(\mathbf{y}-\overline{\mathbf{y}})^T} = \overline{\mathbf{y}\mathbf{y}^T} = \overline{\mathbf{n}\mathbf{n}^T} + \mathbf{S}^T\mathbf{A}\,\overline{\mathbf{b}\mathbf{b}^T}\mathbf{A}^T\mathbf{S} \\ &= \sigma^2\mathbf{I}_N + \mathbf{S}^T\mathbf{A}^2\mathbf{S},\end{aligned} \tag{3.6}$$

since $\overline{\mathbf{y}} = \mathbf{0}$, $\overline{\mathbf{n}\mathbf{n}^T} = \mathbf{R}_n = \sigma^2\mathbf{I}_N$ and $\overline{\mathbf{b}\mathbf{b}^T} = \mathbf{I}_K$. According to maximal entropy theorem [13], the maximum of $H(Y)$ is achieved with Gaussian output statistics having correlation matrix of (3.6). Basically, that is possible only with the Gaussian input vector $\mathbf{x}$. In this case the capacity is according to (3.1)–(3.6)

$$\begin{aligned} C &= \frac{1}{2}\log\left((2\pi e)^N \det(\sigma^2\mathbf{I}_N + \mathbf{S}^T\mathbf{A}^2\mathbf{S})\right) - \frac{1}{2}\log\left((2\pi e)^N(\sigma^2)^N\right) \\ &= \frac{1}{2}\log\left(\det\left(\mathbf{I}_N + \frac{\mathbf{S}^T\mathbf{A}^2\mathbf{S}}{\sigma^2}\right)\right) \end{aligned} \tag{3.7}$$

In [52] the relation between CDMA capacity (3.7) and the capacity of Gaussian channel not restrained to CDMA is established. To derive this the determinant of matrix $\mathbf{S}^T\mathbf{A}^2\mathbf{S}$ is expressed with its eigenvalues, λ_i as

$$\det \mathbf{S}^T\mathbf{A}^2\mathbf{S} = \prod_{i=1}^{n}\lambda_i \tag{3.8}$$

Moreover, the eigenvalues of matrix $\mathbf{I} + \mathbf{R}_y$ are $1 + \lambda_i$. Then, (3.7) becomes

$$\begin{aligned} C &= \frac{1}{2}\log\prod_{i=1}^{N}\left(1 + \frac{\lambda_i}{\sigma^2}\right) \\ &= \frac{N}{2}\cdot\frac{1}{N}\sum_{i=1}^{N}\log\left(1 + \frac{\lambda_i}{\sigma^2}\right) \end{aligned} \tag{3.9}$$

Function $\log(x)$ is concave function for which Jensen's inequality [85] applies

$$\frac{1}{n}\sum_{i=1}^{n} f(x_i) \le f\left(\frac{1}{n}\sum_{i=1}^{n} x_i\right). \tag{3.10}$$

Thus,

$$C \le \frac{N}{2}\log\left(1 + \frac{1}{N\sigma^2}\sum_{i=1}^{N}\lambda_i\right). \tag{3.11}$$

Furthermore, the sum of eigenvalues is the trace of a matrix. Thus,

$$\begin{aligned} \sum_{i=1}^{N}\lambda_i &= \text{tr}\ \left(\mathbf{S}^T\mathbf{A}^2\mathbf{S}\right) \\ &= \sum_{i=1}^{N}\sum_{l=1}^{K}\sum_{m=1}^{K} a_{i,l}(A_l^2\delta_{l,m})a_{i,m} \\ &= \sum_{i=1}^{N}\sum_{l=1}^{K} a_{i,l}a_{i,l}A_l^2 = NP_{\text{tot}}, \end{aligned} \tag{3.12}$$

where $a_{i,l}$,$a_{i,m}$ denote i-th chip for users l and m, A_l is the amplitude of l-th user, $\delta_{l,m}$ is Kronecker delta, and $P_{\text{tot}} = \sum_{l=1}^{K} A_l^2$ is the total power of all users when average chip energy is normalized to one. Now, (3.11) becomes

$$C \leq \frac{N}{2} \log \left(1 + \frac{P_{\text{tot}}}{\sigma^2} \right). \tag{3.13}$$

To compare the result obtained with classical Shannon theorem for a single user, the capacity must be divided by N, since (3.13) is calculated for N dimensions instead of a single dimension of classical result. Therefore, the final upper bound on the capacity of S-CDMA becomes

$$C \leq \frac{1}{2} \log \left(1 + \frac{P_{\text{tot}}}{\sigma^2} \right). \tag{3.14}$$

To arrive at the most familiar form of Shannon capacity (3.14) should be divided by the time unit $t = 1/2W$ [13]:

$$C \leq W \log \left(1 + \frac{P_{\text{tot}}}{\sigma^2} \right), \tag{3.15}$$

which shows that the capacity of CDMA is never higher than the limit imposed by total power of all users and available bandwidth resource. The required conditions to achieve equality in (3.14) are discussed in the next section.

3.2 Signature ensemble that maximizes the channel capacity of S-CDMA

It can be now shown [52] that the capacity of CDMA may achieve Shannon's limit in (3.14) in only saturated or oversaturated CDMA. Indeed, equality in (3.11) is attainable if and only if all λ_i are equal. That is if and only if

$$\mathbf{S}^T \mathbf{A}^2 \mathbf{S} = (\mathbf{AS})^T \mathbf{AS} = P_{\text{tot}} \mathbf{I}_N, \tag{3.16}$$

where $\mathbf{S}^T\mathbf{A}$ is a $N \times K$ matrix. To fulfill (3.16) $\mathbf{S}^T\mathbf{A}$ should be a matrix with orthogonal rows. Its rows have dimension K so to make the matrix orthogonal the number of rows, N, should be equal or smaller than the dimension K:

$$K \geq N. \tag{3.17}$$

Hence, the capacity of S-CDMA can equal the capacity of a Gaussian channel only in a saturated or an oversaturated situation. If all powers for different users are equal (3.16) becomes

$$\mathbf{S}^T \mathbf{S} = K \mathbf{I}_N, \tag{3.18}$$

which means that the columns of the signature matrix are orthogonal. Equivalent condition to (3.18) is that the signature ensemble attains Welch bound [86], i.e. has the TSC equal to its minimum, established by the abovementioned bound:

$$\mathrm{TSC} = \sum_{k,l=1}^{K} |\mathbf{s}_k \mathbf{s}_l^*|^2 \geq \frac{K^2}{N} \tag{3.19}$$

Signatures that reach the equality in (3.19) are called WBE signatures. They are inspected more closely in the section 5.2.

3.3 Channel capacity of oversaturated S-CDMA with binary input symbols

In the derivation of channel capacity of oversaturated S-CDMA (3.14) it was assumed that transmitted symbols are Gaussian to provide Gaussian statistics of channel output. However, the emphasis of this thesis is to investigate binary data transmission. In the binary case the derived results are still valid in the asymptotic case signal-to-noise ratio (SNR) $<< 1$, since in this case the channel output statistics are controlled by the Gaussian noise only. However, as binary signal energy grows the binary input channel capacity only yields to the capacity of channel with no limits on input alphabet. The channel capacity for binary input symbols is investigated in two asymptotic cases, first for weak signals (SNR $<< 1$).

3.3.1 Channel capacity for the asymptotic case of weak signals

The transmitted (fixed) group signal is denoted with $\mathbf{x} = (x_1, x_2, \ldots, x_N)$ where x_i, $i = 1, 2, \ldots, N$ denote components of the group signal vector. The conditional observation pdf is

$$P(\mathbf{y}|\mathbf{x}) = \frac{1}{\sqrt{(2\pi)^N}} \exp\left(-\frac{1}{2}\sum_{i=1}^{N}(y_i - x_i)^2\right), \tag{3.20}$$

where $\sigma^2 = 1$ is assumed for simplified notation without the loss of generality. With very weak signal the Taylor series around $\mathbf{x} = \mathbf{0}$ is

$$f(\mathbf{x}) \approx f(0) + \sum_i \left[\frac{df(\mathbf{x})}{dx_i}\right]_{x_i=0} x_i + \frac{1}{2}\sum_i \sum_j \left[\frac{d^2 f(\mathbf{x})}{dx_i dx_j}\right]_{x_i,x_j=0} x_i x_j + \cdots, \tag{3.21}$$

which for

$$f(\mathbf{x}) = \exp\left(\frac{1}{2}\sum_i 2x_i y_i - \frac{1}{2}\sum_i x_i^2\right) \tag{3.22}$$

results in

$$P(\mathbf{y}|\mathbf{x}) \approx P(\mathbf{y}|\mathbf{x}=\mathbf{0})\left(1 + \frac{1}{2}\sum_{i=1}^{N} 2y_i x_i - \frac{1}{2}\sum_{i=1}^{N}|x_i|^2 + \frac{1}{2}\sum_{i=1}^{N}\sum_{j=1}^{N} y_i y_j x_i x_j\right), \tag{3.23}$$

where terms containing $O(||\mathbf{x}||^2)$ are dropped. To obtain unconditional pdf, $P(\mathbf{y})$, the conditional pdf, $P(\mathbf{y}|\mathbf{x})$, must be averaged over all group signals.

$$P(\mathbf{y}) = \int \ldots \int P(\mathbf{y}|\mathbf{x})P(\mathbf{x})\, d\mathbf{x}, \tag{3.24}$$

where $P(\mathbf{x})$ is the pdf of group signal. The result of averaging is

$$P(\mathbf{y}) \approx P(\mathbf{y}|\mathbf{x}=\mathbf{0})\left(1 - \frac{1}{2}\sum_{i=1}^{N}\overline{|x_i|^2} + \frac{1}{2}\sum_{i=1}^{N}\sum_{j=1}^{N} y_i y_j \overline{x_i x_j}\right), \tag{3.25}$$

where the fact that $\overline{x_i} = 0$ is utilized, since any polarity of any transmitted bit of any user has the probability of 1/2. With designation $\mathbf{R}_x$ for correlation matrix of group signal $\mathbf{x}$ that has components $[\overline{x_i x_j}]$, (3.25) becomes

$$P(\mathbf{y}) \approx P(\mathbf{y}|\mathbf{x}=\mathbf{0})\left(1 - \frac{1}{2}\text{ tr }\mathbf{R}_x + \frac{1}{2}\mathbf{y}^T\mathbf{R}_x\mathbf{y}\right). \tag{3.26}$$

To see how (3.26) is related to the pdf of Gaussian random process, consider the pdf of Gaussian vector $\mathbf{x}_g$ with very weak correlation

$$P(\mathbf{x}_g) = \frac{1}{\sqrt{(2\pi)^N \det\mathbf{K}}}\exp\left(-\frac{1}{2}\mathbf{x}_g^T\mathbf{K}^{-1}\mathbf{x}_g\right), \tag{3.27}$$

where $\mathbf{K} = \mathbf{I} + \delta_0\mathbf{K}_0$ and δ_0 is approaching zero ($\delta_0 << 1$). Then, $\det\mathbf{K} = \prod_{i=1}^{n}(1+\delta_0\lambda_i)$, where n is the dimension of $\mathbf{x}_g$ and λ_i, $i = 1, 2, \ldots, n$ are eigenvalues of matrix $\mathbf{K}_0$. Then,

$$\det\mathbf{K} \approx 1 + \delta_0\sum_{i=1}^{n}\lambda_i = 1 + \delta_0\text{ tr }\mathbf{K}_0, \tag{3.28}$$

whereby

$$(\det\mathbf{K})^{-1/2} \approx 1 - \frac{1}{2}\delta_0\text{ tr }\mathbf{K}_0. \tag{3.29}$$

In addition

$$\mathbf{K}^{-1} = (\mathbf{I}+\delta_0\mathbf{K}_0)^{-1} = \mathbf{I} - \delta_0\mathbf{K}_0 + \delta_0^2\mathbf{K}_0^2 - \delta_0^3\mathbf{K}_0^3 + \ldots \approx \mathbf{I} - \delta_0\mathbf{K}_0 \tag{3.30}$$

due to assumption $\delta_0 << 1$. Then, after substituting (3.29) and (3.30) the Gaussian pdf (3.27) can be expressed as

$$P(\mathbf{x}_g) \approx \frac{1}{\sqrt{(2\pi)^N}} \exp\left(-\frac{1}{2}\mathbf{x}_g^T\mathbf{x}_g\right) \cdot \left(1 - \frac{1}{2}\delta_0 \ \mathrm{tr}\mathbf{K}_0\right) \cdot \exp\left(\frac{1}{2}\mathbf{x}_g^T\delta_0\mathbf{K}_0\mathbf{x}_g\right)$$
$$\approx \frac{1}{\sqrt{(2\pi)^N}} \exp\left(-\frac{1}{2}\mathbf{x}_g^T\mathbf{x}_g\right) \cdot \left(1 - \frac{1}{2}\delta_0 \ \mathrm{tr}\mathbf{K}_0 + \frac{1}{2}\mathbf{x}_g^T\delta_0\mathbf{K}_0\mathbf{x}_g\right), \tag{3.31}$$

where approximation $e^x \approx x$, $x << 0$ is utilized. When (3.31) and (3.26) are compared, it can be seen that (3.26) is just the approximation of Gaussian pdf with zero mean and cross-correlation matrix $\mathbf{I}+\mathbf{R}_x$ when all elements of correlation matrix $\mathbf{R}_x$ are small enough. The latter entails that when group signal is weak, the output is Gaussian regardless of input symbols.

The correlation matrix of the observation is

$$\mathbf{R}_y = \sigma^2\mathbf{I} + \mathbf{R}_x, \tag{3.32}$$

where elements of $\mathbf{R}_x$ are

$$\overline{x_i x_j} = \overline{\sum_{k=1}^{K} b_k a_{i,k} A_k \sum_{l=1}^{K} b_l a_{l,j} A_l} = \sum_{k=1}^{K} a_{i,k} a_{k,j} A_k^2, \tag{3.33}$$

since $\overline{b_k b_l} = \delta_{k,l}$ (Kronecker delta). It is seen that $\mathbf{R}_x = \mathbf{S}^T\mathbf{A}^2\mathbf{S}$, which means all results remain the same as with Gaussian input symbols, which was calculated in (3.6). It can be concluded that to maximize the channel capacity in the case of weak group signals the signature design should be done the same way as with Gaussian input symbols. The resulting optimal ensemble is again constructed with WBE sequences as was the case with Gaussian input symbols.

3.3.2 Channel capacity for the asymptotic case of weak noise

On the other hand, for strong signals (SNR $>> 1$) the situation changes. It is intuitively clear that when the noise is very weak the channel capacity approaches the limit, which is simply entropy at the channel output $H(\mathbf{y})$:

$$C \underset{\mathrm{SNR}\to\infty}{\longrightarrow} -\sum_{\mathbf{y}} P(\mathbf{y}) \log P(\mathbf{y}), \tag{3.34}$$

which reaches its maximum only if all 2^K realizations of group signals are distinct and equiprobable. Then

$$C \underset{\mathrm{SNR}\to\infty}{\longrightarrow} -\sum_{i=1}^{2^K} \frac{1}{2^K} \log_2 \frac{1}{2^K} = K. \tag{3.35}$$

The requirement of distinct group signals is crucial for reaching optimal capacity. Therefore, in the presence of noise, though weak, the minimum distance between group signals should be maximized to ensure that group signals remain distinct even after the effect of noise.

To support (3.35) quantitatively let us represent observation pdf as

$$P(Y) = \sum_{\mathbf{x}\in X} P(\mathbf{x}) P_g(\mathbf{x}, \mathbf{R}_n), \tag{3.36}$$

where P_g is the Gaussian pdf of the form (3.3) having cross-correlation matrix $\mathbf{R}_n = \sigma^2 \mathbf{I}_N$. The observation ensemble entropy is

$$\begin{aligned} H(\mathbf{y}) &= -\int_{\mathbf{y}} \dots \int P(\mathbf{y}) \log_2 P(\mathbf{y})\, d\mathbf{y} \\ &= -\int_{\mathbf{y}} \dots \int \sum_{\mathbf{x_0}} \frac{1}{2^K} P_g(\mathbf{x}_0, \mathbf{R}_n) \log_2 \left[\sum_{\mathbf{x}} \frac{1}{2^K} P_g(\mathbf{x}, \mathbf{R}_n) \right] d\mathbf{y}, \end{aligned} \tag{3.37}$$

where $\mathbf{x}$ and $\mathbf{x}_0$ refer to the same set of possible group signal. The denotation is chosen to enable clear illustration of obtained results. Since

$$\log_2 \left[\sum_{\mathbf{x}} \frac{1}{2^K} P_g(\mathbf{x}, \mathbf{R}_n) \right] = -K + \log_2 \left[\sum_{\mathbf{x}} P_g(\mathbf{x}, \mathbf{R}_n) \right];$$

$$H(Y) = K - \frac{1}{2^K} \int_{\mathbf{y}} \dots \int \sum_{\mathbf{x}_0} P_g(\mathbf{x}_0, \mathbf{R}_n) \log_2 \left[\sum_{\mathbf{x}} P_g(\mathbf{x}, \mathbf{R}_n) \right] d\mathbf{y}. \tag{3.38}$$

Now, inside the $\log_2$ take group signal $\mathbf{x_0}$ outside from the summation:

$$\begin{aligned} H(Y) = K - \frac{1}{2^K} \int_{\mathbf{y}} \dots \int \left(\sum_{\mathbf{x}_0} P_g(\mathbf{x}_0, \mathbf{R}_n) \right) \times \\ \times \log_2 \left[P_g(\mathbf{x_0}, \mathbf{R}_n) \left(1 + \sum_{\mathbf{x}, \mathbf{x} \neq \mathbf{x_0}} \frac{P_g(\mathbf{x}, \mathbf{R}_n)}{P_g(\mathbf{x_0}, \mathbf{R}_n)} \right) \right] d\mathbf{y} \end{aligned} \tag{3.39}$$

Again, the output entropy conditioned in the group signal can be calculated as

$$H(Y|X) = -\tfrac{1}{2^K} \sum_{\mathbf{x}_0} \int_{\mathbf{y}} \dots \int P_g(\mathbf{x_0}, \mathbf{R}_n) \log_2 P_g(\mathbf{x_0}, \mathbf{R}_n) = \frac{1}{2} \log_2 \left((2\pi e)^N \sigma^{2N} \right) \tag{3.40}$$

and the entropy $H(Y)$ becomes

$$H(Y) = K + H(Y|X) -$$
$$-\frac{1}{2^K}\sum_{\mathbf{x}_0}\int_{\mathbf{y}}\dots\int P_g(\mathbf{x}_0,\mathbf{R}_n)\log_2\left[1+\sum_{\mathbf{x},\mathbf{x}\neq\mathbf{x}_0}\frac{P_g(\mathbf{x},\mathbf{R}_n)}{P_g(\mathbf{x_0},\mathbf{R}_n)}\right]\,d\mathbf{y}. \tag{3.41}$$

Finally the capacity, C, becomes

$$C = \max_{P(\mathbf{x}_0)}\left\{K - \tfrac{1}{2^K}\sum_{\mathbf{x}_0}\int_{\mathbf{y}}\dots\int P_g(\mathbf{x}_0,\mathbf{R}_n)\log_2\left[1+\sum_{\mathbf{x},\mathbf{x}\neq\mathbf{x}_0}\frac{P_g(\mathbf{x},\mathbf{R}_n)}{P_g(\mathbf{x_0},\mathbf{R}_n)}\right]\,d\mathbf{y}\right\}. \tag{3.42}$$

The capacity in (3.42) will be maximized when the value of integral is minimized, since it is always positive. The minimization is accomplished with proper selection of group signal point locations, which determines $P(\mathbf{x}_0)$. Geometrically, $P_g(\mathbf{x},\mathbf{R}_n)$ is a bell shaped surface centered at $\mathbf{x}$. In the calculation of capacity $P_g(\mathbf{x},\mathbf{R}_n)$ is divided by the similar surface shape centered at $\mathbf{x}_0$. To minimize the contribution of $P_g(\mathbf{x},\mathbf{R}_n)$ inside the integral for any $\mathbf{x}$ the latter should be as far from $\mathbf{x}_0$ as possible, which can be explained as follows. After substituting an explicit form of $P_g(\mathbf{x},\mathbf{R}_n)$

$$C = \max\left\{K - \frac{1}{2^K}\sum_{\mathbf{x}_0}\frac{1}{\sqrt{(2\pi)^N}}\int_{\mathbf{y}}\dots\int\exp\left(-\frac{1}{2}||\mathbf{y}-\mathbf{x}_0||^2\right)\times\right.$$
$$\left.\log_2\left[1+\sum_{\mathbf{x},\mathbf{x}\neq\mathbf{x}_0}\exp\left(\frac{1}{2}||\mathbf{y}-\mathbf{x}_0||^2-\frac{1}{2}||\mathbf{y}-\mathbf{x}||^2\right)\right]\,d\mathbf{y}\right\}. \tag{3.43}$$

For any fixed $\mathbf{x_0}$ the maximal contribution in the integral is of points $\mathbf{y}$ close to $\mathbf{x_0}$, since $\exp(-\frac{1}{2}||\mathbf{y}-\mathbf{x}_0||^2)$ is a sharp peak centered at $\mathbf{y}=\mathbf{x}_0$ whenever SNR is big. Hence, the maximization of capacity corresponds to minimizing the sum

$$\sum_{\mathbf{x},\mathbf{x}\neq\mathbf{x}_0}\exp\left(\frac{1}{2}||\mathbf{x}_0-\mathbf{x}||^2\right), \tag{3.44}$$

which means that all the group signal points should be moved as far from each other as possible. For large enough SNR values the main contribution from $\mathbf{x_0}$ in the sum of (3.44) are due to the closest $\mathbf{x_0}$ signatures, that is, the minimum distance should be maximized. Hence, in signature design the maximal distinction of group signals should be provided. Also, the convergence of C towards maximum is faster when group signals are more distant. Therefore, we can conclude that to maximize channel capacity when

SNR $>> 1$ we should make group signals as distant as possible in Euclidean space.

To conclude this section the main findings are collected. To maximize the channel capacity of S-CDMA for binary input symbols a signature ensemble should

- obey Welch bound if signal energy is weak (SNR $<< 1$);
- provide maximally distant points in group signal constellation if noise is weak (SNR $>> 1$).

3.4 Minimum distance criterion for oversaturated signature ensembles

It was seen in the previous section that the maximization of the minimum distance is necessary to maximize the capacity for binary input symbols in the presence of weak noise. In addition to the channel capacity, another very important criterion is the probability of error in the receiver.

The probability of error in transmission for receiver using the minimum distance rule depends on Euclidean distances between transmitted signals [12, 13, 15, 16]. The signal space is divided to M decision regions Z_i, $i = 1, \ldots M$ representing all possible transmitted signals $\mathbf{x}_i$. When the observation vector $\mathbf{y}$ falls to region Z_j the receiver declares that signal $\mathbf{x}_j$ was transmitted. If some other signal was transmitted originally, receiver outputs erroneous symbol. The minimum Euclidean distance is the most important factor in determining the error performance of transmission, since asymptotically when SNR $>> 1$, the error probability is dominated by the decision region, which has $d = d_{\min}$ distance to adjacent signal point [12,13].

Therefore, it is instructive to analyze pair-wise error probabilities between the closest constellation points. This probability in an AWGN channel is given as

$$P_e = Q\left(\frac{||\mathbf{x}_1 - \mathbf{x}_2||}{\sqrt{2N_0}}\right), \tag{3.45}$$

where $Q(\cdot)$ is the complementary error function, which gives the probability that Gaussian distributed observation crosses the closest decision region boundary. Q-function is defined as

$$Q(x) = \frac{1}{\sqrt{2\pi}} \int_x^\infty \exp\left(\frac{-u^2}{2}\right) du = \frac{1}{2}\text{erfc}\left(\frac{x}{\sqrt{2}}\right). \tag{3.46}$$

The properties of Q-function are collected extensively for example in [12,50].

The overall probability of error for signal point $\mathbf{x}_i$ would be obtained by integrating the likelihood function of $\mathbf{x}_i$ over the regions Z_j, $j \neq i$, or

alternatively by calculating one minus the integration of likelihood function $f(\mathbf{y}|\mathbf{x}_i)$ over region Z_i. The average error probability P_e is obtained by

$$P_e = 1 - \frac{1}{M} \sum_{i=1}^{M} \int_{Z_i} f(\mathbf{y}|\mathbf{x}_i)\, d\mathbf{y}, \tag{3.47}$$

where $f(\mathbf{y}|\mathbf{x}_i)$ is for an AWGN channel pdf given in (3.3). But, as stated earlier, in asymptotic case it is sufficient to inspect only pair-wise error probabilities.

When considering bit error probability, or bit error rate (BER), it is also necessary to inspect the bit patterns carried with signals. In the optimal case signals in adjacent regions would carry bit patterns with only one bit difference, that is their Hamming distance is $d_H = 1$, when it can be assumed that an erroneous decision on signal produces only one bit error [12, 13].

Basing on the discussion above, it is clear that for the fixed signal energy (E) there is an optimal organization of the signature ensemble where the minimum distance between points in the constellation is maximal. In [32] it is proved that the maximal squared minimum Euclidean distance is $d^2_{\text{min,max}} = 4E$, E being symbol energy. Optimal minimum distance between neighboring realizations of the group signal in a constellation is obtained with orthogonal signature ensemble in the saturated case $K = N$. The optimal ensemble in the minimum distance in the oversaturated case is inspected in chapter 5.

Suboptimal constellations have smaller minimum distance, which results as loss in the SNR. The SNR loss is interpreted so that the larger amount of SNR is required to reach some target error probability. In the oversaturated transmission the exhibited energy loss is obtained from comparison to a orthogonal ensemble. The loss γ is calculated as

$$\gamma = \frac{d^2_{\text{min}}}{d^2_{\text{min,max}}} = \frac{d^2_{\text{min}}}{4E} \tag{3.48}$$

3.5 Chapter summary

In this chapter two distinct criteria for labeling a communication system optimal were discussed. First, the channel capacity of S-CDMA in an AWGN channel was analyzed according to existing literature on information theory. The essential result was that S-CDMA may reach Shannon's channel capacity in the oversaturated (or saturated) case, but only with Gaussian distributed input symbols. The signature ensemble providing the optimal channel capacity must obey the Welch bound on the total squared correlation.

The original contribution of this chapter is the analysis of S-CDMA capacity in the case of binary data transmission. For binary input symbols the channel capacity was analyzed in two asymptotic cases. For weak signals (small SNR) the signature ensemble selection should be performed in a similar way to the optimal case with Gaussian input symbols. That is, a WBE ensemble maximizes the channel capacity. However, for strong signals (big SNR) the signature ensemble should be selected to provide maximal minimal distance in the group signal constellation.

The main focus of this thesis is to increase the capacity (the number of users) of S-CDMA by adding users to system with existing time-frequency resources while guaranteeing maximal separation of group signals to minimize error probability in the receiver. The aim of this thesis is finding signatures that have maximal minimum Euclidean distance in N-dimensional signal space. In this chapter, the channel capacity was investigated in two asymptotic cases. For weak signals it was seen that channel capacity is maximized when TSC criterion is fulfilled. However, for the case of weak noise the channel capacity is maximized simultaneously when the Euclidean distance between group signals is maximized. Thus, the approach taken in this thesis is viable considering also channel capacity, and results obtained in this chapter offer good motivation for the research direction chosen in this thesis.

Chapter 4

Receivers for synchronous CDMA

When $K > N$, the system becomes *oversaturated* and signatures can no longer remain orthogonal making MAI unavoidable [36, 37]. Under these circumstances, the performance of a conventional single-user receiver is not acceptable in the most cases (investigated more closely in section 4.1.1). In the oversaturated situation multiuser receiver should be used instead of single-user receiver [50]. However, special measures must be taken in signature ensemble design to avoid prohibitively high complexity in the receiver. Multiuser receiver is the topic of section 4.2.

With a conventional single-user receiver, transmitted bits are acquired by correlation of received signal by user's spreading code followed by integration and thresholding (see (4.2) and (4.4)). However, a conventional receiver suffers from disadvantages such as the near-far effect and unavoidable error floor in the case of non-orthogonal signals. A multiuser receiver, or multiuser detector (MUD), can be used to overcome these shortcomings. With multiuser receiver, the reception procedure is treated as multihypothesis problem where the signals from unintended users are not treated as interference, but bits from all users are processed simultaneously. MUD is based either on joint detection or interference cancellation. Optimal joint detection obviously delivers the best performance but being exponentially complex in the number of users, its usage is limited if no special care is taken in signature ensemble design. Next, the receiver processing of noisy group signal is investigated formally.

The receiver's intention is to retrieve the data from the noisy group signal, which was defined in chapter 2 to be

$$y(t) = \sum_{k=1}^{K} A_k s_k(t; b_k) + n(t) = \sum_{k=1}^{K} A_k b_k s_k(t) + n(t), \tag{4.1}$$

where the last equality is true for any real valued modulation, including BPSK.

4.1 Single-user receiver

The most simple CDMA receiver is a conventional or single-user receiver, which regards interference from other users as noise and simply correlates the received group signal of (4.1) with a time synchronized replica of signature of intended user to obtain decision variable, d_k:

$$d_k = \int_0^T y(t)s_k(t)\,dt = A_k b_k + \sum_{l \neq k} A_l b_l \int_0^T s_l(t)s_k(t)\,dt + \int_0^T n(t)s_k(t)\,dt. \tag{4.2}$$

In the case of orthogonal signatures the single-user receiver is optimal, since the term including MAI caused by correlation between different signatures vanishes and the decision variable becomes

$$d_k = \int_0^T y(t)s_k(t)\,dt = A_k b_k + \int_0^T n(t)s_k(t)\,dt. \tag{4.3}$$

Decision about transmitted bit is made by simply comparing the decision variable d_k to threshold, which is zero in the case of antipodal bits.

$$\hat{b}_k = \text{sign}(d_k). \tag{4.4}$$

However, in the oversaturated case orthogonal signaling is impossible and the performance of conventional receiver may prove to be poor, depending on the selection of N and K, as will be seen next.

4.1.1 Oversaturation with a single-user receiver

To illustrate how poor the performance of CDMA with intense oversaturation can be, consider a simple example of two-dimensional space covering three signatures (oversaturation efficiency $e_{ov} = 1.5$). The signatures are shown in Fig. 4.1. The average bit error probability, P_e, for a fixed user k is

$$P_{e,k} = \frac{1}{4} \sum_{b_i, b_j = \pm 1} Q\left(q(1 + b_i\rho_{i,k} + b_j\rho_{j,k})\right), \tag{4.5}$$

where $i, j, k \in \{1, 2, 3\}$ are all different and ρ is correlation coefficient defined in section 2.3.2. Summation above is asymptotically dominated by terms, which have $b_k\rho_{i,j} = -|\rho_{i,j}|$. Thus, the error probability can be bounded as

$$P_{e,k} > \frac{1}{4} Q\left(q(1 - |\rho_{i,k}| - |\rho_{j,k}|)\right). \tag{4.6}$$

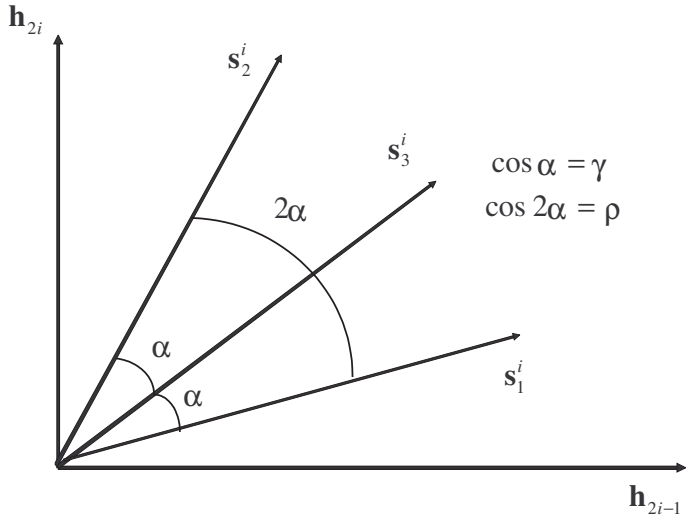

Figure 4.1: Three signatures in two-dimensional signal space.

Three users have different error probabilities. The least favorable user has

$$P_{e,\max} > \frac{1}{4} Q\left(q(1-\Sigma_{\max})\right), \tag{4.7}$$

where $\Sigma_{\max} = \max\{|\rho_{1,2}| + |\rho_{1,3}|, |\rho_{1,3}| + |\rho_{2,3}|, |\rho_{1,2}| + |\rho_{2,3}|\}$. From the geometrical representation of Fig. 4.1, the correlation coefficients are $\rho_{1,2} = \cos(\alpha+\beta)$, $\rho_{1,3} = \cos\beta$ and $\rho_{2,3} = \cos\alpha$. Thus, $\Sigma_{\max} = \max\{|\cos\alpha| + |\cos\beta|, |\cos\alpha| + |\cos(\alpha+\beta)|, |\cos\beta| + |\cos(\alpha+\beta)|\}$. Angles are restricted to be $0 \le \alpha, \beta \le \pi/2$, since the signatures have also antipodal images, which must be taken into consideration. It is proved in appendix B that

$$\Sigma_{\max} \ge 1, \tag{4.8}$$

so that the worst error probability $P_{e,\max}$ (i.e. of the least favorable user) is

$$P_{e,\max} > \frac{1}{8}, \tag{4.9}$$

since $Q(x) > 1/2$ when $x < 0$. The result means that the multiple access interference is such a dominating factor that the bit error probability is always greater than 1/8 regardless of SNR. It will be seen in chapter 6 that for a multiuser receiver, three users in two-dimensional signal space result in BER which approaches zero as SNR grows. It is evident that a multiuser receiver must be employed for oversaturated transmission. Oversaturated signature ensemble facilitating the usage of a conventional receiver is analyzed in section 5.2. The attention of receivers for oversaturated transmission is shifted to multiuser receivers in the next section.

4.2 Optimal multiuser receiver

The optimal strategy for the receiver is to find the minimum among (squared) Euclidean distances from the received observation $y(t)$ to all possible group signals $x(t; \mathbf{b})$. The squared Euclidean distance, denoted with d^2, is calculated as

$$d^2\left(y(t), x(t;\mathbf{b})\right) = \int_0^T \left[y(t) - x(t;\mathbf{b})\right]^2 \, dt. \tag{4.10}$$

After inserting (2.9) and opening brackets (4.10) becomes

$$d^2\left(y(t), x(t;\mathbf{b})\right) = \int_0^T y^2(t)\, dt - 2\sum_{k=1}^{K} A_k z_k + \sum_{k=1}^{K}\sum_{l=1}^{K} A_k A_l \int_0^T s(t;b_k)s(t;b_l)\, dt, \tag{4.11}$$

where z_k is the correlation between received signal and k-th user's signal

$$z_k = \int_0^T y(t) s_k(t;b_k)\, dt \tag{4.12}$$

The correlations z_k are obtained with a bank of matched filters. Amplitudes A_k can be assumed to be known precisely, thus the optimal receiving method would be the substitution of all possible combinations of $\mathbf{b} = (b_1, b_2, \ldots, b_K)$ to (4.11) and declaring the combination producing the minimum d^2 as received one. This kind of receiving strategy is called *optimal multiuser detection*.

It is convenient to express signals in vector form physically corresponding to processing samples at the chip matched filter output (bold symbols denote vector or matrix variables), where (4.1) becomes

$$\mathbf{y} = \mathbf{x} + \mathbf{n} = \mathbf{S}^T\mathbf{A}\mathbf{b} + \mathbf{n}. \tag{4.13}$$

The correlation between received signal and user signatures is

$$\mathbf{z} = \mathbf{S}\mathbf{y} = \mathbf{S}\mathbf{S}^T\mathbf{A}\mathbf{b} + \mathbf{S}\mathbf{n} = \mathbf{R}\mathbf{A}\mathbf{b} + \mathbf{n}', \tag{4.14}$$

where $\mathbf{R}$ is the correlation coefficient matrix of signatures and $\mathbf{n}'$ is the correlated noise vector. Then (4.11) becomes

$$d^2(\mathbf{y}, \mathbf{x}) = ||\mathbf{y} - \mathbf{S}^T\mathbf{A}\mathbf{b}||^2 = ||\mathbf{y}||^2 - 2\mathbf{z}^T\mathbf{A}\mathbf{b} + \mathbf{b}^T\mathbf{A}\mathbf{R}\mathbf{A}\mathbf{b}. \tag{4.15}$$

The receiver makes a decision on transmitted bit vector on the following criteria

$$\hat{\mathbf{b}} = \arg\min_{\mathbf{b}} \left(\mathbf{b}^T\mathbf{A}\mathbf{R}\mathbf{A}\mathbf{b} - 2\mathbf{z}^T\mathbf{A}\mathbf{b}\right),\ \mathbf{b}\,\epsilon(1,-1)^K, \tag{4.16}$$

since $||\mathbf{y}||^2$ does not affect the decision.

In practice, (4.16) can be implemented with exhaustive search for all possible bit patterns. Bit vectors are compared to the received signal and the vector providing the smallest Euclidean distance is selected. Optimal MUD can be implemented, for example, with a Viterbi algorithm [50].

The optimal multiuser detection may be impractical due to the exponential complexity of the algorithm. The number of comparisons in (4.16) is 2^K and the number of users can be several tens or hundreds in practical systems. Therefore, a lot of effort is put to find simple algorithms to implement optimal multiuser receiver and to find suboptimal multiuser receivers, which offer trade-off between complexity and performance. Next, two optimal algorithms for special oversaturated signature ensembles are presented.

4.2.1 Learned's algorithm

Learned et al [33] proposed a polynomial complexity multiuser receiver algorithm for detection of oversaturated signals. This is possible when signatures have a tree-like cross-correlation structure. For example, Ross-Taylor (see chapter 5) signatures form such an ensemble, despite that a completely different property was their design criterion. Another possibility is to utilize wavelet packet based signatures [34, 39, 40].

Required relationships for signatures are that all vectors at a given depth of the tree are orthogonal to each other and the signature has correlation only with its ancestor or descendant signatures in the tree. The algorithm utilizes the orthogonality of different branches of the tree to reduce the number of comparisons required. For example, a 16-dimension Ross-Taylor signature ensemble can be created with the tree illustrated in Fig. 4.2. The cross-correlation matrix for this signal set can be obtained with (5.10). Because of the tree-structure, signature at given a node of the tree has some correlation with all signatures of its ancestor and descendant nodes. Therefore, the estimate $\hat{b}$ at a given node will not affect other estimates at the same depth in different branches of the tree. Detection algorithm sweeps through the tree from bottom to top and creates a conditional estimate table at each node. At the top, these conditional estimate tables can be used to produce optimal estimate. Finally, the optimal estimate from top node is propagated back to bottom to determine the rest of optimal estimations.

Mathematically, the conditional decision rule can be expressed from the optimal estimate (4.16), which is transformed to the tree-structure form, where for each node n of the tree, the estimate is calculated conditioned on the values of bits in ancestor nodes, $\mathbf{b}_{an}$.

$$\hat{b}_n(\mathbf{y}|\mathbf{b}_{an}) = \arg\min||\mathbf{y} - \mathbf{s}_n b_n - \mathbf{S}_{an}\mathbf{b}_{an} - \mathbf{S}_{dn}\hat{\mathbf{b}}_{dn}(\mathbf{y}|b_n, \mathbf{b}_{an})||^2, \quad (4.17)$$

where $\mathbf{S}_{an}, \mathbf{S}_{dn}$ are used to denote all signatures in ancestor and descendant

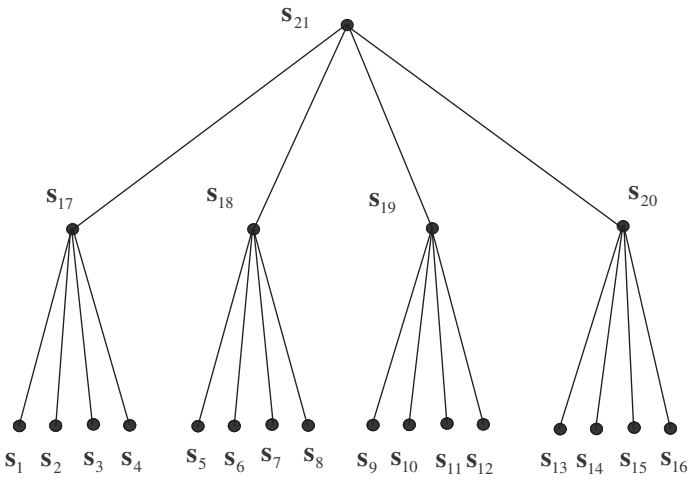

Figure 4.2: Tree-structured signature ensemble.

nodes and $\hat{\mathbf{b}}_{dn}(\mathbf{y}|b_n, \mathbf{b}_{an})$ is the set of estimates for all descendants of the node n.

As an example, the detector algorithm is used to obtain optimal estimates for the tree in Fig. 4.2. In [33] a more detailed example for a three-level tree structure of four initial signals is given. There, at each level, two initial signals are combined to one signal at the upper level.

1. Conditional estimates at node $\mathbf{s}_1$ using (4.17) are calculated and stored for all values of its ancestors $\mathbf{s}_{17}$ and $\mathbf{s}_{21}$. At this point, the sets $\mathbf{S}_{dn}$ and $\hat{\mathbf{b}}_{dn}$ do not exist since the bottom level has no descendants. In binary case $\mathbf{b}_{an} = \{[1,1],[1,-1],[-1,1],[-1,-1]\}$. Similarly, the conditional estimate table for all other nodes $\mathbf{s}_2 \ldots \mathbf{s}_{16}$ at the bottom level is calculated.

2. A conditional estimate table for node $\mathbf{s}_{17}$ is again calculated with (4.17) using node $\mathbf{s}_{21}$ as single ancestor, which can take values ± 1, and conditional $\hat{\mathbf{b}}_{dn}$ estimates of nodes from $\mathbf{s}_1$ to $\mathbf{s}_4$. The conditional estimate table for all other nodes $\mathbf{s}_{18}$–$\mathbf{s}_{20}$ at the middle level is calculated the same way as for $\mathbf{s}_{17}$.

3. Optimal estimation for $\mathbf{s}_{21}$ is calculated with conditional estimate tables $\hat{\mathbf{b}}_{dn}$ of nodes from $\mathbf{s}_{17}$ to $\mathbf{s}_{20}$, since ancestors do not exist in the top level.

4. Optimal estimates for nodes $\mathbf{s}_{17}$–$\mathbf{s}_{20}$ are now obtained, since the optimal estimate $\hat{b}$ for node $\mathbf{s}_{21}$ is available. A simple table look-up from conditional estimates performed in the previous steps can be applied.

5. At the bottom level, conditional estimate tables and obtained values from upper layers are used to find optimal estimations.

The number of comparisons required for Learned's algorithm to reach all estimations is $((8N^{3/2}-1)/7)$. For the Ross-Taylor signatures $K = \frac{4}{3}N - \frac{1}{3}$. Thus, the complexity of receiving algorithm is $O(K^{3/2})$, which is polynomial in the number of users instead of exponential complexity of multiuser receiver in general case.

4.2.2 Trellis decoder

Shi and Schlegel [43] proposed a signature ensemble (see section 5.3) that has band-diagonal cross-correlation matrix. Then, the optimal multiuser receiver can be implemented with a trellis decoder [12] with 2^Z states, where $Z > |i-j|$ for indexes i and j of cross-correlation matrix with $\rho_{i,j} = 0$.

$$\mathbf{R} = \begin{pmatrix} 1 & \rho_{1,2} & \cdots & \rho_{1,j} & 0 & \cdots & 0 \\ \rho_{2,1} & 1 & \rho_{2,3} & \cdots & \rho_{2,j+1} & \cdots & 0 \\ \vdots & & \ddots & & & \ddots & \vdots \\ \rho_{i,1} & & & 1 & & & \rho_{i,N} \\ 0 & \rho_{i+1,2} & & & 1 & & \\ \vdots & & \ddots & & & \ddots & \rho_{N-1,N} \\ 0 & \cdots & 0 & \rho_{N,j} & \cdots & \rho_{N,N-1} & 1 \end{pmatrix} \tag{4.18}$$

For this matrix the optimal detector of equation (4.16) can be calculated recursively after expressing it in a form where equal and normalized user powers are assumed, which makes $\mathbf{A}$ identity matrix

$$\hat{\mathbf{b}} = \arg\min(\mathbf{b}^T(\mathbf{R}-\mathbf{I})\mathbf{b} - 2\mathbf{z}^T\mathbf{b}) \tag{4.19}$$

with partial metric, $J(n)$ defined as

$$J(n) = \sum_{i=1}^{n}\sum_{j\neq i} b_i b_j \rho_{i,j} - 2\sum_{i=1}^{n} b_i z_i, \tag{4.20}$$

and updating this metric is performed for a band-diagonal cross-correlation matrix according to

$$J(n+1) = J(n) + 2\sum_{i=1}^{Z} b_{n+1-i} b_{n+1} \rho_{i,n+1} - 2b_{n+1}z_{n+1}, \tag{4.21}$$

which can be obtained with trellis decoder with 2^Z states. The complexity of receiver is in the order of $O(2^{Z+1}K)$, which is linear in the number of users.

4.2.3 The probability of detection error for an optimal multiuser receiver

Determining the performance when optimal MUD is employed is a difficult task. Since there are 2^K group signal constellation points, the exact bit error probability calculation becomes a very tedious task for large K. Therefore, upper and lower bounds must be established to estimate the performance. As in all communication systems the minimum Euclidean distance is a very important factor in determining transmission fidelity. In the case of multiuser receiver the distance is calculated between all group signals instead of distance between individual signatures. A simple algorithm to calculate minimum distance in multiuser system based on Cholesky factorization of correlation matrix was proposed in [87].

However, because the reception of many users simultaneously is a multihypothesis problem, the BER performance is not solely determined by the minimum Euclidean distance. Correlation structure of signal ensemble and Hamming distances between user bit patterns, i.e. error vectors, also affect it. Exact BER in closed form is practically impossible to obtain due to very complex decision regions. An effort to facilitate decision region calculation is presented in [88]. Thus, asymptotic lower and upper bounds must be obtained in order to investigate the BER performance of communication system using optimal MUD. The BER properties of linear multiuser receivers are analyzed, for example, in [89, 90].

Verdu [50] has derived tight lower and upper bounds for BER when SNR is high. These expressions of BER utilize error vector, $\boldsymbol{\varepsilon} \in \{-2, 0, 2\}^K$, which is defined to be a difference between any pair of distinct transmitted bit vector. The values of error vector are determined by transmitted and received bit vectors as $\varepsilon_k = 0$ if $b_k = \hat{b}_k$ and $\varepsilon_k = 2b_k$ if $b_k \neq \hat{b}_k$. The weight of error vector is defined as $w(\boldsymbol{\varepsilon} = \sum |\varepsilon_k|/2)$.

The derivation of upper bound is based on *decomposable* error vectors. If error vector $\boldsymbol{\varepsilon}$ is decomposable, it fulfills following conditions

1. $\boldsymbol{\varepsilon} = \boldsymbol{\varepsilon}' + \boldsymbol{\varepsilon}''$
2. if $\varepsilon_k = 0$, then $\varepsilon'_k = \varepsilon''_k = 0$
3. $\boldsymbol{\varepsilon}'^T \mathbf{ARA} \boldsymbol{\varepsilon}'' \geq 0$

Geometrically the conditions above ensure that the union bounding of error probability is successful. The item 2 guarantees that decomposable components $\boldsymbol{\varepsilon}'$ and $\boldsymbol{\varepsilon}''$ have the same origin and the item 3 restricts the angle between them so that the $\boldsymbol{\varepsilon}$ is definitively on the erroneous side of the bounded area.

The set of *indecomposable* vectors affecting user k is denoted with F_k. As an example, the case where all users have the same amplitude ($A_k = A$)

and all cross-correlations are equal and positive ($\rho_{kl} = \rho > 0$) is considered. Then, only indecomposable error vectors have the weight of one or two. For user one, the decomposable error vectors are

$$F_1(b_1 = +1) = \left\{ \begin{array}{cccccc} (+2, & 0, & 0, & \cdots & 0, & 0), \\ (+2, & -2, & 0, & \cdots & 0, & 0), \\ (+2, & 0, & -2, & \cdots & 0, & 0), \\ & & & \cdots & & \\ (+2, & 0, & 0, & \cdots & -2, & 0), \\ (+2, & 0, & 0, & \cdots & 0, & -2) \end{array} \right\}$$

plus antipodal images corresponding to $b_1 = -1$. Exhaustive search is required to find indecomposable error vectors in general. More simple ways are presented in [91, 92].

Using the concept of indecomposable error vectors the BER for user k can be upper bounded as

$$P_{e,k} \leq \sum_{\boldsymbol{\varepsilon} \in F_k} 2^{-w(\boldsymbol{\varepsilon})} Q\left(\frac{\boldsymbol{\varepsilon}^T \mathbf{ARA} \boldsymbol{\varepsilon}}{\sqrt{2N_0}} \right). \tag{4.22}$$

Detailed proof of (4.22) can be found from [50]. It should be noted, that for low SNR values error estimation using values for conventional receiver is tighter than (4.22). Also, lower bound for BER was derived in [50] that uses the assumption of genie aided receiver. Trivial lower bound is orthogonal signaling using a single-user receiver, which gives optimal result. Tighter lower bound is

$$P_{e,k} \geq 2^{1-w_{k,\min}} Q\left(\frac{d_{k,\min}}{\sqrt{2N_0}} \right), \tag{4.23}$$

where $d_{k,\min}$ is one half of the minimum distance between two group signals that differ in the k-th bit, and $w_{k,\min}$ is the corresponding error vector weight between these group signals. The minimum weight is chosen if there are more than one signal having $d_{k,\min}$.

4.3 Suboptimal multiuser receivers

Due to the complexity of optimal MUD, several suboptimal MUDs have been investigated [50, 56]. The best known linear suboptimal MUDs are the MMSE receiver and the decorrelating receiver. The latter removes the MAI completely (while increasing noise intensity) but it is not available for receiving oversaturated signature ensembles. MMSE receiver tries to minimize the effects of MAI and noise simultaneously, and is applicable also for oversaturated situation. It will be presented due to its remarkable properties when utilized with a WBE signature ensemble. The other receiver structure presented here is a group orthogonal system, which divides users to non-interfering groups and utilizes the optimal receiver for each group.

4.3.1 MMSE receiver

The description of MMSE receiver can be found, for example, in [32, 45, 50]. MMSE, or alternatively a maximal signal-to-interference-and-noise ratio (SINR) receiver, is obtained by choosing reference (row) vector $\mathbf{u}_k$ for each user to minimize mean square error (MSE)

$$\min_{\mathbf{u}_k} E[(b_k - \mathbf{u}_k \mathbf{y})], \tag{4.24}$$

where $E[\cdot]$ denotes expectation. The decision on transmitted bits is

$$\hat{b}_k = \text{sign}(\mathbf{u}_k \mathbf{y}), \tag{4.25}$$

where it is assumed that signatures are real-valued. Thus, the difference to single-user receiver is that MMSE receiver uses mismatched reference vector to obtain decision statistics instead of a matched reference (signature) vector $\mathbf{s}_k$. Other possible direction is to maximize SINR denoted with q_I^2

$$q_I^2 = \frac{P_s}{P_i + P_n} = \frac{A_k^2 |\mathbf{u}_k \mathbf{s}_k^T|^2}{\sum_{l \neq k} A_l^2 |\mathbf{u}_k \mathbf{s}_l^T|^2 + \sigma^2 ||\mathbf{u}_k||^2}, \tag{4.26}$$

where P_s, P_i, P_n denote signal, interference and noise power, respectively. Both optimizations lead to the same reference vector

$$\mathbf{u}_k = \left(\mathbf{S}^T \mathbf{A}^2 \mathbf{S} + \sigma^2 \mathbf{I}_N\right)^{-1} \mathbf{s}_k^T = \mathbf{e}_k \left(\mathbf{S}\mathbf{S}^T + \sigma^2 \mathbf{A}^{-2}\right)^{-1} \mathbf{S}, \tag{4.27}$$

where $\mathbf{e}_k$ is the vector having $K - 1$ zero components and 1 at the k-th position. The first equality in (4.27) is more suitable for the oversaturated situation, since the dimension of matrix in brackets is smaller (N) than in the second variant (K).

For WBE sequences columns of $\mathbf{S}$ (rows of $\mathbf{S}^T$) are orthogonal, thus with equal signal intensities $\mathbf{S}^T \mathbf{A}^2 \mathbf{S} = A^2 \mathbf{I}_N$ and

$$\mathbf{u}_k = c\mathbf{s}_k, \tag{4.28}$$

which means that the reference is just a scaled version of the matched filter [32, 54]. Thus, for the WBE signatures to be discussed in section 5.2 the MMSE receiver degenerates to conventional single-user matched filter. Thus, its complexity in this case remains the same as for a conventional receiver. The gain in performance depends on user amplitude distribution. For equal amplitudes there is no gain available, since the MMSE receiver is just a conventional receiver. But when amplitudes are different the MMSE receiver performs better than a conventional receiver. In general, the performance analysis of MMSE receiver is not a straightforward task, since the decision statistics are not Gaussian. The general error performance of the MMSE receiver is analyzed for example in [50, 93, 94].

4.3.2 Group orthogonal CDMA

Djonin and Bhargava proposed in [56] a group orthogonal signature allocation strategy to alleviate complexity of optimal multiuser detector. Formally, it means that N-dimensional signal space is divided into N/L orthogonal L-dimensional groups or subspaces. The complexity achieved this way is exponential in the subspace dimension but only linear in the number of users. This method is referred as group orthogonal CDMA (GO-CDMA) in this thesis. The GO-CDMA signature ensemble consists of r orthogonal groups of signatures, and thereby possesses a block-diagonal cross correlation matrix

$$\mathbf{R} = \begin{pmatrix} \mathbf{R}_1 & 0 & \cdots & 0 \\ 0 & \mathbf{R}_2 & \cdots & 0 \\ \cdots & \cdots & \cdots & \cdots \\ 0 & 0 & \cdots & \mathbf{R}_r \end{pmatrix}. \tag{4.29}$$

It was concluded in [56] that signatures in each group should be designed to have favorable properties of $\mathbf{R}_i$ in (4.29), but no specific examples were given. Chapters 5, 6 and 7 will be devoted to finding GO-CDMA signature ensembles. Oversaturation is achieved by assigning each of the subspaces $L + s$ signatures so that oversaturation efficiency becomes $e_{ov} = 1 + s/L$. Obtained subspace signature ensembles are denoted with $(L+s, L)$ meaning that $L + s$ users occupy L-dimensional subspace, or group.

The GO-CDMA receiver is very simple. The multiuser detector in this case is decomposed into N/L subdetectors, each being quite simple due to subspace orthogonality and low subspace dimension L. The receiver processing consists of L correlations and optimal multiuser algorithm for $L + s$ users. Observed group signal (see (4.13)) is

$$\mathbf{y} = \sum_{l=1}^{N/L} \mathbf{S}_l^T \mathbf{A}_l \mathbf{b}_l + \mathbf{n} = \sum_{l=1}^{N/L} \sum_{i=1}^{L+s} A_{li} b_{li} \mathbf{s}_{li} + \mathbf{n}, \tag{4.30}$$

where A_{li}, $b_{li} = \pm 1$ and $\mathbf{s}_{li}$ are amplitude, data bit and signature vector of i-th user entering l-th subspace ($i = 1, \ldots, L + s$; $l = 1, 2, \ldots, N/L$, N and L assumed even for simplicity), $\mathbf{n}$ is an AWGN component, and immaterial details like common time delay are omitted. The $\mathbf{y}$ is correlated with orthonormal vectors, $\mathbf{h}_i$, constituting a basis of l-th subspace ($l = 1, 2, \ldots, N/L$). As a result from correlations, sufficient statistics $d_{l,i}$ are obtained for decisions on bits of $L + s$ users occupying l-th subspace. For the decision on transmitted bits in every subspace the optimal multiuser algorithm is used. Receiver block diagram is illustrated in Fig. 4.3.

For (4.30), optimal multiuser rule of (4.16) for GO-CDMA above becomes

$$\hat{\mathbf{b}}_i = \arg \min_{\mathbf{b}_i \epsilon \{-1,1\}_i^K} ||\mathbf{y} - \mathbf{S}_i^T \mathbf{A}_i \mathbf{b}_i||^2 \tag{4.31}$$

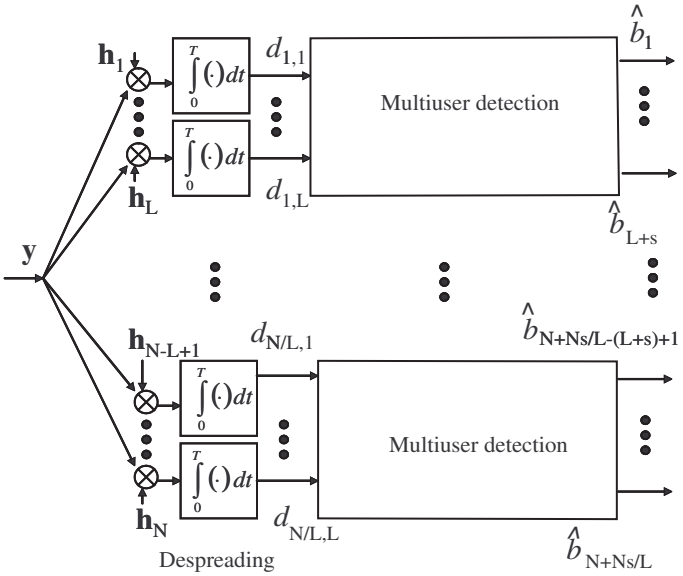

Figure 4.3: GO-CDMA receiver block diagram.

where $i = 1, 2, \ldots, r$, and all the vector-matrix entities have the same meaning as in (4.16), but marked by index i to stress that they are defined for isolated i-th group, as though only its users are present.

Thus, to reiterate, the receiver end consists of N/L parallel independent (due to orthogonality of subspaces) multiuser receivers, each recovering the data transmitted by $L + s$ users. The receiver strategy described requires only L correlations and 2^{L+s} comparisons, which makes the receiver very simple considering that L and s are small.

4.4 Chapter summary

In this chapter, different receiver structures and their suitability to oversaturated S-CDMA were analyzed. It was shown that the most simple solution, a single-user matched filter receiver, performs poorly in the presence of MAI. The best performance would be obtained with an optimal multiuser receiver, but its complexity can become prohibitive. Therefore, lower complexity optimal algorithms for special signature ensembles were also presented. Another option is to use a simple but suboptimal multiuser receiver. There are a lot of different solutions for them. In this chapter, MMSE receiver and group orthogonal system were presented. In the following chapters the focus shifts to signature ensemble design for optimal and group orthogonal receivers.

Chapter 5

Oversaturated signature ensembles

5.1 Maximal minimum Euclidean distance signature ensemble

Optimal multiuser receiver benefits from the large distance between all possible group signals. It is proved in [32] that the maximal minimum distance for group signals is bounded as

$$d^2_{\min} \leq 4 \tag{5.1}$$

for unit energy signals. This bound is achieved by an orthonormal signature ensemble. It was proved in [36] that it is also possible to obtain the upper limit of (5.1) in an oversaturated case for $N \geq 4$. The optimal signature ensemble is a special case of structure depicted in section 4.2.1.

Work by Ross and Taylor [36, 37] has received much attention during recent years. In [36] an oversaturated system, which does not compromise the minimum Euclidean distance of N-dimensional orthogonal signal space in synchronous AWGN channel, was proposed based on a hierarchical signature set structure of the form of Fig. 4.2. The first layer of supplementary signals is formed by incorporating an additional vector into each of the four-dimensional subspaces of an N-dimensional signal space. The initial N orthogonal signals are supplemented by $N/4$ extra signals, then, the four supplemented subspaces are concatenated, and supplemented by one extra signal to have 21 signals in 16 dimensions. This procedure can be continued to have 85 users in 64 dimensions and so on. In the tree-structure depicted in Fig. 4.2 the Ross-Taylor scheme has always four branches connected at the upper layer. Oversaturation efficiency obtained in this manner approaches 1.33 when the number of users is large. In [36] it was assumed that N is a natural power of four. However, this condition is not necessary and as

shown below, the generalization of the construction from [36] for arbitrary N is rather straightforward.

Let $\mathbf{h}_0, \mathbf{h}_1, \ldots, \mathbf{h}_{N-1}$ be orthonormal vectors in N-dimensional vector space[1], which serve as basis signatures

$$\mathbf{s}_i = \mathbf{h}_i,\ i = 0, 1, \ldots, N-1. \tag{5.2}$$

Supplementary signatures are special linear combinations of basis vectors. The mechanism of generating supplementary signatures is as follows: supplementary signature number k of the first layer is

$$\mathbf{s}_k^1 = \frac{1}{2}\sum_{t=0}^{3} \mathbf{h}_{4k+t}\,, k = 0, 1, \ldots, \Omega_1 - 1, \tag{5.3}$$

where Ω_1 denotes a quotient after division of N by four. Denote a remainder of division N by four with Ψ_1. Ω_1 and Ψ_1 refer to the number of supplementary signatures produced and the number of basis signatures not utilized in the forming of supplementary signatures at the first layer, respectively:

$$\Omega_1 = \left\lfloor \frac{N}{4} \right\rfloor,\ \Psi_1 = N - 4\Omega_1. \tag{5.4}$$

Ω_1 first layer supplementary signatures are produced at this stage. When forming second layer supplementary signatures there are $\Omega_1 + \Psi_1$ basis signatures available, which gives

$$\Omega_2 = \left\lfloor \frac{\Omega_1 + \Psi_1}{4} \right\rfloor,\ \Psi_2 = \Omega_1 + \Psi_1 - 4\Omega_2. \tag{5.5}$$

The supplementary signature number k of the second layer is

$$\mathbf{s}_k^2 = \frac{1}{4}\sum_{t=0}^{15} \mathbf{h}_{16k+t}\,, k = 0, 1, \ldots, \Omega_2 - 1. \tag{5.6}$$

The procedure can be generalized and continued until $\Omega_s + \Psi_s < 4$:

$$\Omega_s = \left\lfloor \frac{\Omega_{s-1} + \Psi_{s-1}}{4} \right\rfloor,\ \Psi_s = \Omega_{s-1} + \Psi_{s-1} - \Omega_s \tag{5.7}$$

with initialization

$$\Omega_0 = N,\ \Psi_0 = 0. \tag{5.8}$$

For the scheme presented in [36] $\Psi_s = 0$. The supplementary signature number k of the s-th layer is

$$\mathbf{s}_k^s = \frac{1}{2^s}\sum_{t=0}^{4^s-1} \mathbf{h}_{4^s k+t}\,, k = 0, 1, \ldots, \Omega_s - 1. \tag{5.9}$$

[1]It is convenient to start signature indexing from zero in section 5.1.

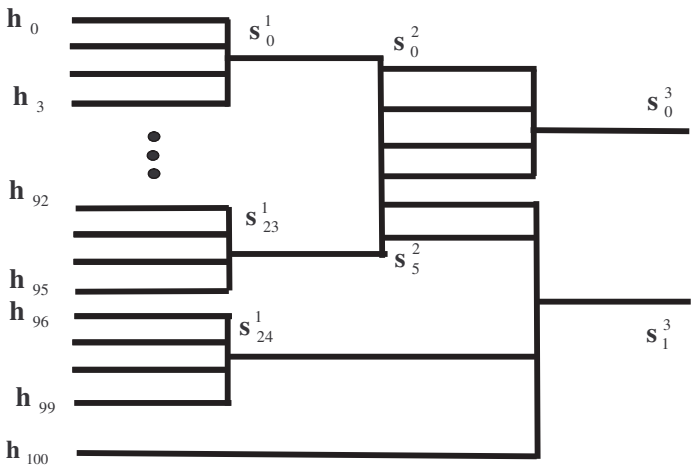

Figure 5.1: Optimal signature ensemble for $N = 101$.

In [32] it was proved that signatures obtained the illustrated way have Euclidean distance $d^2 \geq 4$ between different group signals. Thus, the upper bound in (5.1) is achieved. The correlation coefficient between arbitrary supplementary and basis signature is

$$(\mathbf{s}_k^s, \mathbf{s}_i) = \frac{1}{2^s} \sum_{t=0}^{4^s-1} (\mathbf{h}_{4^s k+t}, \mathbf{h}_i) =$$

$$= \begin{cases} \frac{1}{2^s}, & i \in \{4^s k, 4^s k + 1, , \ldots, 4^s k + 4^s - 1\} \\ 0, & \text{otherwise} \end{cases} \tag{5.10}$$

Take for example $N = 101$. Then $\Omega_1 = 25$, $\Omega_2 = 6$, $\Omega_3 = 2$, $\Psi_3 = 0$, thus the number of supplementary signatures is 33. The procedure is illustrated in Fig. 5.1.

The oversaturation efficiency of the optimal signature ensemble is not a monotonic function of N, which is illustrated in Fig. 5.2. The oversaturation efficiency approaches 4/3 asymptotically, which was also the case for Ross-Taylor signature ensemble in [36]. The oversaturation efficiency can be approximated as follows. The number of supplementary signatures at s-th layer is

$$\Omega_s \geq \left\lfloor \frac{N}{4^s} \right\rfloor \geq \frac{N}{4^s} - 1. \tag{5.11}$$

Then, the total number of supplementary signatures is

$$\sum_{s=1}^{l} \Omega_s \geq \sum_{s=1}^{l} \frac{N}{4^s} - l = \frac{1 - 4^{-l}}{3} N - l, \tag{5.12}$$

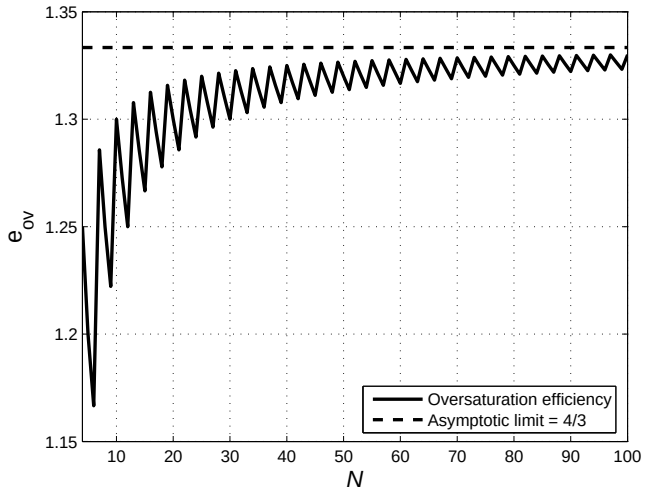

Figure 5.2: The oversaturation efficiency of the optimal signature ensemble.

where $l = \lceil \log_4 N \rceil$. When $N \to \infty$, also $l \to \infty$ but much slower. Therefore, for N big enough $\sum_{s=1}^{l} \Omega_s$ may be estimated as $N/3$ and the total number of signatures approaches $K = N + N/3$, which results in oversaturation efficiency $e_{ov} = 4/3$.

Since supplementary signatures are formed by addition of already obtained ones, alphabet size of supplementary signatures grows from layer to layer and with binary basis signatures supplementary signatures are non-binary. Certainly, it would be much more convenient from the implementation point-of-view to have binary supplementary signatures along with the basis ones. It is demonstrated in the next section that this problem is feasible.

5.1.1 Binary optimal signatures

Next, the conditions guaranteeing that binary supplementary signatures result from binary basis signatures are derived and a practical method of constructing binary oversaturated signature set is proposed [67].

To come to binary both supplementary and basis signatures, we start with the same specification of basis signatures as in the previous section. Take $N = 4^l$ and define $\mathbf{H}_4$ as Hadamard matrix of the order four meeting only one restriction. Every column of Hadamard matrix should contain either 1 or 3 positive (or negative) ones. Denote this Hadamard matrix of

size four fulfilling the restriction set above with $\mathbf{H}_4$:

$$\mathbf{H}_4 = \begin{pmatrix} + & + & + & + \\ - & - & + & + \\ + & - & + & - \\ + & - & - & + \end{pmatrix}. \tag{5.13}$$

Now, the basis signatures are chosen to be rows of the l-th Kronecker power of $\mathbf{H}_4$:

$$\mathbf{E} = \begin{pmatrix} \mathbf{e}_0 \\ \mathbf{e}_1 \\ \vdots \\ \mathbf{e}_{N-1} \end{pmatrix} = [e_{ij}] = \frac{1}{\sqrt{N}}(\underbrace{\mathbf{H}_4 \otimes \mathbf{H}_4 \otimes \cdots \otimes \mathbf{H}_4}_{l}). \tag{5.14}$$

Thus, $\mathbf{E}$ is a Hadamard matrix itself of size $N = 4^l$, and the rows of $\mathbf{E}$ are orthogonal and appropriate to be basis signatures. Now, the supplementary signatures can be calculated with (5.9).

Proposition 1

The elements of supplementary signatures obtained according to (5.9) from the basis binary signatures (5.13) belong to binary $\{\pm 1\}$ alphabet.

Proof of Proposition 1

Transform row (i) and column (j) indexes of $\mathbf{E}$ calculated with (5.14) to quaternary number system

$$\begin{aligned} i &= \sum_{m=0}^{l-1} i_m 4^m \\ j &= \sum_{m=0}^{l-1} j_m 4^m \end{aligned}$$

where i_m and j_m are m-th digits in a quaternary representation of i and j. Then, it can be seen from (5.14) that arbitrary binary element of any basis signature can be represented as

$$e_{ij} = \frac{1}{\sqrt{N}} \prod_{m=0}^{l-1} h_{i_m j_m}, \tag{5.15}$$

where $h_{i_m j_m}$ are elements of $\mathbf{H}_4$. Arbitrary element of k-th supplementary signature in s-th layer

$$s^s_{k,j} = \frac{1}{2^s} \sum_{t=0}^{4^s-1} e_{4^s k+t,j} \tag{5.16}$$

can be then calculated by substituting (5.15) into (5.9)

$$s_{k,j}^{s} = \frac{1}{2^s} \sum_{t=0}^{4^s-1} \frac{1}{\sqrt{N}} \prod_{m=0}^{l-1} h_{i_m j_m}. \tag{5.17}$$

After changing also t to quaternary number system the signature number becomes $4^s k + t = 4^s k + t_{s-1} 4^{s-1} + \ldots + t_0$ in equation (5.17). Now it can be seen that t affects only s minor digits in those numbers, hence

$$\begin{aligned} s_{k,j}^{s} &= \frac{1}{2^s} \frac{1}{\sqrt{N}} \prod_{m=s}^{l-1} h_{i_m j_m} \sum_{t=0}^{4^s-1} \prod_{m=0}^{s-1} h_{i_m j_m} \\ &= \frac{1}{2^s} \frac{1}{\sqrt{N}} \underbrace{\prod_{m=s}^{l-1} h_{i_m j_m}}_{=\pm 1} \sum_{i_0=0}^{3} \sum_{i_1=0}^{3} \cdots \sum_{i_{s-1}=0}^{3} \prod_{m=0}^{s-1} h_{i_m j_m} \\ &= \frac{\pm 1}{\sqrt{N}} \frac{1}{2^s} \sum_{i_0=0}^{3} h_{i_0 j_0} \sum_{i_1=0}^{3} h_{i_1 j_1} \cdots \sum_{i_{s-1}=0}^{3} h_{i_{s-1} j_{s-1}}. \end{aligned}$$

Each sum is ± 2 according to restriction on $\mathbf{H}_4$. Therefore,

$$s_{k,j}^{s} = \frac{\pm 2^s}{\sqrt{N} 2^s} = \pm \frac{1}{\sqrt{N}} \tag{5.18}$$

and all elements of supplementary signatures are also binary.

Example

The binary optimal signatures are illustrated with example for $N = 4^2 = 16$. Starting with Hadamard matrix of (5.13) basis signatures are calculated with (5.14)

$$\mathbf{E} = \begin{pmatrix} \mathbf{e}_0 \\ \mathbf{e}_1 \\ \vdots \\ \mathbf{e}_{15} \end{pmatrix} = \frac{1}{\sqrt{16}} (\mathbf{H}_4 \otimes \mathbf{H}_4) = \begin{pmatrix} \mathbf{s}_0 \\ \mathbf{s}_1 \\ \vdots \\ \mathbf{s}_{15} \end{pmatrix} =$$

$$= \frac{1}{4}\begin{pmatrix}
+ & + & + & + & + & + & + & + & + & + & + & + & + & + & + & + \\
- & - & + & + & - & - & + & + & - & - & + & + & - & - & + & + \\
+ & - & + & - & + & - & + & - & + & - & + & - & + & - & + & - \\
+ & - & - & + & + & - & - & + & + & - & - & + & + & - & - & + \\
- & - & - & - & - & - & - & - & + & + & + & + & + & + & + & + \\
+ & + & - & - & + & + & - & - & - & - & + & + & - & - & + & + \\
- & + & - & + & - & + & - & + & + & - & + & - & + & - & + & - \\
- & + & + & - & - & + & + & - & + & - & - & + & + & - & - & + \\
+ & + & + & + & - & - & - & - & + & + & + & + & - & - & - & - \\
- & - & + & + & + & + & - & - & - & - & + & + & + & + & - & - \\
+ & - & + & - & - & + & - & + & + & - & + & - & - & + & - & + \\
+ & - & - & + & - & + & + & - & + & - & - & + & - & + & + & - \\
+ & + & + & + & - & - & - & - & - & - & - & - & + & + & + & + \\
- & - & + & + & + & + & - & - & + & + & - & - & - & - & + & + \\
+ & - & + & - & - & + & - & + & - & + & - & + & + & - & + & - \\
+ & - & - & + & - & + & + & - & - & + & + & - & + & - & - & + \\
\end{pmatrix} \tag{5.19}$$

Supplementary signatures for layer one are

$$\mathbf{s}_k^1 = \frac{1}{2}\sum_{t=0}^{3}\mathbf{e}_{4k+t},\ k = 0, 1, 2, 3$$

and the supplementary signature for layer 2 is

$$\mathbf{s}_0^2 = \frac{1}{4}\sum_{t=0}^{15}\mathbf{e}_t$$

which result in supplementary signatures

$$\begin{pmatrix} \mathbf{s}_0^1 \\ \mathbf{s}_1^1 \\ \mathbf{s}_2^1 \\ \mathbf{s}_3^1 \\ \mathbf{s}_0^2 \end{pmatrix} = \frac{1}{4}\begin{pmatrix}
+ & - & + & + & + & - & + & + & + & - & + & + & + & - & + & + \\
- & + & - & - & - & + & - & - & + & - & + & + & + & - & + & + \\
+ & - & + & + & - & + & - & - & + & - & + & + & - & + & - & - \\
+ & - & + & + & - & + & - & - & - & + & - & - & + & - & + & + \\
+ & - & + & + & - & + & - & - & + & - & + & + & + & - & + & + \\
\end{pmatrix}$$

The minimum distance between group signals created with signature ensemble $\mathbf{S} = (\mathbf{s}_0, \ldots, \mathbf{s}_{15}, \mathbf{s}_0^1, \ldots, \mathbf{s}_3^1, \mathbf{s}_0^2)$ is $d_{\min}^2 = 4$. Thus, it is seen that using (5.9) and (5.13) the oversaturated signature ensemble having optimal minimum distance can be obtained.

5.2 Welch bound equality signature ensemble

WBE signatures have already been mentioned several times in this thesis. In section 3.2 it was concluded that in order to maximize channel capacity

S-CDMA, the system should utilize a signature ensemble that has optimal total squared correlation. As a consequence, the MAI power is also minimized. The ensemble achieving optimal TSC is called a Welch bound equality signature ensemble. In addition, it was observed in section 4.3.1 that MMSE receiver degenerates to a conventional matched filter receiver if the optimal TSC condition

$$TSC = \sum_{k=1}^{K} \sum_{l=1}^{K} |\mathbf{s}_k \mathbf{s}_l^*|^2 = \frac{K^2}{N} \tag{5.20}$$

is valid.

General methods to produce WBE ensembles are given, for example, in [95–97]. Binary saturated or non-saturated WBE ensembles may exist for only for N divisible by four. In this case $K \leq N$ signatures are just K rows of a $N \times N$ Hadamard matrix (if the latter exists). Binary oversaturated ensembles may exist only for K divisible by four. In this case they are just K rows of $K \times K$ Hadamard matrix where $K - N$ columns are deleted [98,99].

It should be stressed that for binary signatures Welch bound is tight only for N divisible by four [100]. More tight bounds for TSC, and algorithms for producing ensembles obtaining them, for other values of N are derived in [98,99,101]. As an example of the WBE ensemble a case is shown, where four rightmost columns of $\mathbf{S}$ in (5.19) are deleted and signature energies normalized to unity [32]. Hence, the WBE signature ensemble for $K = 16$, $N = 12$ ($e_{ov} = 1.33$) is obtained

$$\mathbf{S} = \frac{1}{\sqrt{12}} \begin{pmatrix} + & - & + & + & - & + & - & - & + & - & + & + \\ + & - & - & - & - & + & + & + & + & - & - & - \\ + & + & + & - & - & - & - & + & + & + & + & - \\ + & + & - & + & - & - & + & - & + & + & - & + \\ + & - & + & + & - & + & - & - & - & + & - & - \\ + & - & - & - & - & + & + & + & - & + & + & + \\ + & + & + & - & - & - & - & + & - & - & - & + \\ + & + & - & + & - & - & + & - & - & - & + & - \\ + & - & + & + & + & - & + & + & + & - & + & + \\ + & - & - & - & + & - & - & - & + & - & - & - \\ + & + & + & - & + & + & + & - & + & + & + & - \\ + & + & - & + & + & + & - & + & + & + & - & + \\ + & - & + & + & + & - & + & + & - & + & - & - \\ + & - & - & - & + & - & - & - & - & + & + & + \\ + & + & + & - & + & + & + & - & - & - & - & + \\ + & + & - & + & + & + & - & + & - & - & + & - \end{pmatrix}, \tag{5.21}$$

which has $TSC = 16^2/12 \approx 21.3333$ as expected. The error probability for WBE ensembles experiences error floor due to MAI. This loss is significant

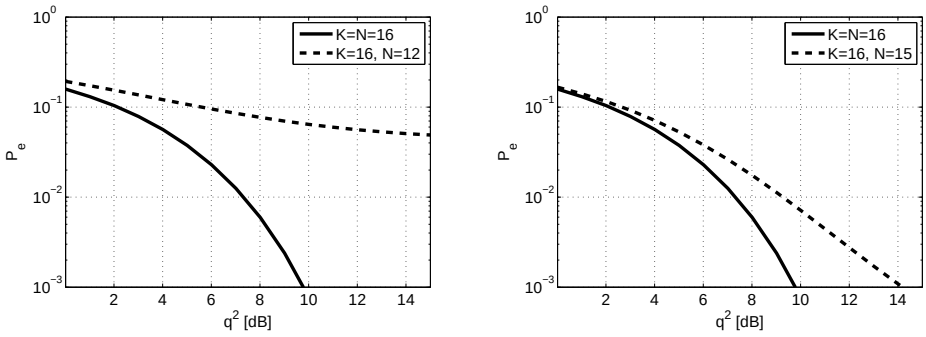

(a) (b)

Figure 5.3: The probability of error for the WBE ensemble using matched filter receiver.

and implies that either joint non-linear processing is necessary [55] or that small oversaturation efficiency should be selected. The SINR, q_I^2, of equal energy users with a WBE signature ensemble is [32, 102]

$$q_I^2 = \left(\frac{K-N}{N} + q^{-2} \right)^{-1}, \tag{5.22}$$

where q^2 is signal-to-noise ratio. The noise-free signal-to-interference ratio (SIR) of a WBE signature ensemble is then

$$q_I^2 = \frac{N}{K-N} = \frac{1}{e_{ov}-1}. \tag{5.23}$$

The effect of MAI to error performance is illustrated in Fig. 5.3(a) for signature ensemble from (5.21) and Fig. 5.3(b), where smaller oversaturation efficiency $e_{ov} = 16/15 \approx 1.07$ is chosen, that is, only one row is deleted from (5.19) to obtain the WBE ensemble. Curves are obtained by plotting $Q(q)$ for saturated situation and $Q(q_I)$ for oversaturated situation (see section 3.4). The error floor is clearly visible in the figures which means that the error probability of a WBE ensemble cannot be driven to zero in any conditions when matched filter receiver is used [103]. Although WBE signatures are optimal when considering channel capacity, MAI and optimal linear receiver complexity, there are some practical problems in the utilization of WBE signatures [102]. If the number of active users varies dynamically, all user signatures must be modified and re-assigned each time a user enters or leaves the system to preserve optimality. Signatures providing optimality (or quasi-optimality) while being scalable are investigated in [20, 66, 102].

5.3 The signature ensemble of linearly combined interpolated Walsh-Hadamard functions

Shi and Schlegel [43] constructed a signature ensemble using linearly combined Walsh-Hadamard codes to have band-diagonal cross-correlation matrix. Oversaturation efficiency obtained with this method is approximately 2 with 3 dB loss. Optimal detection of signatures is accomplished with trellis structure described in section 4.2.2.

Additional signatures are formed by interpolation and linear combinations of Walsh-Hadamard codes

$$\begin{aligned} \mathbf{w}_{2i-1} &= \mathbf{h}_i \\ \mathbf{w}_{2i} &= \frac{1}{2}\sum_{k=i}^{i+3} \mathbf{h}_k,\ i = 1, \ldots, N-3 \\ \mathbf{w}_{2N-6+1} &= \mathbf{h}_{N-3+i},\ i = 1, 2, 3 \end{aligned} \tag{5.24}$$

The number of additional signatures is $N-3$, and the minimum Euclidean distance in signature set $d^2_{\min} = \sqrt{2N}$ resulting in 3 dB loss against purely orthogonal signatures. Also, larger signal sets are possible with this method. The signature set of size $K = 3N-5$ results in the minimum Euclidean distance $d^2_{\min} = 2\sqrt{0.2679N}$, which implies 5.7 dB loss.

Example

A case with a Hadamard matrix of size $N = 16$ produces the result shown next page in (5.25), which has a cross-correlation matrix where the number of trellis states is six. Thus, the decoding complexity is of the order $O(2^7 K)$. When compared to the optimal case it has eleven signatures more, but the minimum distance is reduced to $d^2_{\min} = 2$ at the same time. Also, oversaturated signatures are not binary.

5.4 Chapter summary

In this chapter, different oversaturated signature ensembles were presented. The Ross-Taylor ensemble provides optimal minimum distance properties. The original proposal given in [36] was generalized for arbitrary N and a binary version was also given. As shown in chapter 3, such ensembles minimize asymptotic pair-wise error probability and maximize the channel capacity of a binary-input CDMA channel under the strong signal condition. Other ensembles presented in this chapter are a WBE ensemble and linearly combined interpolated Walsh-Hadamard sequences. The former maximizes oversaturated CDMA channel capacity up to a potential limit (see section

3.2), minimizes MAI power, and reduces MMSE receiver to conventional matched filter while the latter gives greater oversaturation efficiency than the optimal minimum distance ensemble at the expense of smaller minimum distance.

$$\mathbf{S} = \begin{pmatrix}
1 & 1 & 1 & 1 & 1 & 1 & 1 & 1 & 1 & 1 & 1 & 1 & 1 & 1 & 1 & 1 \\
2 & 0 & 0 & 0 & 2 & 0 & 0 & 0 & 2 & 0 & 0 & 0 & 2 & 0 & 0 & 0 \\
1 & -1 & 1 & -1 & 1 & -1 & 1 & -1 & 1 & -1 & 1 & -1 & 1 & -1 & 1 & -1 \\
2 & 0 & 0 & 0 & 1 & -1 & -1 & -1 & 2 & 0 & 0 & 0 & 1 & -1 & -1 & -1 \\
1 & 1 & -1 & -1 & 1 & 1 & -1 & -1 & 1 & 1 & -1 & -1 & 1 & 1 & -1 & -1 \\
2 & 0 & 0 & 0 & 0 & 0 & -2 & 0 & 2 & 0 & 0 & 0 & 0 & 0 & -2 & 0 \\
1 & -1 & -1 & 1 & 1 & -1 & -1 & 1 & 1 & -1 & -1 & 1 & 1 & -1 & -1 & 1 \\
2 & 0 & 0 & 0 & -1 & -1 & -1 & 1 & 2 & 0 & 0 & 0 & -1 & -1 & -1 & 1 \\
1 & 1 & 1 & 1 & -1 & -1 & -1 & -1 & 1 & 1 & 1 & 1 & -1 & -1 & -1 & -1 \\
2 & 0 & 0 & 0 & -2 & 0 & 0 & 0 & 2 & 0 & 0 & 0 & -2 & 0 & 0 & 0 \\
1 & -1 & 1 & -1 & -1 & 1 & -1 & 1 & 1 & -1 & 1 & -1 & -1 & 1 & -1 & 1 \\
2 & 0 & 0 & 0 & -1 & 1 & 1 & 1 & 1 & -1 & -1 & -1 & -2 & 0 & 0 & 0 \\
1 & 1 & -1 & -1 & -1 & -1 & 1 & 1 & 1 & 1 & -1 & -1 & -1 & -1 & 1 & 1 \\
2 & 0 & 0 & 0 & 0 & 0 & 2 & 0 & 0 & 0 & -2 & 0 & -2 & 0 & 0 & 0 \\
1 & -1 & -1 & 1 & -1 & 1 & 1 & -1 & 1 & -1 & -1 & 1 & -1 & 1 & 1 & -1 \\
2 & 0 & 0 & 0 & 1 & 1 & 1 & -1 & -1 & -1 & -1 & 1 & -2 & 0 & 0 & 0 \\
1 & 1 & 1 & 1 & 1 & 1 & 1 & 1 & -1 & -1 & -1 & -1 & -1 & -1 & -1 & -1 \\
2 & 0 & 0 & 0 & 2 & 0 & 0 & 0 & -2 & 0 & 0 & 0 & -2 & 0 & 0 & 0 \\
1 & -1 & 1 & -1 & 1 & -1 & 1 & -1 & -1 & 1 & -1 & 1 & -1 & 1 & -1 & 1 \\
2 & 0 & 0 & 0 & 1 & -1 & -1 & -1 & -2 & 0 & 0 & 0 & -1 & 1 & 1 & 1 \\
1 & 1 & -1 & -1 & 1 & 1 & -1 & -1 & -1 & -1 & 1 & 1 & -1 & -1 & 1 & 1 \\
2 & 0 & 0 & 0 & 0 & 0 & -2 & 0 & -2 & 0 & 0 & 0 & 0 & 0 & 2 & 0 \\
1 & -1 & -1 & 1 & 1 & -1 & -1 & 1 & -1 & 1 & 1 & -1 & -1 & 1 & 1 & -1 \\
2 & 0 & 0 & 0 & -1 & -1 & -1 & 1 & -2 & 0 & 0 & 0 & 1 & 1 & 1 & -1 \\
1 & 1 & 1 & 1 & -1 & -1 & -1 & -1 & -1 & -1 & -1 & -1 & 1 & 1 & 1 & 1 \\
2 & 0 & 0 & 0 & -2 & 0 & 0 & 0 & -2 & 0 & 0 & 0 & 2 & 0 & 0 & 0 \\
1 & -1 & 1 & -1 & -1 & 1 & -1 & 1 & -1 & 1 & -1 & 1 & 1 & -1 & 1 & -1 \\
1 & 1 & -1 & -1 & -1 & -1 & 1 & 1 & -1 & -1 & 1 & 1 & 1 & 1 & -1 & -1 \\
1 & -1 & -1 & 1 & -1 & 1 & 1 & -1 & -1 & 1 & 1 & -1 & 1 & -1 & -1 & 1
\end{pmatrix}, \tag{5.25}$$

Chapter 6

Signature ensembles for group orthogonal CDMA

In section 4.3.2 a group orthogonal receiver was presented. In this chapter, group orthogonal signature ensembles referred to as GO-CDMA ensembles are derived for different oversaturation efficiencies. The results first published in [68, 69] are extended and presented in more detail. The goal of the signature ensemble design is to provide a trade-off between oversaturation efficiency and the minimum distance. Obtained ensembles differ from the Ross-Taylor strategy in a sense that initial orthogonal signatures are not included in the signature ensemble. Instead, the degree of linear dependence of all signatures in the ensemble is optimized.

After the signature ensemble design, they are compared to the optimal Ross-Taylor ensemble in the minimum Euclidean distance and the oversaturation efficiency. Since the minimum distance does not exhaustively determine the performance of the receiver, the bit error probability is also calculated for obtained GO-CDMA ensembles. Oversaturated signature ensembles are denoted as $(L+s, L)$, where L is the signal subspace dimension and $L+s$ is the number of users or signatures contained in the subspace.

The group orthogonal signature ensembles can be created with methods presented in the previous chapter. However, the attainable oversaturation efficiency is only 25% when the first stage of Ross-Taylor scheme is used. If a simple receiver or a greater oversaturation efficiency is required than with the Ross-Taylor ensemble, some loss in the minimum distance must be accepted. The gain in the oversaturation efficiency can be obtained by using smaller subspace dimensions than $L = 4$, or adding more than one supplementary signature into each subspace.

The complexity of the GO-CDMA receiver is well below all optimal multiuser receiver structures presented in the previous section. The complexity is of the order $O(2^{L+1}N)$, and since the considered values of L are restricted

to very small numbers the overall complexity is also very modest.

The optimization criteria in designing signatures is to maximize the minimum Euclidean distance between all possible group signals to reach optimal performance when a multiuser receiver is employed for each subspace. The Euclidean distance between two transmitted group signals can be calculated with

$$d^2(\boldsymbol{\varepsilon}) = \boldsymbol{\varepsilon}^T \mathbf{R}_i \boldsymbol{\varepsilon} \tag{6.1}$$

where $\boldsymbol{\varepsilon}$ is ternary error vector $\boldsymbol{\varepsilon} = (\varepsilon_1, \ldots, \varepsilon_{L+1})^T$, $\varepsilon_i = 0, \pm 2$ discussed in section 4.2.3. The goal is to maximize $\min d^2(\boldsymbol{\varepsilon})$ over all vectors $\boldsymbol{\varepsilon}$ by adjusting correlation coefficients of $\mathbf{R}_i$.

6.1 Signature optimization with symmetry restriction

During the optimization it is assumed that signatures form a symmetric group signal constellation, $\mathbf{R}_i$ being of the general form

$$\mathbf{R}_i = \begin{pmatrix} 1 & \rho & \cdots & \rho & \gamma \\ \rho & 1 & \rho & \cdots & \gamma \\ \vdots & & \ddots & & \vdots \\ \rho & & & 1 & \gamma \\ \gamma & & \cdots & \gamma & 1 \end{pmatrix}, \tag{6.2}$$

which gives more room to analytical study. In more loose case of asymmetry the attainable gain appears to be immaterial. This matter is discussed in section 6.3.

Let $\mathbf{H}_N$ denote an orthonormal matrix of size N (e.g. a Hadamard matrix after normalizing rows to have unit energy) with rows $\mathbf{h}_i, i = 1, \ldots, N$, which constitute the basis vectors for subspaces.

$$\mathbf{H}_N = \begin{pmatrix} \mathbf{h}_1 \\ \vdots \\ \mathbf{h}_N \end{pmatrix}. \tag{6.3}$$

Next, the optimal signatures of i-th orthogonal group having cross-correlation matrix of the form (6.2) are calculated as the linear combinations of $\mathbf{h}_i$. The signature matrix resulting in that kind of a cross-correlation matrix is obtained for $L + s$ signatures with linear combinations of L initial orthogonal signatures. The first of the oversaturated signatures is fixed by just summing all initial orthogonal signatures and by normalizing the result to unit energy. The cross-correlation coefficients of (6.2) can be adjusted with single weighting factor, which multiplies $L - 1$ initial orthogonal signatures before all L of them are summed together. The result of summation

is normalized to make the energy of all signatures equal to unity. At this point $L+1$ signatures are available in each subspace. More signatures are obtained by multiplying $L-2\,(L \geq 3)$ initial orthogonal signatures with the same weighting factor before summation. The procedure can in principle be continued even further, but as will be seen in section 6.1.4 good ensembles are obtained only for $s = 1$.

The Euclidean distance between group signals is calculated using the concept of error vector. Minimum distance as a function of cross-correlation coefficients is calculated for all combinations of error vectors. As a result, a small set of functions are obtained for candidates to provide the value for the minimum distance as a function of cross-correlation coefficients. Minimum distance appears to be a piece-wise polynomial curve. Using graphical illustration, where candidate functions are plotted (see Fig. 6.2 and Fig. 6.4), the approximate value for maximal minimum distance is identified. The exact value is then calculated by equating two candidate functions that intersect at the approximated optimal cross-correlation value. As a result the cross-correlation coefficient value producing the minimum Euclidean distance is achieved. The analysis starts with a $(3, 2)$ ensemble.

6.1.1 Three users in a two-dimensional subspace

Let $\{\mathbf{h}_{2i-1}, \mathbf{h}_{2i}\}$ be an orthonormal basis of a plane. Three normalized signature vectors of i-th group $\mathbf{s}_1^i, \mathbf{s}_2^i, \mathbf{s}_3^i$ are formed as a linear combination from the basis vectors:

$$\mathbf{s}_1^i = \frac{\mathbf{h}_{2i-1} + c\mathbf{h}_{2i}}{\sqrt{1+c^2}}, \mathbf{s}_2^i = \frac{c\mathbf{h}_{2i-1} + \mathbf{h}_{2i}}{\sqrt{1+c^2}}, \mathbf{s}_3^i = \frac{\mathbf{h}_{2i-1} + \mathbf{h}_{2i}}{\sqrt{2}}, \tag{6.4}$$

with c being a real scalar. In the symmetric set of vectors resulting in (6.2), the angle between adjacent signals is acute since all signals can be rotated 180° by multiplication of the signal with an antipodal information bit to have angles smaller than 90° among the nearest vectors.

The correlation coefficients of (6.2) for signatures in (6.4) are

$$\gamma = \frac{1+c}{\sqrt{2(1+c^2)}}, \rho = \frac{2c}{1+c^2} = 2\gamma^2 - 1. \tag{6.5}$$

The cross-correlation coefficient between adjacent signatures is restricted as $0 \leq \gamma \leq 1$ due to acute angles between them. The Euclidean distance between the two transmitted group signals, corresponding to different patterns of users' bits, is calculated in quadratic form from (6.1), where $\boldsymbol{\varepsilon}$ is

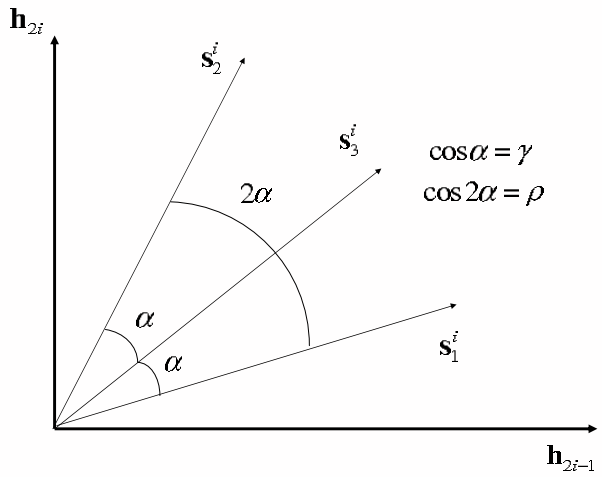

Figure 6.1: Two-dimensional subspace signatures.

$\boldsymbol{\varepsilon} = (\varepsilon_1, \varepsilon_2, \varepsilon_3)^T$, $\varepsilon_i = 0, \pm 2$. The result of the matrix multiplication is

$$d^2(\boldsymbol{\varepsilon}) = \boldsymbol{\varepsilon}^T \mathbf{R} \boldsymbol{\varepsilon} = (\varepsilon_1, \varepsilon_2, \varepsilon_3) \begin{pmatrix} 1 & \rho & \gamma \\ \rho & 1 & \gamma \\ \gamma & \gamma & 1 \end{pmatrix} \begin{pmatrix} \varepsilon_1 \\ \varepsilon_2 \\ \varepsilon_3 \end{pmatrix} =$$
$$= \varepsilon_1^2 + \varepsilon_2^2 + \varepsilon_3^2 + 2\gamma(\varepsilon_1\varepsilon_3 + \varepsilon_2\varepsilon_3) + 2\rho\varepsilon_1\varepsilon_2. \tag{6.6}$$

The goal is to maximize the minimum (over all $\boldsymbol{\varepsilon}$) value of $d^2(\boldsymbol{\varepsilon})$ by adjusting the correlation coefficient γ (ρ depends on γ). Next, candidate functions to provide maximal minimum distances are sought by testing different error vector values.

1. Starting with case, where two of ε_1, ε_2, ε_3 are zero

$$d^2(\boldsymbol{\varepsilon}) = 4. \tag{6.7}$$

2. Then, assuming that ε_1, $\varepsilon_2 \neq 0$ and $\varepsilon_3 = 0$

$$d^2(\boldsymbol{\varepsilon}) \geq 8 - 8|\rho| = 8(1 - |2\gamma^2 - 1|), \tag{6.8}$$

   since the ρ may be also negative.

3. If either ε_1 or ε_2 is zero and $\varepsilon_3 \neq 0$

$$d^2(\boldsymbol{\varepsilon}) \geq 8 - 8\gamma. \tag{6.9}$$

4. When ε_1, ε_2, $\varepsilon_3 \neq 0$ and $\varepsilon_1 = \varepsilon_2 = -\varepsilon_3$

$$d^2(\boldsymbol{\varepsilon}) = 12 - 16\gamma + 8\rho = 4(2\gamma - 1)^2 \leq 4, \tag{6.10}$$

since $\gamma < 1$. Thus, (6.7) can be rejected from the candidate list.

5. The last non-trivial combination is ε_1, ε_2, $\varepsilon_3 \neq 0$ and $\varepsilon_1 = -\varepsilon_2 = \varepsilon_3$ for which

$$d^2(\boldsymbol{\varepsilon}) \geq 12 - 8\rho = 20 - 16\gamma^2 \geq 4, \tag{6.11}$$

which is rejected from the candidate list, since according to (6.10) $d^2_{\min}$ is either 4 or smaller.

After testing all non-trivially distinct error vectors it is seen from (6.8), (6.9) and (6.10) that the minimum Euclidean distance as a function of γ appears to be

$$d^2_{\min}(\gamma) = \min_{\gamma}\{8(1-\gamma), 8(1-|2\gamma^2-1|), 4(2\gamma-1)^2\} \tag{6.12}$$

The middle term in (6.12) can be expressed as

$$8(1-|2\gamma^2-1|) = \begin{cases} 16\gamma^2, & 0 \leq \gamma \leq 1/\sqrt{2} \\ 16(1-\gamma^2), & 1/\sqrt{2} < \gamma \leq 1 \end{cases}. \tag{6.13}$$

The γ is restricted as $0 \leq \gamma \leq 1$ due to acute angles between the adjacent signal vectors. It can be seen from Fig. 6.2 that the maximum of the minimum squared distance is found where curves $8(1-\gamma)$ and $4(2\gamma-1)^2$ intersect. Straightforward calculation shows that the optimal value of γ, maximizing the minimum distance, is

$$\gamma_0 = \frac{1+\sqrt{5}}{4} \approx 0.809 \Rightarrow \rho_0 = \frac{\sqrt{5}-1}{4} \approx 0.310 \tag{6.14}$$

which corresponds to $\pi/5$-angle between the nearest signal vectors ($\mathbf{s}_1^i$ and $\mathbf{s}_3^i$, or $\mathbf{s}_2^i$ and $\mathbf{s}_3^i$). The corresponding value of scalar c is

$$c_0 = \frac{4-\sqrt{10+2\sqrt{5}}}{\sqrt{5}-1} \approx 0.1584 \tag{6.15}$$

and the value of the maximal squared minimum distance is

$$d^2_{\min,\max} = 2(3-\sqrt{5}) \approx 1.528. \tag{6.16}$$

The constellation of all possible group signals and their distances to adjacent signals are illustrated in Fig. 6.3. The signs in parentheses denote antipodal bits for users $1, 2, 3$ in their corresponding order.

Formally, the signatures for i-th group are given with

$$\mathbf{S}_i = \begin{pmatrix} \mathbf{s}_1^i \\ \mathbf{s}_2^i \\ \mathbf{s}_3^i \end{pmatrix} = \frac{1}{\sqrt{1+c_0^2}} \begin{pmatrix} 1 & c_0 \\ c_0 & 1 \\ \sqrt{\frac{(1+c_0^2)}{2}} & \sqrt{\frac{(1+c_0^2)}{2}} \end{pmatrix} \begin{pmatrix} \mathbf{h}_{2i-1} \\ \mathbf{h}_{2i} \end{pmatrix}. \tag{6.17}$$

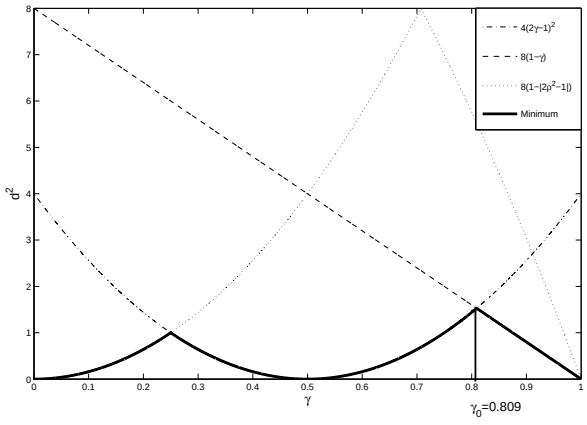

Figure 6.2: Minimum squared distance as a function of correlation coefficient γ.

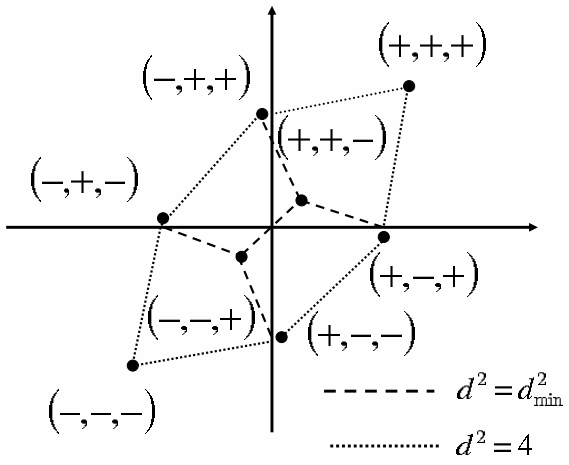

Figure 6.3: Resulting two-dimensional group signal constellation.

6.1.2 Four users in three-dimensional subspace

Next, a $(4, 3)$ constellation is optimized. An oversaturated normalized signature set for three-dimensional subspace fulfilling (6.2) is defined analogously to the two-dimensional case as the following linear combinations

$$\mathbf{s}_1^i = \frac{\mathbf{h}_{3i-2} + c\mathbf{h}_{3i-1} + c\mathbf{h}_{3i}}{\sqrt{1+2c^2}}, \mathbf{s}_2^i = \frac{c\mathbf{h}_{3i-2} + \mathbf{h}_{3i-1} + c\mathbf{h}_{3i}}{\sqrt{1+2c^2}},$$

$$\mathbf{s}_3^i = \frac{c\mathbf{h}_{3i-2} + c\mathbf{h}_{3i-1} + \mathbf{h}_{3i}}{\sqrt{1+2c^2}}, \mathbf{s}_4^i = \frac{\mathbf{h}_{3i-2} + \mathbf{h}_{3i-1} + \mathbf{h}_{3i}}{\sqrt{3}} \tag{6.18}$$

of the orthonormal basis vectors $\mathbf{h}_{3i-2}, \mathbf{h}_{3i-1}, \mathbf{h}_{3i}$. The correlation coefficients in the matrix of (6.2) are

$$\gamma = \frac{1+2c}{\sqrt{3(1+2c^2)}}, \rho = \frac{c(2+c)}{1+2c^2} = \frac{3\gamma^2 - 1}{2}. \tag{6.19}$$

The optimal value for the scalar c, corresponding to the maximal minimum Euclidean distance between different group signals, is calculated the same way as in the two-dimensional case. The squared distance as a function of ternary error vector is

$$\begin{aligned} d^2(\boldsymbol{\varepsilon}) = \boldsymbol{\varepsilon}^T \mathbf{R} \boldsymbol{\varepsilon} = (\varepsilon_1, \varepsilon_2, \varepsilon_3, \varepsilon_4) \begin{pmatrix} 1 & \rho & \rho & \gamma \\ \rho & 1 & \rho & \gamma \\ \rho & \rho & 1 & \gamma \\ \gamma & \gamma & \gamma & 1 \end{pmatrix} \begin{pmatrix} \varepsilon_1 \\ \varepsilon_2 \\ \varepsilon_3 \\ \varepsilon_4 \end{pmatrix} = \\ = \varepsilon_1^2 + \varepsilon_2^2 + \varepsilon_3^2 + \varepsilon_4^2 + 2\gamma(\varepsilon_1\varepsilon_4 + \varepsilon_2\varepsilon_4 + \varepsilon_3\varepsilon_4) \\ +2\rho(\varepsilon_1\varepsilon_2 + \varepsilon_1\varepsilon_3 + \varepsilon_2\varepsilon_3) \end{aligned} \tag{6.20}$$

1. Starting with the assumption that three of the ε_1, ε_2, ε_3, ε_4 are zero. Then,
$$d^2(\boldsymbol{\varepsilon}) = 4. \tag{6.21}$$

2. Next, $\varepsilon_4 = 0$ and

   (a) one of the ε_1, ε_2, ε_3 is zero. Then, again
   $$d^2(\boldsymbol{\varepsilon}) \geq 8 - 8|\rho|, \tag{6.22}$$
   which covers cases where the two non-zero values are equal and when they have opposite sign, since ρ can be positive or negative.

   (b) For $\varepsilon_1 = \varepsilon_2 = \varepsilon_3 \neq 0$
   $$d^2(\boldsymbol{\varepsilon}) = 12 + 24\rho = 36\gamma^2. \tag{6.23}$$

   (c) When $\varepsilon_1, \varepsilon_2, \varepsilon_3 \neq 0$ and one of them has an opposite sign to two others
   $$d^2(\boldsymbol{\varepsilon}) = 12 - 8\rho \geq 4. \tag{6.24}$$
   Since it is no smaller than 4, it can be removed from the candidate list.

3. When $\varepsilon_4 \neq 0$ and

(a) Two of the ε_1, ε_2, ε_3 are zeros

$$d^2(\boldsymbol{\varepsilon}) \geq 8 - 8\gamma. \tag{6.25}$$

(b) If only one of the ε_1, ε_2, ε_3 is zero and those non-zero are opposite to each other

$$d^2(\boldsymbol{\varepsilon}) = 12 - 8\rho \geq 4. \tag{6.26}$$

Being no smaller than four this function is removed from the candidate list.

(c) If only one of the ε_1, ε_2, ε_3 is zero and non-zero values are equal

$$d^2(\boldsymbol{\varepsilon}) \geq 12 - 16\gamma + 8\rho = 8 - 16\gamma + 12\gamma^2. \tag{6.27}$$

4. If all components are non-zero and

(a) $\varepsilon_1 = \varepsilon_2 = \varepsilon_3 = -\varepsilon_4$

$$d^2(\boldsymbol{\varepsilon}) = 16 - 24\gamma + 24\rho = 4 - 24\gamma + 36\gamma^2. \tag{6.28}$$

(b) Taking two of ε_1, ε_2, ε_3 equal to each other but not equal to ε_4:

$$d^2(\boldsymbol{\varepsilon}) \geq 16 - 8\gamma - 8\rho. \tag{6.29}$$

Noting that (6.29) can be re-written as $8 - 8\gamma + 8 - 8\rho \geq 8 - 8\gamma$, and therefore removed from the candidate list, since it cannot be smaller than the right-hand side of (6.25).

(c) If only two of ε_1, ε_2, ε_3 are equal to each other and also ε_4

$$d^2(\boldsymbol{\varepsilon}) = 16 + 8\gamma - 8\rho = 20 + 8\gamma - 12\gamma^2. \tag{6.30}$$

This function is always greater than the previous one and therefore it is dropped from the final analysis.

(d) Finally, consider $\varepsilon_1 = \varepsilon_2 = \varepsilon_3 = \varepsilon_4$

$$d^2(\boldsymbol{\varepsilon}) = 16 + 24\gamma + 24\rho = 4 + 24\gamma + 36\gamma^2 > 36\gamma^2, \tag{6.31}$$

which is dropped from the candidate list according to (6.23).

One more candidate function can be excluded. If (6.22) is expressed as

$$d^2(\boldsymbol{\varepsilon}) = 8 - 4|3\gamma^2 - 1| = \begin{cases} 4 + 12\gamma^2 \geq 4, & \gamma \leq \frac{1}{\sqrt{3}} \\ 12 - 12\gamma^2 \geq 12(1-\gamma) \geq 8(1-\gamma), & \gamma > \frac{1}{\sqrt{3}} \end{cases} \tag{6.32}$$

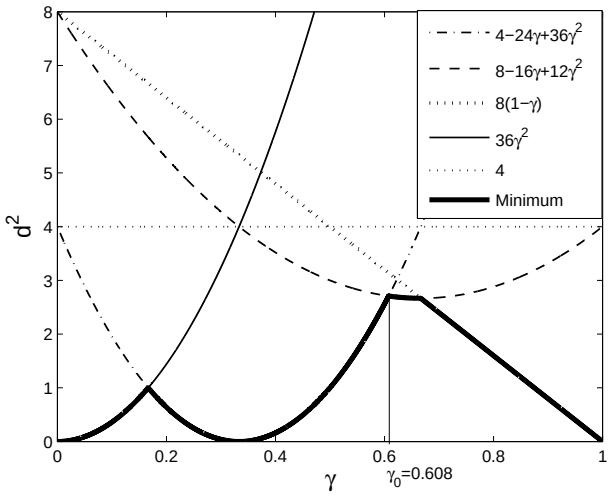

Figure 6.4: Minimum squared distance as a function of the correlation coefficient γ.

it can be covered by (6.21) and (6.25). Thus, after testing all non-trivially distinct error vectors $\boldsymbol{\varepsilon}$ and combining results from (6.21), (6.23), (6.25), (6.27) and (6.28) the squared minimum distance appears to be

$$d^2_{\min} = \min\{4, 36\gamma^2, 8(1-\gamma), 8-16\gamma+12\gamma^2, 4-24\gamma+36\gamma^2\}. \tag{6.33}$$

The γ is restricted as $0 \leq \gamma \leq 1$ since the nearest signal vectors have acute angles among them. The optimal value for γ is found from the intersection of $4-24\gamma+36\gamma^2$ and $8-16\gamma+12\gamma^2$ as shown in Fig. 6.4. The optimal value for γ is

$$\gamma_0 = \frac{1+\sqrt{7}}{6} \approx 0.608 \Rightarrow \rho_0 = \frac{-2+\sqrt{7}}{12} \approx 0.0538 \tag{6.34}$$

(angle between the nearest vectors is 52,6°), and the optimal value for the scalar c is

$$c_0 = \frac{-12+(1+\sqrt{7})\sqrt{14-\sqrt{7}}}{16-2\sqrt{7}} \approx 0.0266. \tag{6.35}$$

Corresponding value for the maximal minimum squared distance is

$$d^2_{\min,\,\max} = 2(4-\sqrt{7}) \approx 2.709. \tag{6.36}$$

Formally, the obtained signatures are given with

$$\mathbf{S}_i = \begin{pmatrix} \mathbf{s}_1^i \\ \mathbf{s}_2^i \\ \mathbf{s}_3^i \\ \mathbf{s}_4^i \end{pmatrix} = \frac{1}{\sqrt{1+2c_0^2}} \begin{pmatrix} 1 & c_0 & c_0 \\ c_0 & 1 & c_0 \\ c_0 & c_0 & 1 \\ \sqrt{\frac{1+2c_0^2}{3}} & \sqrt{\frac{1+2c_0^2}{3}} & \sqrt{\frac{1+2c_0^2}{3}} \end{pmatrix} \begin{pmatrix} \mathbf{h}_{3i-2} \\ \mathbf{h}_{3i-1} \\ \mathbf{h}_{3i} \end{pmatrix}. \tag{6.37}$$

6.1.3 Five users in four-dimensional subspace

The same kind of optimization as in previous examples for the signal set

$$\begin{aligned} \mathbf{s}_1^i &= \frac{\mathbf{h}_{4i-3} + c\mathbf{h}_{4i-2} + c\mathbf{h}_{4i-1} + c\mathbf{h}_{4i}}{\sqrt{1+3^2}}, \mathbf{s}_2^i = \frac{c\mathbf{h}_{4i-3} + \mathbf{h}_{4i-2} + c\mathbf{h}_{4i-1} + c\mathbf{h}_{4i}}{\sqrt{1+3c^2}}, \\ \mathbf{s}_3^i &= \frac{c\mathbf{h}_{4i-3} + c\mathbf{h}_{4i-2} + \mathbf{h}_{4i-1} + c\mathbf{h}_{4i}}{\sqrt{1+3c^2}}, \mathbf{s}_4^i = \frac{c\mathbf{h}_{4i-3} + c\mathbf{h}_{4i-2} + c\mathbf{h}_{4i-1} + \mathbf{h}_{4i}}{\sqrt{1+3c^2}}, \\ \mathbf{s}_5^i &= \frac{\mathbf{h}_{4i-3} + \mathbf{h}_{4i-2} + \mathbf{h}_{4i-1} + \mathbf{h}_{4i}}{\sqrt{4}} \end{aligned} \tag{6.38}$$

gives $c_0 = 0$, which is exactly the same result as in [36]. The obtained minimum distance and cross-correlation values are

$$d_{\min}^2 = 4,\ \gamma_0 = 0,\ \rho_0 = 0.5. \tag{6.39}$$

Formally, the obtained GO-CDMA signature ensemble is given with

$$\mathbf{S}_i = \begin{pmatrix} \mathbf{s}_1^i \\ \mathbf{s}_2^i \\ \mathbf{s}_3^i \\ \mathbf{s}_4^i \\ \mathbf{s}_5^i \end{pmatrix} = \begin{pmatrix} 1 & 0 & 0 & 0 \\ 0 & 1 & 0 & 0 \\ 0 & 0 & 1 & 0 \\ 0 & 0 & 0 & 1 \\ 0.5 & 0.5 & 0.5 & 0.5 \end{pmatrix} \begin{pmatrix} \mathbf{h}_{4i-3} \\ \mathbf{h}_{4i-2} \\ \mathbf{h}_{4i-1} \\ \mathbf{h}_{4i} \end{pmatrix}. \tag{6.40}$$

6.1.4 Other user configurations

Subspace dimensions greater than four cannot have $d_{\min,\max}^2 > 4$ because $d^2 = \boldsymbol{\varepsilon}^T \mathbf{R} \boldsymbol{\varepsilon} = 4$ for all error vectors having only one nonzero component, e.g. $\boldsymbol{\varepsilon} = (\pm 2, 0, \ldots, 0)$. Thus, there is no point to increase dimension beyond $L = 4$ if $s = 1$ when Euclidean distance is concerned.

Using larger subspace dimensions ($L \geq 4$) and more additional signals ($s \geq 2$) would offer more flexibility in choosing the oversaturation efficiency, but unfortunately the minimum Euclidean distance seems to be worse than in the case with only one extra signal in subspace. The situation is illustrated in Fig. 6.5, where the obtained minimum distance is given as a function of oversaturation efficiency for fixed value of s ($e_{ov} = K/N = (L+s)/L$). Correlation coefficient matrix design is not a trivial task when $s > 1$. Exhaustive

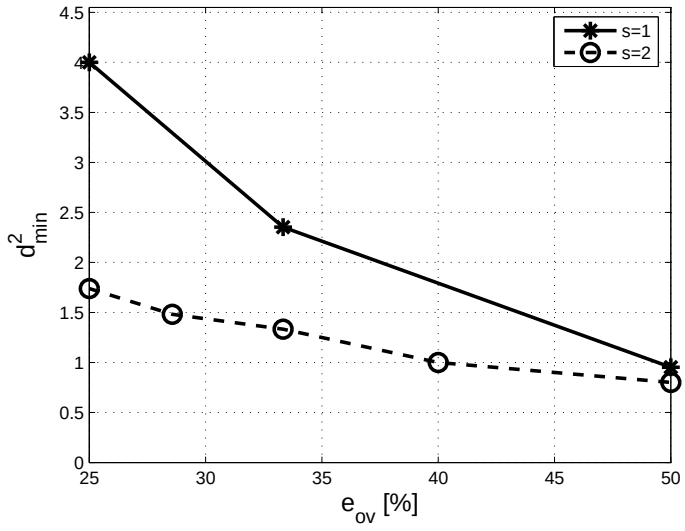

Figure 6.5: Energy loss as a function of oversaturation efficiency e_{ov}.

search was performed for $L = 4$, $s = 2$. For values of $L = 5, 6, 7, 8$, $s = 2$ extensive trials were performed, and tests show that results in the best case are worse when compared to the same oversaturation efficiencies having $s = 1$.

Greater oversaturation efficiencies than 50% were not considered since the minimum Euclidean distance of $d^2 = 1.527$ produces already a great loss in performance, which is shown in the next section. The higher oversaturation efficiencies would lead to intolerable losses as will be seen in section 6.3.

6.1.5 Examples of optimal GO-CDMA signature ensembles

Next, GO-CDMA signature ensemble examples are illustrated for $(3, 2)$, $(4, 3)$ and $(5, 4)$ cases. The considered signal space dimension is $N = 12$ because it is conveniently divisible by two, three, and four. The initial orthogonal matrix is given by (6.41). It is created from the sequence of length $N = 11$ that has minimax autocorrelation function by adding a column and a row of $+1$ symbols to the matrix. Obtained signatures are denoted as $\mathbf{s}^i_j$, where i stands for the group number and j for the signature number in the i-th group.

For $L = 2$ six subspaces are created each containing three users, thus $K = 18$. Those six two-dimensional subspaces $\mathbf{S}_1, \ldots, \mathbf{S}_6$ containing user signatures $\mathbf{s}^1_1, \mathbf{s}^1_2, \mathbf{s}^1_3, \ldots, \mathbf{s}^6_1, \mathbf{s}^6_2, \mathbf{s}^6_3$ are formed with bases $\{\mathbf{h}_1, \mathbf{h}_2\}, \ldots, \{\mathbf{h}_{11}, \mathbf{h}_{12}\}$.

The signature ensemble obtained using (6.4) and (6.41) are given in in (6.42).

$$\mathbf{H} = \begin{pmatrix} \mathbf{h}_1 \\ \mathbf{h}_2 \\ \mathbf{h}_3 \\ \mathbf{h}_4 \\ \mathbf{h}_5 \\ \mathbf{h}_6 \\ \mathbf{h}_7 \\ \mathbf{h}_8 \\ \mathbf{h}_9 \\ \mathbf{h}_{10} \\ \mathbf{h}_{11} \\ \mathbf{h}_{12} \end{pmatrix} = \frac{1}{\sqrt{12}} \begin{pmatrix} + & + & + & + & + & + & + & + & + & + & + & + \\ + & - & + & - & + & + & + & - & - & - & + & - \\ + & - & - & + & - & + & + & + & - & - & - & + \\ + & + & - & - & + & - & + & + & + & - & - & - \\ + & - & + & - & - & + & - & + & + & + & - & - \\ + & - & - & + & - & - & + & - & + & + & + & - \\ + & - & - & - & + & - & - & + & - & + & + & + \\ + & + & - & - & - & + & - & - & + & - & + & + \\ + & + & + & - & - & - & + & - & - & + & - & + \\ + & + & + & + & - & - & - & + & - & - & + & - \\ + & - & + & + & + & - & - & - & + & - & - & + \\ + & + & - & + & + & + & - & - & - & + & - & - \end{pmatrix} \tag{6.41}$$

$$\mathbf{S} = \begin{pmatrix} \mathbf{S}_1 \\ \vdots \\ \mathbf{S}_6 \end{pmatrix} = (\mathbf{s}_1^1, \mathbf{s}_2^1, \mathbf{s}_3^1, \ldots, \mathbf{s}_1^6, \mathbf{s}_2^6, \mathbf{s}_3^6)^T =$$

$$= \frac{1}{\sqrt{6}\chi} \begin{pmatrix} \xi & \eta & \xi & \eta & \xi & \xi & \xi & \eta & \eta & \eta & \xi & \eta \\ \xi & -\eta & \xi & -\eta & \xi & \xi & \xi & -\eta & -\eta & -\eta & \xi & -\eta \\ \chi & 0 & \chi & 0 & \chi & \chi & \chi & 0 & 0 & 0 & \chi & 0 \\ \xi & -\eta & -\xi & \eta & -\eta & \eta & \xi & \xi & -\eta & -\xi & -\xi & \eta \\ \xi & \eta & -\xi & -\eta & \eta & -\eta & \xi & \xi & \eta & -\xi & -\xi & -\eta \\ \chi & 0 & -\chi & 0 & 0 & 0 & \chi & \chi & 0 & -\chi & -\chi & 0 \\ \xi & -\xi & \eta & -\eta & -\xi & \eta & -\eta & \eta & \xi & \xi & -\eta & -\xi \\ \xi & -\xi & -\eta & \eta & -\xi & -\eta & \eta & -\eta & \xi & \xi & \eta & -\xi \\ \chi & -\chi & 0 & 0 & -\chi & 0 & 0 & 0 & \chi & \chi & 0 & -\chi \\ \xi & -\eta & -\xi & -\xi & \eta & -\eta & -\xi & \eta & -\eta & \eta & \xi & \xi \\ \xi & \eta & -\xi & -\xi & -\eta & \eta & -\xi & -\eta & \eta & -\eta & \xi & \xi \\ \chi & 0 & -\chi & -\chi & 0 & 0 & -\chi & 0 & 0 & 0 & \chi & \chi \\ \xi & \xi & \xi & -\eta & -\xi & -\xi & \eta & -\eta & -\xi & \eta & -\eta & \eta \\ \xi & \xi & \xi & \eta & -\xi & -\xi & -\eta & \eta & -\xi & -\eta & \eta & -\eta \\ \chi & \chi & \chi & 0 & -\chi & -\chi & 0 & 0 & -\chi & 0 & 0 & 0 \\ \xi & -\eta & \eta & \xi & \xi & -\eta & -\xi & -\xi & \eta & -\eta & -\xi & \eta \\ \xi & \eta & -\eta & \xi & \xi & \eta & -\xi & -\xi & -\eta & \eta & -\xi & -\eta \\ \chi & 0 & 0 & \chi & \chi & 0 & -\chi & -\chi & 0 & 0 & -\chi & 0 \end{pmatrix}, \tag{6.42}$$

where $\xi = 1 + c_0$, $\eta = 1 - c_0$, $\chi = \sqrt{2(1 + c_o)^2}$ and c_0 is given by (6.15).

For $L = 3$ four subspaces $(\mathbf{S}_1, \ldots, \mathbf{S}_4)$ are created all containing four users, thus the number of users is $K = 16$. The signature ensemble that contains user signatures $\mathbf{s}_1^1, \mathbf{s}_2^1, \mathbf{s}_3^1, \mathbf{s}_4^1, \ldots, \mathbf{s}_1^4, \mathbf{s}_2^4, \mathbf{s}_3^4, \mathbf{s}_4^4$ is formed with bases $\{\mathbf{h}_1, \mathbf{h}_2, \mathbf{h}_3\}, \ldots, \{\mathbf{h}_{10}, \mathbf{h}_{11}, \mathbf{h}_{12}\}$. Using (6.18) and (6.41) signature ensemble

is

$$\mathbf{S} = \begin{pmatrix} \mathbf{S}_1 \\ \vdots \\ \mathbf{S}_4 \end{pmatrix} = (\mathbf{s}_1^1, \mathbf{s}_2^1, \mathbf{s}_3^1, \mathbf{s}_4^1, \ldots, \mathbf{s}_1^4, \mathbf{s}_2^4, \mathbf{s}_3^4, \mathbf{s}_4^4)^T =$$

$$= \frac{1}{\sqrt{12}\sqrt{1+2c_0^2}} \begin{pmatrix} \zeta & \nu & 1 & 1 & 1 & \zeta & \zeta & 1 & \nu & \nu & 1 & 1 \\ \zeta & -1 & 1 & -\nu & 1 & \zeta & \zeta & -\nu & -1 & -1 & 1 & -\nu \\ \zeta & -1 & -\nu & 1 & -\nu & \zeta & \zeta & 1 & -1 & -1 & -\nu & 1 \\ 3\varsigma & -\varsigma & \varsigma & \varsigma & \varsigma & 3\varsigma & 3\varsigma & \varsigma & -\varsigma & -\varsigma & \varsigma & \varsigma \\ \zeta & \nu & -1 & -1 & \nu & -1 & 1 & 1 & \zeta & -\nu & -1 & -\zeta \\ \zeta & -1 & \nu & -1 & -1 & \nu & -\nu & 1 & \zeta & 1 & -1 & -\zeta \\ \zeta & -1 & -1 & \nu & -1 & -1 & 1 & -\nu & \zeta & 1 & \nu & -\zeta \\ 3\varsigma & -\varsigma & -\varsigma & -\varsigma & -\varsigma & -\varsigma & \varsigma & \varsigma & 3\varsigma & \varsigma & -\varsigma & -3\varsigma \\ \zeta & -\nu & -1 & -\zeta & \nu & -1 & -1 & \nu & -1 & 1 & 1 & \zeta \\ \zeta & 1 & -1 & -\zeta & -1 & \nu & -1 & -1 & \nu & -\nu & 1 & \zeta \\ \zeta & 1 & \nu & -\zeta & -1 & -1 & \nu & -1 & -1 & 1 & \nu & \zeta \\ 3\varsigma & \varsigma & -\varsigma & -3\varsigma & -\varsigma & -\varsigma & -\varsigma & -\varsigma & -\varsigma & \varsigma & \varsigma & 3\varsigma \\ \zeta & 1 & 1 & \zeta & -\nu & -1 & -\zeta & \nu & -1 & -1 & \nu & -1 \\ \zeta & -\nu & 1 & \zeta & 1 & -1 & -\zeta & -1 & \nu & -1 & -1 & \nu \\ \zeta & 1 & -\nu & \zeta & 1 & \nu & -\zeta & -1 & -1 & \nu & -1 & -1 \\ 3\varsigma & \varsigma & \varsigma & 3\varsigma & \varsigma & -\varsigma & -3\varsigma & -\varsigma & -\varsigma & -\varsigma & -\varsigma & -\varsigma \end{pmatrix}, \tag{6.43}$$

where $\zeta = 1 + 2c_0$, $\nu = 1 - 2c_0$, $\varsigma = \sqrt{(1+2c_0)/3}$ and c_0 is given by (6.35).

For $L = 4$ three subspaces $(\mathbf{S}_1, \ldots, \mathbf{S}_3)$ are created all containing five users, thus the number of users $K = 15$. The signature ensemble that contains user signatures is formed with bases $\{\mathbf{h}_1, \ldots, \mathbf{h}_4\}, \{\mathbf{h}_5, \ldots, \mathbf{h}_8\}$, $\{\mathbf{h}_9, \ldots, \mathbf{h}_{12}\}$. Using (6.38) and (6.41) signatures are

$$\mathbf{S} = \begin{pmatrix} \mathbf{S}_1 \\ \vdots \\ \mathbf{S}_3 \end{pmatrix} = (\mathbf{s}_1^1, \mathbf{s}_2^1, \mathbf{s}_3^1, \mathbf{s}_4^1, \mathbf{s}_5^1, \ldots, \mathbf{s}_1^3, \mathbf{s}_2^3, \mathbf{s}_3^3, \mathbf{s}_4^3, \mathbf{s}_5^3)^T =$$

$$= \frac{1}{\sqrt{12}} \begin{pmatrix} 1 & 1 & 1 & 1 & 1 & 1 & 1 & 1 & 1 & 1 & 1 & 1 \\ 1 & -1 & 1 & -1 & 1 & 1 & 1 & -1 & -1 & -1 & 1 & -1 \\ 1 & -1 & -1 & 1 & -1 & 1 & 1 & 1 & -1 & -1 & -1 & 1 \\ 1 & 1 & -1 & -1 & 1 & -1 & 1 & 1 & 1 & -1 & -1 & -1 \\ 2 & 0 & 0 & 0 & 1 & 1 & 2 & 1 & 0 & -1 & 0 & 0 \\ 1 & -1 & 1 & -1 & -1 & 1 & -1 & 1 & 1 & 1 & -1 & -1 \\ 1 & -1 & -1 & 1 & -1 & -1 & 1 & -1 & 1 & 1 & 1 & -1 \\ 1 & -1 & -1 & -1 & 1 & -1 & -1 & 1 & -1 & 1 & 1 & 1 \\ 1 & 1 & -1 & -1 & -1 & 1 & -1 & -1 & 1 & -1 & 1 & 1 \\ 2 & -1 & -1 & -1 & -1 & 0 & -1 & 0 & 1 & 1 & 1 & 0 \\ 1 & 1 & 1 & -1 & -1 & -1 & 1 & -1 & -1 & 1 & -1 & 1 \\ 1 & 1 & 1 & 1 & -1 & -1 & -1 & 1 & -1 & -1 & 1 & -1 \\ 1 & -1 & 1 & 1 & 1 & -1 & -1 & -1 & 1 & -1 & -1 & 1 \\ 1 & 1 & -1 & 1 & 1 & 1 & -1 & -1 & -1 & 1 & -1 & -1 \\ 2 & 1 & 1 & 1 & 0 & -1 & -1 & -1 & -1 & 0 & -1 & 0 \end{pmatrix}. \tag{6.44}$$

In the light of section 5.1.1 it is rather disappointing that with even smaller oversaturation efficiency we obtained non-binary extra signatures in every subspace. The prescription of section 5.1.1 is working only with a signature length of the form 4^l. In the presented examples, like in any case of N non-divisible by 8, extra signatures cannot be binary in principle. The following proposition will be proved:

Proposition: Let $\mathbf{a}, \mathbf{b}$ be two rows of Hadamard matrix of size $N > 4$. Let $\mathbf{c}$ be a binary sequence of length N orthogonal to $\mathbf{a}$ but having correlation coefficient with $\mathbf{b}$ equal to $\pm 1/2$. Then, N is divisible by 8.

Proof: First of all, the case of negative correlation between $\mathbf{c}$ and $\mathbf{b}$ can be discarded, since changing the polarity of $\mathbf{c}$ leads to the transforming of correlation into positive values without losing orthogonality of $\mathbf{c}$ to $\mathbf{a}$. To prove the proposition it is necessary to obtain Hamming distances between $\mathbf{a}$, $\mathbf{b}$ and $\mathbf{c}$. The correlation coefficient of two binary sequences is related to their Hamming distance, d_H, as [79]

$$\rho = \frac{N - 2d_H}{N}. \tag{6.45}$$

Thus, it is obvious that Hamming distances between $\mathbf{a}$ and $\mathbf{b}$, and $\mathbf{a}$ and $\mathbf{c}$ are both $N/2$, while Hamming distance between $\mathbf{b}$ and $\mathbf{c}$ is $N/4$.

Now, let w_a, w_b and w_c be weights (the number of minus ones) of $\mathbf{a}, \mathbf{b}, \mathbf{c}$, while $\lambda_{ab}, \lambda_{ac}, \lambda_{bc}$ denote the number of coincidences of minus ones in pairs $(\mathbf{a}, \mathbf{b})$, $(\mathbf{a}, \mathbf{c})$ and $(\mathbf{b}, \mathbf{c})$, respectively. Then, the Hamming distances of these three pairs are

$$\begin{aligned} d_H(\mathbf{a}, \mathbf{b}) &= w_a + w_b - 2\lambda_{ab} = \frac{N}{2} \\ d_H(\mathbf{a}, \mathbf{c}) &= w_a + w_c - 2\lambda_{ac} = \frac{N}{2} \\ d_H(\mathbf{b}, \mathbf{c}) &= w_b + w_c - 2\lambda_{bc} = \frac{N}{4}, \end{aligned}$$

which gives three necessary conditions on N:

$$\begin{aligned} N &= 2(w_a + w_b) - 4\lambda_{ab} \\ N &= 2(w_a + w_c) - 4\lambda_{ac} \\ N &= 4(w_b + w_c) - 8\lambda_{bc}. \end{aligned}$$

Since $N > 4$ is the size of the Hadamard matrix, it is divisible by 4, meaning that all three weights w_a, w_b, w_c are of the same parity (otherwise the first term in right-hand side of at least one of the first two equations is not divisible by 4). This means that $w_b + w_c$ is even, hence, from the third equation it is seen that N is divisible by 8. With this, it is proved that in order to obtain binary ensemble N should be divisible by 8.

6.1.6 Scalability of the GO-CDMA signature ensemble

In [20] Vanhaverbeke has addressed the importance of scalability in oversaturated systems. In perfectly scalable system no modifications to existing signatures are required if users enter or exit the system. A totally unscalable system requires the allocation of signatures of all users to be performed every time a new user arrives or an existing user terminates the transmission. An example of a scalable system would be the utilization of PN codes, and an example of an unscalable signature set are WBE signatures discussed in section 5.2. In [20] the term quasi-scalability is introduced for systems where only few user's signatures are affected by the decreasing or increasing number of users.

Using terminology of [20], the GO-CDMA concept is quasi-scalable. Assume that initially K' users are active ($N \leq K' \leq K_{\max} = \lfloor N/L \rfloor (L + s) + N \bmod L$, where $\lfloor \cdot \rfloor$ is used to denote rounding towards zero). The change in the number of users inside one group is denoted with τ. It is sufficient to investigate changes inside groups individually, since all groups are independent.

- First, consider the case $K' = N$ and new users start entering the system. For each new user (assuming $s = 1$) L orthogonal signatures are required to form a group to support new user. Thus, for each new user, L existing users are affected making the system quasi-scalable.

- Next, consider the case where for $K' > N$ and τ users become inactive inside some group. Then, there are $L + s - \tau$ users that are affected from the change, thus the system is still quasi-scalable. Signatures for those remaining users must be re-designed to retain the maximal minimum distance available, since there are still L dimensions, where $L + s - \tau$ user signatures can be placed. Thus, their transmission fidelity improves. In the case of $\tau = L + s$, the whole group is removed and other users are not affected by the change.

6.2 Comparison of GO-CDMA signatures to the optimal ensemble

In section 6.1 $(L, L + 1)$ GO-CDMA signature ensembles were designed for $L = 2, 3, 4$ ($e_{ov} = 1 + 1/L$). The conventional orthogonal signaling with single-user receiver has $d^2_{\text{min,o}} = 4$ squared minimum distance between different unit energy group signals, which is not compromised by Ross-Taylor signatures [32, 36]. For GO-CDMA signature ensembles the minimum Euclidean distance is sacrificed for the simple receiver and greater oversaturation efficiency ($L = 2, 3$), or oversaturation efficiency for receiver simplicity.

Thus, the GO-CDMA signature ensemble offers trade-off between performance, capacity and receiver complexity.

For the $(3, 2)$ ensemble the oversaturation efficiency $e_{ov} = 1.5$. When its minimum distance is compared to the Ross-Taylor signatures the loss is

$$\frac{d^2_{\text{min,o}}}{d^2_{\text{min,max}}} = \frac{4}{1.528} \approx 2.618 \approx 4.18 \text{ dB}. \tag{6.46}$$

This distance (energy) loss is the penalty for the greater oversaturation efficiency. For the $(4, 3)$ ensemble the oversaturation efficiency $e_{ov} = 1.33$. When compared to the Ross-Taylor signatures, the loss due to the simple receiver

$$\frac{d^2_{\text{min,o}}}{d^2_{\text{min,max}}} = \frac{4}{2.709} \approx 1.477 \approx 1.69 \text{ dB}. \tag{6.47}$$

The oversaturation efficiency obtained in this manner is the same as in [36]. Thus, 1.69 dB energy loss may be accepted as the cost for receiver simplicity. For the $(5, 4)$ constellation the squared minimum distance between different group signals is $d^2_{\text{min,max}} = 4$ so there is no distance (energy) loss when compared to the Ross-Taylor signatures while the number of users served is increased by 25%. This is not as great as in [36] which means sacrificing the oversaturation efficiency in exchange for receiver simplification.

6.3 Signature optimization without symmetry restriction

In [104] similar analysis as in section 6.1 was performed with a software optimization tool without any assumptions about the resulting signatures. Optimal constellations were obtained for $L = 2, s = 1, 2, 3, 4$ and $L = 3, s = 1, 2, 3$. The results show that assumption of symmetric signature constellations in section 6.1 is well justified. The result for the $(3, 2)$ constellation is equal, and the result for the $(4, 3)$ constellation is only 0.02 dB better. Author of [104] also analyzed greater oversaturation efficiencies than 50%. The results indicate that by abandoning the symmetry requirement for signatures, it is possible to obtain better minimum Euclidean distances for certain oversaturation efficiency by increasing L and s. Yet real prospects of this oversaturation mode are rather doubtful because of intolerably big energy losses. Take for example $e_{ov} = 2.0$, where for $L = 2$ $(s = 2)$ the minimum distance is 1.0718, but for $L = 3$ $(s = 3)$ the minimum distance is 1.3333. Thus, it is seen that the loss in minimum distance diminishes from 5.7 dB to 4.8 dB when a larger signal space dimension is used. But, the scale of loss makes oversaturation efficiencies beyond 1.50 seem impractical.

Results of optimization of section 6.1 (symmetric) are summarized in Table 6.1 with the results from [104] (asymmetric). From the table it can

		Symmetric		Asymmetric [104]	
L	e_{ov}	$d^2_{\min}$	Loss [dB]	$d^2_{\min}$	Loss [dB]
2	1.50	1.5279	4.19	1.5279	4.19
2	2.00			1.0718	5.72
2	2.50			0.5196	8.86
2	3.00			0.3946	10.06
3	1.33	2.7085	1.69	2.7251	1.67
3	1.66			1.6991	3.72
3	2.00			1.3333	4.77
4	1.25	4	0		

Table 6.1: Summary of results

be seen that symmetric signature ensemble design is a sensible approach, since the results are equal, except for 0.02 dB loss for the $(4, 3)$ case, to the approach without any restrictions to final outcome. It is also evident that the loss increases quickly as the oversaturation efficiency grows. Therefore, in the next chapter an alternative approach to designing GO-CDMA signature ensembles is considered.

6.4 BER analysis

Minimum Euclidean distances alone calculated in the previous section are not sufficient enough to characterize the BER behaviour of the oversaturation method presented in this chapter. Next, the exact BER is calculated for signals obtained in section 6.1.1. For the higher signal subspace dimension only upper bounds for BER are derived due to complex decision regions.

6.4.1 BER calculation for non-rectangular decision regions

Generally, exact BER calculation can be performed as summations of complementary error functions familiar from numerous sources [12, 13, 50]

$$Q(x) = \frac{1}{\sqrt{2\pi}} \int_x^\infty \exp\left(-\frac{x^2}{2}\right) dx, \tag{6.48}$$

and Owen's T-functions [105]. The usage of Owen's T-function is briefly introduced next.

In the Fig. 6.6 the signal point is in the origin. Owen's T-function gives the probability that the point falls to the shaded area due to disturbances in the AWGN channel. The variance of noise $= \sigma^2 = var\{x\} = var\{y\} = 1$.

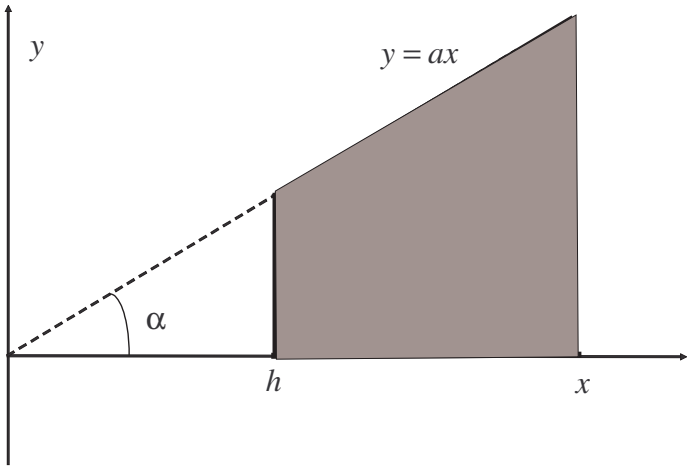

Figure 6.6: The usage of Owen's T-function.

If the angle between $y = ax$ and x-axis is α, then $a = \tan\alpha$. Probability that the received point falls to the shaded region:

$$T(h,a) = \frac{1}{2\pi}\int_{x=h}^{\infty}\int_{y=0}^{ax}\exp\left(-\frac{x^2+y^2}{2}\right)dydx. \tag{6.49}$$

To express (6.49) in the form tabulated in the literature variables x and y are transformed to polar coordinates: $x = \rho\cos\gamma$, $y = \rho\sin\gamma$ and $dxdy = \rho\, d\rho\, d\gamma$. Then,

$$T(h,\alpha) = \frac{1}{2\pi}\int_0^{\alpha} d\gamma \int_{\frac{h}{\cos\gamma}}^{\infty} \rho\,\exp\left(-\frac{\rho^2}{2}\right)d\rho = \frac{1}{2\pi}\int_0^{\alpha}\exp\left(-\frac{h^2}{2\cos^2\gamma}\right)d\gamma. \tag{6.50}$$

With the exchange of variable

$$\tan\gamma = x \Rightarrow \frac{1}{\cos^2\gamma} = 1 + x^2 \text{ and } d\gamma = \frac{1}{1+x^2}dx$$

we have same form as in tables [105]

$$T(h,\alpha) = \frac{1}{2\pi}\int_0^{\alpha}\frac{1}{1+x^2}\exp\left(-\frac{h^2}{2}(1+x^2)\right)dx. \tag{6.51}$$

Thus, the probability can be calculated by numerical integration with (6.50) or by table lookup according to (6.51) [105].

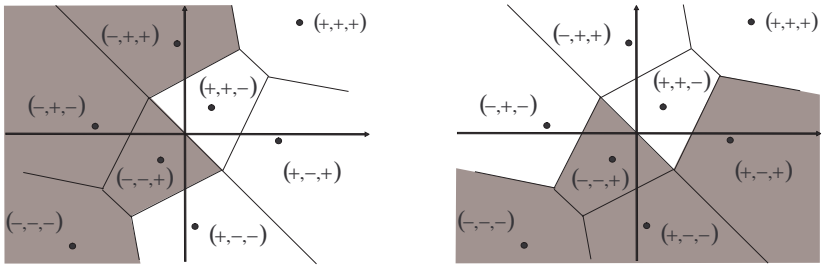

(a) User 1 (b) User 2

Figure 6.7: Decision regions of users 1 and 2 in the $(3, 2)$ constellation.

6.4.2 Closed-form expression of BER

Optimal group signal constellation for the $(3, 2)$ GO-CDMA signature ensemble was presented in Fig. 6.3. Optimal decision regions for received bits of each of three users are illustrated in Fig. 6.7 for users 1 and 2, and Fig. 6.8 for user 3, white area corresponding to decision that transmitted bit is $+1$.

Let $P_{e,j}(b_1, b_2, b_3)$ designate bit error probability for the user j conditioned in bits $b_i = \pm 1$, $i = 1, 2, 3$ transmitted by all three users. Then the total bit error probability $P_{e,j}$ for user j $(j = 1, 2, 3)$ is

$$P_{e,j} = \frac{1}{8} \sum_{b_1,b_2,b_3=\pm 1} P_{e,j}(b_1, b_2, b_3) = \frac{1}{4} \sum_{b_2,b_3=\pm 1} P_{e,j}(+1, b_2, b_3), \qquad (6.52)$$

where the obvious invariance with respect to simultaneous change of all transmitted bits is used.

Every term in (6.52) can be found by integration of pdf of the noise-corrupted group signal over the decision region producing error (see section 3.4):

$$P_{ej} = \int\int_{Z_j} P_g \left(q(\mathbf{s}_1 + b_2\mathbf{s}_2 + b_3\mathbf{s}_3), 1\right) \, dxdy, \qquad (6.53)$$

where $P_g(\boldsymbol{\mu}, \sigma^2)$ stands for two-dimensional Gaussian pdf with mean vector $\boldsymbol{\mu}$ and variance σ^2, q is SNR per user's bit after matched filtering, and Z_j is integration area. When the transmitted bit for the user j is $+1$, Z_j is a shaded region in Fig. 6.7 and 6.8.

Due to the complexity of exact calculation, only one case is presented here as an example. Other cases can be found from appendix A.

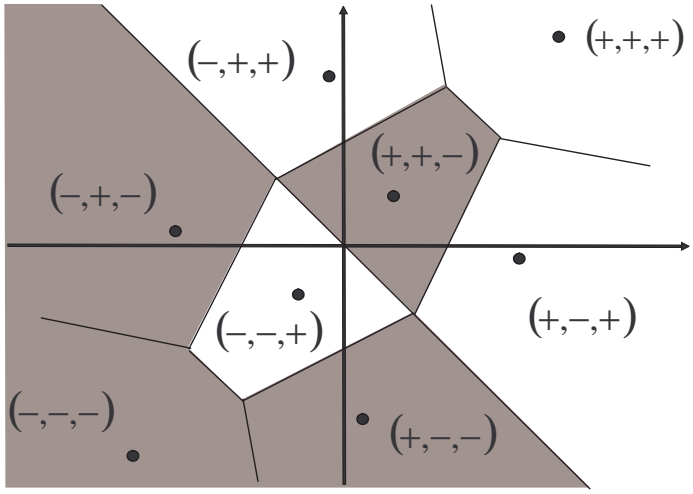

Figure 6.8: Exact BER calculation for user 3 when bit pattern (+,+,+) is transmitted.

The calculation of $P_{e,3}(+,+,+)$

The group signal corresponding to bit pattern (+,+,+) is transmitted and probability of user 3 receiving '−' is calculated. Decision regions are illustrated in Fig. 6.8. The shaded part is the area resulting in bit error. The group signal constellation is divided into different zones and final error probability is calculated with the combination of Q- and T-functions. The calculation in this case can be divided into three phases: the probability of error is the area left of the line $y = -x$ (Fig. 6.9) **plus** the shaded area to the right of the line $y = -x$ (Fig. 6.10) **minus** the white area left of the line $y = -x$ (Fig. 6.11).

In the following derivations $Q(h)$ means actually $Q(h/\sqrt{2N_0})$ and $T(h, \alpha)$ is used to denote $T(h/\sqrt{2N_0}, \alpha)$. The shorter denotations are chosen for convenience. First, the probability that the received point appears to the left of curve $y = -x$ can be calculated with $Q(h_2)$. The probability that the received signal point enters the remaining shaded area can be incorporated with subtraction of two T-functions $2(T(h_1, \beta_1) - T(h_2, \beta_1))$, since without the subtraction the area continues infinitely. The result is multiplied by two to include both halves of the shaded area (see Fig. 6.8). In this part, the result includes also the white area left to the line $y = -x$, which must be subtracted to obtain the exact solution. It can be accomplished with the subtraction of $2T(h_2, \beta_1)$. However, this operation also removes a part of the shaded area. This is compensated with the addition of $2[T(h_4, \beta_3) - T(h_4, \beta_2)]$ and further subtraction of $2T(h_3, \beta_4)$. Combining aforementioned

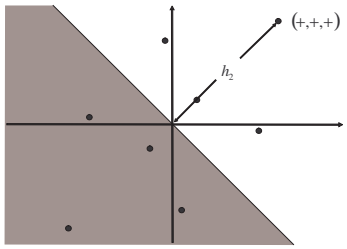

Figure 6.9: The first phase of calculation of $P_e(+,+,+)$.

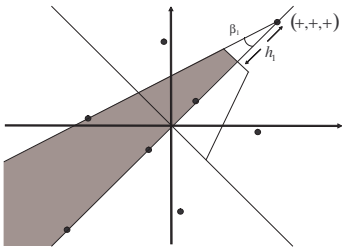

(a) Area right to $y = -x$

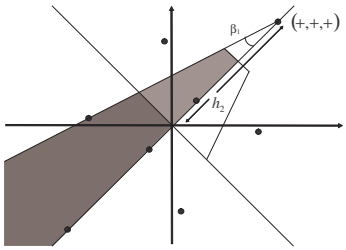

(b) Subtract extra area

Figure 6.10: The second phase of calculation of $P_e(+,+,+)$.

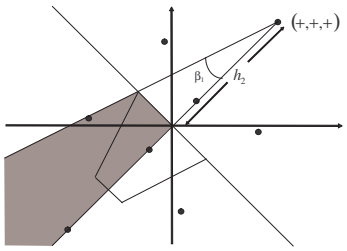

(a) Area left to $y = -x$

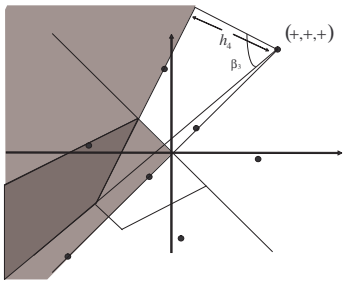

(b) Subtract part of extra area

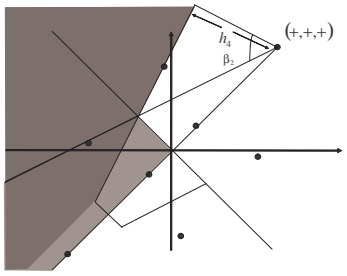

(c) Add to extra removed area

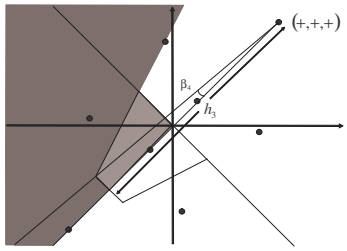

(d) Subtract extra area

Figure 6.11: The third phase of calculation of $P_e(+,+,+)$.

Table 6.2: Parameters for BER calculation for user 3 when (+++) is transmitted.

h_1	h_2	h_3	h_4
$\sqrt{E_b}$	$2.618\sqrt{E_b}$	$4.236\sqrt{E_b}$	$1.6206\sqrt{E_b}$
β_1	β_2	β_3	β_4
0.3141	0.9425	1.1884	0.0682

Table 6.3: Group signal point coordinates

Point	x-coordinate	y-coordinate
$(+,+,+)$	$1.8512\sqrt{E_b}$	$1.8512\sqrt{E_b}$
$(+,+,-)$	$-0.1241\sqrt{E_b}$	$1.5383\sqrt{E_b}$
$(+,-,+)$	$1.5383\sqrt{E_b}$	$-0.1241\sqrt{E_b}$
$(+,-,-)$	$-0.4370\sqrt{E_b}$	$-0.4370\sqrt{E_b}$
$(-,+,+)$	$0.4370\sqrt{E_b}$	$0.4370\sqrt{E_b}$
$(-,+,-)$	$-1.5383\sqrt{E_b}$	$0.1241\sqrt{E_b}$
$(-,-,+)$	$0.1241\sqrt{E_b}$	$-1.5383\sqrt{E_b}$
$(-,-,-)$	$-1.8512\sqrt{E_b}$	$-1.8512\sqrt{E_b}$

results the error probability is

$$P_{e3}(+,+,+) = Q(h_2) + [2\,(T(h_1,\beta_1) - T(h_2,\beta_1)) - 2T(h_2,\beta_1)] + [2\,(T(h_4,\beta_3) - T(h_4,\beta_2)) - 2T(h_3,\beta_4)]\,. \quad (6.54)$$

Values of parameters $h_i, \beta_i, i = 1,\ldots,4$ in (6.54) are listed in the Table 6.2. They are obtained by elementary geometry. Group signal coordinates used to calculate parameters are tabulated in Table 6.3. The distances are obtained as $h_1 = d(+++,++-)/2$, $h_2 = d(+++,++-) + d(++-,--+)/2$, $h_3 = d(+++,++-) + d(++-,--+) + d(--+,---)/2$. The h_4 can be only calculated after obtaining β_2. To find out angles β_i it is necessary to calculate coordinates of some intersecting decision region boundaries. From the obtained coordinates it is possible to derive equations of lines used to calculate values for T-functions. All these lines originate from the signal point (+,+,+). The other point in the plane used to determine the equation of line is some other group signal in most of the cases. However, it can also be an intersection of two lines representing boundaries between decision regions. Using these equations of lines it is easy to determine the tangent of angle between them, which between two lines having slopes m_1 and m_2 is

$$\tan\beta = (m_2 - m_1)/(1 + m_1 m_2). \quad (6.55)$$

Take for example Fig. 6.11(a). The equation of the line passing the origin

and signal point (+,+,+) is simply

$$y = x. \tag{6.56}$$

The equation of the line passing through signal points (+,+,+) and (–,+,–) is

$$y = 0.5095x + 0.908\sqrt{E_b}. \tag{6.57}$$

Thus, the tangent of angle between them is

$$\tan\beta_1 = (1 - 0.5095)/(1 + 0.5096) \approx 0.3249, \tag{6.58}$$

from which the angle can also be calculated as

$$\beta = \arctan 0.3249 = 0.3141.$$

Other β_i are calculated as follows: To obtain $\tan\beta_2$ only one equation of the line must be calculated, since the other is obtained in (6.57). The required line is perpendicular to the line connecting signal points (–,+,+) and (–,–,–) and passes through the point (+,+,+). The equation of that line is

$$y = 1.9626x + 1.782\sqrt{E_b}, \tag{6.59}$$

thus the slope perpendicular to it is $-1/m = -0.5095$, and using (6.55)

$$\tan\beta_2 = 1.3764 \tag{6.60}$$

and

$$\beta_2 = 0.9425. \tag{6.61}$$

When calculating $\tan\beta_3$ it is necessary to first calculate the slope of line connecting point (+,+,+) and the intersection of line from (6.59) and the one perpendicular to $y = x$ going through the point having coordinates

$$\left(-\frac{1}{\sqrt{2}}(h_3 - h_2), -\frac{1}{\sqrt{2}}(h_3 - h_2)\right) = (-1.2077\sqrt{E_b}, -1.2077\sqrt{E_b}),$$

where $h_3 - h_2$ is the distance of that point from the origin. Using the information available, the wanted equation of the line is

$$y = -x - \sqrt{2}(h_3 - h_2) = -x - 2.4155\sqrt{E_b}. \tag{6.62}$$

The x-coordinate of the intersection point used to calculate β_3 is found by solving x from

$$1.9626x + 1.782\sqrt{E_b} = -x - 2.4155\sqrt{E_b},$$

which produces

$$x = -1.4168\sqrt{E_b}$$

and

$$y = -0.9987\sqrt{E_b}.$$

Now, it is possible to calculate the slope of the required line, which is

$$(-0.9987\sqrt{E_b} - 1.8512\sqrt{E_b})/(-1.4168\sqrt{E_b} - 1.8512\sqrt{E_b}) = 0.8721.$$

Thus, using again (6.55)

$$\tan\beta_3 = 2.4864 \tag{6.63}$$

and

$$\beta_3 = 1.1884 \tag{6.64}$$

The value of $\tan\beta_4$ can be calculated with previously obtained slopes from (6.56) and (6.63) as

$$\tan\beta_4 = (1 - 0.8721)/(1 + 0.8721) \approx 0.0683. \tag{6.65}$$

Thus,

$$\beta_4 = 0.0682 \tag{6.66}$$

Other group signal points

The probability of error $P_{e,3}(+,+,+)$ was calculated above. To obtain the total BER of the $(3, 2)$ GO-CDMA system, six more similar operations must be performed consisting of the division of the plane to parts that can be covered with either Q-functions or T-functions, and the calculation of parameters for those functions. The calculations are presented in appendix A to avoid tedious explanations here. To obtain the final result for user 3 the probabilities $P_{e,3}(-,-,+)$ and $P_{e,3}(-,+,+)$ should also be calculated, which is done in A.1.1 and A.1.2, respectively. The fourth required error probability is $P_{e,3}(+,-,+) = P_{e,3}(-,+,+)$ (see Fig. 6.8).

Users 1 and 2 have identical BER performance, which is seen from Fig. 6.7, where it is evident that decision regions are rotated copies of each other. The rotation does not affect to relative distances between points. In appendix A the probabilities are calculated for $P_{e,1}(+,+,-)$, $P_{e,1}(+,-,-)$, $P_{e,1}(+,-,+)$ and $P_{e,1}(+,+,+)$ in A.2.1, A.2.2, A.2.3 and A.2.4, respectively. The results from appendix A can be summarized to

$$P_{e,1} = P_{e,2} = \frac{1}{4}(P(-xx|++-) + P(-xx|+--) + P(-xx|+-+) + P(-xx|+++)) \tag{6.67}$$

and

$$P_{e,3} = \frac{1}{4}(P(xx-|--+) + P(xx-|+++) + 2P(xx-|-++)), \tag{6.68}$$

where x is used to denote bit value that does not affect to the result of calculation. The curves illustrating (6.67) and (6.68) are presented in section 6.4.4 along with the approximated BER curves to be calculated next.

6.4.3 Upper bounds

As can be seen from appendix A, exact BER formulas are very complex and impractical. In addition, they are very difficult to obtain for higher subspace dimensions due to complicated decision regions. Thus, upper bounds for BER are necessary. A general idea of above-bordering BER is quite straightforward and consists of covering the area of erroneous decision by an appropriate union of half-spaces [12, 13].

Bounding in two-dimensional signal space

The principle of upper bounding becomes clear from detailed consideration of the simplest case $L = 2$, $s = 1$. Since $P_{e,1} = P_{e,2}$, it is sufficient to analyze BER only for users 1 and 3. Starting with user 1, take signal point (+,+,+) in Fig. 6.7 and try to separate it from erroneous (shaded) area with as small a number of straight lines as possible, each being maximally distant from the signal point (+,+,+). Fig. 6.12(a) shows that it is possible with only one line, which is perpendicular to the line connecting points (+,+,+) and (−,+,+). Thus, upper bound on $P_{e,1}(+,+,+)$ is derived:

$$P_{e,1}(+,+,+) \leq Q\left(\frac{h_1}{\sqrt{2N_0}}\right), \tag{6.69}$$

where h_1 is distance from the point (+,+,+) to the line mentioned above ($h_1 = \sqrt{E_b}$, see Fig. 6.3).

Next, the point (+,−,+) is taken into consideration. Fig. 6.12(b) shows that two straight lines are required – one being perpendicular to the line connecting points (+,−,+) and (+,−,−), and the other perpendicular to the line connecting points (+,−,+) and (−,+,+). Thus, union bound gives $P(+,-,+) \leq Q(h_2)+Q(h_3)$, with h_2, h_3 once more denote distances from the point (+,−,+) to the lines mentioned above. The distance h_2 is simply $h_2 = h_1$, but h_3 must be calculated as a distance from the (+,−,+) to the line connecting points (+,+,+) and (−,+,−). If the equation of the line is given in general form $Ax + By + C = 0$ the distance d of point (x_1, y_1) from it is given with

$$d = \frac{Ax_1 + By_1 + C}{\pm\sqrt{A^2 + B^2}}, \tag{6.70}$$

where the sign is chosen so that the distance is non-negative. The equation of the line was calculated to be $y = 0.5095x + 0.908\sqrt{E_b}$. When substituted to (6.70) along with point coordinates $(x_1, y_1) = (1.5383\sqrt{E_b}, -0.1241\sqrt{E_b})$ $h_3 = 1.7169\sqrt{E_b}$ and

$$P_{e,1}(+,-,+) \leq Q\left(\frac{h_2}{\sqrt{2N_0}}\right) + Q\left(\frac{h_3}{\sqrt{2N_0}}\right) \tag{6.71}$$

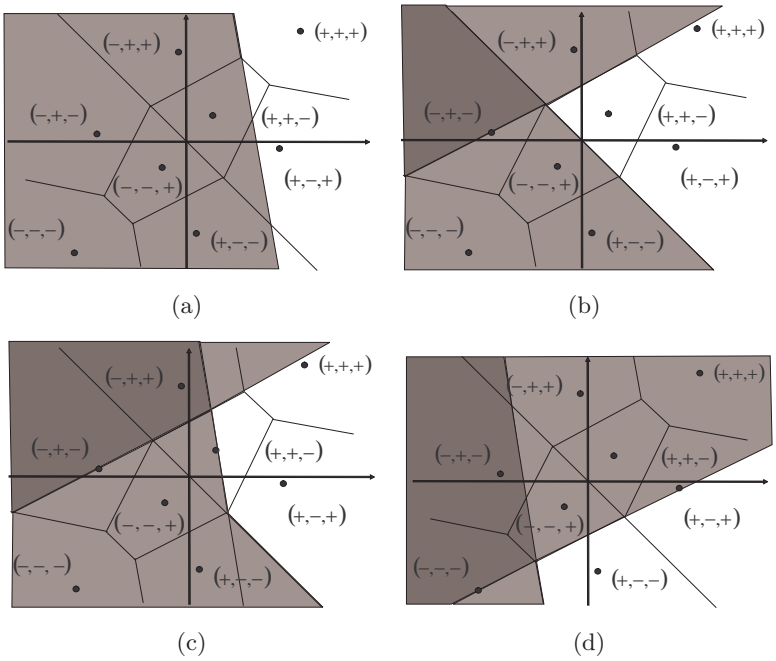

Figure 6.12: Bounding of BER for user 1.

For the point (+,−,+) the covering of erroneous areas requires also two straight lines. From Fig. 6.12(c) it is seen that the closest area resulting in error is the decision region of the point (−,−,+), thus the first line is drawn half way between points (+,−,+) and (−,−,+). The distance of the line to those points is denoted with h_4. To also include the part not covered by the first line from the decision region of point (−,+,+) the same line is drawn as in the case for the point (+,−,+). It is at the distance h_1 from the point (+,−,+).

Finally, the bounding for point (+,−,−) is also covered by two straight lines as shown in Fig. 6.12(d). The two lines are located at the distance h_1 from (+,−,−), since they are obtained by lengthening the decision region boundaries. After combining all the results and expressing h_i as a function of bit energy E_b the error probability for the first and the second user is estimated as

$$P_{e,1} = P_{e,2} < \frac{3}{4}Q\left(0.618q\right) + \frac{3}{4}Q\left(q\right) + \frac{1}{4}Q\left(1.203q\right) \tag{6.72}$$

Similar procedure applied to user 3 gives

$$P_{e3} < \frac{5}{4}Q\left(0.618q\right) + Q\left(q\right), \tag{6.73}$$

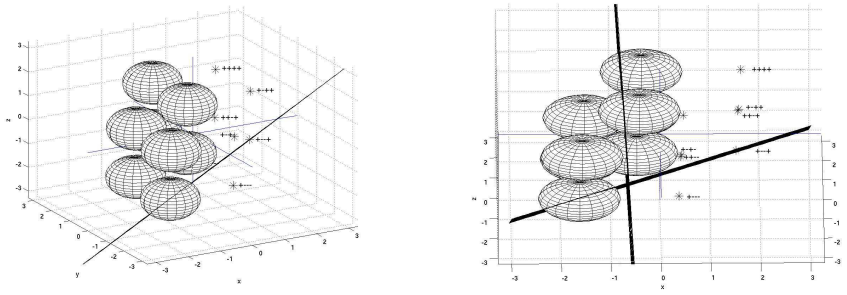

(a) (b)

Figure 6.13: Example of upper bounding in 3D-case.

after which average BER can be given

$$P_{av} < \frac{11}{12}Q(q) + \frac{11}{12}Q(0.618q) + \frac{1}{4}Q(1.203q) \tag{6.74}$$

Bounding in three-dimensional signal space

The procedure in three-dimensional space is illustrated with an example for user 1 when (+,–,–,–) is sent. Spheres in Fig. 6.13 represent erroneous signal points, and they have radius of $d_{\min}/2$. First, a plane is drawn between (+,–,–,–) and (–,–,–,+), because the (–,–,–,+) is the closest point. Now, all signal points except of (–,–,–,–) are 'behind' the plane, and have distance greater than $d_{\min}/2$ from it. After drawing another plane between (+,–,–,–) and (–,–,–,–) all erroneous points are covered and we have $P_{e1}(+,-,-,-) < P(---+|+---) + P(----|+---)$. All the remaining operations for obtaining error probabilities for different users follow the same procedure and bear no new relevant information to the discussion here. Therefore, only results are shown.

Users 1,2,3 have equal error probability, so only users 1 and 4 are necessary to consider.

$$P_{e1} = P_{e2} = P_{e3} < \frac{5}{8}Q\left(0.823q\right) + \frac{1}{4}Q\left(0.886q\right) + Q\left(q\right) + \frac{1}{8}Q\left(1.701q\right) \tag{6.75}$$

$$P_{e4} < \frac{7}{8}Q\left(0.823q\right) + \frac{3}{2}Q\left(0.886q\right) + Q\left(q\right) \tag{6.76}$$

$$P_{av} < Q(q) + \frac{11}{16}Q(0.823q) + \frac{9}{16}Q(0.886q) + \frac{3}{32}Q(1.701q) \tag{6.77}$$

Bounding in four-dimensional signal space

Bounding for four-dimensional space cannot be illustrated with figures. Nevertheless, the bounding procedure is identical to the three-dimensional case.

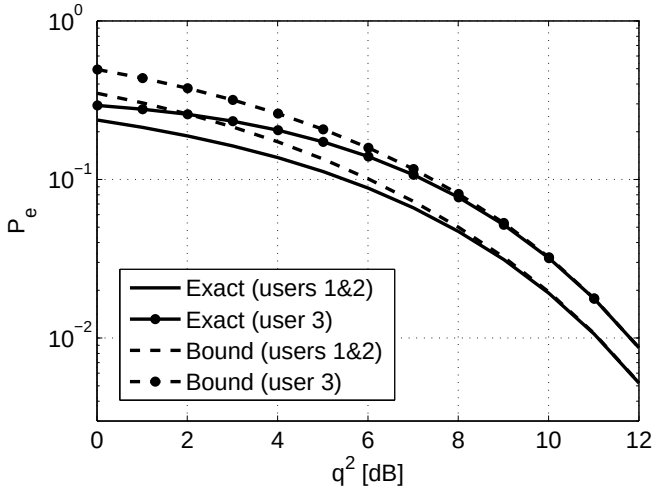

Figure 6.14: Comparison of exact BER to upper bound in two-dimensional case.

For each point the closest adjacent point producing an erroneous decision is isolated by inserting space between them. After that, it is checked if all erroneous decision regions are covered by this space. If not, more spaces are inserted until all erroneous decision regions are isolated. Thus, For the $(5, 4)$ constellation analogous bounding as with the three-dimensional case gives

$$P_{e1} = P_{e2} = P_{e3} = P_{e4} < \frac{43}{16} Q\left(q\right) \tag{6.78}$$

$$P_{e5} < \frac{81}{16} Q\left(q\right). \tag{6.79}$$

The average BER is calculated from (6.78) and (6.79)

$$P_{av} < \frac{4P_{e1} + P_{e5}}{5} = \frac{253}{80} Q(q) \tag{6.80}$$

6.4.4 Comparison of BER results

It is interesting to see how tight the obtained bound for $L = 2$ is, since also exact calculations exist. In Fig. 6.14 exact BER and upper bound for the $(3, 2)$ constellation are given. It is seen that the bound is quite tight and converges with the exact curve after $q^2 \approx 7.5$ dB. BER estimates for $(4, 3)$ and $(5, 4)$ constellations from equations (6.77) and (6.80) are given in Fig. 6.15 along with an estimate for the $(3, 2)$ constellation from (6.74) and curve for the orthogonal single-user case. Exact reference curves do not exist for $(4, 3)$ and $(5, 4)$ constellations, but in chapter 8 they are compared to

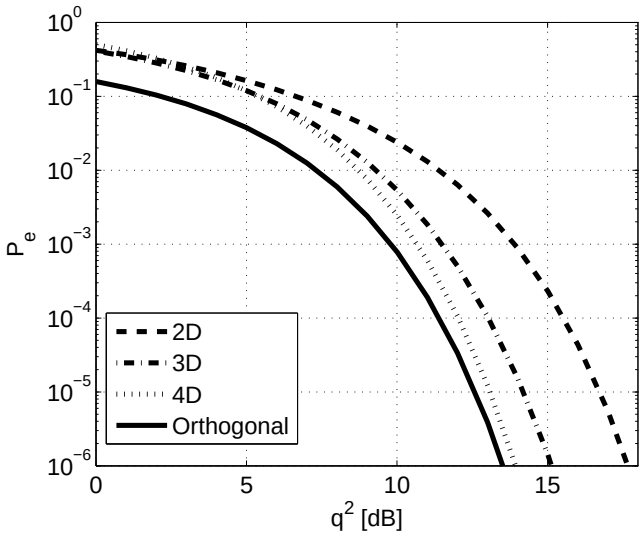

Figure 6.15: Estimated BER curves.

simulation results in the AWGN channel. Results indicate that these bounds are also tight. It can be seen that the loss in BER is larger for the $(5, 4)$ constellation at $P_e = 10^{-6}$ than indicated by loss in minimum Euclidean distance, which gives the loss in asymptotic case. Losses from Fig. 6.15 at $P_e = 10^{-6}$ are approximately 0.5 dB, 1.7 dB, and 4.1 dB for $(5, 4)$, $(4, 3)$, and $(3, 2)$ constellations, respectively. Losses for $(4, 3)$ and $(3, 2)$ constellations correspond accurately to values given in Table 6.1.

6.5 Chapter summary

In this chapter, extensive study on GO-CDMA signature ensemble design was given. The signature ensemble design was performed with unique signature per user strategy, where signatures are special linear combinations of initial orthogonal signatures. The design aimed to optimize the linear dependence of signatures to have maximal separation of all possible group signals. The chapter started with symmetric group signal constellations. Signature ensembles were analytically derived for subspace dimensions 2, 3 and 4 populated with one supplementary user. After comparison to results from literature it was concluded that the chosen approach to concentrate on symmetric constellation was valid. Detailed examples of signature ensembles for $N = 12$ were given, and the necessary conditions to obtain binary ensembles was discussed. After the design, BER performances of obtained ensembles were also calculated in the presence of AWGN. It was possible

to calculate closed form expression of BER for subspace dimension 2. For higher dimensions union bounding was performed due to very complex decision regions. Also, the scalability issue of GO-CDMA signature ensembles was discussed. It was concluded that they are quasi-scalable, meaning that only subset of all users is affected by the changes of the number of active users.

Chapter 7

Collaboratively coded group orthogonal CDMA

In previous chapters it has been assumed that each user is distinguished from other users by his signature. However, rigid one-to-one correspondence between signatures and users may be considered as needlessly binding in some cases. For instance, in the cellular radio downlink, the data of all users is under the control of the base station and may be in principle encoded jointly on the basis of so-called collaborative coding or *collaborative coding multiple access* (CCMA) [106]. Term collaborative coding was first used in [107]. Before that, the problem has been investigated under the name *coding for multiple access channels* (see [108, 109] and references therein). The basic idea of collaborative coding is quite similar to spread spectrum multiple access, or CDMA. It aims towards isolation of different users in channel based on code structure and without the division in time of frequency domain. For CDMA, the isolation is obtained with appropriate correlation properties of signatures.

As discussed in previous chapters, synchronous CDMA is mostly utilized in the downlink of a cellular system, or alternatively to separate different channels of one user. In both cases the transmitter controls all transmissions. Therefore, the combination of collaborative coding with S-CDMA is reasonable to investigate. In general, the idea of oversaturation CDMA combined with CCMA scheme was formulated by Fan and Darnell in [110]. Their aim was to show that hybrid system would gain better performance by exploiting merits from both systems and by compensating drawbacks in each system. CCMA permits high capacity and a large number of users (oversaturation) while CDMA is a very reliable communication method.

The oversaturation scheme combining group orthogonal CDMA and collaborative coding has been considered in [70, 71]. Here, the oversaturated synchronous CDMA using group orthogonal ensembles combined with collaborative coding is referred to as collaborative coded GO-CDMA (CCGO-CDMA). For GO-CDMA collaborative coding entails that N-dimensional space is divided into N/L orthogonal subspaces each of dimension L, and data bits of group of $L+s$ users within one subspace are jointly one-to-one mapped onto 2^{L+s} L-dimensional signal vectors. Every subspace is used to transmit data of $L+s$ users as described in chapter 6, but with no assignment of specific signatures to users. Instead of having unique signatures for each user, L-dimensional signature subspace is used to transmit bits of $L+s$ users ($s>0$). Transmitter structure for CCGO-CDMA system is illustrated in Fig. 7.1. Notations b_i, $\mathbf{h}_i$ and $\mathbf{y}$ are used for bit, orthogonal signature and observation, respectively.

Now, the signature ensemble design is not bound by the restraint of the previous chapter which states that group signals are only linear combinations of $L+s$ bit-manipulated fixed L-dimensional vectors. It enables finding the best possible $(L+s, L)$ constellation of subspace signal vectors with globally maximal distinguishability between them, which utilizes available time-frequency resource in the most effective way. It will be shown in the following sections that CCGO-CDMA possesses significantly higher performance than pure GO-CDMA.

CCGO-CDMA receiver, illustrated in Fig. 7.2 with notations d_i for decision statistic and $\mathbf{p}$ for constellation point vector, intended to retrieve i-th data stream is actually tuned to the signature subset covering i-th user. It is not subject to MAI from the other received signature subsets because all of these subsets are orthogonal. Receiver first restores bit pattern of all $L+s$ users knowing the rule of correspondence between transmitted signals and users' bit patterns, and afterwards abandons needles data of all users but the i-th one. If the proposed scheme is applied to channelization, all received bits belong to user in question, and bits are not dropped.

Now, the key issue is discussed: How to design an appropriate CCGO-CDMA signature ensemble, or in other words, $(L+s, L)$ constellation for each subspace?

7.1 CCGO-CDMA signature ensemble design

In the following formulation, average energy E_S over all 2^{L+s} different signal vectors is set equal to the total energy of signatures employed in the scheme of chapter 6:

$$E_S = \frac{1}{2^{L+s}} \sum_{k=1}^{2^{L+s}} E_{ck} = (L+s)E_b, \tag{7.1}$$

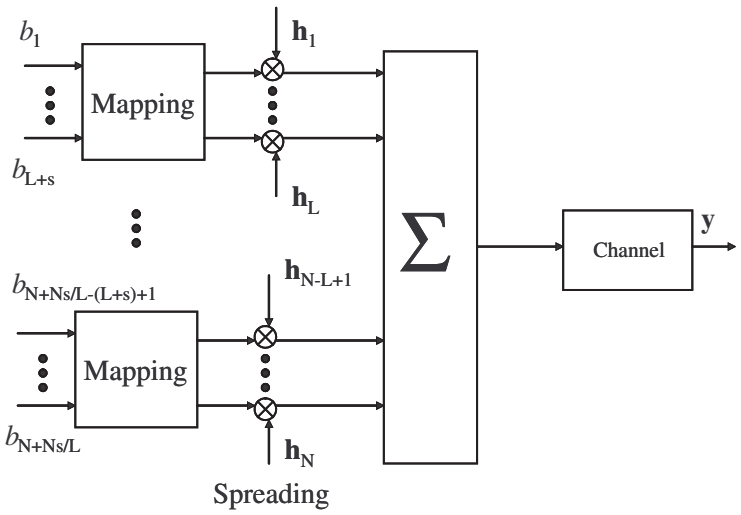

Figure 7.1: Block diagram for CCGO-CDMA transmitter.

where E_{ck} is the energy of k-th signal vector in the collaborative coding scheme and E_b is energy per bit per signature in the signature per user scheme. Such a normalization puts both schemes into equivalent conditions considering energy consumption.

From the geometrical point of view, finding a constellation of maximally distant 2^{L+s} L-dimensional vectors of fixed average energy (i.e. squared length) may be treated in terms of a densest packing of 2^{L+s} spheres in the L-dimensional space. Classical sphere packing theory [13,111] aims to find such a packing of equal non-overlapping spheres that the ratio between the sum of volumes of all the packed spheres and the volume of the obtained packing is maximal. Globally optimal results are not known for space dimension $L \geq 3$. However, among lattice structures optimal packing is known for space dimension $L \leq 8$. Lattice packing is defined by the following property: origin is one of sphere centers, and if there are sphere centers $\mathbf{u}$ and $\mathbf{v}$, then there are also spheres with centers $\mathbf{u} + \mathbf{v}$ and $\mathbf{u} - \mathbf{v}$, i.e. possible center points form an additive group [111].

It should be noted, that in this case, density criterion according to (7.1), differs from a classical approach, since spheres should be packed to guarantee minimal average squared distance of sphere centers from the origin. However, as it will be shown, the solutions taken from classical sphere packing theory may assist (at least for small dimensions L) in finding good collaborative codes.

Two approaches from sphere packing theory are interesting when spheres represent signals: lattice volume packing (LVP) and packing of points on sphere surface (SSP). Volume packing results in optimal constellations from

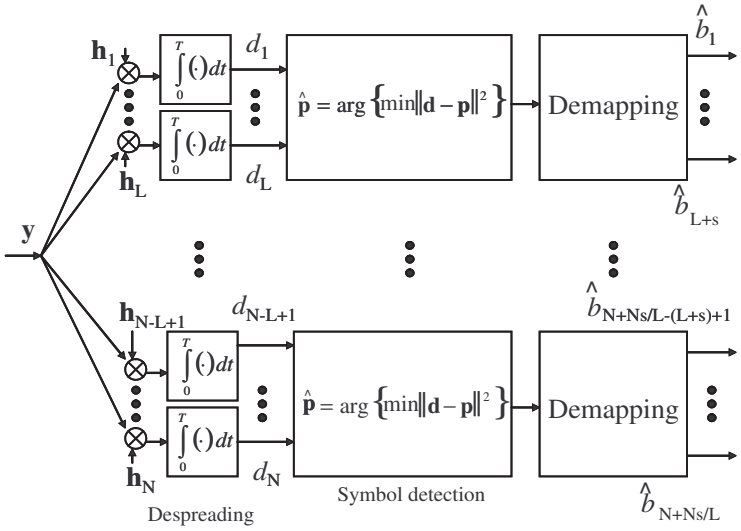

Figure 7.2: Block diagrams for CCGO-CDMA receivers.

the viewpoint of sphere packing theory. However, as we will see later, this in not necessarily the case for signal design, where the optimization criteria is actually to maximize the radius of sphere while keeping average energy of signal constellation fixed. The restriction of lattice structure is imposed to utilize results from sphere packing efficiently. The regular structure of lattice also alleviates the task of receiver. The packing points on a sphere surface correspond to the case where all signals have equal energy.

Optimal LVP constellation includes the origin, or zero-vector, as one of the symbol points. Therefore, symmetrical version of LVP, denoted with SLVP, is also considered. The zero-vector is excluded because it can be problematic in some applications. Additionally, constellation points are placed to achieve symmetry between all coordinate axes. Asymmetry of LVP enables of shifting to constellation so that the centroid falls into origin. This lowers the average energy requirement. The obtained constellation is denoted as balanced LVP (BLVP). To complete the signal design a version of SSP, denoted with ZSSP that includes the zero-vector is also considered.

SLVP is constructed by first assigning signal points to 2^L apex points of square (or cubic in three-dimensional space), whose center resides in the origin. Next $2L$ signal points are assigned along the coordinate-axes outside this square (cubic). For the $(3, 2)$ constellation all points can be assigned this way (see Fig. 7.3(c)), while for the $(4, 2)$ constellation familiar 16-QAM (quadrature amplitude modulation) constellation is chosen. For constellations having $L > 2$ remaining points that do not fit to apex points or cannot be put on the axis are assigned so that sphere surface touches the middle

point of edge of cubic (see for example (7.22)). For $(5,3)$, $(6,5)$ and $(7,5)$ the SLVP is formed from LVP by just moving zero-vector to position that makes the constellation symmetric (compare (C.17) with (C.18)). The reason is that the required condition to have completely symmetric constellation leads to unnecessarily complex geometrical considerations, i.e. determining coefficients α and β as was done in (7.22), while the achievable gain is negligible. To generalize a signal design task with high space dimensions it is reasonable to choose a method, which is as easy as possible to express as a systematic procedure.

Optimal SSP and ZSSP constellations may be found from [112], where packing points on sphere surface that have maximal separation between them is considered. Putatively optimal designs are given for $L = 3, 4, 5$ with up to 130 points packed on the sphere surface. From that selection, packings having 2^{L+s} points are chosen for SSP and packings having $2^{L+s}-1$ for ZSSP, where the zero-vector is one of the signals.

In principle, there is no upper limit on the subspace dimension, or in the number signal points inserted to chosen subspace dimension. The structure for optimal lattice structure is different for dimension $L > 5$ than for smaller dimensions [111], but they are still easily obtained. The problem with packing on sphere surface is that packings must be optimized numerically. For this thesis this procedure was not attempted and the largest investigated dimension is five, since packings are not tabulated in [112] for $L > 5$, or $2^{L+s} > 128$.

Specific examples are given for $L = 2, 3, 4, 5$ and $s = 1, 2$. It is impractical to give exhaustive list of performances of different constellation types, signal space dimensions, and the number or signal points due to very large number of parameter combinations. However, it is possible to draw some conclusions and general considerations based on given examples, which indicate that

- Increasing $L > 4$ is reasonable. The maximum minimum Euclidean distance can be improved beyond the limit discussed in section 6.1.4.

- Also, increasing $s > 1$ is reasonable. With fixed oversaturation efficiency, the constellation with higher dimension having more supplementary users performs better. It is also possible to increase oversaturation efficiency over 50%, which was considered to be the upper limit of GO-CDMA with reasonable loss.

- Restriction of lattice form of LVP becomes prohibitive, when the signal space dimension grows.

The choice of signal space dimension, the number of signal points in the constellation and constellation type requires trade-off between oversaturation efficiency, energy efficiency, and receiver complexity. Specific examples

starting with oversaturation of L-dimensional space by only one extra user ($s = 1$) are presented next.

7.2 Oversaturation of one subspace with one user

7.2.1 Two-dimensional subspace

In the case of a $(3, 2)$ constellation spheres reduce to circles. Thus, the aim is to place $2^3 = 8$ circles on the plane with equal diameter that is as great as possible at average squared distance from the origin fixed by (7.1).

Lattice Volume Packing

First, consider the densest two-dimensional LVP [111] of Fig. 7.3(a). Signal vectors, $\mathbf{p}_i$, forming constellation point matrix $\mathbf{P}$ (with $\mathbf{p}_i$ as columns) can be directly given from the Fig. 7.3(a) with elementary geometry remembering that the distance between adjacent sphere centers is equal to the minimum Euclidean distance $d_{\min}$:

$$\mathbf{P}_{LVP}^{2D} = d_{\min} \begin{pmatrix} 0 & \cos\frac{\pi}{6} & \cos\frac{3\pi}{6} & \cos\frac{5\pi}{6} & \cos\frac{7\pi}{6} & \cos\frac{9\pi}{6} & \cos\frac{11\pi}{6} & \sqrt{3}\cos\frac{\pi}{3} \\ 0 & \sin\frac{\pi}{6} & \sin\frac{3\pi}{6} & \sin\frac{5\pi}{6} & \sin\frac{7\pi}{6} & \sin\frac{9\pi}{6} & \sin\frac{11\pi}{6} & \sqrt{3}\sin\frac{\pi}{3} \end{pmatrix}, \tag{7.2}$$

which results in average energy and minimum distance

$$\begin{aligned} E_S &= \frac{1}{8}\left(1 \cdot 0 + 6 \cdot d_{\min}^2 + 1 \cdot 3d_{\min}^2\right) = \frac{9}{8}d_{\min}^2 \\ \Rightarrow d_{\min}^2 &= \frac{8E_S}{9} = \frac{8E_b}{3} \approx 2.67E_b. \end{aligned}$$

Comparison of this figure with minimum distance of orthogonal signaling mentioned earlier ($d_{\min}^2 = 4E_b$) shows energy loss due to oversaturation $\gamma = 4/(8/3) = 3/2 \approx 1.76$ dB, which is significantly (2.4 dB) lower than with the optimal signature per user $(3, 2)$ constellation (see Table 6.1). Although, this packing is the densest according to sphere packing theory, the minimum distance can still be increased with the constellation illustrated in 7.3(b). The asymmetry of the constellation allows to shift it so that its centroid falls into the origin, which minimizes the average energy of the constellation. Let $\mathbf{u}$ denote vector to be subtracted from each constellation point vectors to enable this shift:

$$\mathbf{u} = \frac{1}{M}\sum_{i=0}^{M-1}\mathbf{p}_i = \frac{1}{8}d_{\min}\begin{pmatrix} \sqrt{3}\cos\frac{\pi}{3} \\ \sqrt{3}\sin\frac{\pi}{3} \end{pmatrix}. \tag{7.3}$$

When the $\mathbf{u}$ is subtracted from each signal, the average energy of constellation is reduced without changing relative distances between constellation

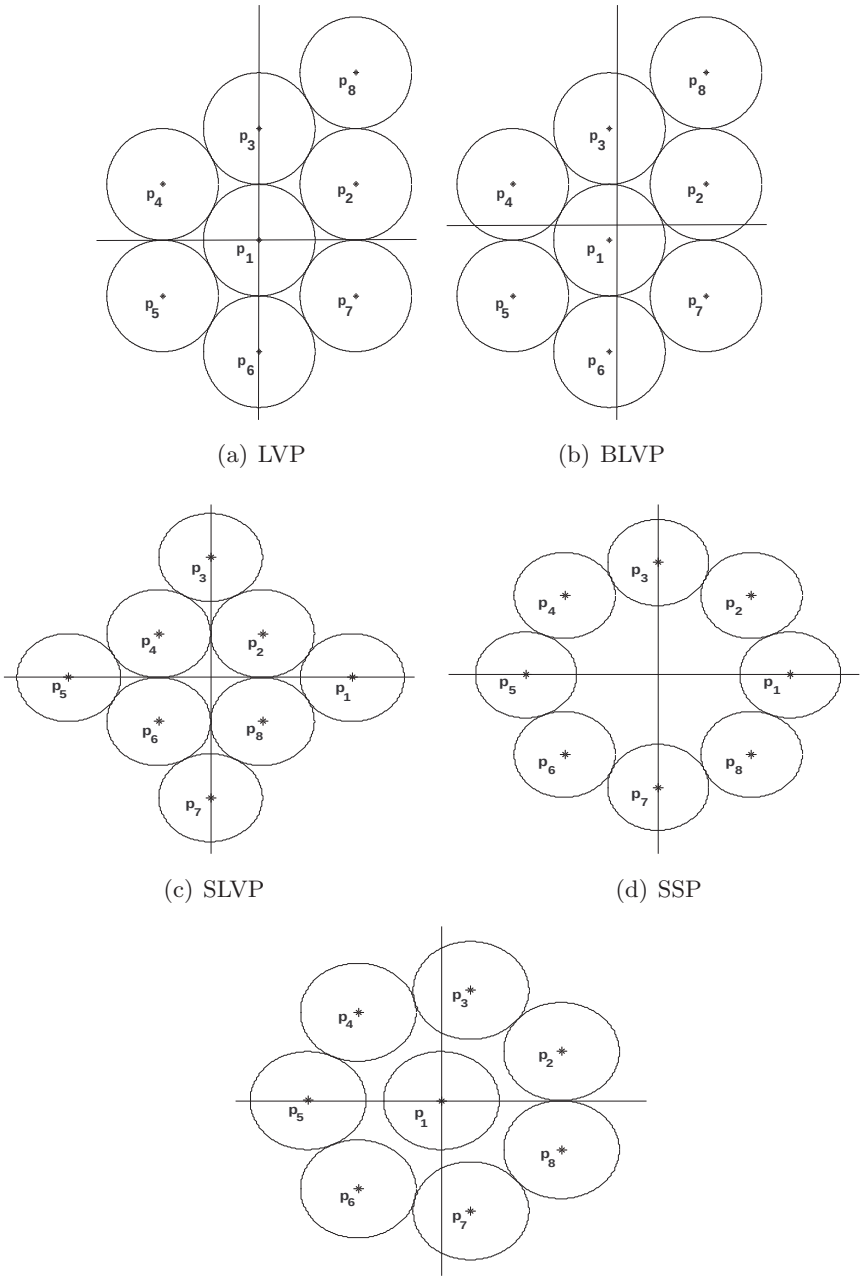

(a) LVP (b) BLVP

(c) SLVP (d) SSP

(e) ZSSP

Figure 7.3: Two-dimensional subspace constellations.

points. The new average energy is

$$E' = \frac{1}{M}\sum_{i=0}^{M-1} ||\mathbf{p}_i - \mathbf{u}||^2 = E_S - ||\mathbf{u}||^2 = \frac{9}{8}d_{\min}^2 - \frac{3}{64}d_{\min}^2 = \frac{69}{64}d_{\min}^2. \quad (7.4)$$

Now, the minimum distance in balanced constellation can be increased so that the average energy $E' = E_S = 3E_b$. From (7.4)

$$d_{\min,b}^2 = \frac{64}{69}E' = \frac{64}{23}E_b \approx 2.78E_b, \quad (7.5)$$

which lowers loss to $\gamma \approx 1.58$ dB. Such a displacement results in constellation

$$\mathbf{P}_{BLVP}^{2D} = \frac{d_{\min,b}^2}{d_{\min}^2}\mathbf{P}_{LVP}^{2D} - \frac{1}{8}d_{\min,b}^2 \begin{pmatrix} \sqrt{3}\cos\frac{\pi}{3} \\ \sqrt{3}\sin\frac{\pi}{3} \end{pmatrix}. \quad (7.6)$$

This constellation type is referred to as balanced LVP (BLVP). Here, it can be seen that classical sphere packing does not necessarily give the optimal constellation directly when the average energy of constellation is considered.

If the zero vector, for some reason, cannot be the one of signals in the constellation, the best constellation when distance property is considered is SLVP, which is illustrated in Fig. 7.3(c) resulting in

$$\mathbf{P}_{SLVP}^{2D} = d_{\min}\begin{pmatrix} \frac{1+\sqrt{3}}{2} & \frac{1}{2} & 0 & -\frac{1}{2} & -\frac{1+\sqrt{3}}{2} & -\frac{1}{2} & 0 & \frac{1}{2} \\ 0 & \frac{1}{2} & \frac{1+\sqrt{3}}{2} & \frac{1}{2} & 0 & -\frac{1}{2} & -\frac{1+\sqrt{3}}{2} & -\frac{1}{2} \end{pmatrix}, \quad (7.7)$$

Average energy of SLVP constellation is calculated as

$$E_S = \frac{1}{8}\left(4\cdot\frac{1}{2}d_{\min}^2 + 4\cdot\frac{(1+\sqrt{3})^2}{4}d_{\min}^2\right) = \frac{3+\sqrt{3}}{4}d_{\min}^2, \quad (7.8)$$

which provides

$$d_{\min}^2 = \frac{12E_b}{3+\sqrt{3}} \approx 2.54E_b, \quad (7.9)$$

which results in $\gamma \approx 1.98$ dB.

Sphere Surface Packing

Another approach in sphere packing theory is packing points on sphere surface aiming for maximal separation of points guaranteeing maximal minimum Euclidean distance between them. For signal constellations it corresponds to equal energy signals, i.e. SSP constellation. For two-dimensional case the signal constellation becomes the familiar 8-PSK pattern as shown in Fig. 7.3(d)

$$\mathbf{P}_{SSP}^{2D} = \sqrt{E_s}\begin{pmatrix} 1 & \cos\frac{\pi}{4} & 0 & -\cos\frac{\pi}{4} & -1 & -\cos\frac{\pi}{4} & 0 & \cos\frac{\pi}{4} \\ 0 & \sin\frac{\pi}{4} & 1 & \sin\frac{\pi}{4} & 0 & -\sin\frac{\pi}{4} & -1 & -\sin\frac{\pi}{4} \end{pmatrix}. \quad (7.10)$$

The squared distance between adjacent points is

$$d_{\min}^2 = 2E_s - 2E_s \cos\frac{\pi}{4} \approx 1.76E_b, \tag{7.11}$$

which results in $\gamma \approx 3.57$ dB. This loss is rather big, but it is still 0.62 dB better than the value obtained with the optimal GO-CDMA 2D-signal set in Table 6.1.

The energy efficiency of SSP can be increased if the zero-vector is included into the constellation. This constellation is denoted with ZSSP. The resulting constellation is shown in Fig. 7.3(e). The constellation points are

$$\mathbf{P}_{ZSSP}^{2D} = \frac{d_{\min}}{2\sin\frac{\pi}{7}} \begin{pmatrix} 0 & \cos\frac{\pi}{7} & \cos\frac{3\pi}{7} & \cos\frac{5\pi}{7} & -1 & \cos\frac{9\pi}{7} & \cos\frac{11\pi}{7} & \cos\frac{13\pi}{7} \\ 0 & \sin\frac{\pi}{7} & \sin\frac{3\pi}{7} & \sin\frac{5\pi}{7} & 0 & \sin\frac{9\pi}{7} & \sin\frac{11\pi}{7} & \sin\frac{13\pi}{7} \end{pmatrix}. \tag{7.12}$$

Average energy is

$$E_S = \frac{1}{8}\left(1 \cdot 0 + 7 \cdot \frac{d_{\min}^2}{4\sin^2\frac{\pi}{7}}\right), \tag{7.13}$$

and the minimum squared distance in this case

$$d_{\min}^2 = \frac{32\sin^2\frac{\pi}{7}}{7} E_S \approx 2.58E_b, \tag{7.14}$$

which in comparison to orthogonal signaling results in loss of $\gamma \approx 1.90$ dB. When compared to best possible packing this suboptimal constellation is only 0.32 dB worse.

7.2.2 Three-dimensional subspace

Lattice Volume Packing

The densest LVP in 3D-space is a well-known face-centered cubic (fcc) lattice [111]. Centers for spheres are obtained by taking points of cubic lattice, whose coordinates add up to even integers. Thus, the signal matrix can be, for example,

$$\mathbf{P}_{LVP}^{3D} = \frac{d_{\min}}{\sqrt{2}} \begin{pmatrix} 0 & 1 & 1 & 0 & -1 & -1 & 0 & 1 & 1 & 0 & -1 & -1 & 0 & 2 & 0 & -2 \\ 0 & 1 & 0 & 1 & -1 & 0 & -1 & -1 & 0 & 1 & 1 & 0 & -1 & 0 & 2 & 0 \\ 0 & 0 & 1 & 1 & 0 & -1 & -1 & 0 & -1 & -1 & 0 & 1 & 1 & 0 & 0 & 0 \end{pmatrix}. \tag{7.15}$$

The average energy is calculated as

$$E_S = \frac{1}{16}\left(1 \cdot 0 + 12 \cdot d_{\min}^2 + 3 \cdot 2d_{\min}^2\right) = \frac{9}{8}d_{\min}^2 = 4E_b. \tag{7.16}$$

Squared minimum distance for this $(4, 3)$ constellation is

$$d_{\min}^2 = \frac{32E_b}{9} \approx 3.56E_b, \tag{7.17}$$

which implies that the loss against orthogonal signals is $\gamma \approx 0.51$ dB. Again, this constellation is asymmetric. If the centroid of constellation is balanced to the origin by subtracting $\mathbf{u}$:

$$\mathbf{u} = \frac{1}{M}\sum_{i=0}^{M-1}\mathbf{p}_i = \frac{1}{16}\frac{d_{\min}}{\sqrt{2}}\begin{pmatrix}0\\2\\0\end{pmatrix} \tag{7.18}$$

from each point vector the average energy of constellation is reduced without changing relative distances between constellation points. The new average energy is

$$E' = \frac{1}{M}\sum_{i=0}^{M-1}||\mathbf{p}_i - \mathbf{u}||^2 = E_S - ||\mathbf{u}||^2 = \frac{9}{8}d_{\min}^2 - \frac{1}{128}d_{\min}^2 = \frac{143}{128}d_{\min}^2. \tag{7.19}$$

Now, the minimum distance in the balanced constellation can be increased so that the average energy $E' = E_S = 4E_b$. From (7.4)

$$d_{\min,b}^2 = \frac{128}{143}E' = \frac{512}{143}E_b \approx 3.58E_b, \tag{7.20}$$

which lowers loss to 0.48 dB, and the obtained constellation is

$$\mathbf{P}_{BLVP}^{3D} = \frac{d_{\min,b}^2}{d_{\min}^2}\mathbf{P}_{LVP}^{3D} - \frac{d_{\min,b}}{16\sqrt{2}}\begin{pmatrix}0\\2\\0\end{pmatrix}. \tag{7.21}$$

The symmetric lattice packing is formed similarly as in two-dimensional case.

$$\mathbf{P}_{SLVP}^{3D} = \frac{d_{\min}}{2} \times \begin{pmatrix} 1 & 1 & 1 & -1 & 1 & -1 & -1 & -1 & \alpha & 0 & 0 & -\alpha & 0 & 0 & \beta & \beta \\ 1 & 1 & -1 & 1 & -1 & 1 & -1 & -1 & 0 & \alpha & 0 & 0 & -\alpha & 0 & \beta & \beta \\ 1 & -1 & 1 & 1 & -1 & -1 & 1 & -1 & 0 & 0 & \alpha & 0 & 0 & -\alpha & 0 & 0 \end{pmatrix}. \tag{7.22}$$

with $\alpha = 1 + \sqrt{2}$ and $\beta = 1 + \sqrt{6}/2$. The average energy is

$$E_S = \frac{1}{16}\left(8 \cdot \frac{3}{4}d_{\min}^2 + 6 \cdot \frac{3+2\sqrt{2}}{4}d_{\min}^2 + 2 \cdot \frac{5+2\sqrt{6}}{4}d_{\min}^2\right) =$$

$$= \frac{(52 + 12\sqrt{2} + 4\sqrt{6})}{64}d_{\min}^2 = 4E_b, \tag{7.23}$$

from where minimum squared distance is calculated as

$$d_{\min}^2 = \frac{128E_b}{26 + 6\sqrt{2} + 2\sqrt{6}} \approx 3.25E_b. \tag{7.24}$$

The resulting loss $\gamma \approx 0.90$ dB.

Packing on sphere surface

If equal energy constellation is of interest, SSP constellation center coordinates can be taken from [112], where points on a sphere surface having maximal separation are found. This choice leads to loss $\gamma \approx 1.10$ dB. Constellation is

$$\mathbf{P}_{SSP}^{3D} = \sqrt{E_S} \cdot 10^{-1} \begin{pmatrix} 1.2661 & 9.6355 & -2.3567 \\ -5.9181 & 7.7086 & 2.3567 \\ 0.8112 & 6.1735 & 7.8249 \\ -3.7917 & 4.9389 & -7.8249 \\ -9.6355 & 1.2661 & -2.3567 \\ -7.7086 & -5.9181 & 2.3567 \\ -6.1735 & 0.8112 & 7.8249 \\ -4.9389 & -3.7917 & -7.8249 \\ -1.2661 & -9.6355 & -2.3567 \\ 5.9181 & -7.70861 & 2.3567 \\ -0.8112 & -6.1735 & 7.8249 \\ 3.7917 & -4.9390 & -7.8249 \\ 9.6355 & -1.2661 & -2.3567 \\ 7.7086 & 5.9181 & 2.3567 \\ 6.1735 & -0.8112 & 7.8250 \\ 4.9390 & 3.7917 & -7.8250 \end{pmatrix}^T . \quad (7.25)$$

If zero vector is allowed to be a signal point and other signal points have equal distance from the origin, the packing from [112] provides $\gamma \approx 0.61$ dB.

$$\mathbf{P}_{ZSSP}^{3D} = \frac{16}{15}\sqrt{E_S} \cdot 10^{-1} \begin{pmatrix} 0 & 0 & 0 \\ 3.0518 & -1.8272 & 9.3460 \\ -4.9070 & -4.0745 & -7.7019 \\ -8.5092 & -5.2297 & 0.4938 \\ 7.0122 & -6.5709 & 2.7664 \\ 9.5556 & -6.2050 & -2.9472 \\ 4.6401 & 7.1616 & -5.2134 \\ 3.2931 & -0.7129 & -9.4152 \\ -9.1977 & 3.7448 & 1.1741 \\ -1.4862 & -8.4243 & 5.1790 \\ -5.8471 & -1.0582 & 8.0431 \\ 2.4506 & -8.4240 & -4.7991 \\ -3.6517 & 4.8611 & -7.9394 \\ -0.5941 & 6.2769 & 7.7619 \\ -2.5575 & 9.6602 & -0.3730 \\ 7.2714 & 5.9964 & 3.3421 \end{pmatrix}^T . \quad (7.26)$$

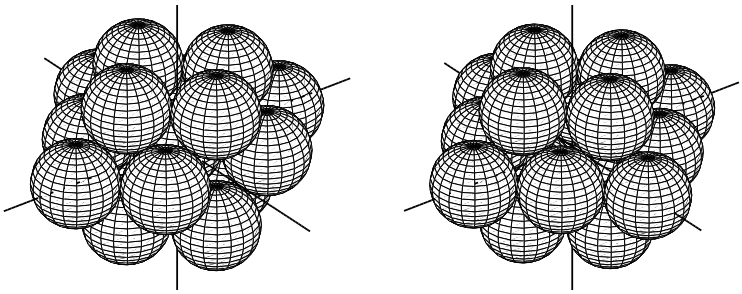

(a) LVP (b) SLVP

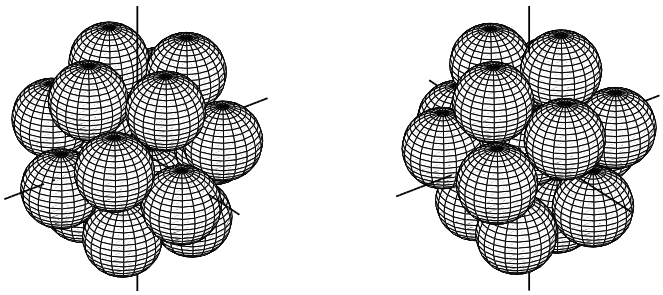

(c) SSP (d) ZSSP

Figure 7.4: Three-dimensional subspace constellations.

Table 7.1: Results for 2D and 3D constellations ($s = 1$)

Constellation	2D ($e_{ov} = 1.50$)		3D ($e_{ov} = 1.33$)	
	$d^2_{\min}$	γ [dB]	$d^2_{\min}$	γ [dB]
SSP	1.76	3.57	3.10	1.10
SLVP	2.54	1.98	3.20	0.90
ZSSP	2.58	1.90	3.45	0.61
LVP	2.67	1.76	3.56	0.51
BLVP	2.78	1.58	3.63	0.48

Signal optimization results for both two- and three-dimensional cases are summarized in Table 7.1. Obtained constellations are illustrated in Fig. 7.4.

7.2.3 Four- and five-dimensional subspaces

The densest lattice in 4- and 5-dimensional cases is a so-called checkerboard lattice where the coordinates of sphere centers add up to an even integers [111]. However, it is interesting to see that the densest packing is no more optimal from the minimum energy point-of-view under small oversaturation efficiencies, as was the case with 2D- and 3D-constellations. In fact, in 4D-

Table 7.2: Results for 4D and 5D constellations ($s = 1$)

Constellation	4D ($e_{ov} = 1.25$)		5D ($e_{ov} = 1.20$)	
	$d^2_{\min}$	γ [dB]	$d^2_{\min}$	γ [dB]
SLVP	4	0	4.36	−0.38
SSP	4.04	−0.05	4.73	−0.73
LVP	4.21	−0.22	4.46	−0.48
BLVP	4.22	−0.23	4.47	−0.48
ZSSP	4.22	−0.24	4.83	−0.82

and 5D-cases the ZSSP constellation is better if maximal minimum distance between signal points is a criterion. In 5D-case, even the equal energy constellation is better than the constellation from optimal lattice packing. Another interesting aspect is that according to the previous chapter, there is no point in increasing subspace dimension to five in the signature per user strategy, since maximal minimum squared distance cannot be greater than $d^2_{\min} = 4$ for $L \geq 4$. However, using collaborative coding in signal design, the minimum distance is improved further when $L \geq 4$. Results for different $(5, 4)$ and $(6, 5)$ constellations are shown in Table 7.2. Constellation matrices are listed in appendix C. LVP constellation is obtained as a checkerboard lattice structure. BLVP is created the same way as for smaller subspace dimension, but the method for SLVP differs from 2- and 3-dimensional cases. This means that constellation point from the origin is just moved so that the constellation becomes symmetric.

Equal energy constellations (SSP and ZSSP) are again taken from [112]. It is seen from the Table 7.2 that the minimum distance is in fact better than with conventional orthogonal signaling (negative loss implies gain). It can be also seen that the effect of balancing is negligible when the number of signal points in constellation is large.

7.3 Oversaturation of one subspace with two users

For GO-CDMA is was seen that oversaturating subspaces with more than one ($s = 1$) user was not profitable. However, the situation changes for CCGO-CDMA. Results become interesting when subspaces are oversaturated by two users ($s = 2$). In the case of signature per user approach similar attempt leads to approximately 1 dB higher energy loss than oversaturation of subspaces with only one extra user. With collaborative coding, the performance can be further enhanced by adding more users to subspaces (increasing s), since the energy of one extra user is available to increase minimum distance. Constellation design follows the same principles as for $s = 1$. Results for $(4, 2)$, $(5, 3)$, $(6, 4)$ and $(7, 5)$ constellations are illustrated

Table 7.3: Results for 2D and 3D constellations ($s = 2$)

Constellation	2D ($e_{ov} = 2.00$)		3D ($e_{ov} = 1.67$)	
	$d^2_{\min}$	γ [dB]	$d^2_{\min}$	γ [dB]
SSP	0.60	8.17	2.06	2.87
ZSSP	0.74	7.34	2.16	2.68
SLVP	1.60	3.98	2.42	2.17
LVP	1.78	3.52	2.53	1.97
BLVP	1.79	3.49	2.54	1.97

Table 7.4: Results for 4D and 5D constellations ($s = 2$)

Constellation	4D ($e_{ov} = 1.50$)		5D ($e_{ov} = 1.40$)	
	$d^2_{\min}$	γ [dB]	$d^2_{\min}$	γ [dB]
SSP	3.13	1.07	3.92	0.08
ZSSP	3.19	0.99	3.97	0.03
SLVP	3.20	0.97	4.15	−0.16
LVP	3.28	0.86	4.19	−0.20
BLVP	3.28	0.86	4.19	−0.20

in Tables 7.3 and 7.4, where, again, negative loss means gain. Constellation matrices are given in appendix C.

7.4 Modulation mapping

The goal of modulation mapping is to assign bit patterns to constellation points in a way that symbol error results in minimum amount of bit errors, i.e. the Hamming distance, d_H, should be as small as possible between the bit patterns in the neighboring symbol points. In the optimal situation neighboring symbols differ only in one bit position. Then, a symbol error results only in one bit error assuming that errors happen only between adjacent decision regions. Preferable encoding, for example, for PSK and QAM signal constellations is Gray coding [13]. For the constellations designed in previous sections it is impossible to map bit patterns to symbols to guarantee the $d_H = 1$ between two constellation points at minimal Euclidean distance apart from the $(3, 2)$ SSP constellation and the $(4, 2)$ SLVP constellation, which are the familiar 8-PSK and 16-QAM constellations.

Since Hamming distance of unity between all neighboring symbol points is impossible to obtain with most constellation types in this chapter, some metric assessing of the efficiency of modulation mapping is required. Gray code penalty, G_p, is proposed in [113] for odd-bit QAM constellations. It is defined as "the average number of bit differences per adjacent decision re-

gion". In [113] peak Gray penalty (G_{pk}) is also defined to be "the maximum number of bit-errors per single symbol threshold error". Good modulation mappings have G_p near unity and G_{pk} equal to two. Penalty criteria can be formally given as

$$G_p = \frac{1}{M} \sum_{l=1}^{M} \frac{\sum_{i=1}^{I_l} d_H(i,l)}{I_l} \tag{7.27}$$

$$G_{pk} = \max_{l} \max_{i \in I_l} d_H(i,l), \tag{7.28}$$

where $M = 2^{L+s}$ is the number of constellation points, I_l is the number of neighbors (adjacent decision regions) of constellation point l at the minimum distance and $d_H(i,l)$ is the Hamming distance between constellation points i and l.

Using (7.27) bit error probability, P_b, can be estimated from symbol error probability P_e as [113]

$$P_b = \frac{G_p}{\log_2 M} P_e, \tag{7.29}$$

and P_e can be given with (3.45) in asymptotic case, or more accurately with [113]

$$P_e = \bar{I}_l Q(\Delta), \tag{7.30}$$

where $\bar{I}_l$ is the average number adjacent decision regions (Gilbert number) and Δ is the minimum distance (given with SNR) from signal point to decision region boundary (Gilbert distance). Thus, $\Delta = d_{\min}/(2\sqrt{2N_0})$. Fig. 7.5 shows potential effect of Gray code penalty. The experienced loss was calculated as

$$\text{loss [dB]} \ = 20 \log_{10} \left(\frac{\Delta_{G_p=1}}{\Delta} \right), \tag{7.31}$$

where

$$\Delta = Q^{-1} \left(\frac{\log_2 M \cdot P_b}{\bar{I}_l G_p} \right). \tag{7.32}$$

In Fig. 7.5 the loss is illustrated as a function of G_p for $M = 8, 32$. Parameter $\bar{I}_l = \log_2 M - 1$. It is seen that the energy loss due to bad modulation mapping may be significant. Hence, special attention is given on how to obtain mapping achieving low values of G_p.

In the following, three different strategies are considered for modulation mapping of constellations presented in this chapter. These procedures were presented in [71]. Here, the Gray code penalty is used to assess modulation mappings.

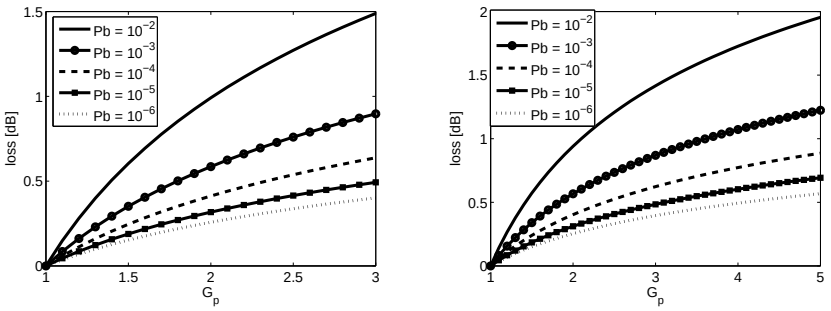

(a) $M = 8$ (b) $M = 32$

Figure 7.5: Potential effect of G_p ($\bar{I}_l = \log_2 M - 1$).

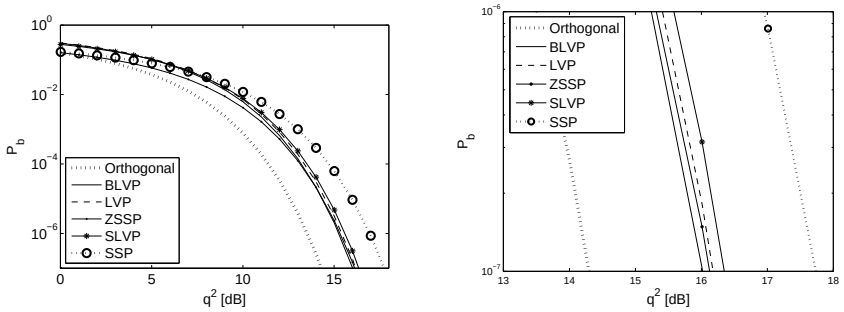

(a) LVP (b) SLVP

Figure 7.6: Estimated BER performance for $(3, 2)$ constellations.

7.4.1 Exhaustive search

The optimal solution could be found by exhaustive search, but its complexity becomes prohibitive when the number of constellation points is large. In this case, exhaustive search is feasible only for the two-dimensional constellations. Three-dimensional case with one supplemental user has up to $15! > 1.3 \cdot 10^{12}$ different permutations of four bit patterns to sixteen constellation points.

Mappings obtained with exhaustive search are presented in Table 7.5, where also corresponding Gray penalties and $\bar{I}_l$ are calculated. When interpreting the result, it should be noted that in the calculation of G_p for ZSSP constellation the zero vector is excluded in (7.27) and (7.28), since the distance from constellation point in the origin to any other point is greater than $d_{\min}$. Resulting BER from inserting $d_{\min}$ from Table 7.1 and $G_p, \bar{I}_l$ from 7.5 to (7.29) and (7.30) are illustrated in Fig. 7.6. Losses against orthogonal system depicted from Fig. 7.6(b) at $P_b = 10^{-7}$ are approximately 1.72 dB,

Table 7.5: Optimal modulation mapping for two-dimensional subspace.

	LVP	SLVP	SSP	ZSSP
$\mathbf{p}_1$	000	101	000	000
$\mathbf{p}_2$	100	000	100	101
$\mathbf{p}_3$	101	100	101	100
$\mathbf{p}_4$	001	110	111	110
$\mathbf{p}_5$	011	111	110	111
$\mathbf{p}_6$	010	011	010	011
$\mathbf{p}_7$	110	010	011	010
$\mathbf{p}_8$	111	001	001	001
G_p	1.27	1.31	1.00	1.14
G_{pk}	2	2	1	2
$\bar{I}_l$	3.5	3	2	2

1.83 dB, 1.88 dB, 2.05 dB, and 3.43 dB, for BLVP, ZSSP, LVP, SLVP, and SSP constellations. When compared to results presented in Table 7.1 it is observed that smaller G_p of ZSSP constellation than for LVP constellation results in smaller BER even though the minimum distance is larger. The topic will be further investigated with simulations in chapter 8.

7.4.2 Mapping by division of constellation to two subconstellations

Due to the huge amount of computation resources required by the exhaustive search, a suboptimal mapping algorithm must be employed for constellations with $L \geq 3$. The chosen mapping method follows the approach from [114], where the algorithm that has small running time for mapping bits to constellation points is considered. The idea is to partition the original signal constellation into two subconstellations in such a way that the minimum Euclidean distance in a subconstellation is maximum, or alternatively the occurrence of the minimum distance of the original constellation between points in subconstellation is as rare as possible.

In the initialization phase of mapping algorithm subconstellation points are labeled from $1, \ldots, M/2$ in one set and from $M/2+1, \ldots, M$ in the other set in such a way that any given point l in the first set and the point $l+M/2$ in the other set have the smallest Euclidean distance. The initialization can be described as follows:

1. Take a random pair of adjacent points, i.e. that have minimum distance, $d_{\min}$, and use them as initial points of two sets.

2. Take the closest point to the initial point of the second set, which is yet to be assigned, and assign it to the first set.

Table 7.6: Sub-optimal modulation mapping for two-dimensional subspace.

	LVP	SLVP	SSP	ZSSP
$\mathbf{p}_1$	101	000	000	110
$\mathbf{p}_2$	100	100	100	010
$\mathbf{p}_3$	001	111	101	000
$\mathbf{p}_4$	110	101	001	100
$\mathbf{p}_5$	011	011	011	101
$\mathbf{p}_6$	010	001	111	001
$\mathbf{p}_7$	111	110	110	011
$\mathbf{p}_8$	000	010	010	111
G_p	1.30	1.37	1	1.14
G_{pk}	3	3	1	2

3. Continue the procedure by always assigning the closest unassigned neighbor of previously assigned point to the set other than that contains this point.

After dividing signal points to two subconstellations, the mapping algorithm assigns bit patterns to constellation points pairwise such that $d_H = 1$ between constellation points l and $l + M/2$ in different sets. The bit pattern pair consists always of patterns $0x \ldots x$ and $1x \ldots x$. The algorithm tries to find the best bit pattern pair to match already assigned patterns. The best possible match would correspond to the case where all adjacent constellation points at the distance d_{min} have $d_H = 1$ between them. The algorithm can be described as follows

1. Assign $0 \ldots 0$ to the first point in the first set and $10 \ldots 0$ to the point $1 + M/2$, which is the the first point in the second set.

2. Take next pair of constellation points (2 and $2 + M/2$ in the first iteration) and go through all unassigned pairs of bit patterns. For every bit pattern pair calculate G_p from (7.27), where M now covers current pair and already assigned constellation points. The pair providing the minimum value of G_p is chosen.

3. Step two is repeated until all bit patterns are mapped.

It should be noted that the algorithm does not always produce the best possible solution. In the case of a PSK constellation the algorithm results in the Gray code, but e.g. for a rectangular QAM constellation the result will contain adjacent points having the $G_{pk} = \log_2 M$. The results of sub-optimal algorithm for the 2D-case are given in Table 7.6 for comparison to the exhaustive search in Table 7.5.

Table 7.7: Modulation mappings for three, four and five-dimensional subspaces (G_p / G_{pk} / $\bar{I}_l$).

	LVP	SLVP	SSP	ZSSP
$(4,2)$	1.37/2/4.13	1.00/1/3.00	1.00/1/2.00	1.07/2/2.00
$(4,3)$	1.53/3/6.00	1.37/3/5.00	1.31/2/4.00	1.41/3/4.00
$(5,3)$	1.71/4/6.63	1.67/5/6.13	1.69/3/4.13	1.53/3/3.87
$(5,4)$	1.99/5/10.13	2.03/4/9.00	1.91/4/6.43	2.06/4/6.26
$(6,4)$	2.25/5/11.03	2.24/6/10.00	2.25/5/7.63	2.20/5/6.61
$(6,5)$	2.27/5/14.44	2.38/6/13.38	2.35/6/9.13	2.33/6/8.60
$(7,5)$	2.77/6/17.50	2.71/7/17.06	2.70/7/9.38	2.80/7/9.37

7.4.3 Combination of sub-optimal algorithm with subset exhaustive search

As can be seen from the Table 7.6 of previous section there exists room for improvement in the mapping design for suboptimal algorithm. Therefore a method was implemented, where bit patterns are first assigned into m' constellation points by a suboptimal algorithm and for the rest $M - m'$ points bit patterns are then assigned by exhaustive search to provide the best possible match to the assigned patterns. In this case $M - m' = 10$ was considered feasible, thus the number of bit patterns to assign with suboptimal algorithm is $2^{L+s} - 10$. Gray code penalties for subspace dimensions $L > 2$ are illustrated in Table 7.7, where each cell contains information on obtained G_p / G_{pk} / $\bar{I}_l$. The result for G_p using only sub-optimal algorithm without utilizing exhaustive search is approximately 0.7 larger on average.

7.5 Chapter summary

In this chapter CCGO-CDMA signature ensemble design was considered. The collaborative coding methodology abandons unique signatures for each user. Instead, in the context of group orthogonality, each subspace acts as a common signature for users inside the subspace. In this case, there is much more freedom in subspace constellation design when compared to GO-CDMA.

Five constellation types were considered for $L = 2, 3, 4, 5$ and $s = 1, 2$. The choice of constellation type allows a trade-off in minimum distance and receiver implementation complexity. In addition to constellation design, modulation mapping has to be considered, since optimal Gray coding for bit patterns is not possible. Exhaustive search would be the optimal algorithm for mapping, but its running duration is prohibitive. Thus, a sub-optimal fast mapping algorithm was employed.

Constellation design reveals interesting results. First of all, the minimum Euclidean distance of orthogonal signaling can be surpassed with CCGO-CDMA when the average energy of signatures is set as equal in both systems. When compared to GO-CDMA it was seen that using a subspace dimension beyond four is profitable in increasing the minimum distance. Also, oversaturating subspaces with more than one user provides gain in minimum distance when the oversaturation is fixed.

Chapter 8

Simulated performance of group orthogonal CDMA in the AWGN and multipath channels

8.1 Simulation setup

The goals of the simulations are

- To verify theoretical considerations for BER of GO-CDMA and CCGO-CDMA in the AWGN channel from chapters 6 and 7.
- To observe the effect of multipath propagation on group orthogonal systems and make comparisons to the performance of conventional orthogonal system in similar conditions.
- To show that GO-CDMA and CCGO-CDMA are feasible in practice in the presence of a multipath channel.

The aim of the simulations was to keep the setup as simple as possible and to concentrate only on goals mentioned above. Therefore, many idealizations were utilized and communication system components not relevant to these analyzes were excluded, such as the channel coding. Simulations were performed with MATLAB® software, which enables clear illustration of results. The drawbacks are operation speed and memory consumption, which at times do not allow optimal accuracy of simulation results. All results are presented with error curves as the function of q^2 (SNR). Transmitted signals

for single bit interval are

$$\mathbf{x} = \begin{cases} \sum_{i=1}^{K} b_i \mathbf{h}_i, & \text{for orthogonal CDMA} \\ \sum_{i=1}^{K} b_i \mathbf{s}_i, & \text{for GO-CDMA} \\ \sum_{i=1}^{N/L} \sum_{j=1}^{L} p_i(j) \mathbf{h}_{(i-1)L+j}, & \text{for CCGO-CDMA} \end{cases}, \tag{8.1}$$

where $p_i(j)$ denotes the location of symbol point on j-th coordinate axis in i-th subspace. The observation is

$$\mathbf{y} = \mathbf{x} * \mathbf{g} + \mathbf{n}, \tag{8.2}$$

where $*$ denotes convolution operation and $\mathbf{g}$ is the channel impulse response vector. For the AWGN channel $\mathbf{g} = 1$. Receiver processing for orthogonal CDMA using single-user receiver was described in section 4.1 and for GO-CDMA in section 4.3.2. CCGO-CDMA block diagrams for transmitter and receiver were given by Fig. 7.1 and Fig. 7.2. For multipath channels aforementioned receivers must include processing to mitigate the effects of multipath propagation or resolve and combine different paths before despreading and detection. Otherwise, the inflicted MAI destroys the transmission altogether.

In the simulations of this chapter, the received bit stream is first equalized at the receiver, and despread by multiplying it with a time-synchronized replica of the signature followed by an integrator that aggregates N chips, i.e. all chips from one bit interval. The resulting decision statistics are utilized in detecting transmitted bits. For the orthogonal case the decision for the received bit for user i is simply $\hat{b}_i = \text{sign}(d_i)$ (see section 4.1). For GO-CDMA the receiver must compare observation $\mathbf{y}$ to 2^{L+s} possible transmitted group signal vectors. The decision $\hat{b} = (\hat{b}_1, \ldots, \hat{b}_{L+s})$ is the bit vector minimizing $||\mathbf{y} - \sum_i b_i \mathbf{s}_i||^2$. For CCGO-CDMA the same maximum-likelihood detection is used to find out transmitted symbols. After that, detected bits are obtained by table look-up according to utilized modulation mapping.

8.2 Results in the AWGN channel

8.2.1 GO-CDMA

In the AWGN channel the results do not depend on N, since subspaces do not interfere with each other. Results are illustrated in Fig. 8.1, where a curve of BER for non-oversaturated orthogonal system is also placed for comparison. Curves demonstrate the consistence of simulation results with the results for exact average BER given in 6.4.2 and appendix A for the $(3, 2)$ constellation. In Fig. 8.2 average estimated BER from (6.74), (6.77)

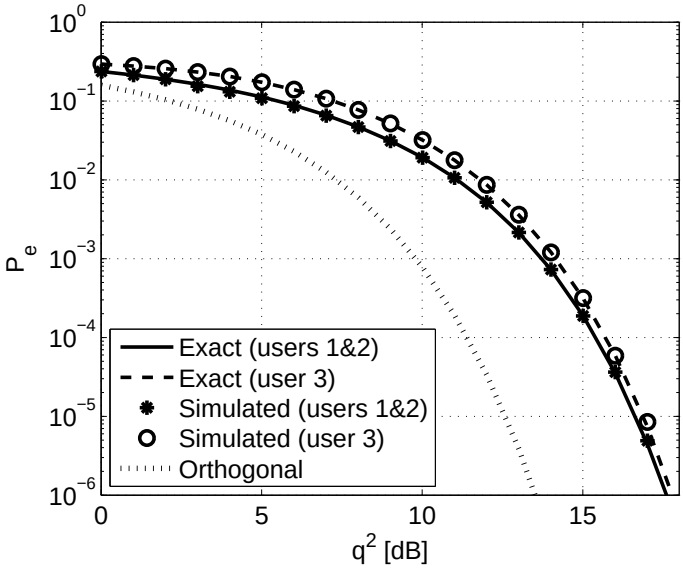

Figure 8.1: Exact and simulated BER for the $(3, 2)$ GO-CDMA constellation.

and (6.80) is compared to simulation results for $(3, 2)$, $(4, 3)$ and $(5, 4)$ constellations. It is seen that BER bounds are tight approximately after $q^2 = 8$ dB for all constellations. Simulation result correspond well to the losses indicated by minimum Euclidean distance from Table 6.1. Only for the $(5, 4)$ ensemble asymptotic loss is smaller (approximately 0.5 dB) than the experienced BER.

8.2.2 CCGO-CDMA

For the BER analysis of CCGO-CDMA all constellation types were analyzed for the $(3, 2)$ case. Results are shown in Fig. 8.3 (and Fig. 8.4 for LVP). For other constellation sizes the LVP constellation was chosen combined with the best possible modulation mapping available. Results are illustrated for $L = 2, 3, 4, 5$ and $s = 1$ in Fig. 8.4 and for $L = 2, 3, 4, 5$ and $s = 2$ in Fig. 8.5. Each figure includes estimated symbol error rate (SER) from (7.30), simulated SER, simulated BER and estimated BER from (7.29). It is seen that estimated curves correspond well to simulation results for two-dimensional constellations. For higher dimensions tighter bounds would be preferable. In the case ZSSP the bound is not adequate to take into account the effect from the symbol point in the origin, which clearly has an impact at small SNR values. It is interesting to notice that none of the CCGO-CDMA BER curves crosses the one for non-oversaturated orthogonal case before $P_e = 10^{-6}$ even though obtained minimum distances for $(5, 4)$, $(6, 5)$

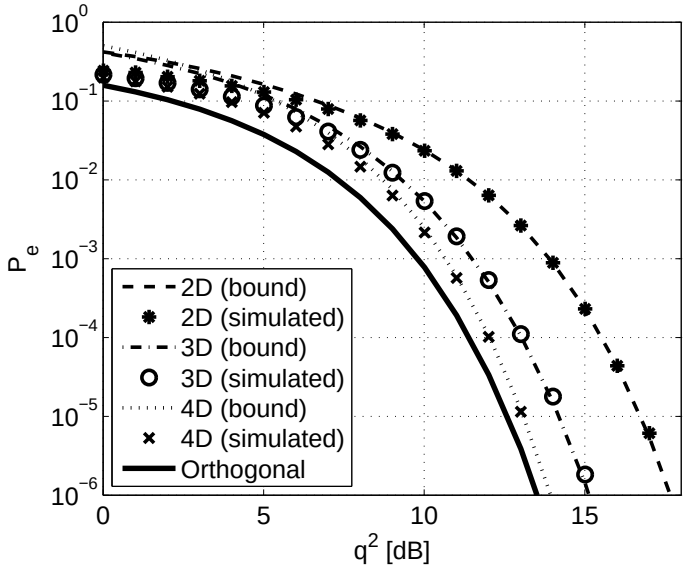

Figure 8.2: Estimated and simulated BER for GO-CDMA (all dimensions).

and $(7, 5)$ constellations indicate better performance. Smaller BER values should be investigated to observe curves reaching the asymptotic gain over orthogonal signaling. When losses in SNR are compared to those indicated by minimum Euclidean distance in chapter 7 it is evident that they are a bit larger due to Gray coding penalty. The difference is small for $L = 2$, but it grows for larger subspace dimensions. For example, when comparing losses from Fig. 8.3 and 7.1 they are only 0.1-0.2 dB larger at $P_e = 10^{-6}$ in simulations. However, the difference can be up to 0.6-0.7 dB for LVP constellations with $L = 4$ or $L = 5$ (see Fig. 8.4, Fig. 8.5, Table 7.2 and Table 7.4). Nevertheless, the estimated performance from chapter 7 offers sufficiently detailed information to allow relative comparisons between constellations.

8.3 Simulations in the presence of multipath propagation

The multipath interference is inflicted when the transmitted group signal propagates through tapped delay line before the noise component is added. For these simulations taps were taken from [115] as TU6 (six-tap typical urban) channel model.

The channel is very severe for the transmitted signal and special mea-

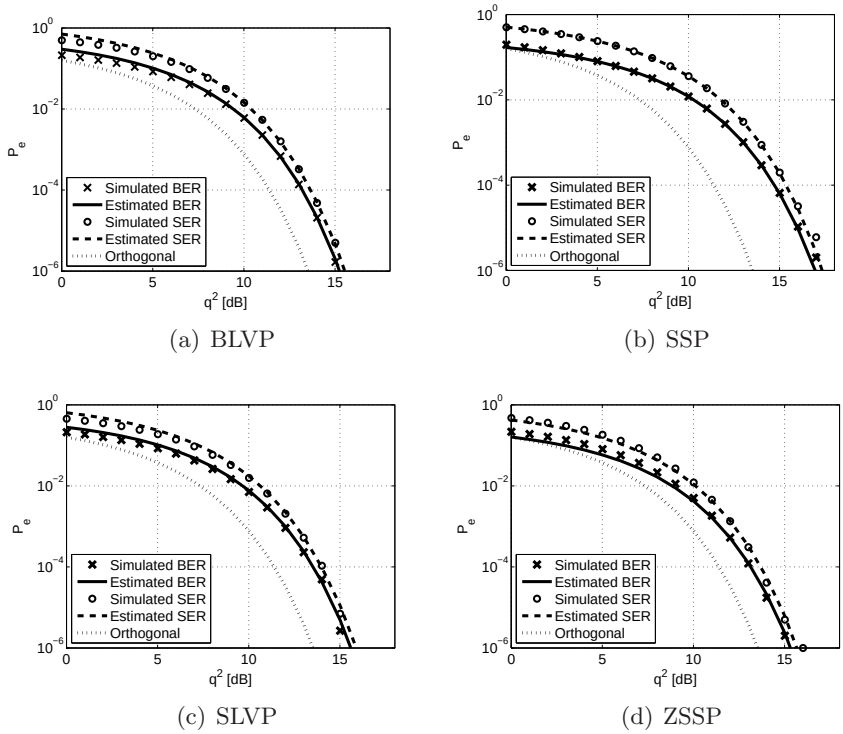

(a) BLVP (b) SSP

(c) SLVP (d) ZSSP

Figure 8.3: CCGO-CDMA with the BLVP, SLVP, SSP and ZSSP $(3, 2)$ constellations and the best obtained modulation mapping.

sures are required to mitigate its effect. The inspected methods are zero-forcing equalizer (ZFE), which tries to reverse the effect of the channel, and the combination of chip interleaving (including zero padding) with ZFE. The merit of chip interleaving is that all reflected signals in a multipath channel will be bit-synchronous at the receiver input.

Chosen simulation parameters are bandwidth of $W = 5$ MHz, which results in chip duration $\Delta_c = 0.2\ \mu s$. Spreading factor $N = 256$. The resulting channel impulse response length l_g equals then to 26 samples, since the delay spread is $5.2\ \mu s$.

8.3.1 Zero-forcing equalizer

When the observation (8.2) is inspected in the frequency domain (noise excluded) it can be given as multiplication of signal and channel frequency responses as

$$Y(f) = X(f)G(f), \tag{8.3}$$

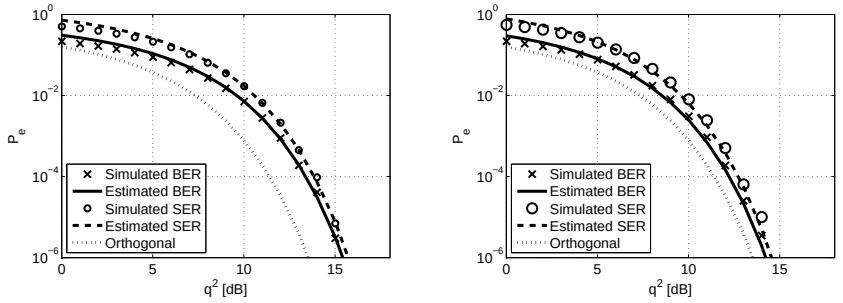

(a) $(3, 2)$ (b) $(4, 3)$

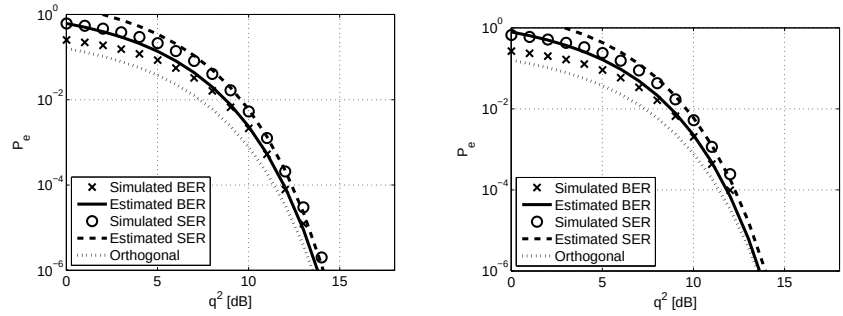

(c) $(5, 4)$ (d) $(6, 5)$

Figure 8.4: CCGO-CDMA with the LVP constellation ($s = 1$) and the best obtained modulation mapping.

since the system is linear. At the output of ZFE (having frequency response $C(f)$) the total frequency response is

$$Y(f) = X(f)G(f)C(f), \tag{8.4}$$

where the specification for ZFE is readily seen to be

$$G(f)C(f) = 1 \Rightarrow C(f) = \frac{1}{G(f)}. \tag{8.5}$$

Unfortunately, to realize equality in (8.5) an infinite impulse response (IIR) filter should be used. It is problematic in practice, since they are very difficult to design to be causal and stable. Therefore, (8.5) cannot be implemented perfectly, and some residual multipath interference remains. The finite impulse response (FIR) equalizer is used to approximate (8.5). In the time domain FIR ZFE provides Z zeros to the both sides of the main lobe of the output signal. The impulse response for the filter can be found from equation

$$\mathbf{Gc} = (\underbrace{0, \ldots, 0}_{Z}, 1, \underbrace{0, \ldots, 0}_{Z})^T = \mathbf{J}, \tag{8.6}$$

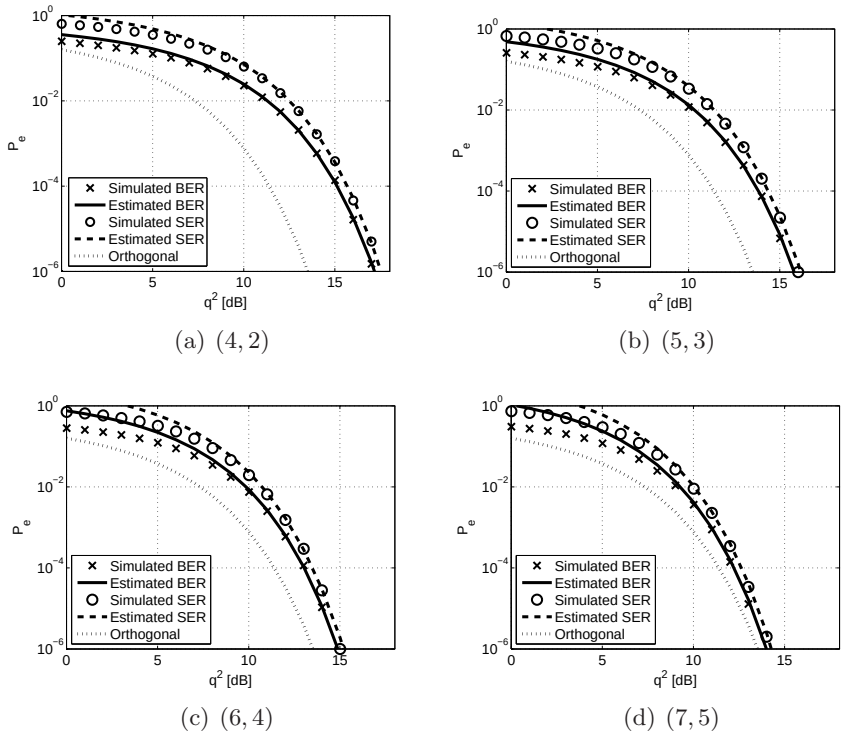

(a) $(4, 2)$ (b) $(5, 3)$

(c) $(6, 4)$ (d) $(7, 5)$

Figure 8.5: CCGO-CDMA with the LVP constellation ($s = 2$) and the best obtained modulation mapping.

where $\mathbf{c} = (c_0, \ldots, c_{n-1})^T$ is FIR-filter vector and $\mathbf{G}$ is matrix where $2Z+1$ rows are just cyclic shifts of channel vector $\mathbf{g}$ of length l_g padded with $2Z$ zeros. With the FIR memory $n > 2Z + 1$ the equation (8.6) has many solutions so that the one minimizing SNR loss is naturally preferred. This solution is expressed in terms of the pseudoinverse matrix of $\mathbf{G}$ giving the minimum norm least squares solution to (8.6) [116]:

$$\mathbf{c} = \mathbf{G}^T(\mathbf{G}\mathbf{G}^T)^{-1}\mathbf{J}. \tag{8.7}$$

The ZFE procedure is illustrated in Fig. 8.6 and Fig. 8.7, where impulse and frequency responses for the multipath channel (TU6 profile), ZFE and convolution of the multipath channel profile with ZFE impulse response are given for filter lengths $n = 74$ and $n = 266$. The frequency axis is normalized so that Nyquist sampling frequency equals to one. It is seen that increasing the length of filter the distorting effect of channel can be almost completely removed. The drawback is noise enhancement, which lowers SNR, and increases processing delay in receivers.

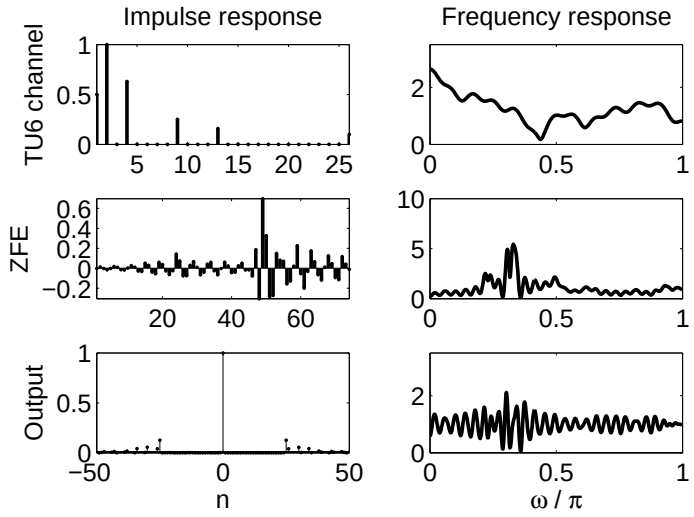

Figure 8.6: Channel impulse and frequency responses for ZFE operations in the multipath channel ($n = 74$).

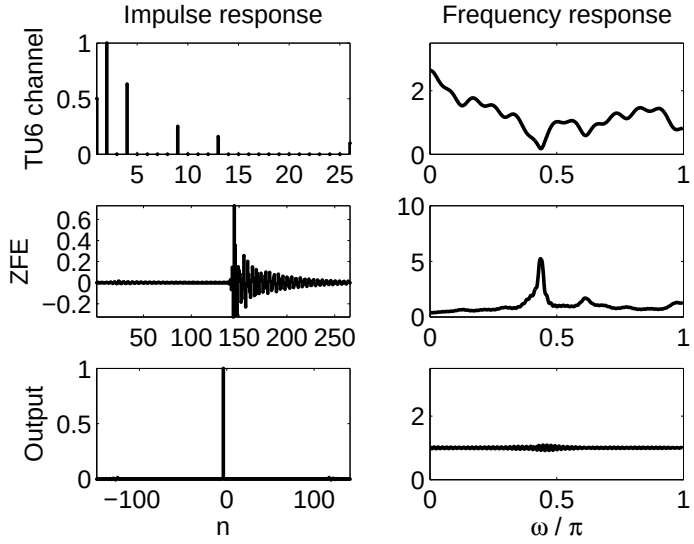

Figure 8.7: Channel impulse and frequency responses for ZFE operations in the multipath channel ($n = 266$).

8.3.2 Chip interleaving

One option of making GO-CDMA operational in the presence of multipath propagation is presented next. The method is called chip interleaving [117], which is combined with ZFE here. The required trade-off is reduced throughput due to zero padding and increased latency due to interleaving.

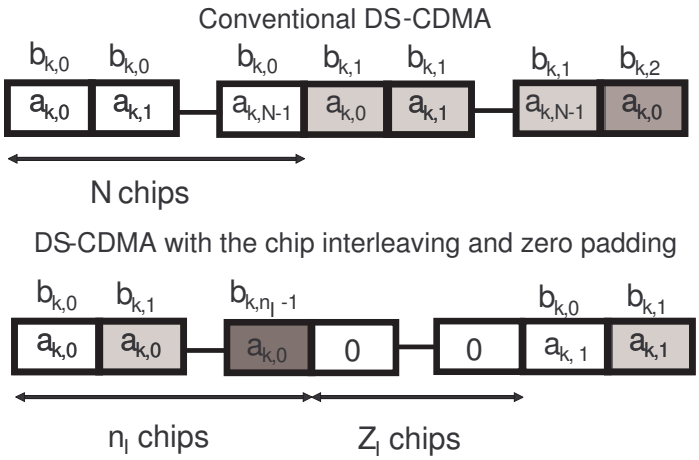

Figure 8.8: The illustration of chip interleaving and zero padding.

Let n_I denote an interleaver depth in bits. The chip interleaved pattern for the k-th user consists of the first chip of the user signature, $a_{k,0}$, modulated by the information bits $b_{k,0}, b_{k,1}, \ldots, b_{k,n_I-1}$, followed by Z_I zeros, then second chip of the user signature, $a_{k,1}$, again modulated by the same information bits and followed by zero padding with Z_I zeros, and up to N-th chip of the user signature, $a_{k,N-1}$, modulated by the same information bits and followed by Z_I zeros (see Fig. 8.8, where chip interleaving is compared to conventional DSSS scheme).

In [117] it is shown that after such a procedure at the receiving end for every bit of the user signatures will remain synchronous *independently* of the multipath propagation profile. In other words, during the time interval of any user signature and for any transmitted bit, signatures of all other users from all reflected paths will be bit-synchronous.

8.3.3 Simulation results for GO-CDMA

The goal of the simulation pursued is to examine the performance degradation due to oversaturation of GO-CDMA operating on a multipath channel destroying the orthogonality between signatures. This is accomplished by comparing simulated BER between orthogonal CDMA ($K = N$) and GO-CDMA. Some of the results have been published in [72].

Simulation results are illustrated in Fig. 8.9 and Fig. 8.10 for ZFE with equalizer length $n = 74$. It can be seen from the Fig. 8.9 that equalizer chosen for simulations could not completely remove the effects of the multipath channel. For all curves there exists error floor after which the performance cannot be improved by increasing SNR. Error floor saturates

Table 8.1: SNR comparison to achieve $P_e = 10^{-2}$.

L	e_{ov}	AWGN [dB]	Fading [dB]
1	1.00	7.3	10.5
2	1.50	11.5	-
3	1.33	9.3	14.3
4	1.25	8.7	12.4

Table 8.2: SNR losses due to oversaturation with $P_e = 10^{-2}$.

L	AWGN [dB]	Fading [dB]
2	4.2	-
3	2.0	3.8
4	1.4	1.9

to $P_e \approx 2 \cdot 10^{-2}$ for the $(3, 2)$ constellation, $P_e \approx 2.5 \cdot 10^{-3}$ for the $(4, 3)$ constellation, $P_e \approx 10^{-3}$ for the $(5, 4)$ constellation, and to $P_e \approx 3 \cdot 10^{-4}$ for the orthogonal system.

The most informative comparison is between two energy losses due to oversaturation: for the non-fading AWGN and multipath channels. As Fig. 8.10 shows, they are of the same order. SNR values to achieve BER value of $P_e = 10^{-2}$ in AWGN channel and in simulated fading channel, and resulting SNR losses when compared to orthogonal case are given in Tables 8.1 and 8.2. The $(3, 2)$ constellation does not reach $P_e = 10^{-2}$ at all. The energy loss due to multipath propagation is 3.2 dB for the orthogonal system, 5.0 dB for the $(4, 3)$ constellation, and 3.7 dB for the $(5, 4)$ constellation. Thus, the higher the initial correlation between signatures the higher the SNR loss. However, the loss for oversaturated case is not dramatically higher than for orthogonal system. When comparing energy loss due to oversaturation in AWGN and multipath channels, the loss grows 0.5 dB for the $(5, 4)$ constellation and 1.8 dB for the $(4, 3)$ constellation.

When chip interleaving is applied to the $(3, 2)$ constellation with the same ZFE length the error floor will be significantly lower. The simulation result is illustrated in Fig. 8.11. It can be seen that the error probability decreases well below 10^{-5}. The curves for $n = 266$ are shown for reference to see how low an error probability is achievable with ZFE if practical issues as complexity and delay are ignored.

8.3.4 Simulation results for CCGO-CDMA

Simulation results are illustrated in Fig. 8.12 and Fig. 8.13. The behavior is very similar to results for GO-CDMA in the previous section. It can be seen that the level of error floor follows the oversaturation efficiency. The

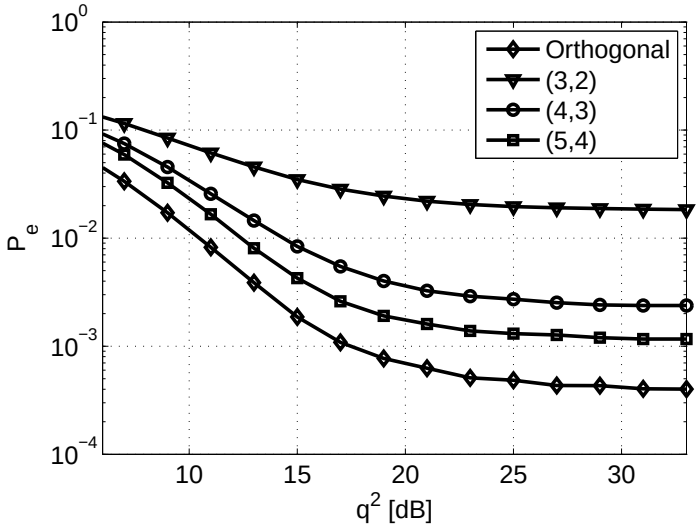

Figure 8.9: GO-CDMA BER in the multipath channel.

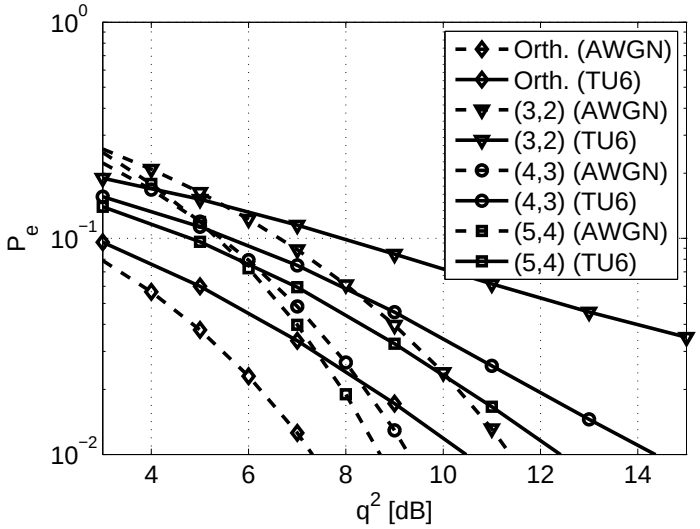

Figure 8.10: GO-CDMA BER in the AWGN and the multipath channel for small SNR values.

higher the oversaturation efficiency the worse the error performance. Only inconsistency is observed with subspace dimension $L = 5$. Its performance seems to be more affected by multipath interference than other subspace dimensions. In Fig. 8.12 the $(6, 5)$ constellation has similar performance as the $(4, 3)$ constellation, and in Fig. 8.13 the $(7, 5)$ constellation overlaps with the curve for the $(6, 4)$ constellation. Explanation might be that

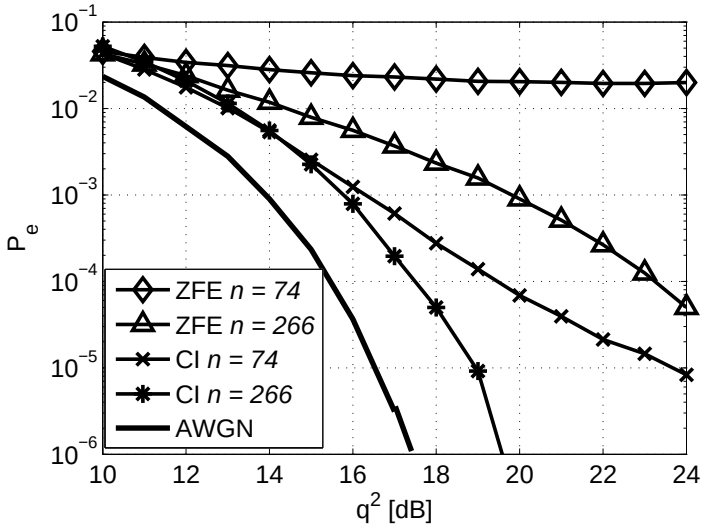

Figure 8.11: GO-CDMA BER comparison for ZFE and chip interleaving.

the gain in minimum Euclidean distances obtained from smaller oversaturation efficiency has been reduced by increased MAI due to larger number of interferers inside subspace.

In Fig. 8.12 error floors for $s = 1$ are at $P_e \approx 3.5 \cdot 10^{-3}, 2.5 \cdot 10^{-3}, 2 \cdot 10^{-3}, 2.5 \cdot 10^{-3}$ for constellations $(3,2)$,$(4,3)$,$(5,4)$,$(6,5)$, respectively. In Fig. 8.13 error floors for $s = 2$ are at $P_e \approx 2 \cdot 10^{-2}, 10^{-2}, 4 \cdot 10^{-3}, 4 \cdot 10^{-3}$ for constellations $(4,2)$, $(5,3)$,$(6,4)$,$(7,5)$, respectively.

The reception using chip interleaving is illustrated in Fig. 8.14 and Fig. 8.15. The performance of the $(3,2)$ LVP constellation with and without chip interleaving (ZFE with $n = 74$) is shown in Fig. 8.14. By comparing the performance to GO-CDMA curves from Fig. 8.11 it is seen that chip interleaving requires smaller filter length to provide good results. Curves in Fig. 8.15 demonstrate that the relative performance of different oversaturation efficiencies is comparable to results in the AWGN channel from Fig. 8.4 and Fig. 8.5.

8.4 Chapter summary

In this chapter simulations were used to verify results from previous chapters in the AWGN channel, and to demonstrate the feasibility of group orthogonality in a multipath channel, which inflicts MAI. First of all, simulation results show that theoretical BER analyses from previous chapters are well supported by simulation results. Secondly, it was demonstrated that GO-CDMA and CCGO-CDMA behave in a similar manner as the non-

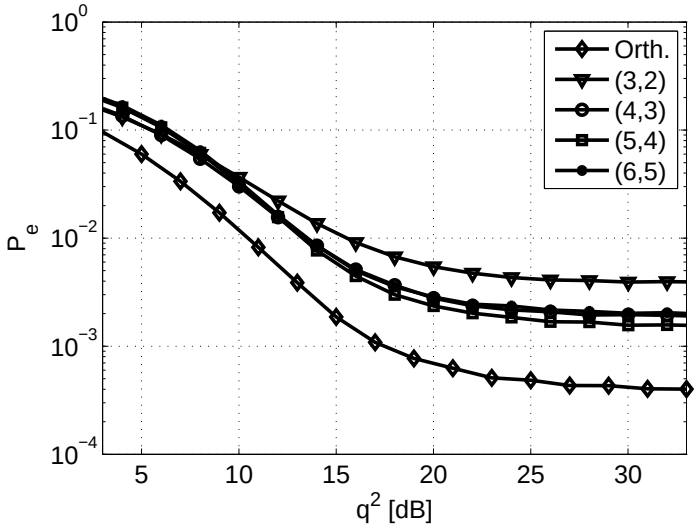

Figure 8.12: CCGO-CDMA BER in the multipath channel ($s = 1$).

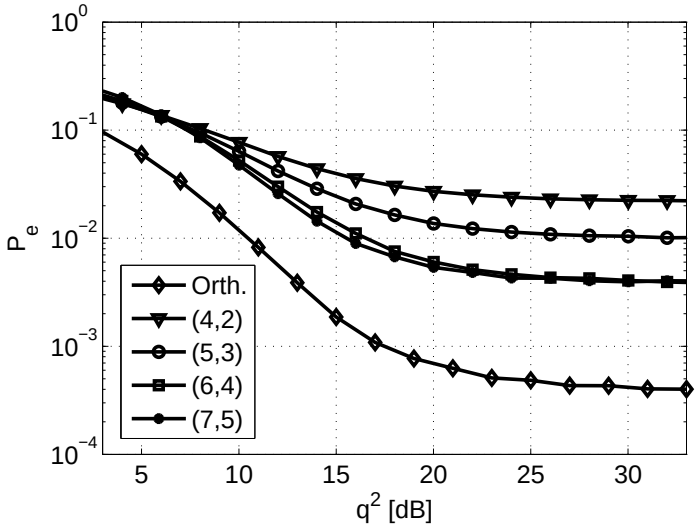

Figure 8.13: CCGO-CDMA BER in the multipath channel ($s = 2$).

oversaturated orthogonal system in both the AWGN and multipath channels. Therefore, it can be concluded that if GO-CDMA or CCGO-CDMA is regarded as feasible in the AWGN channel, it will also be applicable in realistic channel conditions whenever orthogonal signatures perform adequately. Finally, one example of making GO-CDMA operative in multipath channel was shown to be chip interleaving with zero padding.

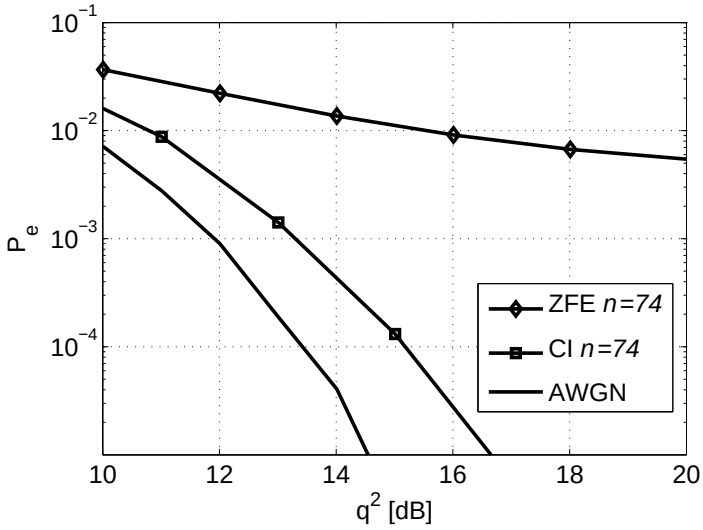

Figure 8.14: CCGO-CDMA BER for the $(3, 2)$ constellation in the multipath channel with ZFE and chip interleaving ($n = 74$).

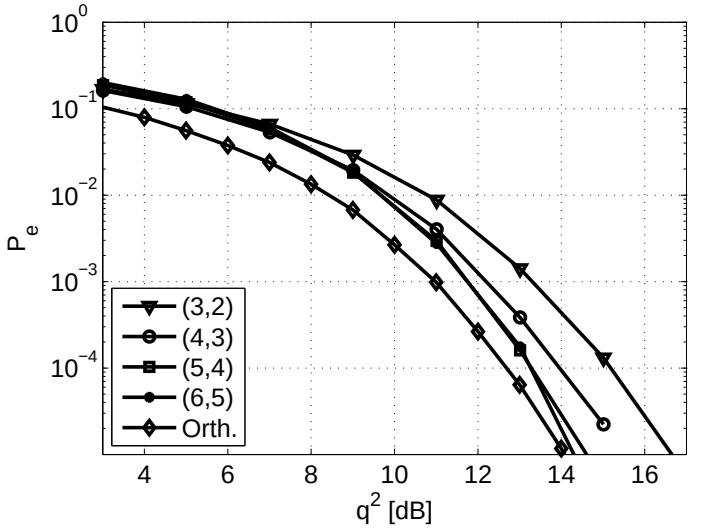

Figure 8.15: CCGO-CDMA BER for all subspace dimensions ($s = 1$) in the multipath channel with chip interleaving ($n = 74$).

Chapter 9

Conclusions

This thesis investigated the capacity (the number of users served) of downlink of cellular S-CDMA systems and signature ensembles providing improvements to this capacity. Downlink capacity is crucial in wireless communication systems, since a great amount of all data is transmitted a base station to a user terminal. CDMA was chosen to be the technology analyzed due to its importance in concurrent and forthcoming cellular systems. The downlink in a CDMA system allows synchronous transmission, where different user signals do not posses mutual time shifts between them. The multiple access free capacity of S-CDMA depends linearly on allocated bandwidth and inversely to the required user data rate. When the number of users exceeds the limit of signal space dimension, a trade-off between capacity, performance and receiver complexity must be decided on. The method considered in this thesis for increasing the number of users is called oversaturation.

The most essential existing literature on oversaturation can be covered with the following: oversaturated signature ensembles have been previously designed based on maximal minimum Euclidean distance [36], minimal mutual correlation between signatures (WBE signature ensembles) [95–97], and feasible receiver complexity [20, 33, 43, 56]. The group orthogonal structure presented in [56] allows utilizing a receiver that has linear complexity as the function of the number of users.

The novel contribution of this thesis is the signature ensemble design for a GO-CDMA system. Obtained signature ensembles are analyzed in detail. It was shown that GO-CDMA enjoys significant oversaturation efficiency while the performance can be maintained at the reasonable level even in multipath channels. Also, previously reported work in literature is continued and improved upon. Channel capacity considerations from [52] are extended to the case, where the transmitter outputs binary symbols instead of symbols having Gaussian distributed amplitude. In addition, oversaturated signature

ensembles having optimal distance property [36] were generalized to cover any signal space dimension. Also, conditions when binary distance-optimal ensembles are feasible were given along with a procedure to produce those binary ensembles. Some of the material from this thesis has been published in [67–72]. Here, results published in aforementioned references are significantly extended and presented more accurately in systematic manner. As a re-cap for the whole thesis, the following should considered:

CDMA technology exhibits some remarkable merits, which were described in chapter 2. These include good performance in multipath environment, resistance to narrow-band interference, privacy, possibility for exact time and location measurement, and good electromagnetic compatibility.

Further motivation to employ CDMA in future wireless systems was investigated in chapter 3. In previous work it was proved that CDMA reaches Shannon capacity in an oversaturated situation if the data symbols are Gaussian. In this thesis, the result is extended by showing that the same is true for binary data whenever the signal is weak. In the case of strong signals, it was proved that the maximization of capacity in CDMA systems is achieved by maximizing the minimum distance in group signal constellation, which also minimizes the symbol error probability. Chapter 3 provides solid foundation for choosing S-CDMA for the thesis topic, and also for signature ensemble design accomplished in this thesis.

Error performance of the receiver is another critical factor for communication system design. Signal and receiver design cannot be separated in CDMA systems. To clarify presented ideas, some different receiver structures available for oversaturated S-CDMA are presented in chapter 4. Then, the main topic of this thesis, signature ensemble design utilizing receiver structures from chapter 4 is presented in chapters 5, 6 and 7.

Each signature ensemble is analyzed considering Euclidean distance between group signals, oversaturation efficiency and the receiver complexity point-of-view. Euclidean distance determines the asymptotic error probability while the oversaturation efficiency describes the obtained capacity increase. Receiver complexity may limit utilizing certain signature ensembles in practical applications.

Conclusions reached from theoretical analysis are tested in chapter 8 by simulations first in the AWGN channel and then in the presence of multipath propagation. Results from the AWGN channel simulations verify the results from chapters 6 and 7. A more realistic channel model is used to find out whether multipath propagation changes the conclusion reached. It was found that performance degradation is similar for the orthogonal transmission, which is free from MAI in the AWGN channel, and oversaturated system, where MAI was present also in the AWGN case.

The aim of this thesis was to answer the question: "How to increase capacity of S-CDMA without inflicting intolerable amounts of MAI while

simple receiver structure is utilized?". GO-CDMA and CCGO-CDMA ensembles are proposed as possible solutions. It was shown that their receiver complexity is very low while the loss compared to orthogonal signaling is tolerable. Also, the signal ensemble design approach is valid from the point-of-view of Shannon's information theory.

Even though this thesis aims to be an exhaustive study on GO-CDMA signature design aspects, this field yields many promising future research directions. The possible future research could include generalized methods for CCGO-CDMA ensemble design and more extensive studies to performance in a fading channel and, consequently, advanced methods to mitigate the effects of fading.

References

[1] "Ministry of transport and communications report, http://www.mintc.fi/oliver/upl237-matkapuh.pdf."

[2] F. Hillebrand, Ed., *GSM and UMTS - The Creation of Global Mobile Communication*. Wiley, 2002.

[3] T. Ojanperä and R. Prasad, *Wideband CDMA for Third Generation Mobile Communications*. Artech House, 1998.

[4] "The 3rd generation partnership project (3GPP), http://www.3gpp.org."

[5] B. Walke, P. Seidenberg, and M. P. Althoff, *UMTS: The Fundamentals*. Wiley, 2003.

[6] M. Etoh, Ed., *Next Generation Mobile Systems - 3G and Beyond*. Wiley, 2005.

[7] "UMTS World, http://www.umtsworld.com/technology/hsdpa.htm."

[8] S. Maniatis, E. Nikolouzou, and L. S. Venieris, "End-to-end QoS specification issues in the converged all-IP wired and wireless environment," *IEEE Communications Magazine*, vol. 42, no. 6, pp. 80–86, June 2004.

[9] A. Ganz, Z. Ganz, and K. Wongthavarawat, *Multimedia Wireless Networks - Technologies, Standards, and QoS*. Prentice Hall, 2004.

[10] O. Benali *et al.*, "A framework for an evolutionary path toward 4G by means of cooperation of networks," *IEEE Communications Magazine*, vol. 42, no. 5, pp. 82–89, May 2004.

[11] S. Verdu, "Wireless bandwidth in the making," *IEEE Communications Magazine*, vol. 38, no. 7, pp. 53–58, July 2000.

[12] J. G. Proakis, *Digital Communications*, 3rd ed. McGraw-Hill, 1995.

[13] S. Haykin, *Communication Systems*, 4th ed. Wiley, 2001.

[14] E. A. Lee and D. G. Messerschmitt, *Digital Communication*, 2nd ed. Kluwer Academic Publishers, 1994.

[15] B. Sklar, *Digital Communications*, 2nd ed. Prentice Hall, 2001.

[16] R. E. Ziemer and R. L. Peterson, *Introduction to Digital Communication*, 2nd ed. Prentice-Hall, 2001.

[17] M. Simon, J. Omura, R. Scholtz, and B. Levitt, *Spread Spectrum Communications Handbook*. New York: McGraw-Hill, 1994.

[18] C. E. Shannon, "A mathematical theory of communication," *Bell Systems Technical Journal*, vol. 27, pp. 379–423,623–656, July–October 1948.

[19] J. S. Lee and L. E. Miller, *CDMA Systems Engineering Handbook*. Artech House, 1998.

[20] F. Vanhaverbeke, "Digital communication through overloaded channels," Ph.D. dissertation, University of Ghent, 2005.

[21] A. J. Viterbi, *CDMA - Principles of Spread Spectrum Communication*. Addison-Wesley, 1995.

[22] R. L. Peterson, R. E. Ziemer, and D. E. Borth, *Introduction to Spread Spectrum Communications*. Prentice-Hall Inc., 1995.

[23] J. Korhonen, *Introduction to 3G mobile communications*. Artech House, 2001.

[24] J. Castro, *The UMTS Network and Radio Access Technology: Air Interface Techniques for Future Mobile Systems*. Wiley, 2001.

[25] H. Schulze and C. Luders, *Theory and Applications of OFDM and CDMA Wideband Wireless Communications*. Wiley, 2005.

[26] B. Vucetic and J. Yan, *Space-time coding*. Wiley, 2003.

[27] R. D. Gaudenzi, C. Elia, and R. Viola, "Band-limited quasi-synchronous CDMA: A novel satellite access technique for mobile and personal communications systems," *IEEE Journal on Selected Areas on Communication*, vol. 10, no. 2, pp. 328–343, February 1992.

[28] A. Kajiwara and M. Nakagawa, "Microcellular CDMA system with a linear multiuser interference canceller," *IEEE Journal on Selected Areas on Communication*, vol. 12, no. 4, pp. 605–611, May 1994.

[29] J. Omura and P. Yang, "Spread spectrum S-CDMA for personal communication services," in *Proc. MILCOM 1992*, San Diego, United States, October 1992.

[30] V. DaSilva and E. Sousa, "Multicarrier orthogonal CDMA signals for quasi-synchronous communication systems," *IEEE Journal on Selected Areas on Communication*, vol. 12, no. 5, pp. 842–852, June 1994.

[31] N. Suehiro, "A signal design without co-channel interference for approximately synchronized CDMA systems," *IEEE Journal on Selected Areas on Communication*, vol. 12, no. 5, pp. 837–841, June 1994.

[32] V. Ipatov, *Spread Spectrum and CDMA - Principles and Applications*. Wiley, 2005.

[33] R. Learned, A. Willsky, and D. Boroson, "Low complexity optimal joint detection for oversaturated multiple access communications," *IEEE Transactions on Information Theory*, vol. 45, no. 1, pp. 113–123, January 1997.

[34] R. E. Learned, H. Krim, and A. S. Willsky, "Examination of wavelet packet signal sets for over-saturated multiple access communications," in *Proc. IEEE-SP International Symposium on Time-Frequency and Time-Scale Analysis*, Paris, France, June 1997.

[35] C. Schlegel and A. Grant, "Polynomial complexity optimal detection of certain multiple access systems," *IEEE Transactions on Information Theory*, vol. 46, pp. 2246–2248, September 2000.

[36] J. Ross and D. Taylor, "Vector assignment scheme for $M+N$ users in N-dimensional global additive channel," *Electronics Letters*, vol. 28, no. 17, pp. 1634–1636, August 1992.

[37] ——, "Multiuser signaling in the symbol-synchronous AWGN channel," *IEEE Transactions on Information Theory*, vol. 41, no. 4, pp. 1174–1178, July 1995.

[38] S. Verdu, "Minimum probability of error for asynchronous Gaussian multiple-access channels," *IEEE Transactions on Information Theory*, vol. 32, no. 1, pp. 85–96, January 1986.

[39] J. Lehtomäki, "Wavelet-based communication in synchronous CDMA and CDM systems (*Licentiate thesis In Finnish*)," University of Oulu, 2003.

[40] H. Zhang, H. H. Fan, and A. Lindsey, "Over-loaded DS-CDMA system waveform design using doubly orthogonal wavelet packets," in *Proc. VTC 2001*, Atlantic City, United States, October 2001.

[41] A. Reid, A. Grant, and P. Alexander, "Direct proof of polynomial complexity optimum multiuser detection algorithm," *IEE Electronics Letters*, vol. 37, no. 19, pp. 1203–1204, September 2001.

[42] C. Sankaran and A. Ephremides, "Solving a class of optimum multiuser detection problems with polynomial complexity," *IEEE Transactions on Information Theory*, vol. 44, September 1998.

[43] Z. Shi and C. Schlegel, "Spreading code construction for CDMA," *IEEE Communications Letters*, vol. 7, no. 1, pp. 4–6, January 2003.

[44] R. Lupas and S. Verdu, "Linear multiuser detectors for synchronous code-division multiple-access channels," *IEEE Transactions on Information Theory*, vol. 35, no. 1, pp. 123–136, January 1989.

[45] U. Madhow and M. Honig, "MMSE interference suppression for direct-sequence spread-spectrum CDMA," *IEEE Transactions on Communications*, vol. 42, no. 12, pp. 3178–3188, December 1994.

[46] M. Varanasi and B. Aazhang, "Near-optimum detection in synchronous code-division multiple access systems," *IEEE Transactions on Communications*, vol. 39, no. 5, pp. 725–736, May 1991.

[47] Z. Xie, R. Short, and C. Rushfort, "A family of suboptimum detectors for coherent multiuser communication," *IEEE Journal on Selected Areas on Communication*, vol. 8, no. 4, pp. 683–690, May 1990.

[48] A. Duel-Hallen, "A family of multiuser decision-feedback detectors for asynchronous code-division multiple-access channels," *IEEE Transactions on Communications*, vol. 43, no. 2, pp. 421–434, February 1995.

[49] P. Patel and J. Holtzman, "Analysis of a simple successive interference cancellation scheme in a DS/CDMA system," *IEEE Journal on Selected Areas on Communication*, vol. 12, no. 5, pp. 796–807, June 1994.

[50] S. Verdu, *Multiuser detection*. Cambridge: University Press, 1998.

[51] A. Kapur and M. Varanasi, "Multiuser detection for overloaded CDMA systems," *IEEE Transactions on Information Theory*, vol. 49, no. 7, pp. 1728–1742, July 2003.

[52] M. Rupf and J. L. Massey, "Optimum sequence multisets for synchronous code-division multiple-access channels," *IEEE Transactions on Information Theory*, vol. 40, no. 4, pp. 1261–1266, July 1994.

[53] P. Viswanath and V. Anantharam, "Optimal sequences and sum capacity of synchronous CDMA systems," *IEEE Transactions on Information Theory*, vol. 45, no. 6, pp. 1984–1991, September 1999.

[54] P. Viswanath, V. Anantharam, and D. Tse, "Optimal sequences, power control, and user capacity of synchronous CDMA systems with linear MMSE multiuser receivers," *IEEE Transactions on Information Theory*, vol. 45, no. 6, pp. 1968–1983, September 1999.

[55] T. Guess, "Optimal sequences for CDMA with decision-feedback receivers," *IEEE Transactions on Information Theory*, vol. 49, no. 4, pp. 886–900, April 2003.

[56] D. Djonin and V. Bhargava, "New results on low complexity detectors for over-saturated CDMA systems," in *Proc. Globecom '01*, San Antonio, United States, November 2001.

[57] L. Junqiang, K. Letaief, and C. Zhigang, "A group oriented multiuser detection with beamforming for multicarrier CDMA system," in *Proc. Globecom '01*, San Antonio, United States, November 2001.

[58] H. H. Nguyen and E. Shwedyk, "A new construction of signature waveforms for synchronous CDMA systems," *IEEE Transactions on Broadcasting*, vol. 51, no. 4, pp. 520–529, December 2005.

[59] F. Vanhaverbeke, M. Moeneclaey, and H. Sari, "An excess signaling concept with Walsh-Hadamard spreading and joint detection," in *Globecom 2000 Conf. Rec.*, San Francisco, USA, November 2000.

[60] H. Sari, F. Vanhaverbeke, and M. Moeneclaey, "Multiple access using two sets of of orthogonal signal waveforms," *IEEE Communications Letters*, vol. 4, no. 1, pp. 4–6, January 2000.

[61] ——, "Extending the capacity of multiple access channels," *IEEE Communications Magazine*, pp. 74–82, January 2000.

[62] F. Vanhaverbeke, M. Moeneclaey, and H. Sari, "DS/CDMA with two sets of orthogonal spreading sequences and iterative detection," *IEEE Communications Letters*, vol. 4, no. 9, pp. 289–291, September 2000.

[63] F. Vanhaverbeke and M. Moeneclaey, "An improved OCDMA/OCDMA scheme based on displaced orthogonal user sets," *IEEE Communications Letters*, vol. 8, no. 5, pp. 265–267, May 2004.

[64] F. Vanhaverbeke, M. Moeneclaey, and H. Sari, "Increasing CDMA capacity using multiple orthogonal spreading sequence sets and successive interference cancellation," in *Proc. ICC 2002*, New York, USA, April 2002.

[65] F. Vanhaverbeke and M. Moeneclaey, "Performance evaluation of three different types of channel overloading," in *Proc. PIMRC '03*, Lisboa, Portugal, September 2003.

[66] ——, "Binary signature sets for increased user capacity on the downlink of CDMA systems," *IEEE Transactions on Wireless Communications*, vol. 5, no. 7, pp. 1795–1804, July 2006.

[67] J. Paavola and V. Ipatov, "Binary CDMA signatures for $M+N$ users in N-dimensional global signal space," *IEE Electronics Letters*, vol. 39, no. 9, pp. 738–740, May 2003.

[68] ——, "Oversaturating synchronous CDMA systems on the signature per user basis," in *Proc.* 5th European Personal Mobile Communications Conference, Glasgow, Scotland, April 2003.

[69] ——, "BER analysis for oversaturated S-CDMA on the signature per user basis," in *Proc. EMC'03*, St. Petersburg, Russia, September 2003.

[70] ——, "Oversaturating synchronous CDMA systems using collaborative coding," in *Proc. PIMRC 2004*, Barcelona, Spain, September 2004.

[71] J. Paavola, "Performance analysis of oversaturated collaboratively coded group orthogonal CDMA in AWGN channel," in *Proc. PIMRC 2006*, Helsinki, Finland, September 2006.

[72] J. Paavola and V. Ipatov, "Performance analysis of oversaturated group orthogonal CDMA system in multipath channel," in *Proc. PIMRC 2006*, Helsinki, Finland, September 2006.

[73] S. Glisić and B. Vucetic, *Spread Spectrum CDMA systems for wireless communication*. Boston: Artech House, 1997.

[74] H. Holma and A. Toskala, *WCDMA for UMTS - Radio Access for the Third Generation Mobile Communications*. Wiley, 2001.

[75] R. Tanner and J. Woodward, Eds., *WCDMA - Requirements and Practical Design*. Wiley, 2004.

[76] L. Korowajczuk, *Designing cdma2000 Systems*. Wiley, 2004.

[77] N. Levanon and E. Mozeson, *Radar Signals*. Wiley, 2004.

[78] R. Dixon, *Spread Spectrum Systems with Commercial Applications*. Wiley, 1994.

[79] S. Golomb, Ed., *Digital Communications with Space Applications*. Prentice-Hall, 1964.

[80] A. Bruen and M. Forcinito, *Cryptography, Information Theory and Error Correction*. Wiley, 2005.

[81] A. Medayat, N. Sloan, and J. Stufken, *Orthogonal Arrays: Theory and Applications*. Springer, 1999.

[82] P. Fan and M. Darnell, *Sequence Design for Communication Applications*. Wiley, 1996.

[83] "3GPP2 C.S00002-0 physical layer standard for cdma2000 spread spectrum systems v1.0."

[84] S. Verdu, "Fifty years of Shannon theory," *IEEE Transactions on Information Theory*, vol. 44, no. 6, pp. 2057–2078, October 1998.

[85] T. Moon and W. Stirling, *Mathematical Methods and Algorithms for Signal Processing*. Prentice Hall, 2000.

[86] L. Welch, "Lower bounds on the maximum cross correlation of signals," *IEEE Transactions on Information Theory*, vol. 20, no. 3, pp. 397–399, May 1994.

[87] C. Schlegel and L. Wei, "A simple way to compute the minimum distance in multiuser CDMA systems," *IEEE Transactions on Communications*, vol. 45, no. 5, pp. 532–535, May 1997.

[88] Q. Li and C. Georghiades, "On a geometric view of multiuser detection for synchronous DS/CDMA channels," *IEEE Transactions on Information Theory*, vol. 46, no. 7, pp. 2723–2731, November 2000.

[89] G. Moustakides and H. Poor, "On the relative error probabilities of linear multiuser detectors," *IEEE Transactions on Information Theory*, vol. 47, no. 1, pp. 450–456, January 2001.

[90] M. Burnashev and V. Poor, "On the probability of error in linear multiuser detection," *IEEE Transactions on Information Theory*, vol. 49, no. 8, pp. 1922–1941, August 2003.

[91] W. Luo and A. Ephremides, "Indecomposable error sequences in multiuser detection," *IEEE Transactions on Information Theory*, vol. 47, no. 1, pp. 284–294, September 2001.

[92] W.-K. Ma, K. Wong, and P. Ching, "On computing Verdu's upper bound for a class of maximum-likelihood multiuser detection and sequence detection problems," *IEEE Transactions on Information Theory*, vol. 47, no. 7, pp. 3049–3053, November 2001.

[93] M. Honig and W. Veerakachen, "Performance variability of linear multiuser detection for DS-CDMA," in *Proc. VTC '96*, Atlanta, United States, May 1996.

[94] H. Poor and S. Verdu, "Probability of error in MMSE multiuser detection," *IEEE Transactions on Information Theory*, vol. 43, no. 3, pp. 858–871, May 1997.

[95] S. Ulukus and R. Yates, "Iterative construction of optimum signature sets in synchronous CDMA systems," *IEEE Transactions on Information Theory*, vol. 47, no. 5, pp. 1989–1998, July 2001.

[96] C. Rose, "CDMA codeword optimization: interference avoidance and convergence via class warfare," *IEEE Transactions on Information Theory*, vol. 47, no. 6, pp. 2368–2382, September 2001.

[97] P. Xia, S. Zhou, and G. Giannakis, "Achieving the Welch bound with difference sets," *IEEE Transactions on Information Theory*, vol. 51, no. 5, pp. 1900–1907, May 2005.

[98] G. Karystinos and D. Pados, "New bounds on the total squared correlation and optimum design of DS-CDMA binary signature sets," *IEEE Transactions on Communications*, vol. 51, no. 1, pp. 48–51, January 2003.

[99] V. Ipatov, "On the Karystinos-Pados bounds and optimal binary DS-CDMA signature ensembles," *IEEE Communications Letters*, vol. 8, no. 2, pp. 81–83, February 2004.

[100] D. Sarwate, "Meeting the Welch bound with equality," in *Sequences and their applications (Singapore, 1998)*. Springer, 1999, pp. 79–102.

[101] C. Ding, M. Golin, and T. Klove, "Meeting the Welch and Karystinos-Pados bounds on DS-CDMA binary signature sets," in *Designs, Codes and Cryptography*. Kluwer, 2003, pp. 73–84.

[102] R. Heath Jr., T. Strohmer, and A. Paulraj, "Grassmannian signatures for CDMA systems," in *Proc. VTC '96*, Atlanta, United States, May 1996.

[103] A. Kapur, M. Varanasi, and C. Mullis, "On the limitation of generalized Welch-Bound equality signals," *IEEE Transactions on Information Theory*, vol. 51, no. 6, pp. 2220–2224, June 2005.

[104] H. H. Nguyen, "Synchronous CDMA systems with group-orthogonal signature waveforms," in *Proc. VTC 2003*, Orlando, United States, October 2004.

[105] D. Owen, *Handbook of statistical tables.* Addison-Wesley, 1962.

[106] F. Ali and B. Honary, "Collaborative coding and decoding techniques for multiple access channel," *IEE Proceedings - Communications*, vol. 141, no. 3, pp. 56–62, April 1994.

[107] B. Honary, F. Ali, and M. Darnell, "Capacity of T-user collaborative coding multiple access scheme operating over a noisy channel," *Electronic Letters*, vol. 25, no. 11, pp. 742–744, May 1989.

[108] S. Chang and E. Weldon Jr., "Coding for T-user multiaccess channels," *IEEE Transactions on Information Theory*, vol. 31, no. 2, pp. 124–142, November 1985.

[109] R. Gallager, "A perspective on multiple access channels," *IEEE Transactions on Information Theory*, vol. 25, no. 6, pp. 684–691, November 1979.

[110] P. Fan and M. Darnell, "Hybrid CCMA/SSMA coding scheme," *Electronics Letters*, vol. 30, no. 25, pp. 2105–2106, December 1994.

[111] J. Conway and N. Sloane, *Sphere Packings, Lattices and Groups*, 3rd ed. Springer, 1999.

[112] "N.J.A. Sloane, with the collaboration of R.H. Hardin, W.D. Smith and others, Tables of Spherical Codes, published electronically at www.research.att.com/ njas/packings/."

[113] J. Smith, "Odd-bit quadrature amplitude-shift keying," *IEEE Transactions on Information Theory*, vol. 23, no. 3, pp. 385–389, March 1975.

[114] N. Guo and L. B. Milstein, "Mapping design for general multidimensional communication systems," in *Proc. MILCOM 1999*, Atlantic City, United States, November 1999.

[115] "3GPP TS 05.05: Digital cellular telecommunications system (phase2+), radio transmission and reception, v8.6.0 release 1999."

[116] C. Rao, *Generalized inverse of matrices and its applications.* Wiley, 1971.

[117] S. Zhou, G. Giannakis, and C. L. Martret, "Chip-interleaved block-spread code division multiple access," *IEEE Transactions on Communications*, vol. 50, no. 2, pp. 235–248, February 2002.

Appendix A

BER calculations for the $(3, 2)$ GO-CDMA constellation

In this chapter, exact BER calculations are given for the $(3, 2)$ GO-CDMA system. They are used to complete calculations in section 6.4.2, where only $P_e(xx-|++)$ was given. Results are illustrated in Fig. 6.14.

A.1 User 3

$$P_{e,3} = \frac{1}{4}(P(xx-|--+) + P(xx-|+++) + 2P(xx-|-++)), \quad \text{(A.1)}$$

since $P(xx-|+-+) = P(xx-|-++)$. The $P(xx-|+++)$ is calculated in the main text in section 6.4.

A.1.1 $P(xx-|--+)$

$$\begin{aligned} P(xx-|--+) &= 2(T(h_1,\beta_3) + T(h_1,\beta_1) + (T(h_1,\beta_1) \\ &-0.5Q(h_1) - T(h_1,\beta_1)) + T(h_1,\beta_1) - (T(h_2,\beta_2) \\ &-T(h_2,\beta_3)) - T(h_3,\beta_4)) \end{aligned} \quad \text{(A.2)}$$

h_1	h_2	h_3	β_1	β_2	β_3	β_4
$0.618\sqrt{E_b}$	$\sqrt{E_b}$	$2.2361\sqrt{E_b}$	0.9425	1.1124	0.3141	0.1443

Table A.1: Parameters for BER calculation for user 3 when $(--+)$ is transmitted.

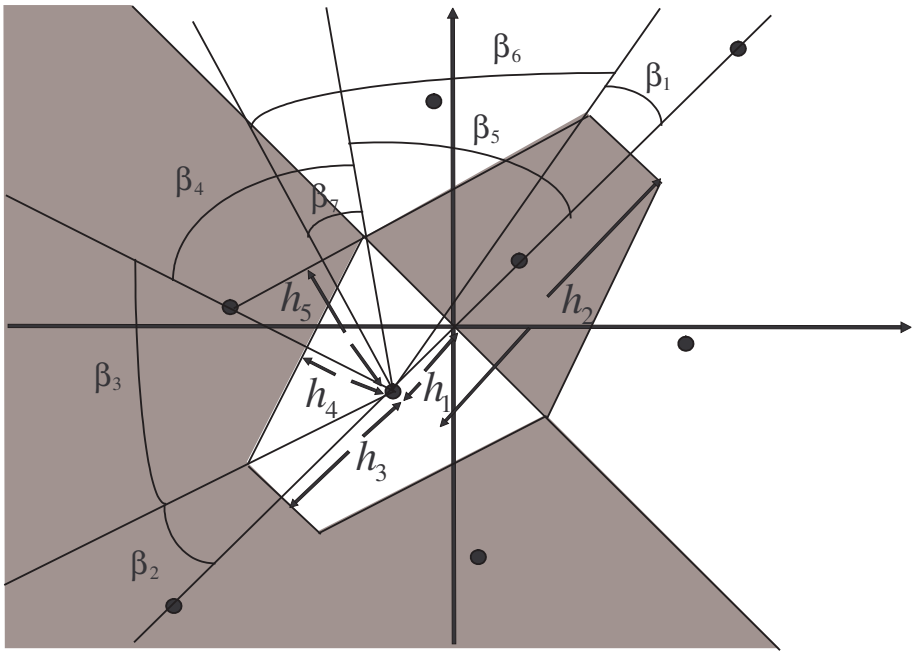

Figure A.1: Calculation of $P(xx-|--+)$.

A.1.2 $P(xx-|+-+) = P(xx-|-++)$

$$
\begin{aligned}
&P(xx-|-++) = (Q(h5) - T(h_5, \beta_8)) + T(h_5, \beta_9) \\
&+(T(h_6, \beta_{11}) - T(h_6, \beta_9)) + T(h_2, \beta_4) + T(h_1, \beta_1) \\
&-T(h_1, \beta_2) - T(h_2, \beta_3) + T(h_3, \beta_4) - (T(h_3, \beta_5) \\
&-T(h_3, \beta_4)) - (T(h_4, \beta_6) - T(h_4, \beta_7)) + T(h_3, \beta_4) \\
&-(T(h_5, \beta_8) - T(h_5, \beta_9)) - (T(h_4, \beta_{10}) - T(h_4, \beta_6)) \qquad \text{(A.3)}
\end{aligned}
$$

h_1	h_2	h_3	h_4	h_5	h_6
$2.2361\sqrt{E_b}$	$2.5043\sqrt{E_b}$	$0.618\sqrt{E_b}$	$1.618\sqrt{E_b}$	$\sqrt{E_b}$	$2.618\sqrt{E_b}$

Table A.2: Distance parameters for BER calculation for user 3 when $(-++)$ is transmitted.

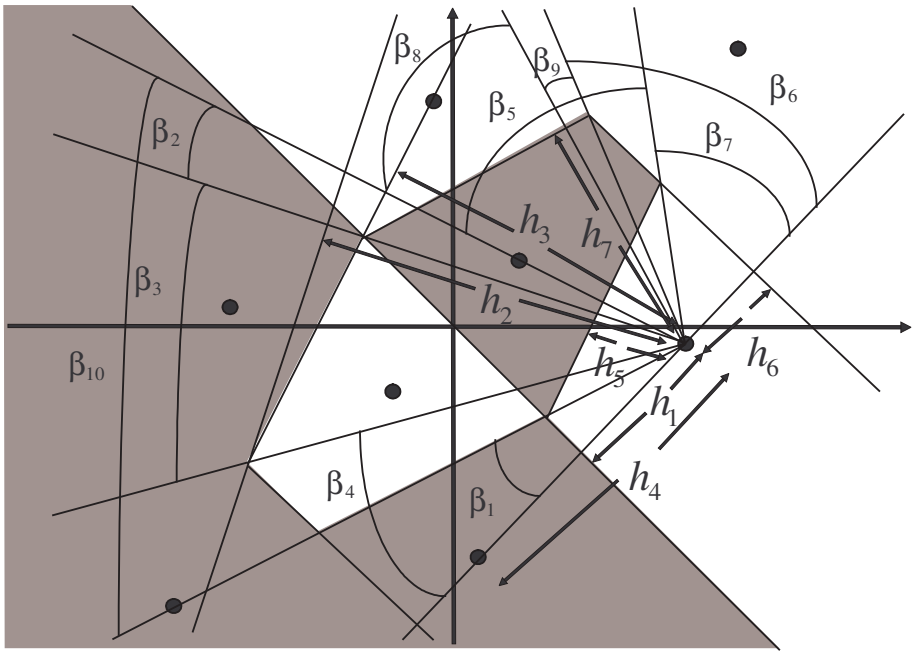

Figure A.2: Calculation of $P(xx-|+-+)$.

β_1	β_2	β_3	β_4	β_5	β_6	β_7	β_8	β_9
0.7362	0.1443	0.5919	0.9425	1.1801	0.6283	0.0766	1.1123	0.3141
β_{10}	β_{11}							
0.7738	0.5204							

Table A.3: Angle parameters for BER calculation for user 3 when $(-++)$ is transmitted.

A.2 Users 1 and 2

$$P_{e,1} = P_{e,2} = \frac{1}{4}(P(-xx|++-)+P(-xx|+--)+P(-xx|+-+)+P(-xx|+++)) \tag{A.4}$$

A.2.1 $P(-xx|++-)$

$$P(-xx|++-) = Q(h_1) + (T(h_1,\beta_1) - 0.5Q(h_1)$$
$$-T(h_1,\beta_1) + (T(h_1,\beta_1) - 0.5Q(h_1) - T(h_1,\beta_1))$$

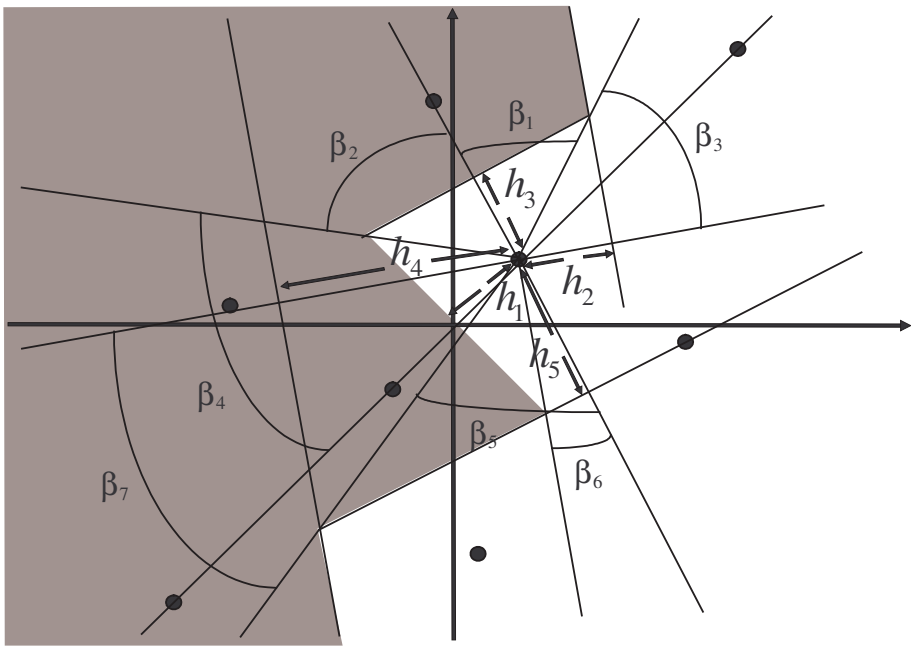

Figure A.3: Calculation of $P(-xx|++-)$.

$$-(0.5Q(h_1) - T(h_1, \beta_1) + T(h_2, \beta_2) - T(h_2, \beta_3) \\ -(0.5Q(h_3)) - T(h_3, \beta_4))) \tag{A.5}$$

h_1	h_2	h_3	β_1	β_2	β_3	β_4
$0.618\sqrt{E_b}$	$\sqrt{E_b}$	$1.618\sqrt{E_b}$	0.9425	1.1124	0.3141	0.7726

Table A.4: Parameters for BER calculation for user 1 when $(++-)$ is transmitted.

A.2.2 $P(-xx|+--)$

$$P(-xx|+--) = Q(h_2) + T(h_4, \beta_6) + T(h_2, \beta_7) \\ +(T(h_4, \beta_4) - 0.5Q(h_1)) - T(h_1, \beta_1) - T(h_2, \beta_2) \\ -T(h_2, \beta_3) - (T(h_3, \beta_4) - T(h_3, \beta_5))) \tag{A.6}$$

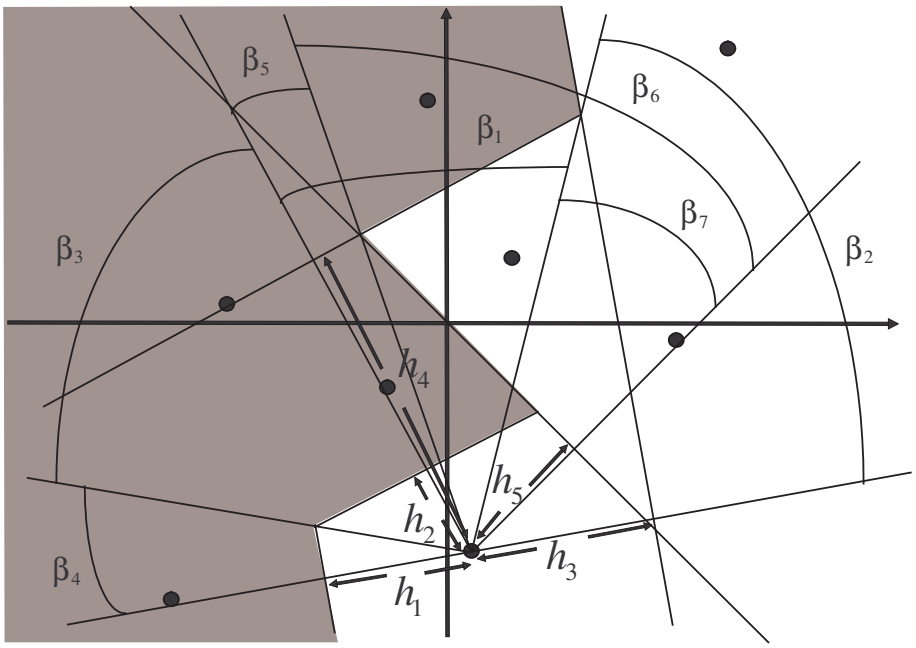

Figure A.4: Calculation of $P(-xx|+-)$.

h_1	h_2	h_3	h_4
$1.236\sqrt{E_b}$	$\sqrt{E_b}$	$2.236\sqrt{E_b}$	$0.618\sqrt{E_b}$

Table A.5: Distance parameters for BER calculation for user 1 when $(+--)$ is transmitted.

β_1	β_2	β_3	β_4	β_5	β_6	β_7
1.1488	1.1124	0.5215	0.7362	0.1443	0.9425	0.3141

Table A.6: Angle parameters for BER calculation for user 1 when $(+--)$ is transmitted.

A.2.3 $P(-xx|+-+)$

$$\begin{aligned} P(-xx|+-+) &= (T(h_3,\beta_3) - T(h_3,\beta_2)) + T(h_4,\beta_4) \\ &+T(h_4,\beta_5) + 0.5Q(h_1)) - T(h_1,\beta_1) \\ &+0.5Q(h_2) - T(h_2,\beta_2) \end{aligned} \tag{A.7}$$

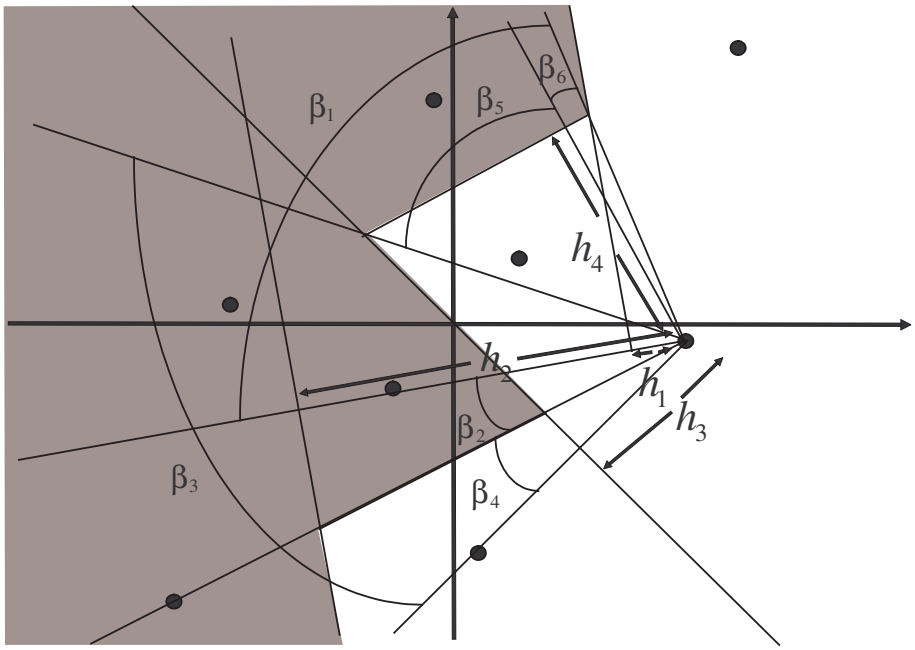

Figure A.5: Calculation of $P(-xx|++-+)$.

h_1	h_2	h_3	h_4
$0.3821\sqrt{E_b}$	$2.6179\sqrt{E_b}$	$\sqrt{E_b}$	$1.618\sqrt{E_b}$

Table A.7: Distance parameters for BER calculation for user 1 when $(+-+)$ is transmitted.

β_1	β_2	β_3	β_4	β_5
1.3331	0.3141	1.1123	0.7726	0.0766

Table A.8: Angle parameters for BER calculation for user 1 when $(+-+)$ is transmitted.

A.2.4 $P(-xx|+++)$

$$
\begin{aligned}
&P(-xx|+++) = 0.5 - (T(h_1,\beta_1) - T(h_2,\beta_1) \\
&+0.5(1 - 2Q(h_3)(1 - Q(h_1)) + T(h_3,\beta_2) - T(h_1,\beta_1) \\
&-T(h_1,\beta_3) + 0.5Q(h_3) - (0.5Q(h_1)) - T(h_1,\beta_3))) \\
&+T(h_2,\beta_1) - (T(h_4,\beta_4) - T(h_4,\beta_3) - (T(h_5,\beta_4)
\end{aligned}
$$

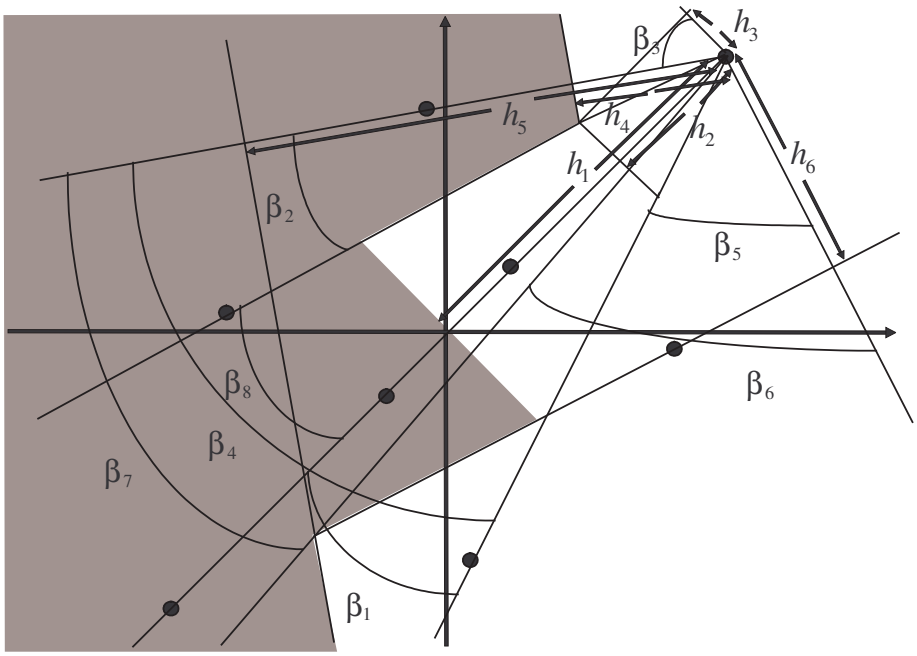

Figure A.6: Calculation of $P(-xx|+++)$.

$$-T(h_5, \beta_5)) + 0.5Q(h_5) - T(h_5, \beta_3)) \tag{A.8}$$

h_1	h_2	h_3	h_4	h_5
$\sqrt{E_b}$	$2.6179\sqrt{E_b}$	$0.3249\sqrt{E_b}$	$1.618\sqrt{E_b}$	$3.2344\sqrt{E_b}$

Table A.9: Distance parameters for BER calculation for user 1 when $(+++)$ is transmitted.

β_1	β_2	β_3	β_4	β_5
0.3141	1.2567	0.9425	1.1801	0.7048

Table A.10: Angle parameters for BER calculation for user 1 when $(+++)$ is transmitted.

Appendix B

The proof of equation (4.8)

In this appendix, the proof of inequality $\Sigma_{\max} \geq 1$ (see section 4.1.1) is given. User signatures are illustrated in Fig. 4.1. The aim is to calculate error probability (4.7):

$$P_{e,\max} > \frac{1}{4} Q\left(q(1-\Sigma_{\max})\right), \tag{B.1}$$

Due to the symmetry of problem it is enough to consider only on the range of angles between signatures α, β (see Fig. 4.1)

$$0 \leq \alpha \leq \beta \leq \frac{\pi}{2},$$

so that

$$\cos\alpha \geq \cos\beta$$

and

$$\Sigma_{\max} = \Sigma_{\max}(\alpha,\beta) = \max\{\cos\alpha + \cos\beta, \cos\alpha + |\cos(\alpha+\beta)|\} \tag{B.2}$$

To estimate $\Sigma_{\max}(\alpha,\beta)$ from below, let us split the area α, β ($0 \leq \alpha \leq \beta \leq \pi/2$) into three regions as shown in Fig. B.1. For the first region

$$0 \leq \alpha \leq \frac{\pi}{3}, \alpha \leq \beta \leq \frac{\pi}{2} - \frac{\alpha}{2},$$

which gives

$$\Sigma_{\max}(\alpha,\beta) \geq \cos\alpha + \cos\left(\frac{\pi}{2} - \frac{\alpha}{2}\right) = \cos\alpha + \sin\frac{\alpha}{2} \tag{B.3}$$

The right-hand side here is concave, since $0 \leq \alpha \leq \pi/3$ and at the borders of this range takes on the value of one. Thus, within the region 1:

$$\Sigma_{\max}(\alpha,\beta) \geq 1. \tag{B.4}$$

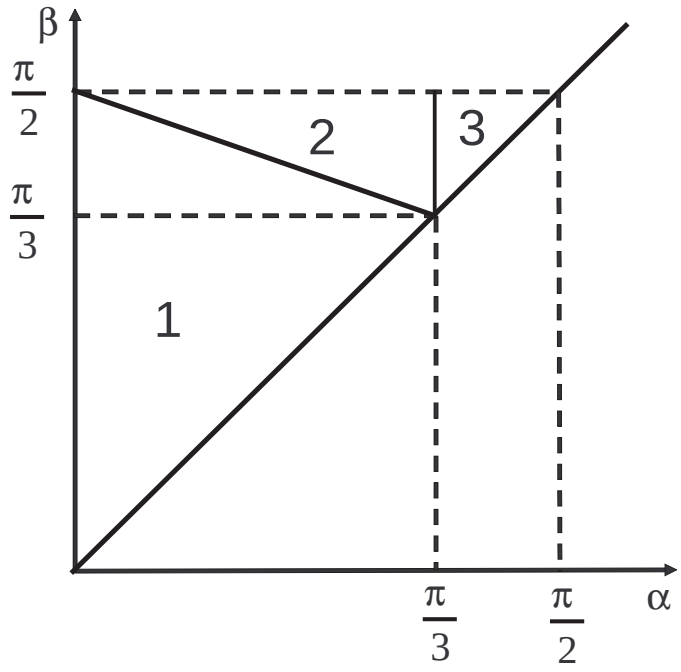

Figure B.1: The division of inspected region to three regions.

The region 2 is defined as

$$0 \leq \alpha \leq \frac{\pi}{3}, \frac{\pi}{2} - \frac{\alpha}{2} \leq \beta \leq \frac{\pi}{2},$$

so that

$$|\cos(\alpha+\beta)| \geq |\cos(\frac{\pi}{2} + \frac{\alpha}{2})| = \sin\frac{\alpha}{2}$$

and

$$\cos\alpha + |\cos(\alpha+\beta)| \geq \cos\alpha + \sin\frac{\alpha}{2},$$

and because the range in α remains the same

$$\Sigma_{\max}(\alpha,\beta) \geq 1 \tag{B.5}$$

also in region 2. In the region 3:

$$\frac{\pi}{3} \leq \alpha \leq \frac{\pi}{2}, \alpha \leq \beta \leq \frac{\pi}{2}$$

and hence

$$|\cos(\alpha+\beta)| \geq |\cos 2\alpha|, |\cos\alpha + |\cos(\alpha+\beta)| \geq \cos\alpha + |\cos 2\alpha|.$$

The right-hand side here is concave in the range $\pi/3 \leq \alpha \leq \pi/2$ and since at the extreme points $\alpha = \pi/3$ and $\alpha = \pi/2$ it equals to one

$$\Sigma_{\max}(\alpha, \beta) \geq 1 \tag{B.6}$$

in the region 3, too. Thus, it has been proved that

$$\Sigma_{\max} \geq 1. \tag{B.7}$$

Appendix C

CCGO-CDMA constellations

In this chapter, signal constellations are given for $(4,2)$, $(5,3)$, $(5,4)$, $(6,4)$, $(6,5)$, and $(7,5)$ for LVP, SLVP, SSP and ZSSP types. BLVP constellation can be obtained from LVP constellations with the similar procedure as for the $(3,2)$ constellation in section 7.2.1. All $(3,2)$ and $(4,3)$ constellations were given in chapter 7.

C.1 $(4,2)$ constellations

$$\mathbf{P}_{LVP}^{2D,s=2} = \sqrt{\frac{4 \cdot 4E_b}{9}} \begin{pmatrix} 0 & 0 \\ \cos\frac{\pi}{6} & \sin\frac{\pi}{6} \\ \cos\frac{3\pi}{6} & \sin\frac{3\pi}{6} \\ \cos\frac{5\pi}{6} & \sin\frac{5\pi}{6} \\ \cos\frac{7\pi}{6} & \sin\frac{7\pi}{6} \\ \cos\frac{9\pi}{6} & \sin\frac{9\pi}{6} \\ \cos\frac{11\pi}{6} & \sin\frac{11\pi}{6} \\ \cos\frac{\pi}{3}\sqrt{3} & \sin\frac{\pi}{3}\sqrt{3} \\ -\cos\frac{\pi}{3}\sqrt{3} & \sin\frac{\pi}{3}\sqrt{3} \\ -\cos\frac{\pi}{3}\sqrt{3} & -\sin\frac{\pi}{3}\sqrt{3} \\ \cos\frac{\pi}{3}\sqrt{3} & -\sin\frac{\pi}{3}\sqrt{3} \\ 0 & 2 \\ 0 & -2 \\ 2\cos\frac{\pi}{6} & 0 \\ -2\cos\frac{\pi}{6} & 0 \\ 2\cos\frac{\pi}{6} & 2\sin\frac{\pi}{6} \end{pmatrix} \tag{C.1}$$

$$\mathbf{P}_{SLVP}^{2D,s=2} = \sqrt{\frac{2E_b}{5}} \begin{pmatrix} 1 & 1 \\ -1 & 1 \\ 1 & -1 \\ -1 & -1 \\ 3 & 1 \\ -3 & 1 \\ 3 & -1 \\ -3 & -1 \\ 1 & 3 \\ -1 & 3 \\ 1 & -3 \\ -1 & -3 \\ 3 & 3 \\ -3 & 3 \\ 3 & -3 \\ -3 & -3 \end{pmatrix} \tag{C.2}$$

$$\mathbf{P}_{ZSSP}^{2D,s=2} = \frac{16}{15}\sqrt{4E_b} \begin{pmatrix} 0 & 0 \\ \cos\frac{\pi}{15} & \sin\frac{\pi}{15} \\ \cos\frac{3\pi}{15} & \sin\frac{3\pi}{15} \\ \cos\frac{5\pi}{15} & \sin\frac{5\pi}{15} \\ \cos\frac{7\pi}{15} & \sin\frac{7\pi}{15} \\ \cos\frac{9\pi}{15} & \sin\frac{9\pi}{15} \\ \cos\frac{11\pi}{15} & \sin\frac{11\pi}{15} \\ \cos\frac{13\pi}{15} & \sin\frac{13\pi}{15} \\ \cos\frac{15\pi}{15} & \sin\frac{15\pi}{15} \\ \cos\frac{17\pi}{15} & \sin\frac{17\pi}{15} \\ \cos\frac{19\pi}{15} & \sin\frac{19\pi}{15} \\ \cos\frac{21\pi}{15} & \sin\frac{21\pi}{15} \\ \cos\frac{23\pi}{15} & \sin\frac{23\pi}{15} \\ \cos\frac{25\pi}{15} & \sin\frac{25\pi}{15} \\ \cos\frac{27\pi}{15} & \sin\frac{27\pi}{15} \\ \cos\frac{29\pi}{15} & \sin\frac{29\pi}{15} \end{pmatrix} \tag{C.3}$$

$$\mathbf{P}_{SSP}^{2D,s=2} = \sqrt{4E_b} \begin{pmatrix} \cos\frac{31\pi}{16} & \sin\frac{31\pi}{16} \\ \cos\frac{\pi}{16} & \sin\frac{\pi}{16} \\ \cos\frac{3\pi}{16} & \sin\frac{3\pi}{16} \\ \cos\frac{5\pi}{16} & \sin\frac{5\pi}{16} \\ \cos\frac{7\pi}{16} & \sin\frac{7\pi}{16} \\ \cos\frac{9\pi}{16} & \sin\frac{9\pi}{16} \\ \cos\frac{11\pi}{16} & \sin\frac{11\pi}{16} \\ \cos\frac{13\pi}{16} & \sin\frac{13\pi}{16} \\ \cos\frac{15\pi}{16} & \sin\frac{15\pi}{16} \\ \cos\frac{17\pi}{16} & \sin\frac{17\pi}{16} \\ \cos\frac{19\pi}{16} & \sin\frac{19\pi}{16} \\ \cos\frac{21\pi}{16} & \sin\frac{21\pi}{16} \\ \cos\frac{23\pi}{16} & \sin\frac{23\pi}{16} \\ \cos\frac{25\pi}{16} & \sin\frac{25\pi}{16} \\ \cos\frac{27\pi}{16} & \sin\frac{27\pi}{16} \\ \cos\frac{29\pi}{16} & \sin\frac{29\pi}{16} \end{pmatrix} \tag{C.4}$$

C.2 $(5, 3)$ constellations

$$\mathbf{P}_{SSP}^{3D,s=2} = 10^{-1}\sqrt{5E_b}\begin{pmatrix} 7.6236 & 3.0833 & -5.6899 \\ 8.7752 & -2.9531 & -3.7783 \\ 1.4220 & 3.6554 & -9.1987 \\ -0.0794 & 9.9997 & 0.0000 \\ 2.7718 & -7.4160 & -6.1090 \\ 4.7123 & -1.8332 & -8.6275 \\ 1.0796 & 3.0313 & 9.4681 \\ -5.1375 & 1.8298 & 8.3820 \\ 3.9930 & -7.4063 & 5.4039 \\ -7.2116 & -3.7014 & 5.8559 \\ -6.5877 & -7.4903 & 0.7051 \\ 2.4063 & 7.9555 & 5.5606 \\ 6.1130 & -7.8879 & -0.6418 \\ 8.7204 & -3.5749 & 3.3427 \\ 9.8053 & 1.9484 & 0.2455 \\ -3.5178 & -7.9643 & -4.9188 \\ -7.6236 & -3.0833 & -5.6899 \\ -8.7752 & 2.9531 & -3.7783 \\ -1.4220 & -3.6554 & -9.1987 \\ 0.0794 & -9.9997 & 0.0000 \\ -2.7718 & 7.4160 & -6.1090 \\ -4.7123 & 1.8332 & -8.6275 \\ -1.0796 & -3.0313 & 9.4681 \\ 5.1375 & -1.8298 & 8.3820 \\ -3.9930 & 7.4063 & 5.4039 \\ 7.2116 & 3.7014 & 5.8559 \\ 6.5877 & 7.4903 & 0.7051 \\ -2.4063 & -7.9555 & 5.5606 \\ -6.1130 & 7.8879 & -0.6418 \\ -8.7204 & 3.5749 & 3.3427 \\ -9.8053 & -1.9484 & 0.2455 \\ 3.5178 & 7.9643 & -4.9188 \end{pmatrix} \tag{C.5}$$

$$\mathbf{P}_{ZSSP}^{3D,s=2} = \frac{32}{31} 10^{-1} \sqrt{5E_b} \begin{pmatrix} 0 & 0 & 0 \\ 7.5847 & 4.1650 & -5.0124 \\ 1.9323 & -9.3788 & 2.8817 \\ -7.4157 & 2.2298 & 6.3274 \\ -3.1801 & -1.7071 & -9.3259 \\ 8.2111 & -0.3364 & 5.6977 \\ 6.9006 & -1.9575 & -6.9678 \\ 8.9028 & 4.3609 & 1.3122 \\ 1.7376 & -5.6972 & -8.0326 \\ -2.4078 & 9.4586 & -2.1765 \\ -6.2329 & 7.3754 & 2.5991 \\ 3.0994 & 0.8570 & 9.4689 \\ -1.7841 & 4.9761 & 8.4885 \\ -3.3088 & 4.6575 & -8.2073 \\ -9.9386 & 0.9827 & 0.5088 \\ 9.8092 & -1.5196 & -1.2124 \\ -7.5900 & 5.5257 & -3.4435 \\ 2.1785 & 7.4745 & -6.2758 \\ -5.4668 & -6.3518 & -5.4562 \\ -0.1708 & 9.2139 & 3.8826 \\ 4.6119 & 8.8616 & -0.4508 \\ 2.3821 & 1.8915 & -9.5262 \\ -5.3575 & -8.4174 & 0.6674 \\ -0.2803 & -9.4732 & -3.1905 \\ 7.4697 & -6.0473 & 2.7630 \\ 5.9662 & -7.2678 & -3.4036 \\ -2.9937 & -1.2995 & 9.4525 \\ -8.2980 & -0.5422 & -5.5542 \\ 4.9990 & 6.0795 & 6.1684 \\ -8.1212 & -3.8844 & 4.3539 \\ 3.3914 & -5.3613 & 7.7301 \\ -2.8980 & -7.0401 & 6.4837 \end{pmatrix} \tag{C.6}$$

$$\mathbf{P}_{LVP}^{3D,s=2} = \sqrt{\frac{16 \cdot 5E_b}{63}} \begin{pmatrix} 0 & 0 & 0 \\ 1 & 1 & 0 \\ 1 & 0 & 1 \\ 0 & 1 & 1 \\ -1 & -1 & 0 \\ -1 & 0 & -1 \\ 0 & -1 & -1 \\ 1 & -1 & 0 \\ 1 & 0 & -1 \\ 0 & 1 & -1 \\ -1 & 1 & 0 \\ -1 & 0 & 1 \\ 0 & -1 & 1 \\ 2 & 0 & 0 \\ 0 & 2 & 0 \\ -2 & 0 & 0 \\ 0 & -2 & 0 \\ 0 & 0 & 2 \\ 0 & 0 & -2 \\ 2 & 1 & 1 \\ -2 & -1 & -1 \\ 1 & 2 & 1 \\ -1 & -2 & -1 \\ 1 & 1 & 2 \\ -1 & -1 & -2 \\ -2 & 1 & 1 \\ 2 & -1 & -1 \\ 1 & -2 & 1 \\ -1 & 2 & -1 \\ 1 & 1 & -2 \\ -1 & & -12 \\ 2 & -1 & 1 \end{pmatrix} \tag{C.7}$$

$$\mathbf{P}^{3D,s=2}_{SLVP} = \sqrt{\frac{8 \cdot 5E_b}{33}} \begin{pmatrix} -2 & 1 & -1 \\ 1 & 1 & 0 \\ 1 & 0 & 1 \\ 0 & 1 & 1 \\ -1 & -1 & 0 \\ -1 & 0 & -1 \\ 0 & -1 & -1 \\ 1 & -1 & 0 \\ 1 & 0 & -1 \\ 0 & 1 & -1 \\ -1 & 1 & 0 \\ -1 & 0 & 1 \\ 0 & -1 & 1 \\ 2 & 0 & 0 \\ 0 & 2 & 0 \\ -2 & 0 & 0 \\ 0 & -2 & 0 \\ 0 & 0 & 2 \\ 0 & 0 & -2 \\ 2 & 1 & 1 \\ -2 & -1 & -1 \\ 1 & 2 & 1 \\ -1 & -2 & -1 \\ 1 & 1 & 2 \\ -1 & -1 & -2 \\ -2 & 1 & 1 \\ 2 & -1 & -1 \\ 1 & -2 & 1 \\ -1 & 2 & -1 \\ 1 & 1 & -2 \\ -1 & -1 & 2 \\ 2 & -1 & 1 \end{pmatrix} \tag{C.8}$$

C.3 $(5, 4)$ constellations

$$\mathbf{P}_{LVP}^{4D,s=1} = \sqrt{\frac{8 \cdot 5E_b}{19}} \begin{pmatrix} 0 & 0 & 0 & 0 \\ 1 & 1 & 0 & 0 \\ 1 & 0 & 1 & 0 \\ 1 & 0 & 0 & 1 \\ 0 & 1 & 1 & 0 \\ 0 & 1 & 0 & 1 \\ 0 & 0 & 1 & 1 \\ 1 & -1 & 0 & 0 \\ 1 & 0 & -1 & 0 \\ 1 & 0 & 0 & -1 \\ 0 & 1 & -1 & 0 \\ 0 & 1 & 0 & -1 \\ 0 & 0 & 1 & -1 \\ -1 & 1 & 0 & 0 \\ -1 & 0 & 1 & 0 \\ -1 & 0 & 0 & 1 \\ 0 & -1 & 1 & 0 \\ 0 & -1 & 0 & 1 \\ 0 & 0 & -1 & 1 \\ -1 & -1 & 0 & 0 \\ -1 & 0 & -1 & 0 \\ -1 & 0 & 0 & -1 \\ 0 & -1 & -1 & 0 \\ 0 & -1 & 0 & -1 \\ 0 & 0 & -1 & -1 \\ 2 & 0 & 0 & 0 \\ 0 & 2 & 0 & 0 \\ 0 & 0 & 2 & 0 \\ 0 & 0 & 0 & 2 \\ -2 & 0 & 0 & 0 \\ 0 & -2 & 0 & 0 \\ 0 & 0 & -2 & 0 \end{pmatrix} \tag{C.9}$$

$$\mathbf{P}_{SLVP}^{4D,s=1} = \sqrt{E_b} \begin{pmatrix} -1 & -1 & -1 & -1 \\ 1 & 1 & 1 & 1 \\ 1 & 1 & 1 & -1 \\ 1 & 1 & -1 & 1 \\ 1 & -1 & 1 & 1 \\ -1 & 1 & 1 & 1 \\ -1 & -1 & -1 & 1 \\ -1 & -1 & 1 & -1 \\ -1 & 1 & -1 & -1 \\ 1 & -1 & -1 & -1 \\ 1 & 1 & -1 & -1 \\ -1 & 1 & 1 & -1 \\ -1 & -1 & 1 & 1 \\ -1 & 1 & -1 & 1 \\ 1 & -1 & 1 & -1 \\ 1 & -1 & -1 & 1 \\ 2 & 0 & 0 & 0 \\ -2 & 0 & 0 & 0 \\ 0 & 2 & 0 & 0 \\ 0 & -2 & 0 & 0 \\ 0 & 0 & 2 & 0 \\ 0 & 0 & -2 & 0 \\ 0 & 0 & 0 & 2 \\ 0 & 0 & 0 & -2 \\ 2 & 2 & 0 & 0 \\ -2 & -2 & 0 & 0 \\ 2 & 0 & 2 & 0 \\ -2 & 0 & -2 & 0 \\ 2 & 0 & 0 & 2 \\ -2 & 0 & 0 & -2 \\ 0 & 0 & 2 & 2 \\ 0 & 0 & -2 & -2 \end{pmatrix} \tag{C.10}$$

$$\mathbf{P}_{SSP}^{4D,s=1} = 10^{-1}\sqrt{5E_b}\begin{pmatrix}
-3.3413 & 5.4758 & 5.2536 & -5.5902 \\
4.8443 & 4.3882 & 7.1217 & -2.5607 \\
-3.3214 & 1.8234 & 0.6444 & 9.2319 \\
2.6076 & -4.1890 & 3.4687 & 7.9762 \\
3.0487 & -2.3937 & -5.3198 & 7.5283 \\
1.0124 & -2.1089 & 6.3186 & -7.3893 \\
7.3347 & 6.4145 & -1.2491 & -1.8696 \\
-6.3266 & -6.4272 & -3.0558 & -3.0541 \\
-3.5847 & 0.0266 & -0.8596 & -9.2957 \\
4.8321 & -4.0875 & 7.7330 & 0.3793 \\
8.7870 & 0.8833 & 2.4847 & 3.9793 \\
1.2016 & -6.0777 & -7.8265 & -0.6027 \\
-6.5100 & 4.8207 & 5.1524 & 2.7989 \\
-8.8413 & -2.6678 & 0.8559 & 3.7391 \\
-2.4192 & -8.1444 & -2.0332 & 4.8664 \\
-3.5472 & -3.1106 & 8.1057 & 3.4697 \\
8.3895 & -1.5644 & 1.8731 & -4.8642 \\
4.0919 & 1.4564 & -5.4421 & -7.1777 \\
2.4171 & 5.0204 & -8.2948 & 0.3861 \\
-8.9628 & 3.2417 & -1.5661 & -2.5897 \\
-5.1370 & -1.3060 & -7.1879 & 4.4989 \\
-4.4678 & 7.0553 & -4.0397 & 3.7339 \\
8.2915 & -1.1676 & -5.4571 & 0.3279 \\
-7.2344 & -2.4843 & 4.9793 & -4.0864 \\
1.6757 & 3.7331 & 7.0205 & 5.8283 \\
2.1536 & -6.4855 & -1.6979 & -7.1006 \\
5.7729 & -8.0349 & -0.2945 & 1.4238 \\
3.7286 & 5.9662 & -2.1692 & 6.7673 \\
0.3648 & 9.6278 & 2.5151 & 9.2001 \\
-1.7900 & 7.6270 & -3.3315 & -5.2466 \\
-3.8451 & 0.4450 & -8.2268 & -4.1637 \\
-1.4732 & -8.8832 & 4.0111 & -1.6820
\end{pmatrix} \tag{C.11}$$

$$\mathbf{P}_{ZSSP}^{4D,s=1} = \frac{32}{31} 10^{-1} \sqrt{5E_b} \begin{pmatrix} 0 & 0 & 0 & 0 \\ -3.5184 & -4.9073 & 5.0383 & -6.1769 \\ -1.7702 & 7.6950 & 6.1337 & 0.1769 \\ 5.8662 & -6.2654 & -4.2121 & 2.9310 \\ 8.0456 & 1.2670 & 0.9345 & 5.7262 \\ -5.6661 & -0.1913 & 8.2212 & 0.5210 \\ 1.4342 & 1.6213 & 7.8437 & 5.8130 \\ 0.3505 & 3.1279 & 6.0202 & -7.3383 \\ -1.4009 & 0.3483 & -2.0790 & -9.6744 \\ 2.4987 & -9.2643 & 1.6437 & -2.2865 \\ 4.8424 & 8.5469 & -1.4742 & 1.1522 \\ -3.8094 & -6.8296 & -3.7187 & -5.0016 \\ -0.6875 & -3.5816 & -9.2970 & 0.5150 \\ -8.1003 & 4.5451 & 1.4940 & 3.3905 \\ 3.1106 & -6.3234 & 3.8566 & 5.9552 \\ -1.3785 & 8.2533 & -0.9650 & -5.3900 \\ -2.6874 & -8.4839 & -2.4108 & 3.8716 \\ 9.1038 & -3.0864 & 1.7812 & -2.1028 \\ 5.2790 & 2.1620 & -7.3777 & 3.6095 \\ -3.0758 & 7.2791 & -5.7896 & 2.0087 \\ 1.3694 & -1.7840 & -3.0177 & 9.2648 \\ 3.1426 & -3.6258 & 8.6689 & -1.3520 \\ -6.4932 & -0.9332 & -5.2123 & 5.4588 \\ 6.571 & 4.3581 & 6.0860 & -0.8861 \\ -6.9432 & 1.0658 & -6.3145 & -3.2838 \\ -9.0280 & -4.2110 & 0.8544 & 0.1793 \\ 4.7157 & -4.2627 & -5.1308 & -5.7677 \\ 1.4933 & 3.5509 & -8.0797 & -4.4586 \\ -7.6554 & 2.6228 & 2.3131 & -5.4006 \\ -4.9004 & -2.5341 & 3.2631 & 7.6757 \\ 6.3527 & 3.7187 & -0.7939 & -6.7219 \\ -0.4429 & 6.2030 & 0.5407 & 7.8125 \end{pmatrix} \tag{C.12}$$

C.4 $(6,4)$ constellations

$$\mathbf{P}_{LVP}^{4D,s=2} = \sqrt{\frac{32 \cdot 6E_b}{117}} \begin{pmatrix}
0 & 0 & 0 & 0 \\
1 & 1 & 0 & 0 \\
1 & 0 & 1 & 0 \\
1 & 0 & 0 & 1 \\
0 & 1 & 1 & 0 \\
0 & 1 & 0 & 1 \\
0 & 0 & 1 & 1 \\
1 & -1 & 0 & 0 \\
1 & 0 & -1 & 0 \\
1 & 0 & 0 & -1 \\
0 & 1 & -1 & 0 \\
0 & 1 & 0 & -1 \\
0 & 0 & 1 & -1 \\
-1 & 1 & 0 & 0 \\
-1 & 0 & 1 & 0 \\
-1 & 0 & 0 & 1 \\
0 & -1 & 1 & 0 \\
0 & -1 & 0 & 1 \\
0 & 0 & -1 & 1 \\
-1 & -1 & 0 & 0 \\
-1 & 0 & -1 & 0 \\
-1 & 0 & 0 & -1 \\
0 & -1 & -1 & 0 \\
0 & -1 & 0 & -1 \\
0 & 0 & -1 & -1 \\
2 & 0 & 0 & 0 \\
0 & 2 & 0 & 0 \\
0 & 0 & 2 & 0 \\
0 & 0 & 0 & 2 \\
-2 & 0 & 0 & 0 \\
0 & -2 & 0 & 0 \\
0 & 0 & -2 & 0 \\
0 & 0 & 0 & -2 \\
1 & 1 & 1 & 1 \\
1 & 1 & -1 & -1 \\
1 & -1 & 1 & -1 \\
1 & -1 & -1 & 1 \\
-1 & 1 & 1 & -1 \\
-1 & 1 & -1 & 1 \\
-1 & -1 & 1 & 1 \\
-1 & -1 & -1 & -1 \\
1 & 1 & 1 & -1 \\
1 & 1 & -1 & 1 \\
1 & -1 & 1 & 1 \\
-1 & 1 & 1 & 1 \\
-1 & -1 & -1 & 1 \\
-1 & -1 & 1 & -1 \\
-1 & 1 & -1 & -1 \\
1 & -1 & -1 & -1 \\
2 & 1 & 1 & 0 \\
2 & -1 & 1 & 0 \\
2 & 1 & -1 & 0 \\
2 & -1 & -1 & 0 \\
2 & 1 & 0 & 1 \\
2 & -1 & 0 & 1 \\
2 & 1 & 0 & -1 \\
2 & -1 & 0 & -1 \\
-2 & 1 & 1 & 0 \\
-2 & -1 & 1 & 0 \\
-2 & 1 & -1 & 0 \\
-2 & -1 & -1 & 0 \\
-2 & 1 & 0 & 1 \\
-2 & -1 & 0 & 1 \\
-2 & 1 & 0 & -1
\end{pmatrix} \tag{C.13}$$

$$\mathbf{P}_{SLVP}^{4D,s=2}\sqrt{\frac{2\cdot 6E_b}{15}}\begin{pmatrix}
-1 & -1 & -1 & -1\\
1 & 1 & 1 & 1\\
1 & 1 & 1 & -1\\
1 & 1 & -1 & 1\\
1 & -1 & 1 & 1\\
-1 & 1 & 1 & 1\\
-1 & -1 & -1 & 1\\
-1 & -1 & 1 & -1\\
-1 & 1 & -1 & -1\\
1 & -1 & -1 & -1\\
1 & 1 & -1 & -1\\
-1 & 1 & 1 & -1\\
-1 & -1 & 1 & 1\\
-1 & 1 & -1 & 1\\
1 & -1 & 1 & -1\\
1 & -1 & -1 & 1\\
2 & 0 & 0 & 0\\
-2 & 0 & 0 & 0\\
0 & 2 & 0 & 0\\
0 & -2 & 0 & 0\\
0 & 0 & 2 & 0\\
0 & 0 & -2 & 0\\
0 & 0 & 0 & 2\\
0 & 0 & 0 & -2\\
2 & 2 & 0 & 0\\
-2 & -2 & 0 & 0\\
2 & 0 & 2 & 0\\
-2 & 0 & -2 & 0\\
2 & 0 & 0 & 2\\
-2 & 0 & 0 & -2\\
0 & 0 & 2 & 2\\
0 & 0 & -2 & -2\\
0 & 2 & 2 & 0\\
0 & -2 & -2 & 0\\
0 & 2 & 0 & 2\\
0 & -2 & 0 & -2\\
2 & -2 & 0 & 0\\
-2 & 2 & 0 & 0\\
2 & 0 & -2 & 0\\
-2 & 0 & 2 & 0\\
2 & 0 & 0 & -2\\
-2 & 0 & 0 & 2\\
0 & 0 & 2 & -2\\
0 & 0 & -2 & 2\\
0 & 2 & -2 & 0\\
0 & -2 & 2 & 0\\
0 & 2 & 0 & -2\\
0 & -2 & 0 & 2\\
2 & 2 & 2 & 0\\
-2 & -2 & -2 & 0\\
2 & 2 & 0 & 2\\
-2 & -2 & 0 & -2\\
2 & 0 & 2 & 2\\
-2 & 0 & -2 & -2\\
0 & 2 & 2 & 2\\
0 & -2 & -2 & -2\\
2 & 2 & -2 & 0\\
-2 & -2 & 2 & 0\\
2 & 2 & 0 & -2\\
-2 & -2 & 0 & 2\\
2 & 0 & 2 & -2\\
-2 & 0 & -2 & 2\\
0 & 2 & 2 & -2\\
0 & -2 & -2 & 2
\end{pmatrix} \tag{C.14}$$

$$\mathbf{P}_{SSP}^{4D,s=2} = \sqrt{E_b} \begin{pmatrix}
2.4296 & -0.1245 & 0.2625 & 0.1129 \\
1.6028 & -1.0041 & 1.5539 & 0.0906 \\
1.8015 & 0.9944 & 0.0268 & -1.3286 \\
-0.8361 & -0.7286 & -0.3068 & -2.1624 \\
0.7868 & -0.4962 & -0.8852 & 2.0860 \\
-1.6378 & -1.3336 & 1.2323 & 0.1445 \\
1.7849 & -0.6659 & 0.6652 & -1.3886 \\
0.5041 & 0.2366 & 0.6861 & 2.2845 \\
0.4711 & 1.6820 & 1.0707 & 1.3426 \\
0.6232 & 2.0388 & -0.6257 & 1.0313 \\
-1.6687 & -0.6389 & 0.5028 & 1.5983 \\
1.6486 & 0.4124 & 1.3558 & 1.1287 \\
1.6573 & -1.0400 & 0.3912 & 1.4208 \\
0.1523 & 2.3733 & 0.5618 & -0.1696 \\
0.4853 & -0.2575 & 1.7721 & -1.5993 \\
-2.3255 & -0.5935 & -0.4244 & 0.2447 \\
0.6712 & 0.0990 & 0.0569 & -2.3530 \\
-2.1903 & 0.7649 & 0.6915 & 0.3729 \\
0.4437 & -0.7779 & 1.8149 & 1.3799 \\
-1.0912 & 0.9340 & -0.7447 & -1.8392 \\
1.8318 & 0.6612 & -0.3563 & 1.4424 \\
-1.6645 & -0.4102 & -1.3809 & -1.0743 \\
-1.1720 & -1.9635 & -0.2421 & 0.8440 \\
1.7426 & -1.7142 & -0.0406 & -0.1531 \\
0.0998 & 1.3800 & 1.7222 & -1.0582 \\
-1.1126 & -0.0526 & 1.9488 & 0.9806 \\
0.7227 & -1.4927 & -0.4214 & -1.7527 \\
-1.3266 & -0.1238 & -1.9869 & 0.5263 \\
0.2401 & -0.8668 & -2.0699 & 0.9521 \\
-0.7751 & 0.5274 & 0.9317 & -2.0623 \\
0.7691 & 0.8850 & -1.3647 & -1.6622 \\
0.8465 & 0.7516 & -1.8031 & 1.2114 \\
-0.9793 & -1.1071 & 1.2735 & -1.4811 \\
0.9317 & 0.0774 & -2.2348 & -0.3625 \\
1.9630 & -0.3768 & -1.0211 & -0.9808 \\
1.6478 & 0.6173 & 1.5905 & -0.6115 \\
1.8645 & -0.7202 & -1.2068 & 0.7406 \\
-0.1015 & -2.0903 & 1.1338 & 0.5788 \\
-0.0287 & -0.6390 & -1.7632 & -1.5755 \\
1.7163 & 1.6685 & 0.4585 & 0.2453 \\
-0.8204 & -1.6341 & -1.6231 & -0.1489 \\
-1.5354 & -1.6933 & -0.1725 & -0.8634 \\
-0.1124 & -1.3641 & 0.3690 & 1.9976 \\
-1.7966 & 0.6346 & -0.7118 & 1.3649 \\
-0.6993 & 1.4754 & -1.6527 & 0.7764 \\
-2.1037 & 0.0798 & 0.2528 & -1.2264 \\
-0.9072 & 1.5723 & 1.6009 & 0.3770 \\
0.5742 & -1.8104 & 1.1537 & -1.0305 \\
-1.2272 & 2.0097 & -0.0557 & 0.6723 \\
-1.4219 & 1.6702 & 0.5477 & -0.9427 \\
1.6378 & 1.3336 & -1.2323 & -0.1445 \\
0.1015 & 2.0903 & -1.1338 & -0.5788 \\
0.7155 & -1.9396 & -0.7535 & 1.0763 \\
0.0181 & -2.3966 & -0.2923 & -0.4128 \\
-1.0518 & 0.9781 & 0.7862 & 1.8218 \\
0.2376 & 1.6991 & 0.1301 & -1.7435 \\
-0.2288 & 0.9440 & -0.7493 & 2.1201 \\
-0.9277 & -0.7855 & -1.0796 & 1.8321 \\
-0.2203 & -0.9602 & 2.2325 & -0.2131 \\
0.9231 & -1.5745 & -1.5758 & -0.4313 \\
-0.6141 & 0.8012 & -2.0845 & -0.7975 \\
-1.9780 & 1.0840 & -0.8983 & -0.3250 \\
-1.4693 & 0.3092 & 1.8019 & -0.7063 \\
0.3780 & 0.5911 & 2.3156 & 0.3818
\end{pmatrix} \tag{C.15}$$

$$\mathbf{P}_{ZSSP}^{4D,s=2} = \sqrt{E_b} \begin{pmatrix} 0 & 0 & 0 & 0 \\ 1.1950 & -1.2353 & -1.1232 & 1.3710 \\ 1.9163 & -0.8893 & -1.2588 & -0.2186 \\ 1.8720 & 0.3801 & -1.1751 & 1.0323 \\ 1.0054 & -0.1438 & -1.6861 & -1.4902 \\ 1.8020 & 1.0753 & -1.1489 & -0.6096 \\ 0.7307 & 1.6265 & -1.5862 & 0.6323 \\ 0.0151 & 1.1855 & -1.9724 & -0.8940 \\ 0.5929 & 1.7690 & -0.5214 & -1.5305 \\ 1.0916 & -1.4452 & -0.4182 & -1.6248 \\ 1.1589 & 0.2593 & -0.0902 & -2.1626 \\ -0.6940 & 0.7224 & -0.9002 & -2.0691 \\ -1.0661 & 1.9045 & 0.0009 & -1.1540 \\ -0.3760 & -0.5522 & 0.2720 & -2.3611 \\ -0.0979 & 1.0735 & 0.8806 & -2.0390 \\ 1.4782 & 1.3556 & 0.9126 & -1.1134 \\ 1.1035 & -0.2087 & 1.5293 & -1.5795 \\ 1.8445 & 0.1664 & 1.6326 & -0.0033 \\ 2.0949 & 1.2054 & 0.2692 & 0.4255 \\ 0.9329 & 1.4813 & 1.5387 & 0.8143 \\ 0.3158 & 0.5620 & 2.3430 & -0.4357 \\ 0.7949 & 2.3356 & -0.0454 & 0.0809 \\ -0.0429 & 1.9886 & 1.3428 & -0.5792 \\ -1.4703 & 0.9691 & 1.6595 & -0.4903 \\ -0.7354 & 0.4308 & 2.0997 & 0.9798 \\ -0.7222 & 1.8564 & 1.0275 & 1.0353 \\ -0.6946 & -0.2477 & 1.7898 & -1.5323 \\ -1.7075 & 0.3948 & 0.4758 & -1.6726 \\ -2.0130 & 1.3929 & 0.1922 & 0.2567 \\ -2.3693 & -0.2501 & 0.6289 & -0.1535 \\ -1.3033 & -0.9293 & 1.8796 & -0.0020 \\ -1.7827 & 0.0173 & 0.8165 & 1.5001 \\ 0.8566 & -0.1702 & 1.8104 & 1.4335 \\ -0.2506 & 0.5956 & 0.9061 & 2.2038 \\ 2.2213 & -0.7125 & 0.1706 & 0.7902 \\ 2.3131 & -0.0167 & 0.1447 & -0.8505 \\ -0.5798 & -1.1504 & 1.4264 & 1.5495 \\ 0.4510 & -1.1449 & 2.1402 & 0.0249 \\ 0.1641 & -1.6657 & 1.1398 & -1.4123 \\ -0.4239 & -2.2044 & 1.0119 & 0.1791 \\ -1.7297 & -1.5332 & 0.2374 & 0.8346 \\ 1.6825 & -1.4120 & 1.0000 & -0.5203 \\ -0.3976 & -2.2191 & -0.3866 & -0.9292 \\ 0.3667 & -1.5626 & -1.8350 & -0.3898 \\ 1.0916 & -2.1801 & -0.3843 & 0.0535 \\ -0.5189 & -0.9671 & -1.3477 & -1.7534 \\ -2.0080 & -0.5631 & -0.8715 & -0.9933 \\ -1.5090 & -1.3319 & 0.6323 & -1.2824 \\ 1.0106 & -1.7025 & 0.9672 & 1.1135 \\ -0.2385 & -2.0700 & -0.4792 & 1.2345 \\ -0.2870 & -0.7926 & -1.9942 & 1.1865 \\ -1.1978 & -0.6272 & -0.6746 & 1.9525 \\ 0.4372 & 0.3074 & -1.1990 & 2.0910 \\ 0.3494 & -0.8847 & 0.1133 & 2.2754 \\ -2.1933 & 0.0663 & -0.9147 & 0.6659 \\ -1.6389 & 1.0692 & -1.3698 & -0.6243 \\ -0.8265 & 0.8821 & -1.9604 & 0.8894 \\ 0.8527 & 0.0651 & -2.3104 & 0.1616 \\ -0.8148 & -0.2907 & -2.2741 & -0.4186 \\ -1.2752 & -1.6274 & -1.3416 & 0.1445 \\ -1.2813 & 1.1284 & -0.4683 & 1.7207 \\ 0.3756 & 1.7371 & -0.2063 & 1.7012 \\ 1.4649 & 0.4431 & 0.3232 & 1.9101 \\ -0.7720 & 2.1615 & -0.8273 & 0.3779 \end{pmatrix} \tag{C.16}$$

C.5 $(6, 5)$ constellations

$$\mathbf{P}_{LVP}^{5D,s=1} = \sqrt{\frac{16 \cdot 6E_b}{43}} \begin{pmatrix} 0 & 0 & 0 & 0 & 0 \\ 1 & 1 & 0 & 0 & 0 \\ 1 & 0 & 1 & 0 & 0 \\ 1 & 0 & 0 & 1 & 0 \\ 1 & 0 & 0 & 0 & 1 \\ 0 & 1 & 1 & 0 & 0 \\ 0 & 1 & 0 & 1 & 0 \\ 0 & 1 & 0 & 0 & 1 \\ 0 & 0 & 1 & 1 & 0 \\ 0 & 0 & 1 & 0 & 1 \\ 0 & 0 & 0 & 1 & 1 \\ 1 & -1 & 0 & 0 & 0 \\ 1 & 0 & -1 & 0 & 0 \\ 1 & 0 & 0 & -1 & 0 \\ 1 & 0 & 0 & 0 & -1 \\ 0 & 1 & -1 & 0 & 0 \\ 0 & 1 & 0 & -1 & 0 \\ 0 & 1 & 0 & 0 & -1 \\ 0 & 0 & 1 & -1 & 0 \\ 0 & 0 & 1 & 0 & -1 \\ 0 & 0 & 0 & 1 & -1 \\ -1 & 1 & 0 & 0 & 0 \\ -1 & 0 & 1 & 0 & 0 \\ -1 & 0 & 0 & 1 & 0 \\ -1 & 0 & 0 & 0 & 1 \\ 0 & -1 & 1 & 0 & 0 \\ 0 & -1 & 0 & 1 & 0 \\ 0 & -1 & 0 & 0 & 1 \\ 0 & 0 & -1 & 1 & 0 \\ 0 & 0 & -1 & 0 & 1 \\ 0 & 0 & 0 & -1 & 1 \\ -1 & -1 & 0 & 0 & 0 \\ -1 & 0 & -1 & 0 & 0 \\ -1 & 0 & 0 & -1 & 0 \\ -1 & 0 & 0 & 0 & -1 \\ 0 & -1 & -1 & 0 & 0 \\ 0 & -1 & 0 & -1 & 0 \\ 0 & -1 & 0 & 0 & -1 \\ 0 & 0 & -1 & -1 & 0 \\ 0 & 0 & -1 & 0 & -1 \\ 0 & 0 & 0 & -1 & -1 \\ 2 & 0 & 0 & 0 & 0 \\ 0 & 2 & 0 & 0 & 0 \\ 0 & 0 & 2 & 0 & 0 \\ 0 & 0 & 0 & 2 & 0 \\ 0 & 0 & 0 & 0 & 2 \\ -2 & 0 & 0 & 0 & 0 \\ 0 & -2 & 0 & 0 & 0 \\ 0 & 0 & -2 & 0 & 0 \\ 0 & 0 & 0 & -2 & 0 \\ 0 & 0 & 0 & 0 & -2 \\ 1 & 1 & 1 & 1 & 0 \\ 1 & 1 & 1 & 0 & 1 \\ 1 & 1 & 0 & 1 & 1 \\ 1 & 0 & 1 & 1 & 1 \\ 0 & 1 & 1 & 1 & 1 \\ -1 & -1 & -1 & -1 & 0 \\ -1 & -1 & -1 & 0 & -1 \\ -1 & -1 & 0 & -1 & -1 \\ -1 & 0 & -1 & -1 & -1 \\ 0 & -1 & -1 & -1 & -1 \\ 1 & -1 & -1 & -1 & 0 \\ -1 & 1 & 1 & 1 & 0 \\ 0 & 1 & 1 & 1 & -1 \end{pmatrix} \tag{C.17}$$

$$\mathbf{P}_{SLVP}^{5D,s=1} = \sqrt{\frac{4 \cdot 6E_b}{11}} \begin{pmatrix}
1 & 1 & 0 & 0 & 0 \\
1 & 0 & 1 & 0 & 0 \\
1 & 0 & 0 & 1 & 0 \\
1 & 0 & 0 & 0 & 1 \\
0 & 1 & 1 & 0 & 0 \\
0 & 1 & 0 & 1 & 0 \\
0 & 1 & 0 & 0 & 1 \\
0 & 0 & 1 & 1 & 0 \\
0 & 0 & 1 & 0 & 1 \\
0 & 0 & 0 & 1 & 1 \\
1 & -1 & 0 & 0 & 0 \\
1 & 0 & -1 & 0 & 0 \\
1 & 0 & 0 & -1 & 0 \\
1 & 0 & 0 & 0 & -1 \\
0 & 1 & -1 & 0 & 0 \\
0 & 1 & 0 & -1 & 0 \\
0 & 1 & 0 & 0 & -1 \\
0 & 0 & 1 & -1 & 0 \\
0 & 0 & 1 & 0 & -1 \\
0 & 0 & 0 & 1 & -1 \\
-1 & 1 & 0 & 0 & 0 \\
-1 & 0 & 1 & 0 & 0 \\
-1 & 0 & 0 & 1 & 0 \\
-1 & 0 & 0 & 0 & 1 \\
0 & -1 & 1 & 0 & 0 \\
0 & -1 & 0 & 1 & 0 \\
0 & -1 & 0 & 0 & 1 \\
0 & 0 & -1 & 1 & 0 \\
0 & 0 & -1 & 0 & 1 \\
0 & 0 & 0 & -1 & 1 \\
-1 & -1 & 0 & 0 & 0 \\
-1 & 0 & -1 & 0 & 0 \\
-1 & 0 & 0 & -1 & 0 \\
-1 & 0 & 0 & 0 & -1 \\
0 & -1 & -1 & 0 & 0 \\
0 & -1 & 0 & -1 & 0 \\
0 & -1 & 0 & 0 & -1 \\
0 & 0 & -1 & -1 & 0 \\
0 & 0 & -1 & 0 & -1 \\
0 & 0 & 0 & -1 & -1 \\
2 & 0 & 0 & 0 & 0 \\
0 & 2 & 0 & 0 & 0 \\
0 & 0 & 2 & 0 & 0 \\
0 & 0 & 0 & 2 & 0 \\
0 & 0 & 0 & 0 & 2 \\
-2 & 0 & 0 & 0 & 0 \\
0 & -2 & 0 & 0 & 0 \\
0 & 0 & -2 & 0 & 0 \\
0 & 0 & 0 & -2 & 0 \\
0 & 0 & 0 & 0 & -2 \\
1 & 1 & 1 & 1 & 0 \\
1 & 1 & 1 & 0 & 1 \\
1 & 1 & 0 & 1 & 1 \\
1 & 0 & 1 & 1 & 1 \\
0 & 1 & 1 & 1 & 1 \\
-1 & -1 & -1 & -1 & 0 \\
-1 & -1 & -1 & 0 & -1 \\
-1 & -1 & 0 & -1 & -1 \\
-1 & 0 & -1 & -1 & -1 \\
0 & -1 & -1 & -1 & -1 \\
1 & -1 & -1 & -1 & 0 \\
-1 & 1 & 1 & 1 & 0 \\
0 & 1 & 1 & 1 & -1 \\
0 & -1 & -1 & 1 & 1
\end{pmatrix} \tag{C.18}$$

$$\mathbf{P}_{SSP}^{5D,s=1} = \sqrt{E_b} \begin{pmatrix}
0.3977 & 0.1899 & -2.1969 & -0.9873 & -0.0667 \\
1.1518 & 1.3004 & -1.6123 & 0.6178 & 0.0324 \\
-0.1405 & 1.2235 & -1.4648 & -0.3306 & 1.4928 \\
0.3334 & 0.5292 & -0.8721 & 1.9280 & -1.0635 \\
-1.1787 & 1.2751 & 0.4748 & -1.2130 & -1.1349 \\
1.1939 & -0.7129 & -1.7520 & 0.6269 & -0.7771 \\
0.5618 & 2.2208 & 0.0746 & 0.3143 & 0.8050 \\
1.6841 & 0.7632 & -0.7712 & -1.0792 & -0.9066 \\
-0.6009 & 0.8264 & -0.2274 & -2.1458 & 0.5478 \\
-0.6694 & 1.0726 & 1.0491 & 0.9652 & 1.5393 \\
1.3912 & 1.0473 & -0.2736 & -1.2395 & 1.1647 \\
0.8756 & 1.8293 & 0.1211 & 0.3984 & -1.3090 \\
0.9920 & 0.9334 & 1.6238 & -0.2615 & 1.1998 \\
-0.0363 & -1.3275 & -0.4873 & 0.7089 & 1.8699 \\
1.0984 & -1.1333 & 0.5445 & -0.7977 & 1.6050 \\
0.9101 & -0.6849 & -0.5484 & -2.0746 & 0.3132 \\
-1.3701 & -0.7789 & 1.3166 & 0.1314 & 1.3287 \\
1.9646 & -0.2828 & 0.9494 & -1.0682 & -0.1343 \\
-2.1972 & -0.0578 & 0.0787 & -1.0627 & 0.1829 \\
-0.6967 & -0.5024 & 0.3389 & 2.0988 & 0.8616 \\
-0.3907 & 1.2143 & -0.8923 & 1.6822 & 0.8642 \\
-1.1979 & -0.3292 & 1.7111 & -0.4213 & -1.1626 \\
-0.4437 & 0.2759 & 0.3731 & -0.9505 & 2.1643 \\
-0.8893 & -1.7766 & 0.1972 & -0.9135 & -1.0860 \\
-0.0117 & -1.0258 & -0.4674 & 0.8544 & -1.9998 \\
-0.1118 & -1.7637 & -0.8752 & 1.4502 & -0.0882 \\
1.0231 & -1.2145 & -0.5744 & -0.9745 & -1.4828 \\
-0.1801 & -0.3549 & -2.1170 & 0.8330 & 0.8161 \\
0.2273 & 0.2971 & 0.4075 & -0.5802 & -2.3146 \\
-1.5574 & 0.7214 & -1.7078 & -0.3663 & -0.0597 \\
0.3397 & -2.0844 & -1.0071 & -0.5839 & 0.4296 \\
-0.0325 & 1.9630 & -1.0569 & -0.9238 & -0.4185 \\
1.8048 & -0.1137 & 0.0961 & 0.5922 & -1.5394 \\
-0.0594 & -2.1983 & 0.8903 & 0.3940 & 0.4648 \\
-0.5615 & 1.8120 & 1.4575 & 0.3722 & -0.3720 \\
-1.4401 & 1.7894 & 0.0030 & -0.4119 & 0.7447 \\
0.6240 & -1.3284 & 1.3230 & 0.0035 & -1.4477 \\
-1.6173 & 0.1569 & -0.6232 & 0.4929 & 1.6518 \\
0.9634 & 0.5520 & -0.1164 & 0.6081 & 2.0938 \\
-1.7610 & -0.1668 & -0.3376 & -0.0399 & -1.6600 \\
1.8155 & -1.5889 & 0.0720 & 0.4145 & 0.0486 \\
-1.5405 & -0.1621 & -1.1025 & 1.5039 & -0.3511 \\
-0.0337 & 0.6454 & -1.5646 & 0.0298 & -1.7701 \\
-2.0740 & 0.5739 & 0.7481 & 0.8995 & -0.0142 \\
0.7969 & 1.5273 & 0.9758 & -1.3743 & -0.4376 \\
-0.5505 & 0.4980 & 0.8917 & 1.2959 & -1.7247 \\
0.6351 & 1.1530 & 0.8440 & 1.8839 & 0.0778 \\
-0.4996 & -0.0662 & 2.0685 & 1.2112 & 0.0123 \\
1.2958 & -0.3450 & -0.6870 & 1.8127 & 0.6662 \\
0.3458 & -0.8459 & 2.1341 & -0.6920 & 0.3629 \\
-0.6394 & -0.1698 & -0.9439 & -1.7897 & -1.2117 \\
0.1556 & -0.4017 & 1.0395 & -1.9666 & -0.9308 \\
1.1255 & 0.6038 & 1.8841 & 0.2894 & -0.8574 \\
0.6651 & -0.8638 & 0.7621 & 1.9228 & -0.7305 \\
1.6066 & -0.5372 & -1.3430 & -0.2256 & 1.1294 \\
2.1843 & 0.8707 & 0.2267 & 0.5403 & 0.3573 \\
-1.0000 & 0.7125 & 1.6700 & -1.1678 & 0.5829 \\
-0.8117 & -0.6195 & -1.3380 & -1.2369 & 1.2795 \\
-0.7097 & -1.2433 & 0.6366 & -1.6986 & 0.8124 \\
-1.3368 & -1.2918 & 0.6918 & 1.1950 & -0.7984 \\
-1.1029 & 1.7170 & -0.5464 & 0.8426 & -0.9093 \\
-0.8079 & -1.1409 & -1.8225 & -0.1009 & -0.8449 \\
1.0481 & -0.6965 & 1.3120 & 1.1428 & 1.1785 \\
-1.6198 & -1.6759 & -0.4931 & 0.0802 & 0.5638
\end{pmatrix} \tag{C.19}$$

$$\mathbf{P}_{ZSSP}^{5D,s=1} = \sqrt{E_b} \begin{pmatrix} 0 & 0 & 0 & 0 & 0 \\ -0.8148 & 2.0600 & -0.0931 & -0.6704 & -0.8541 \\ -0.8938 & -0.3330 & -1.5829 & 0.7552 & 1.4524 \\ -0.2240 & -0.3307 & 0.8733 & -2.1431 & 0.7616 \\ -0.8820 & -0.8124 & -0.6588 & -1.1661 & 1.6921 \\ 0.0521 & 0.6136 & -1.8995 & -0.9269 & 1.1175 \\ -1.2540 & 0.4197 & 0.4499 & -0.1493 & -2.0302 \\ 0.5036 & -0.8518 & 0.4544 & 0.1584 & -2.2101 \\ 0.2640 & -1.4121 & -1.1567 & 1.6379 & 0.1042 \\ 1.2663 & 0.0427 & -1.6119 & 0.8195 & 1.1046 \\ 1.9069 & -0.3833 & 0.4612 & 0.4989 & 1.3604 \\ -0.4144 & -1.3148 & 1.4716 & -0.9935 & -1.0209 \\ -1.8414 & 1.0327 & 0.2505 & 1.1552 & -0.4906 \\ 0.3491 & -1.4538 & -1.7991 & -0.4167 & 0.6704 \\ -0.4026 & 0.4887 & 0.4362 & -2.0050 & -1.2181 \\ 2.3338 & 0.2199 & 0.3807 & 0.0587 & -0.6722 \\ 1.5451 & 0.5228 & 1.2264 & -1.2280 & 0.6500 \\ -0.1584 & 0.6914 & 1.0495 & 2.1179 & 0.0740 \\ -0.3977 & -0.5381 & 0.0302 & 1.9170 & -1.4042 \\ 1.5284 & 1.2005 & -0.0799 & 1.4882 & 0.3112 \\ -0.0291 & 0.0135 & -2.3628 & 0.5312 & -0.4787 \\ -0.4208 & 1.2277 & -0.9880 & 0.9563 & -1.5876 \\ 0.8954 & 0.4422 & 1.6631 & -0.7300 & -1.3414 \\ 0.2292 & 0.3703 & -0.0189 & 1.4623 & 1.9409 \\ 0.1820 & -1.6125 & -0.1718 & 0.5419 & 1.7716 \\ -0.1452 & -1.5141 & -1.2779 & -0.4131 & -1.4065 \\ 1.3976 & -1.2092 & 1.6240 & -0.1810 & -0.0963 \\ -0.9320 & 1.1265 & -0.3495 & -0.2120 & 1.9469 \\ -2.3212 & -0.1029 & -0.2866 & -0.0287 & 0.7834 \\ -0.0129 & -0.6463 & -1.0911 & -2.1130 & -0.1488 \\ -1.8286 & 0.5124 & 1.2534 & -0.9300 & -0.2305 \\ -1.8606 & -0.9703 & 0.9242 & 0.5876 & -0.7018 \\ 1.3858 & -0.7288 & 0.6980 & 1.7445 & -0.3365 \\ -1.3753 & 0.8437 & -0.6032 & -1.7109 & 0.4484 \\ 0.8835 & 0.9217 & 0.7390 & 1.1913 & -1.5811 \\ 1.7600 & -1.6505 & -0.4674 & 0.1790 & -0.1515 \\ 0.2812 & -2.1086 & 0.1858 & -1.1536 & 0.4524 \\ -1.2349 & -0.7904 & 0.1691 & 1.7894 & 0.8456 \\ -0.5093 & 1.5171 & 1.7284 & 0.3696 & -0.6407 \\ 0.0847 & -2.1744 & 0.6214 & 0.7640 & -0.6247 \\ -1.3871 & 1.3232 & -1.5273 & 0.2105 & 0.2087 \\ 1.3573 & -0.9008 & 0.1955 & -1.4990 & -1.0753 \\ 0.2416 & -0.1330 & 0.9511 & -0.5546 & 2.1925 \\ 1.3414 & -0.2559 & -1.0476 & 1.0858 & -1.3978 \\ -0.1417 & 0.0138 & 2.3554 & -0.5974 & 0.4127 \\ 0.7122 & 1.2426 & 1.5426 & 0.5800 & 1.1523 \\ 1.6384 & -0.0367 & -1.6167 & -0.8060 & -0.3825 \\ 0.8254 & 1.2713 & -0.5204 & -1.8744 & 0.1160 \\ 1.2800 & -0.5138 & -0.5393 & -1.4106 & 1.3828 \\ -1.7047 & -0.4499 & -1.1696 & 0.6613 & -1.0870 \\ -0.3217 & 1.6537 & 1.0380 & -1.2194 & 0.8322 \\ -0.2497 & 0.7135 & -1.1393 & 2.0417 & 0.2395 \\ 1.1784 & 2.0291 & 0.6021 & -0.2593 & -0.3994 \\ 0.8130 & 1.7770 & -1.4950 & 0.1519 & -0.1368 \\ -0.0506 & -0.5044 & 1.9796 & 0.9521 & -1.0064 \\ 1.2222 & 1.3639 & -0.3512 & -0.3035 & 1.5893 \\ -0.7588 & 0.4968 & -1.4862 & -1.0208 & -1.4220 \\ 0.2079 & -0.8154 & 1.6740 & 1.1500 & 1.1235 \\ -1.3147 & -1.9491 & -0.6554 & 0.2020 & 0.3122 \\ -0.3350 & 2.1904 & 0.0037 & 0.9313 & 0.5639 \\ -1.6929 & -0.9293 & -0.2455 & -1.2600 & -0.8473 \\ -1.3806 & 0.5941 & 1.3924 & 0.6635 & 1.2072 \\ -1.2216 & -1.3290 & 1.2072 & -0.3691 & 1.1149 \\ 1.0309 & 0.8916 & -0.4479 & -0.6234 & -1.9100 \end{pmatrix} \tag{C.20}$$

C.6 $(7,5)$ constellations

$$\mathbf{P}_{LVP}^{5D,s=2} = \sqrt{\frac{32\cdot 7E_b}{107}} \begin{pmatrix} 0 & 0 & 0 & 0 & 0 \\ 1 & 1 & 0 & 0 & 0 \\ 1 & 0 & 1 & 0 & 0 \\ 1 & 0 & 0 & 1 & 0 \\ 1 & 0 & 0 & 0 & 1 \\ 0 & 1 & 1 & 0 & 0 \\ 0 & 1 & 0 & 1 & 0 \\ 0 & 1 & 0 & 0 & 1 \\ 0 & 0 & 1 & 1 & 0 \\ 0 & 0 & 1 & 0 & 1 \\ 0 & 0 & 0 & 1 & 1 \\ 1 & -1 & 0 & 0 & 0 \\ 1 & 0 & -1 & 0 & 0 \\ 1 & 0 & 0 & -1 & 0 \\ 1 & 0 & 0 & 0 & -1 \\ 0 & 1 & -1 & 0 & 0 \\ 0 & 1 & 0 & -1 & 0 \\ 0 & 1 & 0 & 0 & -1 \\ 0 & 0 & 1 & -1 & 0 \\ 0 & 0 & 1 & 0 & -1 \\ 0 & 0 & 0 & 1 & -1 \\ -1 & 1 & 0 & 0 & 0 \\ -1 & 0 & 1 & 0 & 0 \\ -1 & 0 & 0 & 1 & 0 \\ -1 & 0 & 0 & 0 & 1 \\ 0 & -1 & 1 & 0 & 0 \\ 0 & -1 & 0 & 1 & 0 \\ 0 & -1 & 0 & 0 & 1 \\ 0 & 0 & -1 & 1 & 0 \\ 0 & 0 & -1 & 0 & 1 \\ 0 & 0 & 0 & -1 & 1 \\ -1 & -1 & 0 & 0 & 0 \\ -1 & 0 & -1 & 0 & 0 \\ -1 & 0 & 0 & -1 & 0 \\ -1 & 0 & 0 & 0 & -1 \\ 0 & -1 & -1 & 0 & 0 \\ 0 & -1 & 0 & -1 & 0 \\ 0 & -1 & 0 & 0 & -1 \\ 0 & 0 & -1 & -1 & 0 \\ 0 & 0 & -1 & 0 & -1 \\ 0 & 0 & 0 & -1 & -1 \\ 2 & 0 & 0 & 0 & 0 \\ 0 & 2 & 0 & 0 & 0 \\ 0 & 0 & 2 & 0 & 0 \\ 0 & 0 & 0 & 2 & 0 \\ 0 & 0 & 0 & 0 & 2 \\ -2 & 0 & 0 & 0 & 0 \\ 0 & -2 & 0 & 0 & 0 \\ 0 & 0 & -2 & 0 & 0 \\ 0 & 0 & 0 & -2 & 0 \\ 0 & 0 & 0 & 0 & -2 \\ 1 & 1 & 1 & 1 & 0 \\ 1 & 1 & 1 & 0 & 1 \\ 1 & 1 & 0 & 1 & 1 \\ 1 & 0 & 1 & 1 & 1 \\ 0 & 1 & 1 & 1 & 1 \\ -1 & -1 & -1 & -1 & 0 \\ -1 & -1 & -1 & 0 & -1 \\ -1 & -1 & 0 & -1 & -1 \\ -1 & 0 & -1 & -1 & -1 \\ 0 & -1 & -1 & -1 & -1 \\ 0 & 1 & 1 & 1 & -1 \\ 0 & 1 & 1 & -1 & 1 \\ 0 & 1 & -1 & 1 & 1 \\ 0 & -1 & 1 & 1 & 1 \\ 1 & 0 & 1 & 1 & -1 \\ 1 & 0 & 1 & -1 & 1 \\ 1 & 0 & -1 & 1 & 1 \\ -1 & 0 & 1 & 1 & 1 \\ 1 & 1 & 0 & 1 & -1 \\ 1 & 1 & 0 & -1 & 1 \\ 1 & -1 & 0 & 1 & 1 \\ -1 & 1 & 0 & 1 & 1 \\ 1 & 1 & 1 & 0 & -1 \\ 1 & 1 & -1 & 0 & 1 \\ 1 & -1 & 1 & 0 & 1 \\ -1 & 1 & 1 & 0 & 1 \\ \vdots & \vdots & \vdots & \vdots & \vdots \end{pmatrix} \begin{pmatrix} & & \vdots & & \\ 1 & 1 & 1 & -1 & 0 \\ 1 & 1 & -1 & 1 & 0 \\ 1 & -1 & 1 & 1 & 0 \\ -1 & 1 & 1 & 1 & 0 \\ 0 & -1 & -1 & -1 & 1 \\ 0 & -1 & -1 & 1 & -1 \\ 0 & -1 & 1 & -1 & -1 \\ 0 & 1 & -1 & -1 & -1 \\ -1 & 0 & -1 & -1 & 1 \\ -1 & 0 & -1 & 1 & -1 \\ -1 & 0 & 1 & -1 & -1 \\ 1 & 0 & -1 & -1 & -1 \\ -1 & -1 & 0 & -1 & 1 \\ -1 & -1 & 0 & 1 & -1 \\ -1 & 1 & 0 & -1 & -1 \\ 1 & -1 & 0 & -1 & -1 \\ -1 & -1 & -1 & 0 & 1 \\ -1 & -1 & 1 & 0 & -1 \\ -1 & 1 & -1 & 0 & -1 \\ 1 & -1 & -1 & 0 & -1 \\ -1 & -1 & -1 & 1 & 0 \\ -1 & -1 & 1 & -1 & 0 \\ -1 & 1 & -1 & -1 & 0 \\ 1 & -1 & -1 & -1 & 0 \\ 1 & 1 & -1 & -1 & 0 \\ 1 & -1 & 1 & -1 & 0 \\ 1 & -1 & -1 & 1 & 0 \\ -1 & 1 & 1 & -1 & 0 \\ -1 & 1 & -1 & 1 & 0 \\ -1 & -1 & 1 & 1 & 0 \\ 1 & 1 & -1 & 0 & -1 \\ 1 & -1 & 1 & 0 & -1 \\ 1 & -1 & -1 & 0 & 1 \\ -1 & 1 & 1 & 0 & -1 \\ -1 & 1 & -1 & 0 & 1 \\ -1 & -1 & 1 & 0 & 1 \\ 1 & 1 & 0 & -1 & -1 \\ 1 & -1 & 0 & 1 & -1 \\ 1 & -1 & 0 & -1 & 1 \\ -1 & 1 & 0 & 1 & -1 \\ -1 & 1 & 0 & -1 & 1 \\ -1 & -1 & 0 & 1 & 1 \\ 1 & 0 & 1 & -1 & -1 \\ 1 & 0 & -1 & 1 & -1 \\ 1 & 0 & -1 & -1 & 1 \\ -1 & 0 & 1 & 1 & -1 \\ -1 & 0 & 1 & -1 & 1 \\ -1 & 0 & -1 & 1 & 1 \\ 0 & 1 & 1 & -1 & -1 \\ 0 & 1 & -1 & 1 & -1 \\ 0 & 1 & -1 & -1 & 1 \end{pmatrix} \tag{C.21}$$

$$\mathbf{P}_{SLVP}^{5D,s=2} = \sqrt{\frac{8 \cdot 7E_b}{27}} \begin{pmatrix} 1 & 1 & 0 & 0 & 0 \\ 1 & 0 & 1 & 0 & 0 \\ 1 & 0 & 0 & 1 & 0 \\ 1 & 0 & 0 & 0 & 1 \\ 0 & 1 & 1 & 0 & 0 \\ 0 & 1 & 0 & 1 & 0 \\ 0 & 1 & 0 & 0 & 1 \\ 0 & 0 & 1 & 1 & 0 \\ 0 & 0 & 1 & 0 & 1 \\ 0 & 0 & 0 & 1 & 1 \\ 1 & -1 & 0 & 0 & 0 \\ 1 & 0 & -1 & 0 & 0 \\ 1 & 0 & 0 & -1 & 0 \\ 1 & 0 & 0 & 0 & -1 \\ 0 & 1 & -1 & 0 & 0 \\ 0 & 1 & 0 & -1 & 0 \\ 0 & 1 & 0 & 0 & -1 \\ 0 & 0 & 1 & -1 & 0 \\ 0 & 0 & 1 & 0 & -1 \\ 0 & 0 & 0 & 1 & -1 \\ -1 & 1 & 0 & 0 & 0 \\ -1 & 0 & 1 & 0 & 0 \\ -1 & 0 & 0 & 1 & 0 \\ -1 & 0 & 0 & 0 & 1 \\ 0 & -1 & 1 & 0 & 0 \\ 0 & -1 & 0 & 1 & 0 \\ 0 & -1 & 0 & 0 & 1 \\ 0 & 0 & -1 & 1 & 0 \\ 0 & 0 & -1 & 0 & 1 \\ 0 & 0 & 0 & -1 & 1 \\ -1 & -1 & 0 & 0 & 0 \\ -1 & 0 & -1 & 0 & 0 \\ -1 & 0 & 0 & -1 & 0 \\ -1 & 0 & 0 & 0 & -1 \\ 0 & -1 & -1 & 0 & 0 \\ 0 & -1 & 0 & -1 & 0 \\ 0 & -1 & 0 & 0 & -1 \\ 0 & 0 & -1 & -1 & 0 \\ 0 & 0 & -1 & 0 & -1 \\ 0 & 0 & 0 & -1 & -1 \\ 2 & 0 & 0 & 0 & 0 \\ 0 & 2 & 0 & 0 & 0 \\ 0 & 0 & 2 & 0 & 0 \\ 0 & 0 & 0 & 2 & 0 \\ 0 & 0 & 0 & 0 & 2 \\ -2 & 0 & 0 & 0 & 0 \\ 0 & -2 & 0 & 0 & 0 \\ 0 & 0 & -2 & 0 & 0 \\ 0 & 0 & 0 & -2 & 0 \\ 0 & 0 & 0 & 0 & -2 \\ 1 & 1 & 1 & 1 & 0 \\ 1 & 1 & 1 & 0 & 1 \\ 1 & 1 & 0 & 1 & 1 \\ 1 & 0 & 1 & 1 & 1 \\ 0 & 1 & 1 & 1 & 1 \\ -1 & -1 & -1 & -1 & 0 \\ -1 & -1 & -1 & 0 & -1 \\ -1 & -1 & 0 & -1 & -1 \\ -1 & 0 & -1 & -1 & -1 \\ 0 & -1 & -1 & -1 & -1 \\ 0 & 1 & 1 & 1 & -1 \\ 0 & 1 & 1 & -1 & 1 \\ 0 & 1 & -1 & 1 & 1 \\ 0 & -1 & 1 & 1 & 1 \\ 1 & 0 & 1 & 1 & -1 \\ 1 & 0 & 1 & -1 & 1 \\ 1 & 0 & -1 & 1 & 1 \\ -1 & 0 & 1 & 1 & 1 \\ 1 & 1 & 0 & 1 & -1 \\ 1 & 1 & 0 & -1 & 1 \\ 1 & -1 & 0 & 1 & 1 \\ -1 & 1 & 0 & 1 & 1 \\ 1 & 1 & 1 & 0 & -1 \\ 1 & 1 & -1 & 1 & 0 \\ 1 & -1 & 1 & 1 & 0 \\ -1 & 1 & 1 & 1 & 0 \\ -1 & 0 & 1 & 1 & 1 \\ \vdots & \vdots & \vdots & \vdots & \vdots \end{pmatrix} \begin{pmatrix} \vdots & \vdots & \vdots & \vdots & \vdots \\ 1 & 1 & 1 & -1 & 0 \\ 1 & 1 & -1 & 1 & 0 \\ 1 & -1 & 1 & 1 & 0 \\ -1 & 1 & 1 & 1 & 0 \\ 0 & -1 & -1 & -1 & 1 \\ 0 & -1 & -1 & 1 & -1 \\ 0 & -1 & 1 & -1 & -1 \\ 0 & 1 & -1 & -1 & -1 \\ -1 & 0 & -1 & -1 & 1 \\ -1 & 0 & -1 & 1 & -1 \\ -1 & 0 & 1 & -1 & -1 \\ 1 & 0 & -1 & -1 & -1 \\ -1 & -1 & 0 & -1 & 1 \\ -1 & -1 & 0 & 1 & -1 \\ -1 & 1 & 0 & -1 & -1 \\ 1 & -1 & 0 & -1 & -1 \\ -1 & -1 & -1 & 0 & 1 \\ -1 & -1 & 1 & 0 & -1 \\ -1 & 1 & -1 & 0 & -1 \\ 1 & -1 & -1 & 0 & -1 \\ -1 & -1 & -1 & 1 & 0 \\ -1 & -1 & 1 & -1 & 0 \\ -1 & 1 & -1 & -1 & 0 \\ 1 & -1 & -1 & -1 & 0 \\ 1 & 1 & -1 & -1 & 0 \\ 1 & -1 & 1 & -1 & 0 \\ 1 & -1 & -1 & 1 & 0 \\ -1 & 1 & 1 & -1 & 0 \\ -1 & 1 & -1 & 1 & 0 \\ -1 & -1 & 1 & 1 & 0 \\ 1 & 1 & -1 & 0 & -1 \\ 1 & -1 & 1 & 0 & -1 \\ 1 & -1 & -1 & 0 & 1 \\ -1 & 1 & 1 & 0 & -1 \\ -1 & 1 & -1 & 0 & 1 \\ -1 & -1 & 1 & 0 & 1 \\ 1 & 1 & 0 & -1 & -1 \\ 1 & -1 & 0 & 1 & -1 \\ 1 & -1 & 0 & -1 & 1 \\ -1 & 1 & 0 & 1 & -1 \\ -1 & 1 & 0 & -1 & 1 \\ -1 & -1 & 0 & 1 & 1 \\ 1 & 0 & 1 & -1 & -1 \\ 1 & 0 & -1 & 1 & -1 \\ 1 & 0 & -1 & -1 & 1 \\ -1 & 0 & 1 & 1 & -1 \\ -1 & 0 & 1 & -1 & 1 \\ -1 & 0 & -1 & 1 & 1 \\ 0 & 1 & 1 & -1 & -1 \\ 0 & 1 & -1 & 1 & -1 \\ 0 & 1 & -1 & -1 & 1 \\ 0 & -1 & 1 & 1 & -1 \end{pmatrix} \tag{C.22}$$

$$\mathbf{P}_{SSP}^{5D,s=2} = \sqrt{E_b} \times \tag{C.23}$$

$$\begin{pmatrix} 0.1282 & 0.5478 & -1.1080 & 0.2362 & -2.3238 \\ 1.7764 & -1.7637 & -0.1312 & 0.0934 & 0.8412 \\ -0.5711 & -1.4422 & 1.5546 & -0.8092 & 1.2338 \\ -2.3243 & 1.1794 & 0.0641 & -0.1381 & -0.4281 \\ 0.2323 & -1.5861 & 0.6318 & 0.7286 & 1.8709 \\ -1.5042 & -0.3790 & -0.1914 & 1.1797 & 1.7791 \\ 0.3591 & -1.3703 & -0.3983 & -1.5044 & -1.6035 \\ -0.4413 & 0.2951 & 1.9275 & 0.4672 & -1.6687 \\ -1.0062 & -0.1590 & -2.2415 & -0.2991 & -0.9212 \\ 1.2323 & 0.0406 & 2.2355 & 0.0427 & -0.6931 \\ -0.2549 & 0.0235 & 0.5414 & -0.6311 & -2.4986 \\ -1.3912 & -0.8756 & 0.3669 & -1.4484 & -1.4371 \\ -0.1804 & -1.9151 & 1.0316 & -1.4194 & -0.4699 \\ -1.0015 & -1.0059 & -0.8703 & -0.0902 & -2.0542 \\ -1.7867 & 0.3612 & 1.8427 & 0.4837 & -0.2186 \\ 1.2030 & 0.4040 & 0.0221 & -2.0721 & 1.0467 \\ -0.6577 & 2.2292 & -0.0665 & -1.1076 & -0.6059 \\ 0.4622 & 0.8385 & -2.2801 & 0.5635 & -0.7530 \\ 0.1163 & 0.1935 & -1.0898 & 1.0446 & 2.1611 \\ -1.9518 & 0.2070 & -1.5369 & 0.4290 & 0.7755 \\ 1.5538 & 1.6726 & -0.7293 & 1.1162 & 0.1020 \\ 1.9152 & 1.3646 & -0.3999 & -0.5506 & 1.0034 \\ -0.8510 & -0.9528 & -0.1469 & -0.5367 & 2.2491 \\ 1.4843 & 0.1295 & 0.9083 & -1.8727 & -0.6695 \\ -1.4680 & 1.5366 & 0.8551 & -0.9862 & 0.8830 \\ 0.1280 & 1.1430 & -1.6676 & -1.2112 & -1.1956 \\ 0.9183 & -1.2155 & -0.8531 & 1.5916 & 1.1909 \\ -0.0278 & -0.5472 & -0.0748 & 2.4708 & -0.7678 \\ -0.3696 & -2.3007 & 1.1720 & 0.4421 & 0.0357 \\ 0.6301 & 1.7621 & -0.1481 & 0.6804 & 1.7359 \\ 0.0191 & -2.3516 & -0.0818 & -0.6905 & 0.9931 \\ -0.0784 & 1.4053 & -1.5909 & 1.4128 & 0.7014 \\ -0.4486 & -0.8769 & 2.4445 & -0.0051 & -0.2331 \\ -0.7518 & 0.1392 & 0.6944 & 2.3164 & 0.7534 \\ -0.5108 & 1.0564 & -1.8174 & -0.3012 & 1.4931 \\ 0.9708 & 0.5281 & -0.0558 & 2.0876 & 1.1905 \\ -0.8179 & 1.0078 & -0.0185 & -0.2882 & 2.2873 \\ -0.0931 & 1.2550 & 1.1294 & -2.0349 & -0.0002 \\ -0.9631 & -2.1575 & -0.6502 & -0.7841 & -0.6164 \\ -1.0508 & 2.0667 & 1.1667 & 0.3994 & -0.3223 \\ 2.2143 & -0.1678 & 0.9104 & -0.7553 & 0.8183 \\ -0.0411 & 0.2897 & 0.8806 & 1.1229 & 2.2086 \\ -1.2397 & -1.0443 & 1.2546 & 1.5190 & -0.7009 \\ -0.5473 & 0.2373 & 0.6735 & -1.8616 & 1.6508 \\ -2.4110 & -0.3478 & 0.1379 & 1.0216 & 0.0563 \\ -1.5402 & 1.1532 & 0.9239 & 0.9166 & 1.2665 \\ 1.8093 & 0.2657 & -0.8379 & 0.9327 & -1.4435 \\ 1.3839 & 0.2331 & -0.3409 & -1.0079 & -1.9744 \\ -1.2793 & 1.0758 & 1.1947 & -0.9433 & -1.3743 \\ 0.7803 & 0.3420 & -0.8335 & -0.7972 & 2.2235 \\ -1.3549 & -0.0901 & 1.6914 & -1.4962 & 0.2380 \\ -1.6916 & 0.6035 & 0.0000 & -1.9193 & -0.3011 \\ 1.3934 & 1.4084 & 1.5369 & -0.8178 & 0.2098 \\ 1.3472 & -1.4970 & -0.4901 & 1.4947 & -0.6854 \\ -1.4815 & 0.4238 & -1.0437 & 1.0754 & -1.5427 \\ 0.8057 & -2.4015 & -0.0809 & -0.1547 & -0.7436 \\ -0.3011 & 1.0274 & 2.3563 & -0.5204 & -0.1754 \\ -1.1636 & -1.1971 & -1.7903 & -0.7455 & 0.6724 \\ 0.3758 & -1.2674 & -1.5137 & -0.1257 & 1.7162 \\ -0.4367 & 1.5646 & 0.4397 & 0.4831 & -1.9836 \\ 2.4361 & -0.0188 & -0.6693 & 0.6763 & 0.3993 \\ -1.6396 & 1.2854 & -0.5439 & 1.5342 & 0.0996 \\ 0.0560 & 0.0877 & 2.0915 & 1.6100 & -0.1516 \\ -0.0589 & -0.2581 & 1.8360 & -1.4201 & -1.2419 \\ -1.5010 & -1.2981 & 0.1305 & -1.6225 & 0.6423 \\ 0.5800 & -1.7251 & -1.5402 & -1.1456 & 0.0532 \\ 0.7133 & 1.5659 & 1.5371 & 0.9380 & -0.8924 \\ 0.2678 & 1.1003 & -0.6108 & 1.8268 & -1.4167 \\ -0.8600 & -0.6115 & -1.2847 & -1.9476 & -0.6652 \\ -0.2869 & -0.3156 & -2.4403 & 0.6532 & 0.6605 \\ 1.8563 & 0.7841 & -1.5198 & -0.5973 & -0.5225 \\ -1.9480 & -0.1666 & 0.6067 & 0.2862 & -1.6516 \\ 1.9676 & 0.9808 & 0.9370 & 0.8388 & 0.7649 \\ 0.9736 & 0.0715 & -1.4522 & 1.9800 & -0.1341 \\ -1.6505 & -1.8435 & -0.2733 & 0.2189 & 0.8688 \\ 0.6710 & 1.3608 & 1.1414 & -0.9345 & -1.5880 \\ & & \vdots & & \end{pmatrix}$$

$$\times \begin{pmatrix} & & \vdots & & \\ -0.6526 & 2.0202 & -1.1611 & 0.5255 & -0.9319 \\ 0.4257 & 0.0638 & -2.3426 & -1.1149 & 0.2898 \\ -0.7013 & 0.4070 & 1.9157 & -0.3362 & 1.5999 \\ 1.1443 & 1.8362 & -0.4694 & -0.0056 & -1.4486 \\ 0.0317 & 1.8675 & 0.2886 & 1.8450 & 0.1553 \\ -0.8466 & -0.2354 & -1.2251 & 2.1069 & 0.5367 \\ 0.8768 & -1.1411 & -0.4158 & 0.3110 & -2.1586 \\ 1.2493 & 0.2661 & 0.9092 & 0.5200 & -2.0667 \\ 0.9920 & -1.0254 & 1.0156 & 1.8824 & 0.6241 \\ 0.9651 & -0.1893 & 2.0573 & 0.5485 & 1.2245 \\ 1.3801 & -1.4692 & 0.1613 & -1.6935 & 0.2070 \\ -1.9231 & -1.3395 & 1.1699 & -0.2640 & -0.2628 \\ -1.6394 & 0.2361 & -0.8553 & -1.3157 & 1.3394 \\ 1.3162 & -1.1930 & 1.1043 & -0.6656 & -1.4771 \\ 2.1917 & -0.8586 & 0.9337 & 0.6720 & -0.3689 \\ -0.6327 & -1.6779 & 0.0894 & 1.8488 & 0.5985 \\ -1.3987 & 0.7659 & -0.7054 & -0.8259 & -1.8103 \\ 1.1153 & -0.1519 & -1.0206 & -2.0973 & -0.5408 \\ 0.6555 & -1.1776 & 1.2464 & 1.4331 & -1.2556 \\ -1.0706 & 0.8617 & 0.9353 & 1.8124 & -0.9756 \\ -1.1655 & -0.8774 & 1.5854 & 0.9930 & 1.1713 \\ -0.0741 & -2.1934 & -1.3008 & 0.6613 & 0.2329 \\ 0.2492 & 1.5906 & 1.6647 & 0.7697 & 1.0218 \\ -0.9506 & 2.2522 & -0.5119 & 0.1433 & 0.8611 \\ -0.0071 & -0.8190 & -0.8885 & -1.9091 & 1.3766 \\ -1.6107 & -1.1983 & -1.3706 & 0.9328 & -0.4704 \\ 2.1380 & -1.0652 & -0.6325 & -0.4406 & -0.8368 \\ 0.9025 & -1.0280 & 0.5362 & -1.0606 & 1.9278 \\ 1.2850 & 0.6454 & -1.9079 & 0.3027 & 1.0958 \\ 1.1214 & 1.6351 & -0.2857 & -1.6765 & -0.4201 \\ 0.5949 & 2.0777 & -1.4494 & -0.3993 & 0.2627 \\ -0.4551 & -1.9311 & -0.2017 & 1.2061 & -1.2524 \\ 1.3804 & -1.0375 & -1.9445 & 0.4815 & 0.0701 \\ -0.5979 & -1.4927 & 1.2316 & -0.0004 & -1.7022 \\ 2.3704 & 0.7735 & 0.4045 & -0.2225 & -0.7548 \\ -0.2552 & 0.8785 & -1.0738 & -2.1935 & 0.4456 \\ 0.8081 & -0.5873 & -1.9053 & -0.6080 & -1.4151 \\ 1.8692 & -0.5194 & -1.2047 & -1.0084 & 0.8764 \\ 0.0266 & -0.7786 & -1.7320 & 1.1940 & -1.4027 \\ -2.3452 & -0.5825 & -0.7418 & -0.6807 & -0.3835 \\ 1.6010 & -0.2664 & 0.1057 & 0.5988 & 1.9991 \\ 1.1549 & -1.6064 & 1.6633 & -0.4378 & 0.3569 \\ 0.6395 & 2.5309 & 0.4099 & 0.0850 & 0.1025 \\ 0.5863 & -0.1140 & 1.9505 & -1.4903 & 0.7861 \\ -0.1053 & 0.6069 & -0.0249 & -2.1102 & -1.4721 \\ 0.9698 & 0.8263 & 1.0526 & -0.5992 & 1.9773 \\ 1.4840 & 0.3984 & 0.6116 & 1.9623 & -0.6435 \\ -2.1394 & -0.2211 & 0.7451 & -0.3656 & 1.2981 \\ -0.0923 & -0.5129 & 0.4078 & -2.5614 & 0.0377 \\ -1.4686 & 1.3230 & -1.5261 & -0.8686 & -0.0974 \\ -0.3845 & -0.2149 & 0.2871 & 1.2982 & -2.2446 \\ 0.2087 & 1.9307 & 0.0000 & -1.2945 & 1.2462 \end{pmatrix}$$

$$\mathbf{P}^{5D,s=2}_{ZSSP} = \sqrt{E_b} \times \tag{C.24}$$

$$\begin{pmatrix}
0 & 0 & 0 & 0 & 0 \\
0.3443 & -2.1063 & -1.4317 & 0.3244 & -0.5876 \\
2.2527 & 0.5751 & -1.1833 & 0.2918 & -0.4058 \\
-0.5564 & 0.7351 & 0.2253 & -1.9274 & -1.5618 \\
-0.4514 & 0.0094 & -0.6250 & 2.5354 & 0.1794 \\
0.0160 & 1.8038 & 0.1471 & 1.9315 & -0.2210 \\
-0.5078 & 0.1029 & -1.5820 & -1.7964 & -1.0282 \\
0.8131 & 0.1408 & 2.3917 & -0.3427 & -0.7325 \\
1.0400 & -0.8766 & -0.7022 & -0.0491 & 2.1701 \\
0.7761 & -0.3873 & -2.0457 & -0.9232 & 1.1250 \\
-2.0252 & 1.3395 & 0.7620 & -0.2433 & 0.7206 \\
0.1067 & 0.6298 & 1.1373 & 1.9713 & 1.2115 \\
-2.2489 & -0.5022 & 0.1824 & 0.2481 & 1.2848 \\
1.5878 & -0.3556 & 1.8022 & 1.0651 & 0.1588 \\
0.9573 & -1.1774 & -1.5233 & -1.4659 & -0.5323 \\
0.0664 & -1.3572 & -1.8063 & 0.8192 & 1.1291 \\
-0.0280 & -0.9873 & -1.4069 & -0.5104 & -1.9595 \\
-0.3267 & -0.5067 & 2.2539 & 1.2042 & 0.4017 \\
-2.0107 & -0.6157 & -0.3922 & 1.5587 & -0.2228 \\
-1.1378 & 0.2035 & 1.6020 & 0.4125 & 1.7270 \\
1.4130 & 1.8010 & -0.8060 & 0.7406 & 0.7853 \\
0.7291 & 1.7613 & 1.6953 & -0.7322 & 0.1045 \\
0.6435 & -1.0853 & 1.3361 & 0.8386 & 1.7247 \\
1.7924 & 1.4866 & 0.6013 & 1.0057 & -0.5096 \\
0.5520 & 0.1443 & -1.4893 & 1.0186 & -1.8639 \\
0.8937 & -0.8228 & 0.1760 & -1.2769 & -1.9794 \\
-0.5317 & -1.7401 & -0.1212 & 0.5174 & 1.8606 \\
-0.5615 & -0.7709 & -0.1669 & 1.9675 & -1.4989 \\
-0.5858 & 0.8875 & -2.1539 & -0.0608 & -1.1319 \\
-0.0924 & -1.9523 & 0.8610 & -0.2385 & -1.5611 \\
-1.1365 & -0.8555 & 0.7102 & 1.7914 & 1.1480 \\
1.4659 & 0.0334 & -1.6120 & 1.0200 & 1.1252 \\
0.5848 & -1.8672 & 1.7776 & 0.2579 & -0.0061 \\
1.0385 & 0.5910 & -1.2150 & -2.0342 & 0.1148 \\
-0.5362 & 0.3567 & -2.4271 & 0.5508 & 0.6681 \\
1.9994 & -1.2285 & -1.1152 & -0.1950 & 0.5165 \\
-1.4224 & -1.5514 & 0.0320 & -1.2085 & 1.0788 \\
-1.3046 & -0.2666 & -1.1184 & 1.3901 & 1.4487 \\
1.0597 & -2.1586 & 0.1506 & -1.0563 & -0.3665 \\
-0.0904 & 1.2297 & -0.7161 & 1.6990 & 1.4613 \\
0.9561 & -0.8355 & -1.3192 & 1.8775 & -0.4214 \\
-1.7620 & 1.1966 & -0.7431 & -1.2992 & -0.5278 \\
0.5064 & 1.7292 & 1.1199 & 0.1050 & -1.5948 \\
0.4175 & 0.4772 & 0.3685 & 0.6703 & 2.4633 \\
2.1800 & -0.2005 & -0.2359 & -1.3337 & -0.6543 \\
-1.1656 & -1.6055 & 1.4823 & 0.1264 & 0.9516 \\
-0.9007 & 2.0265 & 0.8360 & -1.0840 & -0.5130 \\
1.0914 & -2.0623 & -0.0954 & 0.9484 & 0.8381 \\
1.7621 & -1.0549 & 1.1336 & 0.0380 & -1.2453 \\
2.2299 & 0.5601 & 1.2394 & -0.4806 & 0.0422 \\
0.8858 & 1.3054 & -2.0962 & -0.4033 & 0.0971 \\
2.0381 & -1.2694 & 0.8685 & -0.2727 & 0.6792 \\
1.3683 & -0.9355 & -0.3105 & -1.8274 & 0.9337 \\
-1.6900 & 1.0388 & 0.1800 & 1.6165 & 0.6887 \\
0.8685 & -1.8605 & 0.1415 & 1.2777 & -1.0895 \\
1.0315 & -0.4828 & -2.3450 & 0.2083 & -0.4644 \\
-0.5488 & -0.6497 & -1.2122 & -2.0707 & 0.7580 \\
2.0743 & 0.2509 & 0.4812 & 0.7305 & 1.3872 \\
-0.4951 & -1.8315 & -0.5702 & 1.7649 & 0.1252 \\
-2.1339 & -1.2922 & 0.6754 & -0.3991 & -0.4652 \\
0.4604 & -0.6455 & 0.1879 & 0.6004 & -2.4558 \\
0.0249 & 0.9347 & -0.4074 & -0.3633 & -2.4255 \\
-0.8385 & 0.8661 & 2.3540 & -0.2061 & 0.1336 \\
-0.8523 & -0.9266 & 2.1862 & -0.2372 & -0.7965 \\
-1.6241 & -1.6449 & -1.1413 & 0.3013 & 0.5641 \\
0.2322 & -2.0346 & -1.0825 & -0.8915 & 0.9461 \\
-1.6178 & -0.4644 & 0.0595 & -2.0209 & -0.3669 \\
-0.4390 & -2.6104 & 0.1635 & 0.0850 & 0.1200 \\
-0.3939 & 1.0892 & 1.4231 & -1.1856 & 1.5109 \\
-0.1347 & -0.4935 & 0.8481 & -2.1642 & 1.1791 \\
0.3249 & 2.6235 & 0.1942 & 0.1476 & -0.0851 \\
-0.2977 & 0.4272 & 1.7411 & -1.9113 & -0.3158 \\
-0.5306 & -1.6710 & 1.1362 & -1.6207 & -0.2523 \\
-1.7765 & 0.3487 & -0.3543 & -1.4057 & 1.2946 \\
1.7283 & -1.1178 & -0.8850 & 0.0477 & -1.4258 \\
-0.5079 & 0.9805 & -0.0958 & -2.3907 & 0.3329 \\
 & & \vdots & &
\end{pmatrix}$$

$$\times$$

$$\begin{pmatrix}
 & & \vdots & & \\
0.0413 & -0.6415 & 2.2825 & -0.8402 & 0.8520 \\
-1.2346 & 1.7392 & 1.1834 & 0.8374 & -0.6359 \\
0.5176 & -0.9485 & 0.8067 & 2.2828 & 0.1606 \\
-0.7999 & 0.3320 & 1.1402 & 2.1743 & -0.5264 \\
0.4270 & 1.1863 & 1.9899 & 1.1945 & -0.2811 \\
1.8004 & 0.5633 & 0.0854 & 0.0024 & -1.8679 \\
1.2482 & 0.8120 & 0.6839 & -1.9919 & 0.6343 \\
1.1116 & 1.6573 & 0.4771 & -0.4959 & 1.6123 \\
-1.2533 & -0.7996 & 0.0869 & -0.9598 & -1.9790 \\
0.3502 & 1.0531 & -1.4942 & -0.0191 & 1.8948 \\
-0.6528 & -0.3999 & 0.3612 & -0.7619 & 2.3996 \\
-2.0424 & -0.0122 & 1.5003 & 0.7953 & -0.0003 \\
1.1882 & -0.1979 & 0.9283 & -0.9366 & 1.9660 \\
-0.5533 & 2.0678 & -1.4324 & 0.4621 & 0.4560 \\
0.2580 & -0.4555 & 1.7831 & 1.2064 & -1.4650 \\
-0.7077 & -1.9213 & -0.7542 & -1.3321 & -0.7207 \\
0.4281 & -0.6786 & -0.3930 & 1.8634 & 1.6688 \\
-2.1065 & 0.6877 & -1.3340 & 0.1096 & 0.5942 \\
0.3737 & 0.5279 & -0.5699 & -1.7035 & 1.8466 \\
-1.2638 & -1.8076 & -0.5484 & 0.4800 & -1.2881 \\
0.2958 & -0.6177 & -0.0597 & -2.5035 & -0.5614 \\
-1.3005 & -0.0064 & -0.9506 & 0.5740 & -2.0324 \\
-0.9374 & -0.5232 & -1.5064 & -0.4705 & 1.8472 \\
2.2516 & -0.7412 & 0.0041 & 1.1801 & -0.2085 \\
-1.3539 & 0.9909 & -1.3002 & 1.4773 & -0.6060 \\
0.5405 & 1.0348 & -1.7461 & 1.6130 & -0.2032 \\
-0.4505 & 1.0461 & 0.2430 & 1.4129 & -1.9241 \\
-0.6331 & -1.0289 & -2.2712 & -0.6566 & -0.0796 \\
-1.7730 & 0.4070 & 1.2996 & -0.9197 & -1.1003 \\
1.1915 & 0.8422 & 1.0252 & -1.5067 & -1.2669 \\
-0.8083 & -0.8072 & -1.9390 & 1.2179 & -0.7123 \\
0.9769 & 1.8224 & -1.0061 & 0.3977 & -1.2685 \\
-1.6880 & -0.2258 & 1.4631 & -1.1990 & 0.7592 \\
-0.4409 & 1.9242 & 1.0058 & 0.5717 & 1.3489 \\
1.7645 & 1.7709 & -0.2077 & -0.8510 & -0.1950 \\
-0.5698 & 2.1108 & -0.2223 & -0.9667 & 1.1362 \\
-1.2561 & 1.0170 & -0.3541 & 0.2258 & 2.0656 \\
-0.8847 & -1.7040 & 1.1659 & 1.2766 & -0.6164 \\
-1.4686 & -0.3331 & 0.9885 & 0.7327 & -1.8092 \\
0.3716 & -1.9035 & 0.8599 & -0.8612 & 1.3463 \\
1.2292 & -0.7903 & 1.4427 & -1.6707 & -0.2166 \\
0.0694 & 1.9294 & -0.8803 & -1.4127 & -0.7463 \\
1.3541 & 0.5680 & -0.2134 & 2.1529 & 0.4676 \\
-2.0869 & -0.5696 & -1.1914 & -0.6024 & -0.7703 \\
1.1584 & 0.1298 & 0.2660 & 1.9208 & -1.3915 \\
2.0214 & 0.5165 & -0.7926 & -0.7681 & 1.2182 \\
1.1831 & 0.4644 & -1.5201 & -0.9304 & -1.5045 \\
-0.9988 & 2.0474 & -0.5441 & 0.1543 & -1.2433 \\
-0.7537 & 1.0258 & -1.8287 & -1.2106 & 0.7906 \\
-0.1468 & 0.1039 & 1.4168 & -0.6002 & -2.1576 \\
-2.3635 & 0.7618 & -0.0302 & 0.3734 & -0.8650 \\
0.7474 & 0.6946 & 1.9908 & 0.3005 & 1.4001
\end{pmatrix}$$

Turku
Centre *for*
Computer
Science

Joukahaisenkatu 3-5 B, 20520 Turku, Finland | www.tucs.fi

University of Turku
- Department of Information Technology
- Department of Mathematics

Åbo Akademi University
- Department of Information Technologies

Turku School of Economics
- Institute of Information Systems Sciences

ISBN 978-952-12-1959-7
ISSN 1239-1883